

**SUSTAINABLE HOUSING IN VIETNAM:
CLIMATE RESPONSIVE DESIGN STRATEGIES
TO OPTIMIZE THERMAL COMFORT**

PhD thesis
submitted in partial fulfillment of the requirements for the Degree of
Doctor in Architecture and Urban planning

by

Anh Tuan NGUYEN

Liège, 2013
Académie Universitaire Wallonie-Europe

This document presents the original results of the doctoral research carried out by

NGUYEN Anh Tuan, Architect, M.Sc.

Université de Liège – Faculté des Sciences Appliquées
Département Architecture, Géologie, Environnement et Constructions
Chemin des Chevreuils 1, Bâtiment B52/3
B-4000 Liège, Belgique
natuan@ud.edu.vn; arcnguyenanhtuan@yahoo.com

The present thesis has been supervised by the promoter
Prof. Dr. Ir. Sigrid Reiter

Jury members

Prof. Dr. Ir. Jacques Teller	Université de Liège, president
Prof. Dr. Ir. Sigrid Reiter	Université de Liège, promoter
Dr. Ir. Arnaud Evrard	Université Catholique de Louvain, member
Prof. Dr. Ir. Pierre Leclercq	Université de Liège, member
Prof. Dr. Ir. André De Herde	Université Catholique de Louvain, member
Prof. Dr. Khoi Doan-Minh	National University of Civil Engineering (Vietnam), member

The research presented in this thesis was financially supported by Ministry of Education and Training of Vietnam (Grant No 624/QĐ-BGDĐT 9/2/2010) and partly by Wallonie Bruxelles International (Grant No 23478/AMG/BE.VN/JP/jp and DWBH/FP/vtd/V084/2011)

Copyright © Nguyen Anh Tuan, 2013
All rights reserved

ACKNOWLEDGMENTS

First of all, I would like to express my greatest thanks to Professor Sigrid Reiter for her guidance and patience over the last three years. Her kind support has been key to my academic development, and her research style has had a profound influence on my work.

Professor Pierre Leclercq (Université de Liège) and Dr. Arnaud Evrard (Université Catholique de Louvain), two members of the committee of this thesis, are acknowledged for their valuable consultancy, encouragement and final approval.

I would like to thank Dr. Jiang Yi (Massachusetts Institute of Technology), Professor T. Katayama (Kyushu University) for their support of experimental settings and results of the wind tunnel experiments. Valuable inputs about CFD from Mathieu Barbason and Dr. Sébastien Erpicum are greatly acknowledged. The author also appreciates initial support for the use of PLEIADES-COMFIE from Dr. Anne Françoise Marique. I'm greatly thankful to many anonymous reviewers who have had many contributions to my publications.

The thermal comfort research in this thesis is completely relied on field survey data from various studies around South-East Asia. I would like to express my appreciation to following professors for their donations of field survey data and useful guides: Nuyk HienWong (National University of Singapore); Henry Feriadi (Duta Wacana Christian University); Yufeng Zhang and his survey team (South China University of Technology); Mary Myla Andamon (University of Adelaide); Ibrahim Hussein (Universiti Tenaga Nasional); and other authors in ASHRAE RP-884 database.

I greatly thank Dr. To Mai Xuan Hong (Hochiminh city University of Medicine and Pharmacy) for the support in statistics. I sincerely thank Dr. Michael Wetter, U.S. Lawrence Berkeley National Laboratory, who kindly gave many instructions and GenOpt optimization program. I'm so grateful to Professor Carl Mahoney for his instruction to rebuild the Mahoney tables. I appreciate Professor Curtis Pedersen (University of Illinois at Urbana-Champaign – EnergyPlus development team) for his guide about the IRT surface used in

atrium modeling. Louise Regnard, among my best friends, patiently helped me in translating many of my works into English. The experimental results of house No. 120 Bui Thi Xuan st, Hanoi of Mr. Tran Quoc Bao is also acknowledged. The U.S. Department of Energy, Autodesk, UCLA and the Unit of Econometrics and Applied Statistics of the Joint Research Centre (European Commission) are greatly acknowledged for making EnergyPlus program, AutoCAD 2010 and Ecotect 2011, Climate consultant 5.0 and Simlab 2.0 free of charge, respectively. The Faculty of Environment – Danang University of Technology is acknowledged for many useful experimental instruments. I would like to thank the Centre for the Preservation and Restoration of Hoian city and the Centre for Heritage and Tourism of Quangnam province for their support and input data of the ancient dwelling No. 75 Tran Phu, Hoi An, Vietnam. Météonorm (Météotest) is acknowledged for the weather files (free of charge) of many locations in Vietnam. National Meteorological and Hydrographical Station - Central Vietnam is acknowledged for the weather data of Danang city during my measuring campaigns.

The research unit LEMA, Faculty of Applied Sciences, University of Liège within which I have conducted my PhD research since March 2010 consistently gave me supports and many opportunities. I am grateful to all members of LEMA, especially Professor Jacques Teller.

This thesis was financially supported by Ministry of Education and Training of Vietnam (Grant No 624/QĐ-BGDĐT: 9th Feb. 2010) and partly by Wallonie Bruxelles International (Grant No 23478/AMG/BE.VN/JP/jp and DWBH/FP/vtd/V084/2011). I would like to thank these institutions for their generous supports.

I am thankful to my family and friends for their support and encouragement, in particular to my parents who always supported me in the academic career. Special thanks go to my wife and my tiny son for providing me with strength and continuous supports through the ups and downs of writing a dissertation.

ABSTRACT

Housing issue in Vietnam is still a big concern as in 2008, 72.2% of the existing housing was semi-permanent or temporary and 89.2% of the poor did not have a permanent shelter. As a response to sustainability, the global aim of this thesis is to develop design strategies toward comfortable, energy-efficient housing with acceptable building cost. Occupants' thermal comfort is the key assessment criterion throughout the research.

First of all, the thesis develops a thermal comfort model for Vietnamese people living in naturally ventilated buildings through the data from field surveys around South-East Asia. This comfort model is then validated by survey data in Vietnam in 2012.

A new simple climate analysis tool is developed, used to analyze the climate of 3 regions in question and to draw preliminary design guidelines. A comprehensive study on climate responsive design strategies of vernacular housing in Vietnam is also carried out. The results to some extent reveal the remaining values of vernacular architecture and provide valuable lessons for modern applications.

Three most common housing prototypes in Vietnam are selected. Afterward a comprehensive framework is implemented to derive thermal performances of 3 typical housing types. Various techniques (in situ monitoring, building thermal simulation, CFD and airflow network model, numerical model calibration, parametric simulation method) are employed to improve the thermal performances and natural ventilation of these houses.

The sensitivity of building performance to the design variables is outlined by Monte Carlo-based sensitivity analysis. The thermal performances of the reference cases are optimized using the simulation-based optimization method and the most influential design variables. Optimization results show the best combinations of design strategies for each climatic region. The performances of the optimal solutions are compared with the references, providing an insight of the efficiency of this approach in building design.

Finally, the different objectives yielded in this thesis are summarized. The possible future extensions of this research are outlined.

TABLE OF CONTENTS

ACKNOWLEDGMENTS	i
ABSTRACT.....	iii
TABLE OF CONTENTS.....	iv
LIST OF PUBLICATIONS	viii
LIST OF SYMBOLS AND ABBREVIATIONS	ix
CHAPTER 1 Introduction	1
1.1 Global environmental issues and the sustainability movement	1
1.2 Housing issues in Vietnam - Identifying problems	6
1.3 Research objectives.....	9
1.4 Research hypotheses	10
1.5 Limits of the research	11
1.6 Structure and methodologies of the thesis	12
CHAPTER 2 Literature review	16
2.1 Literature review on the bioclimatic approach in architecture	16
2.1.1 Terms and definitions	16
2.1.2 Bioclimatic architecture - conventional methods and novel approaches.....	17
2.1.3 Classification of bioclimatic research methodologies	20
2.1.4 The challenges in Vietnam	20
2.2 Literature review on human thermal comfort in built environments.....	21
2.2.1 Thermal comfort and its role in built environments	21
2.2.2 Human thermal regulation mechanism	22
2.2.3 Comfort temperature in climate-controlled environments.....	24
2.2.4 Thermal comfort prediction in actual built environments	25
2.2.5 Thermal comfort studies in Vietnam	35
CHAPTER 3 A thermal comfort model for Vietnamese	36
3.1 Study background and the proposed approach	36
3.2 Adaptive thermal comfort model for hot humid South-East Asia	38
3.2.1 Methodology	38
3.2.2 Raw data standardization	41
3.2.3 Results and discussions.....	43
3.2.4 An adaptive thermal comfort model for South-East Asia.....	48

3.2.5	Other comfort-related issues	54
3.3	Model validation under conditions of Vietnam	56
3.3.1	The thermal comfort survey in Vietnam	56
3.3.2	Survey data and validation results	59
3.4	Long-term evaluation of the general thermal comfort condition.....	62
3.5	Implementation of the adaptive model into a building simulation program.....	63
3.6	Chapter conclusion	64
CHAPTER 4	Climate analysis	66
4.1	An overview about the climate of Vietnam	66
4.1.1	Climatic regions in Vietnam	66
4.1.2	Characteristics of the climate of three climatic regions of Vietnam.....	69
4.2	Climate analyses using methods developed by some authors	71
4.2.1	Climate analysis by Climate Consultant 5.3 program	72
4.2.2	Climate analysis by Mahoney Tables	73
4.2.3	Discussions	76
4.3	An improved climate-comfort analysis method for hot humid climates using a graphical method and TMY weather data sets.....	76
4.3.1	Comfort zone for people living in hot humid climates	77
4.3.2	Extended comfort zones using passive cooling and heating strategies.....	81
4.3.3	Plotting weather data on the Building psychrometric chart.....	85
4.3.4	Results of the method	88
4.4	Climate analysis using the adaptive comfort model	91
4.5	General conclusions about the climates of Vietnam.....	93
CHAPTER 5	Thermal performance of typical housing typologies	95
5.1	Identifying typical housing prototypes in Vietnam	95
5.2	The monitoring campaign.....	96
5.2.1	The selections of case-study houses	96
5.2.2	Monitoring protocol and monitoring results	98
5.2.3	Discussions on the monitoring results	101
5.3	Numerical modeling and simulation of buildings performance	102
5.3.1	Building energy simulation programs and EnergyPlus	102
5.3.2	Airflow prediction in and around buildings using Computational Fluid Dynamics	105
5.4	Modeling the case-study houses in EnergyPlus.....	119
5.4.1	About Airflow Network model and its role in modeling NV buildings	121
5.4.2	Calculation of wind pressure coefficient using CFD.....	121
5.5	Calibration of the three EnergyPlus housing models.....	126

5.5.1	Introduction to the calibration approach.....	126
5.5.2	Criteria to assess the agreement between simulated and measured data	127
5.5.3	Calibration runs.....	129
5.6	Thermal performance of the case-study houses during a year.....	139
5.6.1	Thermal comfort analysis	140
5.6.2	Identifying strong and weak points and potential improvements	145
5.7	Chapter conclusion	149
CHAPTER 6 Climate responsive design strategies of vernacular housing.....		150
6.1	Introduction and background of the study	150
6.2	Materials and methods	151
6.3	Theory, measurement, calculation and results.....	153
6.3.1	Step 1: Climate zoning and selected sites of the survey	153
6.3.2	Step 2: Collecting data.....	153
6.3.3	Step 3: Investigation of housing climate responsive design strategies	156
6.3.4	Step 4: Full-scale measurement of micro-climate in a vernacular house	165
6.3.5	Step 5: Whole – year simulation of building performance.....	170
6.4	Step 6: The lessons given by vernacular architecture - Conclusions.....	177
CHAPTER 7 Climate responsive design strategies to improve thermal comfort.....		179
7.1	Improving the thermal performance by a parametric simulation method	179
7.1.1	The effects of various external wall types	179
7.1.2	Thermal insulation for the roof and thermal performance of the houses.....	181
7.1.3	The effect of color of the external walls	183
7.1.4	The effect of ventilation schemes on thermal performance of the houses.....	184
7.1.5	Other design strategies to improve thermal performance of the houses.....	186
7.1.6	Efficiency of the combination of all positive strategies.....	188
7.2	Design strategies to enhance passive cooling by natural ventilation.....	190
7.2.1	Theory of passive cooling by natural ventilation.....	190
7.2.2	Case study on natural ventilation using the CFD technique.....	195
7.3	Auxiliary strategies to improve building thermal performance.....	211
7.3.1	Climate responsive heating techniques.....	211
7.3.2	Climate responsive cooling techniques.....	212
7.4	Chapter conclusion	214
CHAPTER 8 Combination of design strategies to optimize thermal comfort		215
8.1	Monte Carlo-based sensitivity analysis	215
8.1.1	A brief introduction of sensitivity analysis.....	215
8.1.2	Methodologies of sensitivity analysis.....	217
8.1.3	The selected approach of SA for the present study.....	219

8.1.4	Sensitivity analysis of the EnergyPlus thermal models	222
8.2	Optimizing building thermal performance by numerical optimization	235
8.2.1	An introduction of numerical optimization	235
8.2.2	Definition of an optimization problem and related nominations	237
8.2.3	Optimization methodology	238
8.2.4	Parameters of design and strategies considered in the optimization.....	240
8.2.5	The choice of optimization algorithms for the present problem.....	242
8.2.6	The establishment of objective functions	246
8.2.7	Optimization results	249
8.3	Discussions and comparisons	257
8.3.1	Discussions	257
8.3.2	Comparison of the findings of this work with results of earlier studies	260
8.4	Chapter conclusion	262
CHAPTER 9	Conclusions and further works	264
9.1	Original contributions of the thesis.....	264
9.1.1	A simple climate-comfort analysis tool for hot humid climates.....	264
9.1.2	An adaptive thermal comfort model for South-East Asia.....	265
9.1.3	Thermal performance of vernacular housing and current housing typologies in Vietnam.....	265
9.1.4	A new bioclimatic approach towards sustainable architecture	266
9.2	Conclusions and recommendations	267
9.2.1	Comfort model for Vietnamese	267
9.2.2	The significance of design parameters.....	267
9.2.3	Climate responsive design for optimal thermal comfort.....	268
9.2.4	The efficiency of different design methods	270
9.3	Further works	271
9.3.1	Sustainable housing under the perspective of building materials.....	271
9.3.2	Feasibility of adaptive thermal comfort in climate-controlled buildings.....	271
9.3.3	Climate responsive solutions for non-residential buildings.....	272
9.3.4	Passive design towards zero energy buildings in Vietnam.....	272
9.4	Towards sustainable housing in Vietnam	272
REFERENCES	275
LIST OF FIGURES	286
LIST OF TABLES	292
APPENDIX A	294
APPENDIX B	299
APPENDIX C	304

LIST OF PUBLICATIONS

The following scientific papers have been published as the result of this thesis:

*** In ISI journals (indexed by ISI - Thomson Reuters)¹:**

- Nguyen, A.T.; Reiter, S. *The effect of ceiling configurations on indoor air motion and ventilation flow rates*, Building and Environment 2011; 46:1211-22 (IF=2.4)
- Nguyen, A.T.; Tran, Q.B.; Tran, D.Q.; Reiter, S. *An investigation on climate responsive design strategies of vernacular housing in Vietnam*, Building and Environment 2011, 46: 2088-2106 (IF=2.4)
- Nguyen, A.T.; Reiter, S. *An investigation on thermal performance of a low cost apartment in Danang*, Energy and Buildings 2012, 47:237-246 (IF=2.386)
- Nguyen, A.T.; Singh, M.K.; Reiter, S. *An adaptive thermal comfort model for hot humid South-East Asia*, Building and Environment 2012, 56:291-300 (IF=2.4)
- Nguyen, A.T.; Reiter, S. *A climate analysis tool for passive heating and cooling strategies in hot humid climate based on Typical Meteorological Year data sets*, Energy and Buildings 2012, <http://dx.doi.org/10.1016/j.enbuild.2012.08.050> (IF=2.386)
- Nguyen, A.T.; Reiter, S. *Passive designs and strategies for low-cost housing using simulation-based optimization and different thermal comfort criteria*, Journal of Building Performance Simulation 2013, doi:10.1080/19401493.2013.770067 (IF=0.718)

*** In Proceedings of International Conferences:**

- Nguyen, A.T.; Reiter, S. *Analysis of passive cooling and heating potential in Vietnam using graphical method and Typical Meteorological Year weather file*, in Proceedings CISBAT 2011 International conference, Lausanne, 2011
- Nguyen, A.T.; Reiter, S. *Optimum design of low-cost housing in developing countries using nonsmooth simulation-based optimization*, in Proceedings of International conference of Passive and Low Energy Architecture 2012, Lima, 2012

¹ Source: © Thomson Reuters Journal Citation Reports (2012)

LIST OF SYMBOLS AND ABBREVIATIONS

SYMBOLS

A and A_i	Opening area and its differential, m ²	Q_w	Energy flow rate through window, W
A_{Du}	Dubois skin surface area, m ²	\mathbb{R}	The set of real numbers
A_{ew}	External wall area, m ²	S	Rate of heat storage, W
A_w	Total projected window area, m ²	$SHGC$	Solar heat gain coefficient
C_d	Opening discharge coefficient	S_{ij}	Mean rate of strain tensor
$COST_{max}$	Estimated max construction cost, \$	SR	Standard residual
C_p	Wind pressure coefficient	T	Absolute temperature, K
E	Wall roughness parameter	T_{comf}	Comfort (neutral) temperature, °C
$f_o^{50}(x)$	50-year operation cost function, \$	T_{DB}	Inlet air dry-bulb temperature, °C
$f_c(x)$	Construction cost function, \$	$TDH\%(x)$	Total discomfort hours function, h
$F_{schedule}$	Hourly schedule by users	T_g	Global temperature, °C
G_{cons}	Griffiths constant	T_i	Indoor air temperature, °C
h_o	Conductance of the thin air film on wall surfaces, W/m ² .°C	$T_{i,o}$	Indoor operative temperature, °C
I_i	Reference infiltration rate, m ³ /s	T_{LA}	Leaving air dry-bulb temperature, °C
I_s	Solar irradiation on South-facing surface, W/m ²	T_{mrt}	Mean radiant temperature, °C
i_t	Turbulence intensity, %	T_o	Outdoor ambient temperature, °C
k	Turbulence kinetic energy, m ² /s ²	T_{od-1}	Mean external temperature of the previous day, °C
L	Thermal load on the body, W/m ²	T_{od-2}	Mean external temperature for the day before and so on, °C
l	Characteristic length, m	$T_{o,rm}$	Outdoor running mean temperature, °C
M	Rate of metabolic heat production, W/m ²	T_{out}	Monthly mean outdoor temperature, °C
N	Number of air change per hour	$T_{sol-air}$	Sol-air temperature, °C
n	Local coordinate normal to the wall	T_{WB}	Inlet air wet-bulb temperature, °C
p	Mean pressure, N/m ²	U	Wind velocity through window, m/s
p_∞	Static pressure in free stream, Pa	\bar{U}	Mean wind velocity normal to window, m/s
p_s	Standard atmospheric pressure, Pa	U^*	Friction (or shear) velocity, m/s
p_{st}	Static pressure at the current point, Pa	u, v, w	Velocity vector in u, v, w directions, m/s
p_w	Partial pressure of water vapor, Pa	$u+$	Dimensionless velocity
p_{ws}	Pressure of saturated pure water, Pa	U_{ew}	External wall U-value, W/m ² .°C
Q	Ventilation flow rate, m ³ /s	u_i	Mean and fluctuating velocity component in x_i direction, m/s
Q_c	Energy flow rate through wall, W	$u_{i,A}$	Wind velocity on a differential A_i of the opening, m/s
q_{res}	Rate of heat loss from respiration, W/m ²	u_r	Absolute resultant velocity parallel to the wall at the 1 st grid cell, m/s
q_{sk}	Total rate of heat loss from skin, W/m ²	U_{ref}	Reference velocity, m/s
Q_v	Energy flow rate by ventilation, W		

U_w	Window overall coefficient of heat transfer, $W/m^2 \cdot ^\circ C$	CEN	Comité Européen de Normalisation
u_z	Wind velocity and height z , m/s	CFD	Computational fluid dynamics
u_τ	Resultant friction velocity, m/s	CIBSE	Chartered Institution of Building Services Engineers
V	Volume of the solar heating space, m^3	COP	Coefficient of performance
v_∞	Free stream velocity at reference height, m/s	CPHSC	Central Population and Housing census Steering Committee
V_a	Air velocity, m/s	CPZ	Control potential zone
$V_{outdoor}$	Hourly outdoor wind speed, m/s	CV	Coefficient of Variation of Root Square Mean Error
ν_t	Isotropic eddy viscosity, $kg/m \cdot s$	(RMSE)	
W	Rate of mechanical work accomplished, W	DISC	Thermal discomfort
W_h	Humidity ratio, $kg/kg_{dry-air}$	DNS	Direct Numerical Simulation
y	Normal distance 1 st grid point from wall, m	EPS	Expanded polystyrene
y^+	Dimensionless wall distance	ET*	New effective temperature
Y_o	Observed value	HVAC	Heating, ventilation and air-conditioning
Y_p	Predicted value	IAQ	Indoor air quality
\bar{Y}	Arithmetic mean of observed values	ISO	International Organization for Standardization
z_o	Aerodynamic roughness length, m	LCC	Life cycle cost
τ_w	Wall shear stress, Pa	LES	Large eddies simulation
ψ	Efficiency of evaporative cooler	LHS	Latin hypercube sampling
α	Solar absorptance of external wall	NMBE	Normalized mean bias error
ε	Dissipation rate of kinetic energy, m^2/s^3	NV	Naturally ventilated
κ	von Karman constant	OAT	One-parameter-at-a-time
ρ	Air density, kg/m^3	PCC	Partial correlation coefficient
ρ_∞	Free stream air density, kg/m^3	PMV	Predicted mean vote
σ	Standard deviation	PPD	Predicted percentage dissatisfied
μ	Mean value	PSO	Particle swarm optimization
ΔP	Pressure difference across the opening, Pa	PTAC	Packed terminal air conditioner
ΔT	Indoor-outdoor temperature difference, $^\circ C$	RANS	Reynolds-Averaged Navier-Stokes
(u_n) and (u_t)	Normal and tangential velocity component at 1 st grid cell adjacent to the wall, m/s	RH	Relative humidity
$\sigma_k, \sigma_\varepsilon, C_\mu, c_{\varepsilon 1}, c_{\varepsilon 2}, \eta_\sigma, \beta$	Constants of turbulence model	RMSE	Root mean square error
		RNG	Renormalization group
		SA	Sensitivity analysis
		SET*	Standard effective temperature
		SRRC	Standardized Rank Regression Coefficients
		TDH	Total discomfort hours
		TEC	Total energy consumption
		TMY	Typical meteorological year
		TSEN	Thermal sensation
		TSV	Thermal sensation vote
		UA	Uncertainty analysis
		VND	Vietnam dong (monetary unit)
		WPC	Wind pressure coefficient

ABBREVIATIONS

AC	Air-conditioned
ACH	Air changes per hour
ASHRAE	American Society of Heating, Refrigerating and Air Conditioning Engineers
BPS	Building performance simulation

CHAPTER 1

INTRODUCTION

1.1 Global environmental issues and the sustainability movement

The severe environmental depression and energy crisis in recent decades have required significant changes of human behavior to the nature. The term "sustainable development" was first appeared in 1980 in "*World Conservation Strategy*" published by the International Union for Conservation of Nature and Natural Resources - IUCN (1980). According to this report, sustainable development can be understood as "the development of mankind cannot just focus on economic development but also to respect the essential social needs and the impact on ecological environment".

So far, the term "sustainable development" had been migrated from the conceptions of local ecosystem management to those of the global ecology. It has gradually been popularized in other scientific vocabularies such as economics, tourism, architecture, construction, urbanism...

Thanks to the Brundtland report (World Commission on Environment and Development, 1987), also known as report "*Our common future*", the term "sustainable development" has increasingly been used during the past two decades. This report clearly defined "sustainable development" as "*Development that meets the needs of the present without compromising the ability of future generations to meet their own needs... Sustainable development is not a fixed state of harmony, but rather a process of change in which the exploitation of resources, the direction of investments, the orientation of technological development, and institutional change are made consistent with future as well as present needs*" (World Commission on Environment and Development, 1987). In other words, a sustainable development has to ensure the effectiveness of economic development, social equality and environmental protection and conservation. To achieve these objectives, all economic - social sectors, governments, social organizations... have to harmoniously

control three main aspects: economy - society - environment. This term was once again reminded and emphasized in the United Nations Conference on Environment and Development (UNCED), held in Rio de Janeiro in 1992. The Rio Declaration stressed the importance of a balance between the three dimensions (see Figure 1-1):

- Environmental (protection of ecosystems and biodiversity, wise use of natural resources, fight against pollution, etc),
- Social (fight against exclusion and poverty, social equity, quality of life, public health, etc),
- Economic (cost-effective use of resources, etc).

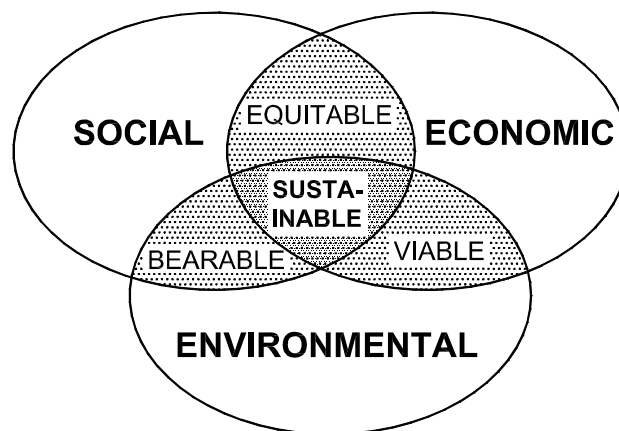


Figure 1-1: The three pillars of sustainable development (Liébard & de Herde, 2005)

Statistical data of different organizations have shown that building construction and operating activities consume approximately 30% of the total global energy in which the residential sector occupies an important part (see Table 1-1). Furthermore, buildings consume a huge amount of natural resources and consequently impose a burden on the environment during its life cycle.

A new mission which is challenging architects and engineers is how to resolve the actual building problems of effective use of energy and resources that are gradually running out, while ensuring occupant's comfort and affordable prices. Immediate actions of architects and engineers are therefore essential if we want to limit hazardous climate changes and environmental impacts. So far, sustainability has come in consciousness of architects and should become the most important concern during their professional works. The term "sustainable architecture" appears as a response of the building research and design community to apply the concept of sustainable development to architecture.

Table 1-1: Percentage of the final energy consumption used in commercial and residential buildings in 2004 (Pérez-Lombarda, et al., 2008)

Final energy consumption (%)	Commercial	Residential	Total
USA	18	22	40
UK	11	28	39
EU	11	26	37
Spain	8	15	23
World	7	16	24

Sustainable architecture is a subcategory of sustainable development and depends on environmental, socio-cultural and economic factors. The idea of sustainability addresses the need to meet our needs today while ensuring that our actions and decisions will not harm the opportunities of future generations. Sustainable architecture's stakes cover a huge area that encompasses political, scientific, technical, financial and human resources. However, sustainable architecture is often used as a generic term that describes only environmentally-conscious design and the usage of environmental techniques in the domain of architecture and urban design. In this sense, sustainable architecture looks for a comprehensive solution for a building to minimize its impacts on the environment through its design solutions and strategies such as architectural configurations, material use, energy use, occupancies, etc.

Considering the enormous responsibility of architects toward sustainability, the World Congress of Architect held in Chicago in 1993 by the Union of International Architects officially placed "sustainable architecture" in its agenda and in the congress declaration (UIA, 1993). The earliest effort to put this term into practice was observed in UK with BREEAM assessment criteria for green buildings in 1990. So far, many countries have had their own Green building standard such as: LEED in the U.S., GBTool in Canada, EcoProfile in Norway and Environmental Status in Sweden... In Vietnam, the first version of Green building assessment criteria was published in 2011 under the name "LOTUS".

In recent years, the appearance of many eco-friendly architectural trends in the world has demonstrated special attentions on sustainability of the design community. Sustainable architecture is not simply a modern trend, but actually an indispensable movement. Sustainable architecture has established firm relationships with many other sciences; thus an idea sustainable project requires not only the contributions of architects, engineers but also the participation of economists, sociologists, psychologists... among which architects must

play the key role. Figure 1-2 summarizes some specific targets of each dimension of sustainable architecture and some architectural design solutions. Dimensions, targets and solutions which are written in bold in Figure 1-2 are those studied in this thesis.

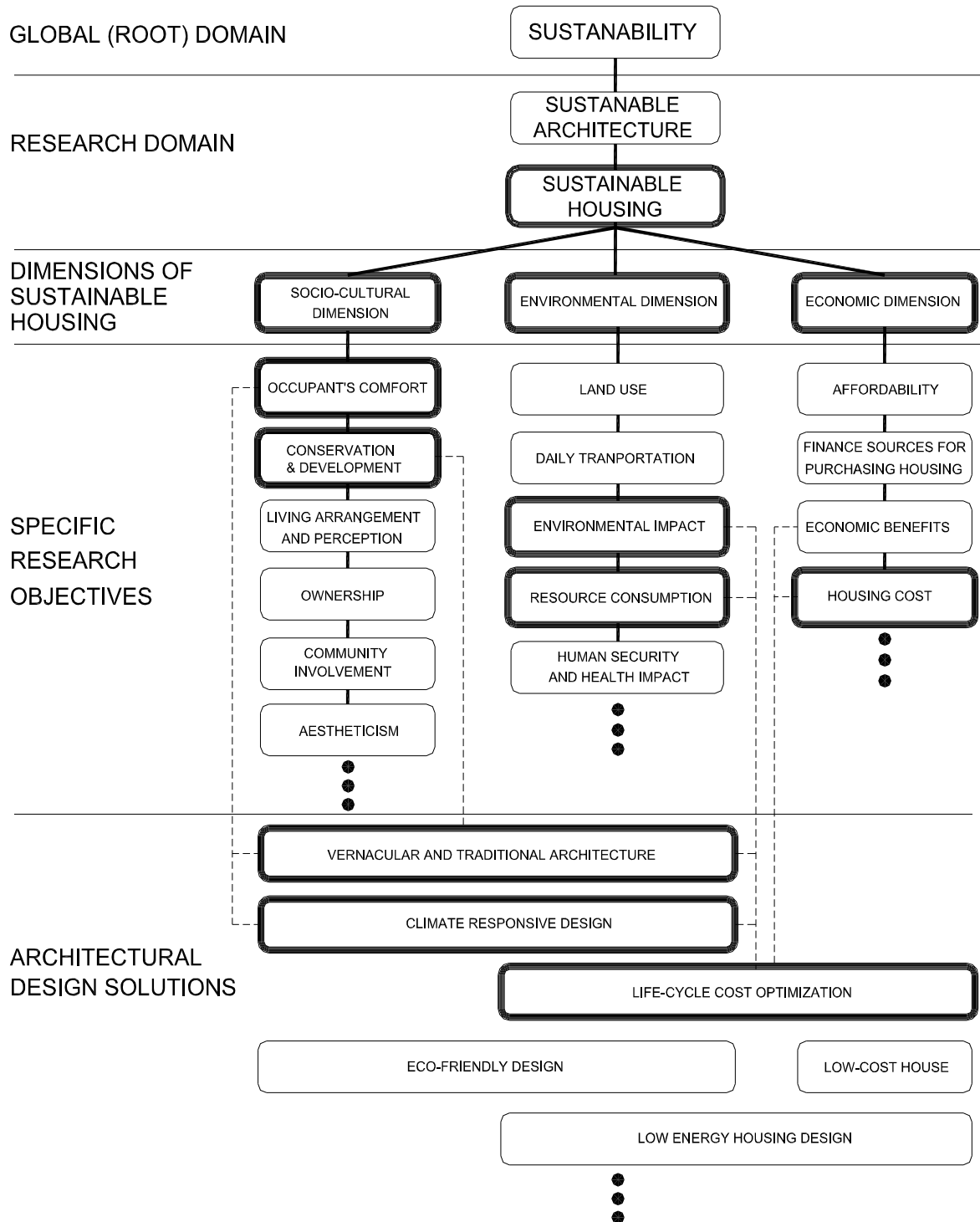


Figure 1-2: The hierarchy of sustainability in architecture

However, in most architects' thinking, the practice of sustainable architecture has largely been reduced to the issue of energy performance and building technologies (McMinn & Polo, 2005) whose importance in architecture is underestimated and considered as engineers' skills. This is due to the fact that architects are often lacking in knowledge of architectural and environmental sciences. Consequently, a gap between sustainability and the building design community does exist, especially for residential buildings. Most architects experience much difficulty in combining sustainability requirements with many other design constraints and criteria. To fill this gap, this thesis is aimed to develop design solutions towards sustainable housing in Vietnam based on a comprehensive approach.

The global aim of this research is to improve the quality of living environment and occupant's comfort while ensuring acceptable cost, reducing building energy consumption and minimizing adverse effects of buildings on the natural environment by promoting applications of advances in building science. This thesis cannot, of course, cover all the aspects of sustainable housing. Instead, it focuses on with the most sensitive aspect that challenges architects and engineers in Vietnam: climate responsive design strategies for human thermal comfort and energy savings. A study on vernacular and traditional housing in Vietnam will complement the socio-cultural aspect of this research and a life-cycle cost optimization will provide strategies towards affordable – comfortable housing in Vietnam.

Historically, the issue of climate responsive design has systematically been studied by the works of Victor Olgyay since 1950, then by his book (Olgyay, 1963) in 1963. So far, many studies conducted in developed countries have significantly enriched the knowledge of the building science and its applications (Givoni, 1969; Koenigsberger, et al., 1973; Liébard & de Herde, 2005). However, such studies for Vietnam are still rare² and very practical. As being based on latest advancements of modern building science and analysis methods, it is expected that this thesis will provide designers in Vietnam more opportunities to reach the targets of sustainable housing.

² In fact, researches on building science and applications in Vietnam are not quite rare, but most of them could only reach qualitative results rather than developing an analytical approach based on advanced building science. These researches are therefore considered insufficient and to some extent unqualified.

1.2 Housing issues in Vietnam - Identifying problems

Vietnam locates in the center of Southeast Asia, expanding from 9° to 23°20' North latitude and 102° to 110° East longitude. The territory of Vietnam covers 331212 km² of land, 3200 km length of the seashore and consists of 64 provinces, 609 districts and 10554 communes. Today, there are 54 different ethnic minorities inhabiting in Vietnam among which the Viet (or Kinh) ethnic group occupies 87% of the total population. Each ethnic group occupies their own living territory, language and culture, but living in harmony together. According to a 10-year national survey conducted by Government and General Statistics Office of Vietnam in April 2009, Vietnamese population was 85.8 millions, ranking third in Southeast Asia and 13th in the world. Sex ratio was 98.1 man/100 women. Approximately 70.4% of the population lives in rural areas. In the period from 1999 to 2009, average population growth-rate was 1.2% per year while urban growth was 3.4% per year and 0.4% per year in rural areas (CPHSC, 2010).

The poverty rate in Vietnam has gradually decreased since 1986 when the “liberalization process” of Vietnamese government was launched. However, it is important to quantify recent economic achievements in Vietnam. The rapid development of the country was based on a very low departure. As reported by World Bank, in 2008 GDP per capita of Vietnam (2787 USD – PPP method) was ranked 118 over 168 countries of the world (PPP takes into account the relative cost of living and the inflation rates of the countries, rather than using just exchange rates which may distort the real differences in income). Whether judged by any standards, GDP per capita income is very low and disparities between urban and rural areas are significant.

The recent economic progress has propelled the country to the ranks of lower-middle-income status, with GDP per capita of approximately 1024 USD in 2008 and 1411 USD in 2011³. A significant proportion of families is, however, still under the level of poverty or a little above it. As shows in Table 1-2, the monthly income per capita in 2008 in Vietnam was as low as 995200 VND (equal to 58.5 USD), while it is even much lower in rural areas.

³ Data available at <http://data.worldbank.org/indicator/NY.GDP.PCAP.CD> [Last accessed 11 Oct 2012]

Table 1-2: Monthly income per capita by urban and rural region - unit: 1000 VND (At exchange rate of 1USD \approx 17.000 VND) (CPHSC, 2010)

	2002	2004	2006	2008
WHOLE COUNTRY	356.1	484.4	636.5	995.2
Urban	622.1	815.4	1058.4	1605.2
Rural	275.1	378.1	505.7	762.2

About the living area, each Vietnamese averagely occupies 16.3 m² in 2008. This threshold is still well under the world average as well as achievements of other countries (around 30.0 m²/person in 2008 in urban China⁴; 43.6 m²/person in 2004 in Sweden; 33.7 m²/person in Belgium in 2001; 41.3 m²/person in Germany in 2001; 22.4 m²/person in Russia in 2009 and 22.5 m²/person in Ukraine in 2007⁵). However, this figure has been gradually improved by over 0.5 m² per year during recent years (see Table 1-3).

Table 1-3: Living area per capita by type of house, urban-rural region (Unit: m²)

	Type of house											
	Total			Permanent house			Semi- Permanent house			Temporary and other house		
	2004	2006	2008	2004	2006	2008	2004	2006	2008	2004	2006	2008
WHOLE COUNTRY	13.5	14.7	16.3	17.8	19.7	21.1	13.2	13.7	15.0	10.3	11.0	12.1
Urban	15.8	16.9	18.7	19.6	21.5	22.5	13.9	14.4	15.8	10.4	10.2	11.2
Rural	12.8	13.9	15.4	16.3	18.1	19.9	13.0	13.6	14.8	10.3	11.2	12.3

A permanent house is the largest investments of most Vietnamese families, requiring long-term saving and a great effort of the owners. Unlike the situation observed in most developed countries, Vietnamese people build their house with no loans from banks. If they cannot pay for the construction cost, they often ask their relatives for the loan or borrow money from informal services at extortionate rates.

The total construction costs in urban and rural areas in Vietnam differ significantly. It was estimated that a 120 m² private house in urban areas with acceptable quality might costs averagely 18000 USD (150 USD/m²)⁶ while in rural areas, people usually build their

⁴ Data available at <http://wenku.baidu.com/view/58a1768302d276a200292e91.html> [Last accessed 11 Oct 2012]

⁵ Data available at <http://www.stainfo.biz/Geomap.aspx?act=1762&lang=2> [Last accessed 11 Oct 2012]

⁶ Value estimated by the author

house within 5000 - 7000 USD (about 40 to 58 USD/m²)⁷ with various kinds of local materials. In most rural areas of Vietnam, people can well make their cement blocks, clay brick from clay soil, and thatch for roofing... themselves. Nevertheless, others materials such as cement, steel, steel sheets, roof tiles, doors and windows... have to be bought from commercial markets.

It is important to emphasize that housing quality and durability in Vietnam is a big issue, especially in rural areas. In 2008, according to the General statistics Office of Vietnam, nearly 80% of houses in rural regions were semi – permanent and temporary shelters (see Table 1-4). These houses are extremely vulnerable to natural disasters which occur very often in Vietnam (storm, typhoon, flood...). An international workshop has estimated that approximately 70% of houses in the coastal areas in central Vietnam has been replaced or renewed over the past 15 years. But the same proportion of these dwellings can only be classified as ‘semi-solid’ or ‘weak’, and thus is very vulnerable to damage (Kenedy, 2004).

Table 1-4: Percentage of house by housing condition, urban - rural area (CPHSC, 2010)

		Type of house in percentage								
Total		Permanent house			Semi- Permanent house			Temporary and other house		
		2004	2006	2008	2004	2006	2008	2004	2006	2008
WHOLE COUNTRY	100.0	20.8	23.7	27.8	58.8	60.3	59.1	20.4	16.0	13.1
Urban	100.0	38.7	41.4	46.2	52.4	51.3	48.4	8.9	7.4	5.5
Rural	100.0	17.4	17.0	20.6	61.0	63.7	63.3	24.3	19.3	16.1

Small residential buildings in Vietnam are usually built with a low investment rate without professional consultation. Larger housing projects were not fully investigated before groundbreaking as these projects are usually aimed to maximize the profit of investors rather than occupant’s comfort and conveniences. Consequently indoor comfort is entirely not ensured by the current design. In any third world countries, having a shelter is nearly a dream of life of the majority. Therefore, people may have some complaints about building services and quality whereas their evaluations on thermal comfort and indoor environment are virtually omitted.

⁷ Value estimated by the author

In the near future, as living standards are improving, housing issues and issues related to indoor comfort will be, of course, the leading concern of building occupants. Vietnam generally has a hot humid climate. Winter is always short and warm whereas summer is much longer and extremely unfavorable. On the other hand, in practice most residential buildings are naturally ventilated (NV), thus the indoor environment is often free-floating along with that out of doors. In such conditions, some significant questions and issues have emerged:

- (1) whether the current design of residential buildings can provide indoor comfort;
- (2) which design strategies can improve thermal comfort;
- (3) about the efficiency and applicability of these solutions.

Research on these housing issues, especially housing issues of the poor - the most vulnerable class - will be very practical and could have significant social impacts in Vietnam. This thesis therefore focuses on resolving the issue of human thermal comfort in NV dwellings which are common shelters for most low-income classes in Vietnam. In a little further extent, it also deals with initial construction cost, energy consumption and life cycle operating cost of air-conditioned (AC) residential buildings.

1.3 Research objectives

The global objective of this thesis is to develop design strategies toward comfortable, environmental-friendly, energy-saving buildings at acceptable building cost. The solutions achieved have to be adapted to the context of Vietnam through the effective use of building materials, the great attention to climate responsive design and intelligent combination of various design parameters. All solutions must consistently satisfy requirements of sustainable development.

To obtain this target, the following specific aims need to be achieved:

- Good understanding of the thermal comfort condition of Vietnamese, corresponding to each climatic region, by using both predictive models and field surveys on thermal comfort;
- Identifying strengths and weaknesses of the current housing design in Vietnam through an investigation on thermal performance of the current housing stock;
- Discovering our ancestors' wisdom underlining the design principles of traditional and vernacular architecture and their applicability in modern housing development;

- Developing passive solutions to improve thermal performance of the current design, based on required thermal conditions for Vietnamese; and quantifying the effectiveness of these solutions;

- Successfully providing general guidelines and recommendations for housing design towards comfortable and sustainable architecture.

Moreover, this work aims to provide valuable materials for academic purposes. Furthermore, as being shown in the conclusions, the results of this thesis can be refined to provide general guidelines and recommendations for direct applications in building design. Intrinsically, the author expects that the analytical approach of this thesis can be combined with the creative aspects of design to develop more aesthetic, comfortable, affordable, energy conscious, secure and healthy built environments.

1.4 Research hypotheses

The above-mentioned objectives are based on a global hypothesis according to which the common housing design in Vietnam can be improved to provide better thermal comfort and to consume less energy. The solutions obtained will be a consistent response towards sustainable housing in Vietnam. Other research hypotheses are also outlined below.

The 1st hypothesis: Many studies have pointed out that thermal conditions required for human comfort in NV buildings are not quite similar to those in climate-controlled environment. On the other hand, people in developing countries in hot and warm climates are believed to be acquainted with long-term warm conditions and may have lower comfort expectation. As a result, their preferred thermal conditions might differ considerably from what have been prescribed by international standards of thermal comfort. This research therefore hypothesizes that Vietnamese people living in NV buildings have specific thermal preferences and thermal comfort conditions. These conditions need to be defined.

The 2nd hypothesis: This research hypothesizes that common design of residential buildings in Vietnam have failed to provide appropriate indoor thermal conditions so that a major part of occupants would be thermally satisfied. It means that the thermal performance of the current housing stock needs to be improved and housing design methods should be subject to modifications and supplementations.

The 3rd hypothesis: Architectural design and occupancy strategies play an important role in protecting building occupants from disadvantageous effects of the climate and

creating favorable indoor environment through various strategies: natural ventilation, building shape, building orientation, sun shading, humidity control, thermal insulation, thermal mass and ventilation control... It is therefore hypothesized that some climate responsive solutions can effectively ameliorate the thermal performance of the current housing stock in Vietnam.

The 4th hypothesis: Traditional - vernacular architecture has been developed over the centuries and is the result of much trial and error. It is generally true to say that traditional - vernacular architecture underlines many effective passive design principles, reflecting excellent knowledge of our ancestors about the climate, natural environment and local cultural institution. This thesis hypothesizes that traditional - vernacular architecture, in general, or specifically vernacular housing in Vietnam is also able to provide valuable lessons for current development and therefore needs to be considered.

The 5th hypothesis: The basic characteristic of the climate of Vietnam is hot and humid. The weather often reaches extreme conditions, e.g. very hot and humid (over 35°C and RH of 75% - 90%). Such a climate type requires indoor environment to be sometimes fully controlled by mechanical systems to ensure thermal comfort. It is hypothesized that design and occupancy strategies derived by using the optimization method are capable to minimize building energy consumption and thus environmental impacts, to maximize thermal comfort and to minimize the construction and operation costs. The optimization method is able to shift the optimal houses into some sustainable building categories, e.g. net-zero energy houses or passive houses, defined in some guidelines and standards.

1.5 Limits of the research

Sustainability and sustainable housing is considered as a large research domain. To ensure quality and clarity of the research, this thesis needs to be concentrated on its specific objectives and hypotheses as described above. The research domain of this thesis will be limited to and excluded some specific aspects as follows:

- Indoor thermal comfort is the main subject of this research. Other occupants' comfort related issues such as indoor air quality (IAQ), visual and acoustic comfort are assumed independent from thermal comfort and are not included in this work.

- This thesis with only focus on passive design strategies that can be controlled by architects during the design phase and by building users in the occupancy phase. Other active methods used in building design such as the design and operation of HVAC systems will not be treated intensively, because it should be out of the scope of this research.
- Only residential buildings, particularly low-rise apartment buildings, low income residential buildings and private dwellings are the subjects of this research. Other building types (e.g. commercial buildings, office buildings, industrial buildings, educational buildings, etc...) are not included in this work.
- This research only conducts investigations on the building-scale issues, e.g. the building design and operation, the indoor micro-climate; it deliberately overlooks other urban-scale issues such as urban morphology and arrangement, urban design and landscape design.

As can be seen in the practice, most residential facilities in Vietnam are NV to favor the advantages of the tropical climate. The research will therefore mainly give discussions on NV buildings which is the most common building type for low income inhabitants. AC buildings will also be mentioned, but with more limited frequency and content.

1.6 Structure and methodologies of the thesis

Figure 1-3 graphically illustrates the workflow of the research. The major steps, methods used, research objectives, final results and reciprocal relationships are shown. The main modules in this figure, which are the kernels of this research, are constituted by the author's peer-reviewed publications. This figure shows a very consistent research target (thermal comfort – thermal performance of the building) and the results will be obtained by using the *inductive method* - also called the *scientific method* that starts with many observations of nature (practice), with the goal of finding a few, powerful statements about how nature works (laws and theories). More specifically, this research is based on intensive surveys and examinations on a number of case-study dwellings (e.g. vernacular dwellings, contemporary dwellings, a generic single-zone housing model, results from literature) under typical climate patterns of Vietnam from which findings and general design

recommendations are derived. It is therefore essential to note that more observations from other variants will further consolidate the findings of this work.

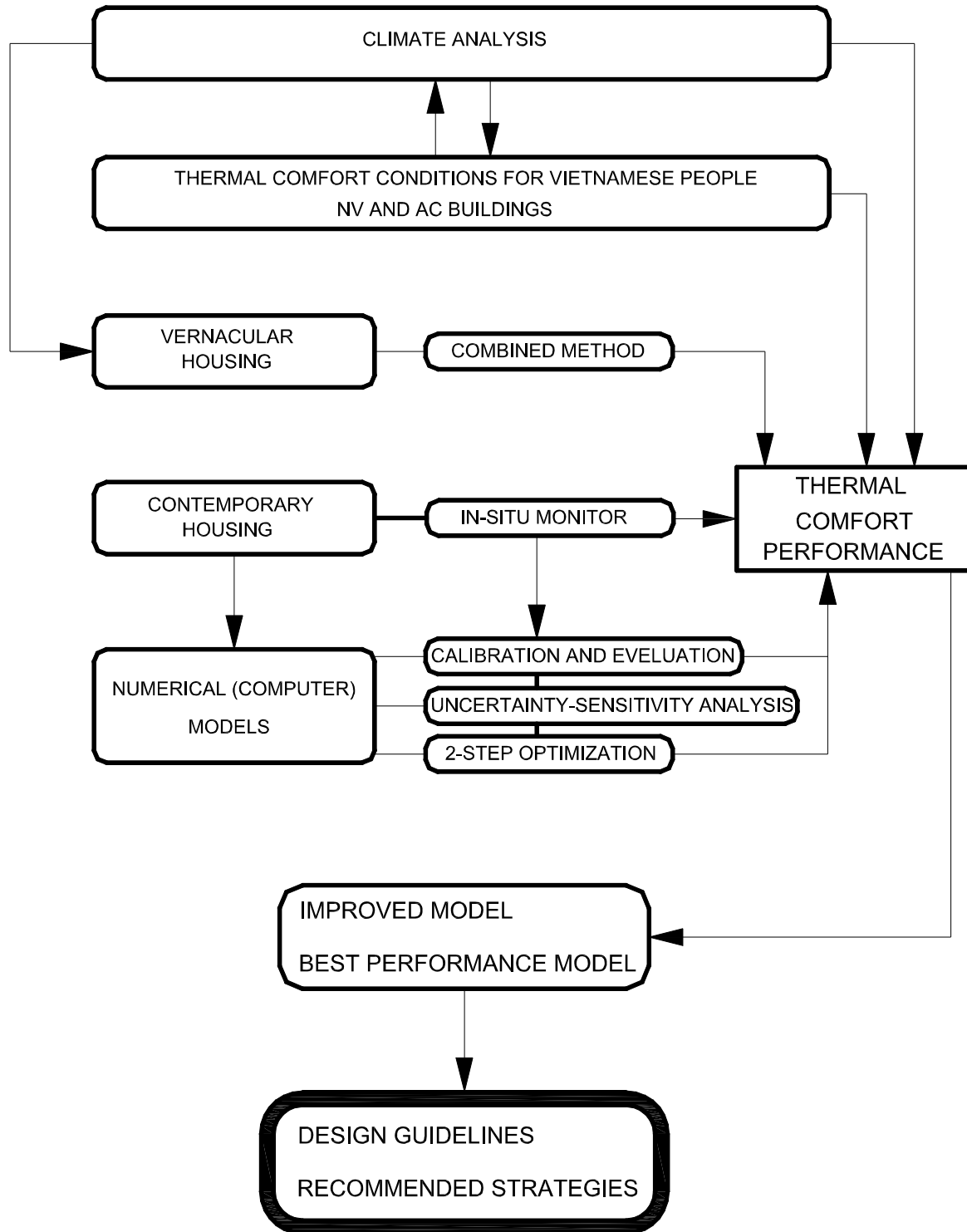


Figure 1-3: The workflow of the thesis

This thesis is constituted by 9 chapters. Summary of the content of the remaining chapters are described as follows:

Chapter 2: This chapter reports the state of the art of sustainable housing, climate responsive architecture, its applications in housing design and human thermal comfort. This chapter gives an idea of the general development and latest advancements in this research domain based on which the research methodology of the thesis is established.

Chapter 3: This chapter develops a thermal comfort model applicable for Vietnamese people. The model is based on the adaptive theory in thermal comfort, which is usually used to explain the deviation between predicted thermal sensation votes by analytical theories and actual thermal sensation votes in NV buildings. The choice and implementation of comfort models for two building types, namely NV and AC buildings, are defined. Many other comfort related issues are also discussed.

Chapter 4: In this chapter, the climates of Vietnam are first described and categorized into three major climatic regions. A new simple climate analysis tool is developed in order to analyze the climate of these 3 regions and to draw preliminary design guidelines. This tool is also applied in CHAPTER 6 to evaluate thermal comfort of some indoor conditions. The “performance of the climate” is also presented and its application is explained.

Chapter 5: Three most common housing prototypes are identified and case-study houses are selected. Afterward this chapter presents a comprehensive framework through which thermal performances of 3 typical housing types are derived. Various techniques, including in situ monitoring, building thermal simulation, CFD and airflow network model, numerical model calibration are employed to obtain the results. Results of these studies provide the reference thermal performances for further improvements.

Chapter 6: This chapter presents a comprehensive investigation on climate responsive design strategies applied in vernacular housing in Vietnam. The investigation employs both qualitative and quantitative assessment methods. The study to some extent reveals the remaining value of vernacular housing and provides valuable lessons for modern applications.

Chapter 7: Based on the thermal models and CFD models of the case-study houses, this chapter uses the parametric simulation method to improve the thermal performances of these houses and thermal comfort by natural ventilation. Performances of the improved

cases are compared with the reference performances obtained in CHAPTER 5. The efficiency of the parametric simulation method is also defined.

Chapter 8: This chapter is divided into two parts. In the first part, the Monte Carlo-based sensitivity analysis method is used to quantify the impact (sensitivity) of design parameters on the thermal performance of the houses. Parameters that have highest impact on the building performance are selected for the next step. In the remaining part, the thermal performances of the reference cases are optimized using the simulation-based optimization method. Optimization results show the best design for each climatic region. The performances of the optimal solutions are compared with the references, providing an insight of the efficiency of the optimization approach in building design. The chapter also gives many discussions on the results obtained and compares them with the results found in the literature.

Chapter 9: This chapter summarizes the different objectives yielded in this thesis and provides general design recommendations for different climate regions in Vietnam. It also outlines limitations and possible future extensions of this thesis through new researches.

CHAPTER 2

LITERATURE REVIEW

This chapter provides an up-to-date overview of recent research advancements related to climate responsive architecture and human thermal comfort in built environments. The aim of this chapter is to thoroughly identify the aspects that have been successfully clarified by other authors and problems that need to be studied, especially those related to Vietnam and Vietnamese people. On this basis, the specific challenges of this research will be outlined.

2.1 Literature review on the bioclimatic approach in architecture

2.1.1 Terms and definitions

Since the first appearance of the term “*bioclimatic approach*” in architecture (Olgay, 1963), building design according to biological and climatological principles has been emerging as a strong movement towards sustainable development. In the original definition (Olgay, 1963), the term “bioclimatic approach to architectural regionalism” emphasizes the importance of the interactions of *living organisms* and the *local climate* through the form and fabric of the *building*. To solve the challenge of climate control in a systematic way, the effort of several sciences is required. The first step is to define and estimate a condition within which a normal person will find comfortable. For this challenge, the answer almost lies in the field of biology. In the second step, the science of climatology has to provide necessary information on the local climate. Finally, a rational architectural solution is proposed based on the engineering sciences (Olgay, 1963).

Climate responsive design strategies are simply the concretization of the bioclimatic approach in building design practice. Today, climate responsive design has become a cornerstone to achieve more sustainable buildings. Climate responsive design principles are

therefore necessary for building design practice as a starting point for architectural conceptions with the climate in mind.

In recent years, there has been a raising concern on sustainability among the building research community and design professionals. Research using the bioclimatic approach has taken a new form of passive low energy architecture and has been carried out worldwide, with a well-developed field. The passive and low energy architecture (PLEA) conference series⁸ is an explicit evidence for such a trend (Hyde, 2008). In housing research and development, some new terminologies have been developed to refer to these new building concepts. “*Eco house*”, “*passive house*”, “*energy-efficient building*”, “*carbon neutral building*”, “*zero energy building*”, “*green building*”... are some examples of the innovative responses to sustainability. Although the design of such building types requires many integrated design tools and methods (e.g. building simulation method), it is important to acknowledge that these new concepts are primarily relied on passive design features of the building form and fabric as a major measure to attain the targets. Hence, the bioclimatic approach in architecture has never lost its important role in building design practice.

2.1.2 Bioclimatic architecture - conventional methods and novel approaches

The origin of the bioclimatic approach can be traced back to the design principles applied in most vernacular and traditional buildings all around the world. Vernacular and traditional architecture evolved over time to reflect the environmental, cultural, technological, and historical context of a specific location in which it was built. Hence, climate responsive design knowledge was accumulated in vernacular architecture during an ‘evolutional’ process.

It was during the year 1930s that the concept of “organic architecture” was founded by a famous American architect – Frank Lloyd Wright. The philosophy of “organic architecture” lies in designing structures which are in harmony with humanity and its environment. At that time, the works of Wright was a “declaration of war” against the modernism in architecture which was being spread throughout the world.

It seems that the first academic publication on the issue of climate responsive architecture was published by Aronin (1953). Nevertheless, the first work that had strong

⁸ See <http://plea-arch.org> for further information

reputation in academic research was published in 1963 (Olgay, 1963). In his work, Olgay established the foundation of the bioclimatic approach which was mainly relied on the bioclimatic chart invented for U.S. moderate zone inhabitants (see Figure 2-1). The bioclimatic chart was used as a tool to analyze the climates of various regions in the U.S. and finally the findings were interpreted into architectural design principles and applications. In his book, Olgay also developed design principles and examples for 4 climatic regions in the U.S. The greatest contribution of Olgay can be seen as the pioneer scholar who systematically integrated the concept of human thermal comfort in climate assessment and in building design.

Givoni (1969) was the next notable scholar in the effort to develop an innovative design method using the bioclimatic approach. Different from Olgay, he developed the building bioclimatic chart on the psychrometric chart which was then widely used in building research (see Figure 2-1). On this psychrometric chart, all thermodynamics processes of moist air could be reproduced, allowing him to outline potential control zones of various passive design strategies. His work also presented a comprehensive review on architectural sciences and provided a number of design guides for 3 common climatic types in the world. It can be said that both the works of Olgay and Givoni basically set fundamental frameworks for next studies on climate responsive architecture.

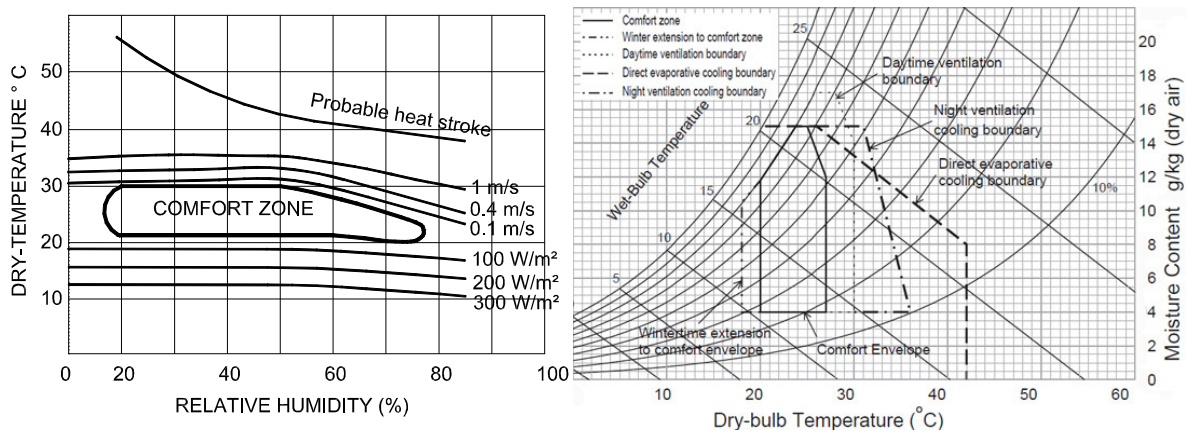


Figure 2-1: The building bioclimatic chart of Olgay (left) and Givoni (right)

Using the similar approach, several authors (Koenigsberger, et al., 1973; O'Cofaigh, et al., 1996; Givoni, 1998; Roaf, et al., 2001; Szokolay, 2004; Liébard & de Herde, 2005) also thoroughly reviewed recent advances of the architectural science and then developed

their design guides for different climatic regions based on their experience and the abundant available literature.

However, there have been some crucial questions which challenge both the building professional and the client during the design process of a ‘high performance’ building, e.g. how much comfort will the building provide without HVAC systems? When and how long will the peak overheating occur? What are the peak heating or cooling loads? How much electricity will the building consume in a year? Using the methods developed by the authors mentioned above, such questions can only be answered qualitatively. Due to many strict design requirements of ‘high performance’ buildings, these questions need to be answered thoroughly with satisfactory accuracy and details. **Numerical modeling and simulation of building performance have emerged as a novel bioclimatic approach which is able to satisfy these requirements in relatively shorter time.** Building simulation can also take into account the simultaneous variations of the local weather as well as different scenarios of the building occupancy (Hyde, 2008). A building simulation program can be used as design advice, a testing tool, a fine-tuning tool, a verification/assessment tool, a diagnostic tool, etc.

It is therefore obvious that the simulation method has an increased role in building research and design practice. In response to this trend, the book on bioclimatic housing of Hyde (2008) presents a number of new ideas and applications of the simulation method in building design practice. Particularly, with the raised concern on energy consumption, Hyde proposed to redefine the terminology “bioclimatic housing” according to which “*energy efficiency*” is now considered as the central issue in the design of more efficient building systems, rather than examining on thermal comfort and passive elements of a building. This means that climate responsive architecture is now a part of the whole solution to achieve the zero carbon target (or energy-efficient buildings). The work of Hyde is a typical representative of the design trend in the computer-based era.

Since the year 2000, some authors have paid more attention on the sustainable aspect in the built environment (Smith, 2005; Bay & Ong, 2006; Glicksman & Lin, 2006; Santamouris, 2006). These works have shown efforts in exploring a new challenge in building design which attracts many research communities. In any case, the passive design principles are always an important part of the synthesized solution.

2.1.3 Classification of bioclimatic research methodologies

By following the “flow” of time, the author found that the development of the bioclimatic approach can be divided into 3 separated periods corresponding to 3 design methods. Table 2-1 summarizes characteristics of these 3 major bioclimatic approaches in building design. The numerical modeling and simulation approach shows a number of capabilities which result in broader applications than the previous approaches.

Table 2-1: Three major bioclimatic approaches in the evolutionary order

	Empirical approach	Analytical approach	Numerical modeling and simulation approach
Estimated effective period	Until the year 1950s	1930 - present	1990 - present
Comfort assessment method	Rules of thumb	Building bioclimatic chart	Standards and codes (thermal comfort model, natural lighting code, IAQ code)
Climate analysis method	Observation	Discrete statistical weather data	TMY weather file
Design objectives	Human comfort and health	Human comfort and health	Human comfort and health Energy consumption Environmental impact
Performance verification method	Trial and error	Monitoring and comparison	Numerical simulation
Diagnostic method	Trial and error	Trial and error, monitoring and analysis	Numerical simulation
Applications and products	Vernacular housing, traditional building	Comfortable building	Energy-efficient building Zero energy building Green building Comfortable NV building

Along with recent advancements in the computer science, research on climate responsive architecture using the 3rd approach has been growing rapidly, continuing to feed recent researches (Wang & Wong, 2007; Singh, 2010; Nguyen, et al., 2011; Nguyen & Reiter, 2012c; Nguyen & Reiter, 2013) and the results can satisfy different research and practical purposes. The numerical modeling approach explicitly shows a great potential in building research and design practice.

2.1.4 The challenges in Vietnam

As many other countries, vernacular housing in Vietnam has illustrated valuable examples of the harmony between the nature and manmade structures (Nguyen, et al.,

2011). Research on building physics, especially the relationship between architecture and climates, has been carried out in Vietnam since 1960. In 1966, some books on the issue relating climates and architecture appeared. However, until 1980, the first academic result which discussed the problem in a systematical way was published in the book “Building Physics” (Pham, et al., 1980). The book carefully describes most basic questions in building physics and applies these to solve some specific problems of building design in Vietnam. After that, some other scholars further studied the climate aspect in architecture (Pham, et al., 1998; Hoang, 2002). In a recent book Pham (2002) mentioned specifically the bioclimatic approach and its potential applications in Vietnam. His effort was to develop a building bioclimatic chart for Vietnamese based on which the climates of Vietnam could be analyzed and the design strategies for each region were proposed. Intrinsically, the method of Pham was mostly relied on the materials and methods that were developed by foreign authors (Givoni, 1969; Watson & Labs, 1983). In general, the principles developed by these authors can be applied in theoretical research and among design professionals, but they are, so far, not able to meet many sophisticated requirements of new building standards and codes such as “Lotus 2011” – the first green building rating tool for Vietnam.

It is therefore essential to re-examine the climate responsive design principles for Vietnam by using a stronger, more reliable and more comprehensive approach. The benefit of such an approach is not only seen in building design practice but also a solid contribution to the architectural theory of Vietnam which is included in the global objective of this thesis.

2.2 Literature review on human thermal comfort in built environments

2.2.1 Thermal comfort and its role in built environments

Comfort designates “*a state of physical ease and freedom from pain or constraint*”⁹ by any factor of the environment. According to ASHRAE (2004), **thermal comfort** is defined as “*condition of mind which satisfaction is expressed with the thermal environment and is assessed by subjective evaluation*”. It emphasizes that the judgment of comfort is a cognitive process involving many inputs influenced by physical, physiological, psychological and other factors.

⁹ Oxford online dictionary: <http://oxforddictionaries.com> (Last accessed Feb 2013)

Thermal comfort is a key issue in building science that has a profound influence on how we design and operate a building, on the energy needed to heat or cool it and on the quality of both natural and built environments (Brager & de Dear, 1998). Because of the large physiological and psychological variation from person to person, it is not possible to create a thermal environment that can satisfy everyone in a space. However, based on statistical results of intensive laboratory works and field experiments, it is now feasible to create a condition that can satisfy a certain percentage of occupants (ASHRAE, 2004). In the built environment, there are six primary factors that affect thermal sensation of an occupant, including: **dry-bulb air temperature, radiant temperature of surrounding surfaces, air humidity, air velocity, his/her metabolic heat production and clothing insulation**. Besides, the subjective thermal perception may vary from person to person due to differences of sex, age, adaptation, seasonal and circadian rhythms and many other factors.

Although thermal comfort is one among the research objectives of human physiology, it has recently gained a great attention of building scientists because thermal comfort standards are required to help architects and building engineers to define an indoor environment in which a major part of building occupants will find thermally comfortable. Thermal comfort is therefore directly related to the issue of occupants' satisfaction, health and productivity. Furthermore, the comfort range given by a thermal comfort standard is usually used to establish the HVAC thermostat in AC buildings. Consequently, thermal comfort significantly influences the amount of building energy consumption and thereby the environmental impacts of a building system.

2.2.2 Human thermal regulation mechanism

Human thermoregulation:

Temperature in the core of a human body is always kept in a very small range around 37°C. A small change of this temperature may cause a lot of physiological reactions. Temperature of the brain at rest is about 36.8°C. It will rise up to 37.4°C when walking and almost higher when jogging up to 37.9°C (ASHRAE, 2009).

The hypothalamus located in the brain is the central control organ for body temperature. It has hot and cold temperature sensors and it is completely embedded into arterial blood. The hypothalamus receives thermal information mainly from the blood and

partly from the skin temperature sensors as well as other parts of the body (Hensel, 1981). The most important mechanism of controlling body temperature is the regulation of blood flows to the skin. When the internal temperatures rise above a ‘setpoint’, more blood will be directed to the skin, diffusing heat to the surrounding environment. Conversely, the skin blood flow decreases to preserve heat. If the body is put in a state of extreme heat loss, muscle tensing and shivering will happen to produce supplemental metabolic heat which may reach 260 W/m^2 (compared with 60 W/m^2 for a seated person). As internal temperature is elevated, sweating will occur. According to Givoni (1969), for a man working in the heat, sweating rate can reach 1 liter per hour. In a very hot environment, it can achieve 2.5 liters per hour. Assuming that latent heat of evaporation of water is 2270 kJ/kg , one kilogram of sweat evaporation in one hour can provide a heat dissipation rate of $2270 \text{ kJ} / 3600\text{s} \approx 0.63 \text{ kW}$.

Heat balance:

The means by which a human body exchanges heat with surrounding environment consist of: evaporation, radiation, convection and conduction. The heat production and heat exchange processes are illustrated in Figure 2-2.

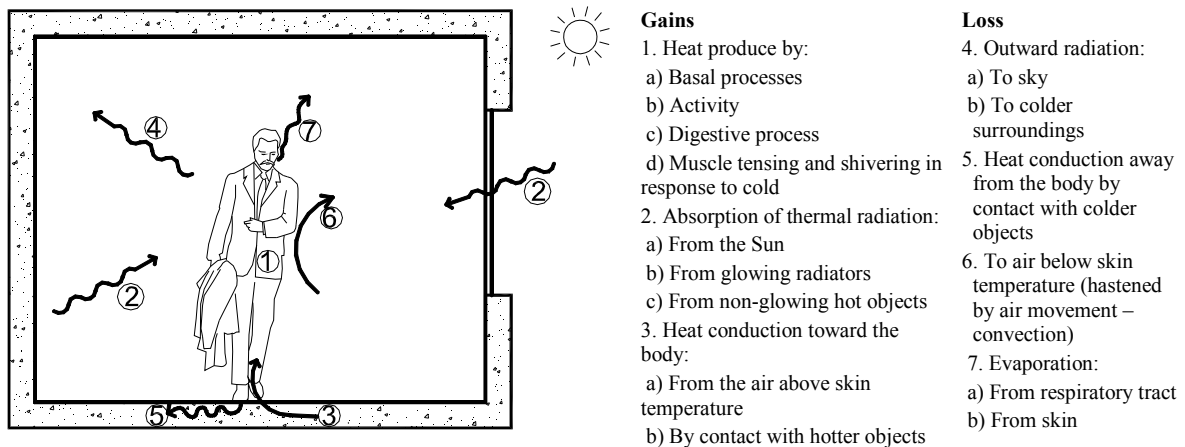


Figure 2-2: Heat exchange between man and his environment

Heat production in a body is the result of the metabolism process through which components of digested foods is oxidized in cells, generating energy required for the functions of various organs in the body (i.e. the contraction of muscles during work, the involuntary activities of the internal organs: heart work, respiration, digestion) and maintaining the body temperature stable. It is unusual if more than 5 - 10% of this energy production is used for mechanical work done by the muscles (Nishi, 1981). Hence metabolic

activities result almost in heat that must be continuously dissipated and regulated to maintain normal body temperatures (ASHRAE, 2009). Even when the body is completely at rest and in warm surrounding, its heat production does not fall below a certain minimum lever – the basal metabolism – usually taken as about 85W for an average person. This figure raises to 117 W for sedentary activities, to 223 W walking 3.22 km/h, to 323 W walking 6.4 km/h, and to 880 – 1400 W at maximum exertion.

The mechanism of heat balance between a human body and the environment can be expressed in a mathematical equation as shown in Figure 2-3.

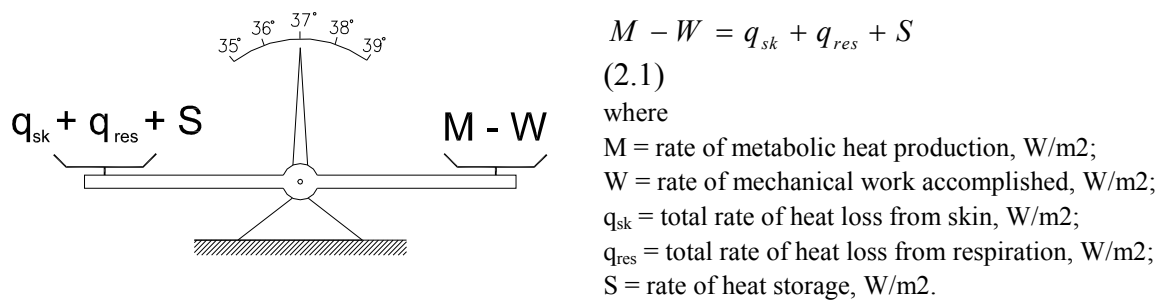


Figure 2-3: Heat balance mechanism and body temperature

In this figure, for some reasons W is usually assumed to be zero in most thermal comfort calculation (ASHRAE, 2009). In a normal condition, this balance is maintained by the human thermoregulation. This natural mechanism and some personal adaptations can help man to feel thermally comfortable within a range of about $\pm 1.7^{\circ}\text{C}$ to $\pm 2.5^{\circ}\text{C}$ around the optimal comfort temperature. Under unfavorable conditions unbalance occurs, resulting in excessive heat gain/loss which in turn results in hot or cold thermal sensation. Thus the most important questions of thermal comfort in built environment are: (i) what is the optimal condition for occupants’ thermal comfort; and (ii) how to predict the thermal sensation if thermal unbalance occurs.

2.2.3 Comfort temperature in climate-controlled environments

Rohles and Nevins (1971) carried out a comprehensive thermal comfort survey on 1600 college-age students in the U.S. These subjects were asked to stay in a climatic chamber during 3 h, doing sedentary tasks and wearing 0.6 clo clothing. Ambient humidity was kept around 50%. The preferred temperature of both male and female subjects was 25.6°C .

Fanger explored the influence of different cold climatic experience of different Danish subjects: normal college-age students, winter swimmers and meat packers from a refrigerated storeroom. Although these experiments were conducted in different periods in 1970s, the same experimental procedure was imposed (sedentary activity, 0.6 clo clothing, 3 h exposure in the chamber). Fanger found that these three groups almost have the same preferred temperature of about 25.0°C to 25.7°C (Brager & de Dear, 1998).

To examine the effect of acclimatization on the thermal preference, Fanger (1970) conducted a thermal comfort experiment on 16 long-term tropical people right after their arrival in Copenhagen airport. Under the same experimental procedure, preferred temperature of this group was 26.2°C, slightly differing from 25.5°C. In addition, de Dear et al. (1991) performed an experiment on 32 Singaporean students under hot and humid conditions of Singapore. They found that the upper limit of the acceptable comfort zone at 70% humidity was established at 27.6°C.

Chung and Tong (1990) investigated the thermal comfort of 134 college-age Chinese subjects in the warm humid climate of Hong Kong. These subjects were exposed under sedentary activity for 3h to several different thermal conditions while they were wearing 0.6 clo standard clothing. Their neutral temperature was observed at 24.9°C and the neutral zone was found to be between 22.2°C and 25.2°C.

Tanabe et al. (1987) carried out a thermal comfort survey for 172 Japanese college-age students under hot and humid weather of Japan in a climatic chamber. The same experimental procedure of other authors was imposed. They found that the neutral temperature of Japanese subjects was 26.3°C, slightly higher than American and Danish subjects.

The consistent results of these experiments strongly confirm that preferred or neutral temperature of a man (wearing standard clothing at sedentary activity and moderate humidity) was around 25.5°C to 26°C. This range seems identical throughout the world, regardless of the differences in climates, ethnic groups and cultural context.

2.2.4 Thermal comfort prediction in actual built environments

The significance of thermal comfort issue in building research has promoted many studies on thermal comfort in both experimental environment and “real-world” conditions. These studies resulted in a number of thermal comfort prediction models, both

deterministically and empirically. Most of the recently-developed models as well as field surveys often evaluate occupants' thermal sensation one of the two 7-point thermal sensation scales from ASHRAE and Bedford as reported in Table 2-2.

Table 2-2: ASHRAE and Bedford thermal sensation scales

ASHRAE scale		Bedford scale	
+3	Hot	7	Too much warm
+2	Warm	6	Too warm
+1	Slightly warm	5	Comfortably warm
0	Neutral	4	Comfortable – neither cool nor warm
-1	Slightly cool	3	Comfortably cool
-2	Cool	2	Too cool
-3	Cold	1	Too much cool

The ASHRAE sensation scale is used more frequently than the Bedford scale. However, thermal comfort evaluations based on the ASHRAE scale must be assumed that the perceptions of thermal comfort and thermal sensation vary on the same scale (i.e. occupant's vote at zero on ASHRAE scale means he/she is thermally comfortable) although in practice, this assumption is not always true (Wong, et al., 2002).

2.2.4.1 Empirical models

Empirical models are usually built on results of field surveys. Based on some studies on 1600 college-age American students (Rohles & Nevins, 1971; Rohles, 1973), some correlations between thermal sensation votes (TSV) on the ASHRAE scale, temperature, humidity, sex, and length of exposure were established as shown in Table 2-3. The regressions equations reveal that about a 3°C change of temperature or a 3 kPa change of vapor pressure is needed to create a deviation of the TSV by 1 unit.

To see the deviation of thermal perception of subjects in different regions over the world, a comparison of the results of various studies has been done as shown in Table 2-4. It should be noted that all these results were obtained from experiments conducted in climate chambers where environmental conditions were stringently controlled. It can be seen that neutral temperature of these groups of subjects were similar and the differences were not statistically significant. Similar regression coefficients of these equations indicate that these groups of subjects had the same sensitivity to temperature changes. With these empirical equations, it is quite simple to predict people's thermal sensation if the ambient temperature is known.

Table 2-3: Thermal sensation prediction by temperature and humidity (adapted from (La Roche, 2012))

Exposure period, h	Subjects	Regression equations
1h	Man	$TSV = 0.220T_i + 0.233p_w - 5.673$
	Woman	$TSV = 0.272T_i + 0.248p_w - 7.245$
	Both	$TSV = 0.245T_i + 0.248p_w - 6.475$
2h	Man	$TSV = 0.221T_i + 0.270p_w - 6.024$
	Woman	$TSV = 0.283T_i + 0.210p_w - 7.694$
	Both	$TSV = 0.252T_i + 0.240p_w - 6.859$
3h	Man	$TSV = 0.212T_i + 0.293p_w - 5.949$
	Woman	$TSV = 0.275T_i + 0.255p_w - 8.622$
	Both	$TSV = 0.243T_i + 0.278p_w - 6.802$

where T_i is dry-bulb air temperature, °C; p_w is partial water vapor pressure, kPa; TSV is thermal sensation vote on the ASHRAE scale; subjects with sedentary activities, wearing clothing with thermal resistance of 0.5 clo, in still air; mean radiant temperature is equal to air temperature.

Table 2-4: Sensation prediction and neutral temperature of different groups of subjects

	Sex	Number of subjects	Regression equations	Neutral temperature, °C
College-age Japanese (Tanabe, et al., 1987)	Both	172	$TSV = 0.3448T_i - 5.080$	26.3
	Man	84	$TSV = 0.3663T_i - 5.821$	26.8
	Woman	88	$TSV = 0.3130T_i - 4.337$	25.8
College-age Danish (Fanger, 1970)	Both	128	$TSV = 0.3048T_i - 3.836$	25.7
	Man	64	$TSV = 0.3907T_i - 5.963$	25.5
	Woman	64	$TSV = 0.2109T_i - 1.709$	26.1
College-age American (Rohles & Nevins, 1971)	Both	720	$TSV = 0.3376T_i - 4.625$	25.6
	Man	360	$TSV = 0.3735T_i - 5.678$	25.9
	Woman	360	$TSV = 0.3019T_i - 3.574$	25.1

T_i is dry-bulb air temperature (equal to mean radiant temperature)

TSV is thermal sensation vote on the Bedford scale

The thermal comfort standard 55 of ASHRAE has been periodically evolved on a 12-year cycle. The version 2004 (ASHRAE, 2004) introduces a simple graphical method to assess an environmental condition by giving a comfort zone on the psychrometric chart (see Figure 2-4). According to this method, the comfort zone (zone with inclined hatch patterns) may be varied due to changes of clothing and wind velocity. The building bioclimatic charts of Olgyay (1963) and Givoni (1969) presented in Figure 2-1 were the alternative means to assess thermal comfort. Adaptive thermal comfort models can also be seen as empirical models. They will be presented in the next sections.

The above mentioned methods were mostly developed in temperate climatic regions, using local subjects under special laboratory conditions. The applicability of these models for developing countries in hot and humid regions is therefore still in question.

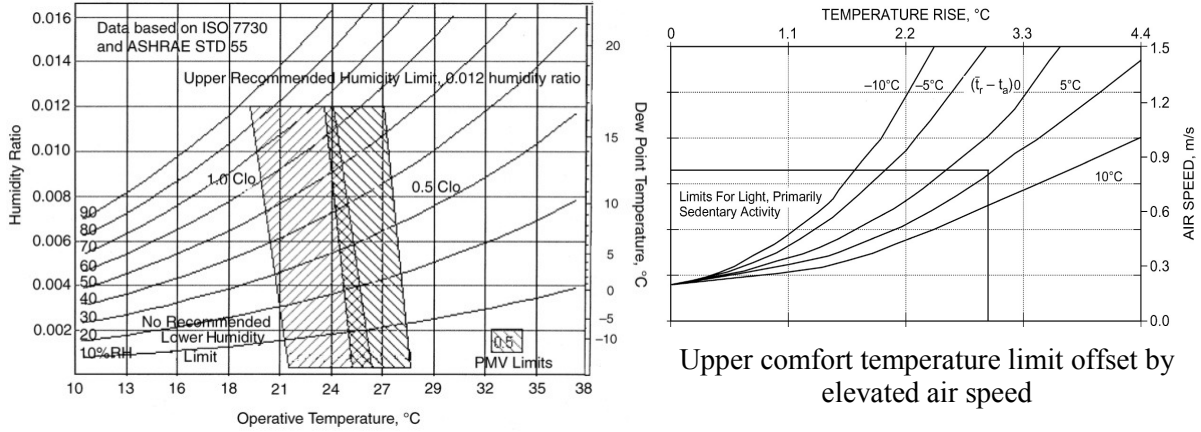


Figure 2-4: The comfort chart recommended by ASHRAE (2004)

2.2.4.2 Models based on the heat balance principle

In recent decades, there have been a number of physiologically based methods developed to predict the thermal sensation and thermal comfort. Due to space constraints, this thesis only introduces two most significant and widely used models, the PMV-PPD model and the two-node model.

The PMV-PPD model of Fanger (1970)

P.O. Fanger (1934 - 2006) exploited the heat balance principle presented in Figure 2-3 to develop the PMV-PPD model. Firstly, from equation (2.1) Fanger defined the thermal load L of the body as the difference between internal heat production and the heat loss to the actual environment as follows:

$$L = (M - W) - (q_{sk} + q_{res} + S) \quad (2.2)$$

where

L = thermal load, W/m^2 ; M = rate of metabolic heat production, W/m^2 ; W = rate of mechanical work accomplished, W/m^2 ; q_{sk} = total rate of heat loss from skin, W/m^2 ; q_{res} = total rate of heat loss from respiration, W/m^2 ; S = rate of heat storage, W/m^2 .

In an optimal comfort condition, L in the above equation is zero. In other conditions, the human thermoregulation system changes its control so as to maintain the heat balance,

thus $L \neq 0$. The most important assumption of Fanger's theory is that **the thermal sensation TSV at a given activity level is a function of the thermal load L of the body** (Fanger, 1970), and can be expressed as follows:

$$TSV = f(L, M) \quad (2.3)$$

It can be seen that the function in equation (2.3) cannot be derived by any deterministic method. Fanger then solved this equation by using the regression method on experimental data from the literature. All the experiments that Fanger relied on were conducted in climatic chambers in the U.S. and in Denmark. By doing that, he reached a regression equation that determines the connection between TSV, L and M as follows:

$$TSV = (0.352e^{-0.042(M/A_{Du})} + 0.032)L \quad (2.4)$$

where A_{Du} is total skin surface area of the subject (Dubois surface area), m^2 .

Finally, by combining equation (2.2) and (2.4), the prediction model is obtained:

$$TSV \text{ (or PMV)} = (0.352e^{-0.042(M/A_{Du})} + 0.032)[(M - W) - (q_{sk} + q_{res} + S)] \quad (2.5)$$

This equation is the compact form of the PMV-PPD model. More details of the elements in this equation can be found in (Fanger, 1970; ISO, 2005). In this equation, the TSV was referred to as the so-called “**Predicted Mean Vote**” (PMV) by Fanger. PMV is the index used to predict the mean thermal sensation vote of a large group of subjects on the 7-point thermal sensation scale of ASHRAE. The independent variables required for this model are: metabolic heat production rate ($Kcal/h.m^2$), clothing thermal resistance (clo), air temperature ($^{\circ}C$), mean radiant temperature ($^{\circ}C$), relative air velocity (m/s) and air humidity (mmHg).

The PMV index can give a prediction of the thermal comfort sensation of a group of persons; however it is much more practical to know the percentage of satisfied/dissatisfied occupants. Fanger introduced another index called the “**Predicted Percentage of Dissatisfied**” (PPD). PPD index is used to predict the percentage of dissatisfied subjects, defined as anybody not voting -1 , $+1$, or 0 on the ASHRAE scale. By using the probit analysis on the experimental data mentioned previously, Fanger related the PMV and the PPD as follows (Fanger, 1982):

$$PPD = 100 - 95e^{(-0.03353PMV^4 - 0.2179PMV^2)} \quad (2.6)$$

This relationship is graphically shown in Figure 2-5. A PPD smaller than 10% corresponds to the PMV range of ± 0.5 . Even with $PMV = 0$ (an optimal thermal condition), about 5% of the people are still dissatisfied. This relation becomes less reliable if the absolute PMV is greater than 2.

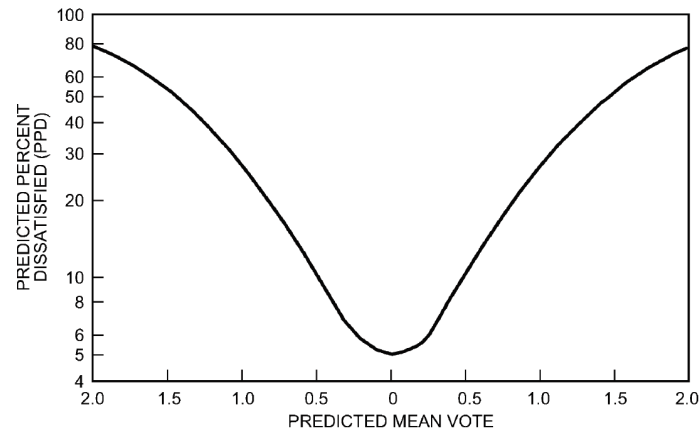


Figure 2-5: PPD as the function of PMV

The PMV-PPD model of Fanger is now widely used and approved in some international/national standards (CIBSE, 1999; ASHRAE, 2004; ISO, 2005; CEN, 2007). Due to the fact that PMV-PPD model relied on the experimental data from comfort surveys in controlled environment, the model was proved to be quite satisfied in AC built environment under steady-state conditions (de Dear & Brager, 1998). However, in NV buildings and under hot conditions, the predictions of the PMV-PPD model showed significant bias, compared with the actual mean thermal sensation vote (de Dear & Brager, 2002; Nguyen, et al., 2012). Although there have been some efforts to revise the PMV-PPD model so as to overcome this limitation (Fanger & Tøftum, 2002), none of them reaches a feasible solution.

The two-node model of Gagge et al. (1971)

The two-node model is a thermal sensation and comfort prediction algorithm applied to predict physiological responses or responses to steady-state or transient situations. It was first proposed by Stolwijk and Hardy (1966). It was then simplified by Gagge et al. (1971) and supplemented by Gagge et al. (1986). This model considers a human body as two concentric thermal compartments - skin compartment and core compartment - as shown in Figure 2-6.

Temperature of each compartment was assumed to be uniform so that the temperature gradient only exists between these two compartments. In comfort condition during rest, 33.5°C and 36.6°C were observed as the average temperature of the skin and core. Based on the heat balance principle in section 2.2.2, the model calculates 3 important indices: skin temperature t_{sk} , core temperature t_{cr} , and skin wettedness w of a human body in a specific environment at a given activity level. After obtaining the t_{sk} , t_{cr} and w , the model uses empirical expressions to relate these indices with the thermal sensation (TSEN) and thermal discomfort (DISC).

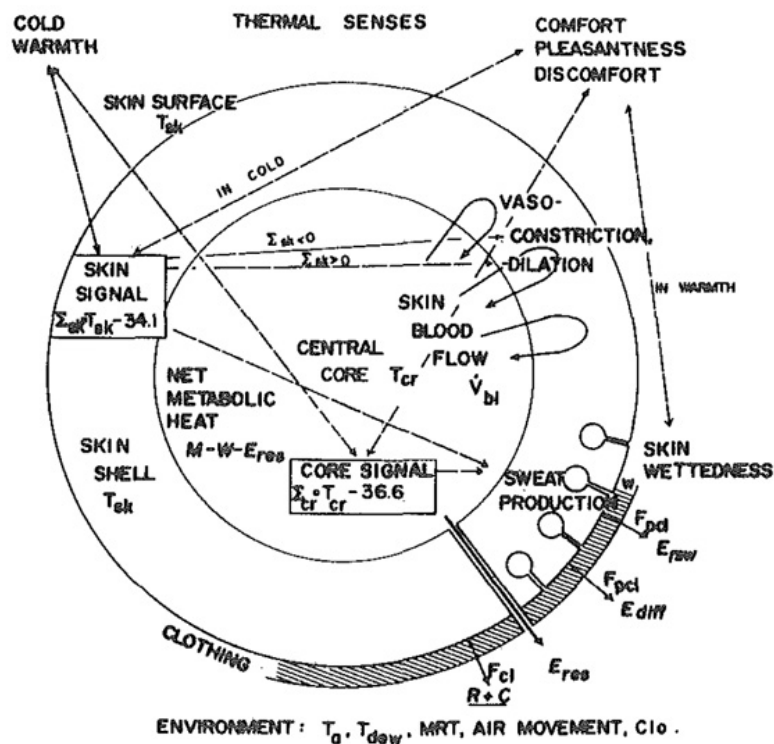


Figure 2-6: The concentric model of a man and his environment (Gagge, et al., 1971)

The thermal sensation scale TSENS and comfort scale DISC are presented in Table 2-5. The TSENS scale is rather similar to the 7-point scale of ASHRAE, but with two extra terms for ± 4 and ± 5 . As a result, this model is able to predict thermal sensations in extreme conditions which usually fail with the PMV-PPD model.

The algorithm of the two-node model is not complicated, but rather wordy; it is therefore not presented in this work. Readers should refer to (Gagge, et al., 1971; Gagge, et al., 1986; ASHRAE, 2009) for details.

Table 2-5: Thermal sensation and comfort scale of the two-node model

TSENS		DISC	
±5	Intolerably hot/cold	5	Intolerable
±4	Very hot/cold	4	Limited tolerance
±3	Hot/cold	3	Very uncomfortable
±2	Warm/cool	2	Uncomfortable and unpleasant
±1	Slightly warm/cool	1	Slightly uncomfortable but acceptable
0	Neutral	0	Comfortable

In practice, the application of the two-node model in predicting thermal sensation and comfort is not very common. But the two-node model offers a great contribution by introducing a new environmental index called “New effective temperature” (ET*)¹⁰ and its extension “Standard effective temperature” (SET*). The ET* is the temperature at 50% humidity that yields the same total heat loss from the skin as for the actual environment. The SET* is a sub-set of the ET* and is defined as equivalent temperature under standardized conditions (pressure at sea level with 50% RH, still air at 0.1 to 0.15 m/s and standard clothing for a given activity level). The ET* and SET* are usually used to normalize and then to compare the thermal effects of different thermal conditions and situations.

2.2.4.3 Models based on adaptive thermal comfort theory

As mentioned earlier, considerable discrepancies between the predictions given by heat balance-based comfort models (e.g. PMV-PPD model) and the field measurements have been observed. Particularly in NV buildings, other simple comfort models which use a simple predictor (e.g. air or operative temperature) were found more accurate (Nicol & Humphreys, 2002). This discrepancy can be explained by the results of a feedback between subjects’ comfort and their behaviors (Nicol & Humphreys, 1973), resulting in considerable changes in thermal perception. Research on these changes and its consequences are the objective of an emerging approach so-called “adaptive comfort theory”. Adaptive thermal comfort models often predict comfort (or neutral) temperature in an environment by assuming a linear relationship between comfort temperature and a predictor, usually the mean outdoor temperature of a prevailing period. The basis of the adaptive theory is that, *if changes occur in the thermal environment to produce discomfort, then people will generally*

¹⁰ The “*” is to distinguish ET* with another effective temperature (ET) developed previously.

change their behavior and act in a way that will restore it (Nicol & Humphreys, 2002). This means that people adapt themselves to the context they are living in so as to maintain thermal comfort. Adaptive actions can be categorized into three groups (Brager & de Dear, 2000):

- Behavioral adaptation refers to deliberate changes of occupants, e.g. changing clothing, posture, controlling nearby windows or fans, adjusting activities... Behavioral adaptation provides occupants best opportunities to maintain their thermal comfort.
- Physiological adaptation (also known as acclimatization) refers to biological responses which results from prolonged exposure to harsh environment, e.g. the increase of sweating setpoint temperature of a man living in hot climates.
- Psychological adaptation is assumed to relate to the social aspect of thermal perception. The past experience and expectation seem to be the motivation.

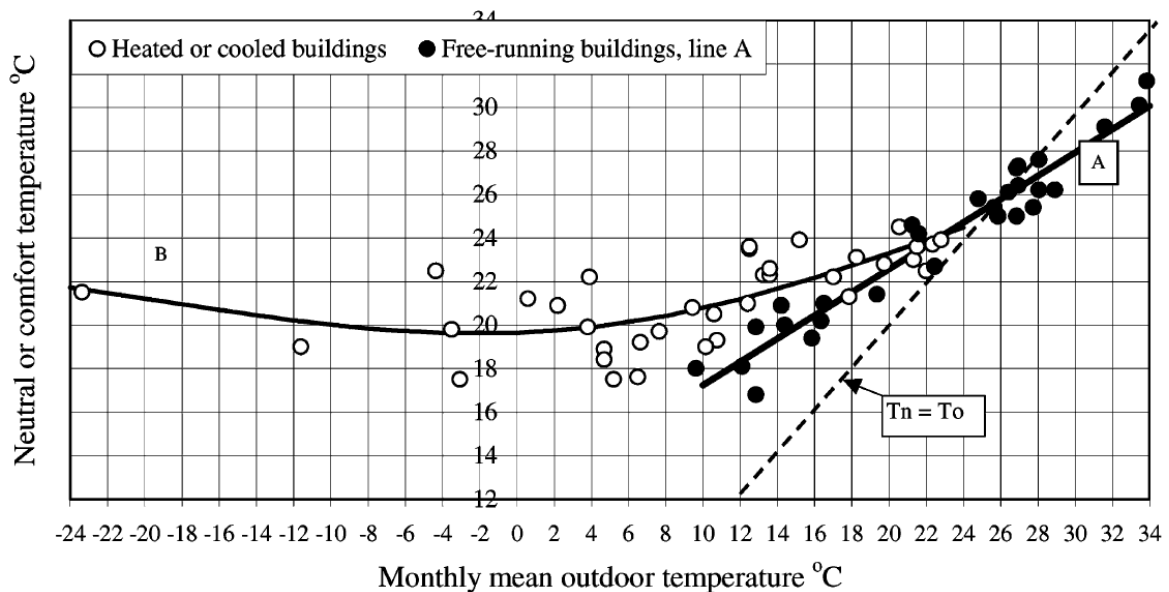


Figure 2-7: The change in comfort temperature with monthly mean outdoor temperature (Humphreys, 1978)

It has been observed that through adaptation mechanism, occupants' comfort may be achieved over a wide range of indoor temperature, from 17 – 31°C (Humphreys & Nicol, 1998). In NV buildings, the prime motivation of occupants' adaptation is the ambient temperature which is usually correlated well with outdoor conditions. Based on data from surveys performed worldwide, Humphreys (1978) found a strong correlation between

indoor comfort temperature and monthly mean outdoor temperature. He also found a clear distinction between subjects' votes in free-running buildings and those in climate-controlled buildings (see Figure 2-7).

Since the first adaptive comfort model of Humphreys (1978), different adaptive models have been developed. This thesis only reports the most widely-recognized models. In 1995 ASHRAE launched the RP-884 project in which more than 22000 set of data from field surveys around the world were gathered. Based on this database, de Dear and Brager (2002) then developed an adaptive thermal comfort model as follows:

$$T_{conf} = 0.31T_{out} + 17.8 \quad (10^{\circ}\text{C} \leq T_{out} \leq 33^{\circ}\text{C}) \quad (2.7)$$

where T_{conf} is comfort temperature; T_{out} is monthly mean outdoor temperature. This model was recommended to apply in NV buildings worldwide and was adopted in the comfort standard 55 of ASHRAE (2004).

Humphreys and Nicol (2000) reanalyzed the database of ASHRAE RP-884 project and that of Humphreys (1978). The resulting adaptive comfort models are remarkably stable between these two databases (R^2 of 0.95 to 0.97) and almost identical as shown below:

$$T_{conf} = 0.54T_{out} + 13.5 \quad (2.8)$$

The SCAT project (1997-2000) funded by the European Union was aimed to develop an adaptive control algorithm in climate-controlled buildings so as to reduce building energy consumption. The project has resulted in an adaptive thermal comfort model for free-running buildings in Europe and was then adopted in the CEN standard of indoor environment (CEN, 2007) as follows:

$$T_{conf} = 0.33T_{o,rm} + 18.8 \quad (2.9)$$

where $T_{o,rm}$ is outdoor running mean temperature, defined by the weighted mean temperature of some prevailing days. $T_{o,rm}$ can be estimated by the following equation:

$$T_{o,rm} = (T_{ed-1} + 0.8T_{ed-2} + 0.6T_{ed-3} + 0.5T_{ed-4} + 0.4T_{ed-5} + 0.3T_{ed-6} + 0.2T_{ed-7}) / 3.8 \quad (2.10)$$

where T_{ed-1} is the daily mean external temperature of the previous day, T_{ed-2} is the daily mean external temperature for the day before and so on.

As adaptive comfort models almost rely on the field survey data, their applicability in free floating environment is obviously reliable. In NV buildings in hot climates, adaptive comfort models usually predict much higher comfort temperature than that predicted by heat balance comfort models (Wong, et al., 2002; Feriadi & Wong, 2004; Nicol, 2004; Zhang, et al., 2010). This shows an explicit evidence of human adaptation in hot climates. This also results in less cooling demand and thereby less energy consumption in buildings.

In practice, the adaptive comfort approach does not reject the achievements of steady-state heat balance theories, but it helps to clarify the mechanism through which people adapt themselves to surrounding environment as well as gives a supplemental method to assess different thermal environment and situations.

2.2.5 Thermal comfort studies in Vietnam

The issue of thermal comfort for Vietnamese has been studied since 1966. Pham (2002) conducted a field survey with only 12 subjects in 2002. Other effort was very modest. The methodologies used were out of date and the sample size was not large enough. Consequently, the results of these comfort studies were not remarkable. As a result, Vietnam thermal comfort standards (Ministry of Science and Technology, 2005; 2010) are completely relied on the PMV-PPD indices of Fanger (1970) while these national standards are designed for the applications in moderate (climate-controlled) environments.

NV buildings, which occupy an overwhelming portion in the current building stock of Vietnam, require another thermal comfort guide for design. The building code TCXD VN 306 (MOC, 2004) prescribed some fixed indoor conditions for hot and cold periods for residential buildings, regardless of building climate control strategies and building locations. One can be seen from the adaptive comfort theory is that (i) comfort temperature continuously changes in accordance with prevailing outdoor conditions; and (ii) comfort temperatures in AC and NV buildings are not the same. Hence, the proposals in this building code are obviously inappropriate, compared with modern thermal comfort theories. A comfort model for NV buildings in various climatic regions of Vietnam becomes an important challenge of this research.

CHAPTER 3

A THERMAL COMFORT MODEL FOR VIETNAMESE

3.1 Study background and the proposed approach

Thermal standards applied to the built environment are very important for architects and engineers to ensure comfort, health and work productivity of occupants in a building. A good estimation of the environment not only offers comfortable thermal sensation to occupants, but it also determines the amount of energy that will be consumed by cooling and heating systems of the building. In the context of climate change and global warming, the inclusion of advanced thermal comfort concepts in thermal comfort standards which allows adopting new energy efficiency strategies, consistently helps meeting the requirement of sustainable development and makes them more relevant to the present context.

The ‘steady-state’ thermal comfort theory proposed by Fanger (1970) has become the foundation of international/national thermal comfort standards (ASHRAE, 1992; CIBSE, 1999; ISO, 2005; CEN, 2007). As indoor environment of climate-controlled buildings is rather stable and quite similar to that in climatic chambers (used to develop the model of Fanger), the PMV-PPD comfort model of Fanger have widely been used to predict occupant’s comfort in climate-controlled environments. Based on a large number of comfort studies in climate chambers in the literature, Fanger and Tøftum (2002) stated that the PMV-PPD model had been validated with Asian subjects. The result of ASHRAE RP-884 project also confirmed the validity of the PMV-PPD model in AC buildings (de Dear & Brager, 1998).

However, many field studies have shown that this model has failed to predict the thermal sensation of occupants living in "free-running" or NV buildings, not only in hot climates but also in temperate climates. This failure occurs because of the fact that the

PMV-PPD model cannot take into account complex human interactions with surrounding environment by changing their behaviors and slowly getting adapted by adjusting their expectations and preferences. Consequently, the *adaptive comfort approach* has emerged as an alternative method of thermal comfort assessment in such situations. Detailed research (McCartney & Nicol, 2002) has also pointed out that the application of adaptive comfort standards in real office buildings offers a huge potential in energy saving. The above saving translates to approximately 30% of the cooling load, compared to that of a fixed thermostat as indicated by the conventional comfort theory.

The validity of the adaptive comfort theory has been continuously clarified during the last 2 decades. Thus this thesis focuses on the development of an applied comfort model for NV buildings in hot humid climates in Vietnam using the adaptive comfort approach.

To develop an adaptive comfort model for a region, many transverse field surveys need to be conducted and repeated during a long period of time (e.g. a few years) so that the surveys cover various ranges of outdoor conditions (from cold to hot weather). Besides, a large number of observations (or respondents) should be obtained to ensure that the results would be statistically meaningful and reliable. That would be a time consuming and strenuous job. Therefore, an adaptive comfort model for Vietnamese based on direct field surveys is out of the scope of this thesis.

South–East Asia including Vietnam commonly has hot and humid climates all year round. The majority of the population almost originates from similar cultural background. They prefer to live in NV buildings because the socio-economic and socio-cultural preferences are optimally addressed in these buildings. We hypothesize that people in this region have identical or at least similar thermal preference. The author therefore proposes an approach to develop an adaptive thermal comfort model for Vietnamese through 2 phases:

- First, an adaptive comfort model for people living in hot humid climate South-East Asia is established by reusing the data from earlier field surveys conducted within this region.
- Then, the applicability of the developed adaptive comfort model for Vietnamese will be validated by conducting a transverse comfort survey in Vietnam on large observations and comparing the results with those of South-East Asia.

The subsequent sections will describe in detail the two steps mentioned above.

3.2 Adaptive thermal comfort model for hot humid South-East Asia

Recently, there have been many thermal comfort studies conducted around the world using the adaptive comfort theory (Humphreys, 1978; de Dear & Brager, 2002; Bouden & Ghrab, 2005; Manoj, et al., 2011). However, the validity for global application is still in question because human adaptation happens in different manners through various climatic and cultural regions. Nicol (2004) carried out a meta-analysis on the database of 25 comfort field surveys in hot humid climates and reported that the adaptive comfort temperature in hot humid climates significantly differs from that in temperate or hot dry climates. Therefore, the determination of an adaptive comfort model which can be widely applied within hot humid South-East Asia is needed. This section describes the research methodology in detail, followed by the results and discussions through which the adaptive comfort model for this region is generated. Other comfort related issues, the differences and similarities between various adaptive comfort models were also addressed.

3.2.1 Methodology

The adaptive approach in thermal comfort relies on the analysis of the data collected from field surveys on thermal comfort. Then statistical methods are often used to analyze the recorded data from field surveys. Since errors can rise from many sources, e.g. measuring error, data recording error or calculating error etc., a large sample is usually required for reliable statistics. Meta-analysis (Glass, 1976) which combines the results of several surveys to address a set of related research hypotheses was applied in this study. The general aim of the meta-analysis is to generate a reliable adaptive comfort model through a large database collected from methodologically sound studies. Data of such studies must be refined by removing the inconsistent data and then standardized. Although this method has both advantages and weaknesses (Rosenthal, 1979; Hunter & Schmidt, 1990), it has been frequently used in other thermal comfort studies related to data from field surveys (Humphreys, 1978; de Dear, et al., 1997; Nicol & McCartney, 2001; Nicol, 2004).

The comfort surveys selected were based on the following criteria:

(1) Survey locations are scattered around hot humid regions of South-East Asia (climatic boundary instead of political one);

(2) Quality of the survey and subsequently the data was ensured by final research publications;

(3) Raw data file (not only the research reports or publications) created by the original researchers is available.

Table 3-1: Summary of the field survey database for the present adaptive model

Location and Research leader	Building type	Climate type ¹¹	Year of survey	ASHRAE Classification ¹²	Type of survey	Sample size	Sources
Singapore, R. de Dear	NV	Wet equatorial	1987	Class 2	cross-sectional	583	(de Dear, et al., 1997)
Bangkok, J.F. Busch	NV	Tropical savanna	1990	Class 2	cross-sectional	391	(de Dear, et al., 1997)
Jakarta – Indonesia, T.H. Karyono	NV	Wet equatorial	1995	Class 3	cross-sectional	97	(de Dear, et al., 1997)
Singapore, N. H. Wong	NV	Wet equatorial	2001	Class 2	cross-sectional	538	(Wong, et al., 2002)
Jogjakarta – Indonesia, H. Feriadi	NV	Wet equatorial	2002	Class 2	Hybrid	525	(Feriadi & Wong, 2004)
Johor Bahru – Malaysia, I. Hussein	NV	Wet equatorial	2009	Class 3	cross-sectional	375	(Hussein & Rahman, 2009)
Guangzhou – China, Y. Zhang	NV	Tropical savanna	2009-2010	Class 1	Longitudinal	921	(Zhang, et al., 2010)
Singapore, R. de Dear	AC	Wet equatorial	1986	Class 2	cross-sectional	235	(de Dear, et al., 1997)
Bangkok – Thailand, J.F. Busch	AC	Tropical savanna	1990	Class 2	cross-sectional	776	(de Dear, et al., 1997)
Jakarta – Indonesia, T.H. Karyono	AC	Wet equatorial	1995	Class 3	cross-sectional	458	(de Dear, et al., 1997)
Manila – Philippines, M. M. Andamon	AC	Wet equatorial	2002-2003	Class 2	Longitudinal	277	(Andamon, 2005)

Table 3-1 summarizes basic information of 11 comfort surveys included in this research database. All observations of gathered surveys were then transferred into a meta-file in a spreadsheet for statistical analysis. Totally 5176 sets of environmental and

¹¹ By the classification developed for the Macquarie University undergraduate teaching program in climatology

¹² By the classification system used in the final report of the ASHRAE RP-884 project

subjective observations were included in the database (3430 records in NV buildings). Only 402 observations of this database will be then eliminated by the data standardization. Comparing with other surveys (e.g. European SCATs project (Nicol & McCartney, 2001) with total 4655 records – 1449 in free running building), this amount is considered to be sufficiently large for a reliable meta-analysis.

For the purpose of statistical analysis, the responses of all subjects of longitudinal surveys (few subjects, sampled many times during a long period, as in case of Guangzhou and Manila) were assumed to be independent. It means that observations of longitudinal surveys were treated in the same manner as cross-sectional surveys. Since the earliest survey was carried out 25 years ago, we also assumed that human thermal perception and preference does not change over time.

In ASHRAE RP-884 project (de Dear, et al., 1997), all individual responses in the database were aggregated into the statistical unit of each building, thus the 21000 responses were able to reduce to 160 buildings. The buildings for which the regression analysis failed to reach statistical significance ($P = 0.05$) were eliminated. This method has a small drawback that if the temperature range or the number of respondents in a building is small, the corresponding linear regression may result in an inaccurate model and the mean thermal sensation vote will not always reflect the thermal environment inside the building.

This work aggregated the large quantity of building observations into half-degree ($^{\circ}\text{C}$) increments, attributed by its sample size. The weighted regression was then performed to obtain the relationship between the variables. As presented in the next sections, each scatter point in the graph has its own weight shown by its relative area. The purpose of using the weighted regression is to minimize the impact of outlying bins which consist of small number of observations. This method has an advantage that the temperature range of each bin is small (0.5°C), therefore the mean thermal sensation vote closely corresponds with the thermal environment. For example, the scatter plot of operative temperature ($T_{i,o}$) versus thermal sensation vote (TSV) is reduced from 3430 observations in the database to about 36 weighted bins (see Figure 3-2). Each bin is the mean of comfort votes corresponding to a mean of a half-degree ($^{\circ}\text{C}$) indoor temperature range (which was carefully sorted before by Excel[®] spreadsheet). We imposed a stringent criterion according to which only significant weighted regression ($P < 0.01$, correlation $R^2 > 0.50$) was accepted.

3.2.2 Raw data standardization

Each comfort study included in the present database employed a specific method, although most of these studies on adaptive comfort basically relied on a relatively homogeneous modality. Therefore, for a meta-analysis, data normalization is essential. Most information related to research methodologies were obtained through the official publications or by exchanging e-mails with the original authors. This section reports in detail the data assimilation procedure.

3.2.2.1 Consistency in clothing insulation and chair insulation effects

Clothing insulation is always the most troublesome in any comfort field survey because of the great variety of subject's clothes. It can only be estimated precisely by using a thermal manikin. However, even in an experiment in a climate controlled chamber where clothing insulation was calculated using sophisticated thermal manikins, the obtained insulation values varied considerably between manikins (de Dear, et al., 1997). In ASHRAE database, all clothing insulation estimations of the field surveys were converted using ASHRAE 55-1992 clo estimation method. Meanwhile, our newly gathered data in South-East Asia used ISO 9920-1995 (ISO, 1995), ASHRAE 55-2004 and ASHRAE 55-1992 as clo estimation methods. As all these methods were used in the database of this study, the consistency between these four methods must be verified. It was found that these three methods are almost similar since they are based on the data from the works of McCullough (McCullough & Wyon, 1983; McCullough, et al., 1985) and Olesen (Olesen, 1985; Olesen & Dukes-DuBos, 1988). Therefore, the clo estimation method throughout the database was considered to be identical. Besides, the insulation effect of chairs of 0.1 - 0.15 was consistently added into the database by the original authors.

3.2.2.2 Consistency in calculated parameters

The calculated parameters consist of mean radiant temperature (T_{mrt}), operative temperature ($T_{i,o}$), new effective temperature (ET*), standard effective temperature (SET*), predicted mean vote (PMV) and predicted percentage dissatisfied (PPD). These parameters were carefully checked for consistency and recalculated wherever inconsistencies were detected. A PMV-PPD calculator on Spreadsheet which allows calculations of PMV-PPD indices in series was built on the code recommended by ISO 7730 (ISO, 2005). ET* and

SET* were calculated by the calculator of de Dear (2010) (slightly different, but acceptable results were yielded, compared with those given by Wincomf[®] used in the RP-884 project). The operative temperature was directly recalculated by simple equations presented in ASHRAE 55-2004, based on mean radiant temperature and air temperature plus air speed. Only for mean radiant temperature (T_{mrt}), this study have not collected enough information about measuring instruments and calculation methods, therefore the T_{mrt} given by the original authors were accepted.

3.2.2.3 Gathering means of outdoor temperature

Outdoor environmental conditions corresponding to each observation must be obtained so as to establish a correlation between observed neutral temperature and the weather. It is obvious that the exponentially weighted running mean outdoor temperature ($T_{o,rm}$) used in European SCATs project (McCartney & Nicol, 2002) is the most appropriate index for this purpose. However, $T_{o,rm}$ requires continuous and detailed information of outdoor conditions which are only available in pre-designed surveys (e.g. SCATs project). An acceptable and widely used outdoor reference index is the monthly mean outdoor temperature which is calculated by the average of daily maxima and minima. Monthly mean outdoor temperature is a suitable climate reference since weather conditions are rather stable and the day - night temperature variation/swing over an entire year is small in hot humid regions. In the surveys for which this value was not reported, the historical mean monthly temperature from official climatological data resources, e.g. (U.S. Department of Energy, 2012), was assigned to each observation.

3.2.2.4 Refining the data and bias control in meta-analysis

A Chi-squared test was applied to each regression analysis to verify whether the linear relationship between two examined variables is statistically significant. The choice of significance threshold depends critically on the sample size because equilibrium will always be rejected at a conventional level ($P = 0.05$) with large sample sizes. Since the database of this study is very large, we decided to set a stringent threshold - P-value of 0.01 - as statistical significance. All the surveys and the corresponding data after analysis which failed to reach the statistical significance were eliminated or rejected.

According to the above criterion, 158 observations (4.6% of the total) obtained from the survey in Johor Bahru - Malaysia (in Nong Chik primary school, very young subjects - around 10 years old) were eliminated because the correlation coefficient of determination R^2 of some regressions were too low and the relations were not statistically significant. The regression between $T_{i,o}$ and TSV gave P-value = 0.023 > 0.01, $R^2 = 0.033$; and the regression between PMV and TSV gave P-value = 0.021 > 0.01, $R^2 = 0.034$. A possible reason for these inconsistencies is that many young subjects didn't understand the questionnaire and the requirements of the survey.

During the regression analysis using scatter graphs, it was found that a few responses exhibited very large bias from the principle scatter clouds. These responses can be seen as survey errors which are inevitable in any field survey. They may come from measuring errors, data entry errors, health problems of occupants or because an occupant have special needs about the thermal environment at that moment. Standard Residual (SR) of each TSV was calculated and then used to detect abnormal bias as follows:

$$SR = \frac{Y_o - Y_p}{\sqrt{\frac{\sum_{i=1}^n (Y_i - \bar{Y})^2}{n}}} \quad (3.1)$$

where

Y_o is observed value (in this case: observed TSV by occupants); Y_p is predicted value (in this case PMV); Y_i is i^{th} observed value; \bar{Y} is arithmetic mean of the observed values.

Observed TSVs with absolute SR greater than 2 were eliminated since they exhibit large bias from the scatter cloud. For example, in a case where $T_{i,o} = 30.1$, TSV = 3 while PMV = -0.91, SR = 2.87 > 2, therefore this vote should be eliminated. After Standard Residual analysis, 196 observations (5.7% of the total) in the NV database and 48 observations (2.7% of the total) in the AC database were eliminated. The bias percentage observed in NV buildings was about two times higher than that in AC buildings. Finally, the refined database consisted of 4774 observations ready for use.

3.2.3 Results and discussions

Although the purpose of this study is to define an adaptive comfort model for NV buildings, another analysis based on survey data collected from AC buildings were also carefully examined. The similarities and differences between results of these two building

types are important to strengthen our understanding about the adaptation and thermal comfort. For this reason, analysis results of both NV and AC buildings were always presented together in the following sections.

3.2.3.1 Distribution of indoor operative temperature and relative humidity

The histograms of distribution of indoor operative temperature and relative humidity during all surveys are presented in Figure 3-1. It is notable that only the survey in Guangzhou – China in mild seasons (from October to April of the next year) had low a temperature range - from 17°C to 26°C and extremely low humidity (not shown in Figure 1). The result of this survey is significantly different from that of other surveys, as being discussed in the next sections. In other surveys, the operative temperature range is 26°C to 35°C (mean 29.8°C) in NV buildings and 20°C to 32°C (mean 24.4°C) in AC buildings. Humidity in NV buildings is rather high (mean 71.7%) and about 14% higher than that in AC buildings (mean 57.9%). It can be seen that South-East Asia almost has hot and humid climates that may result in different human thermal perception.

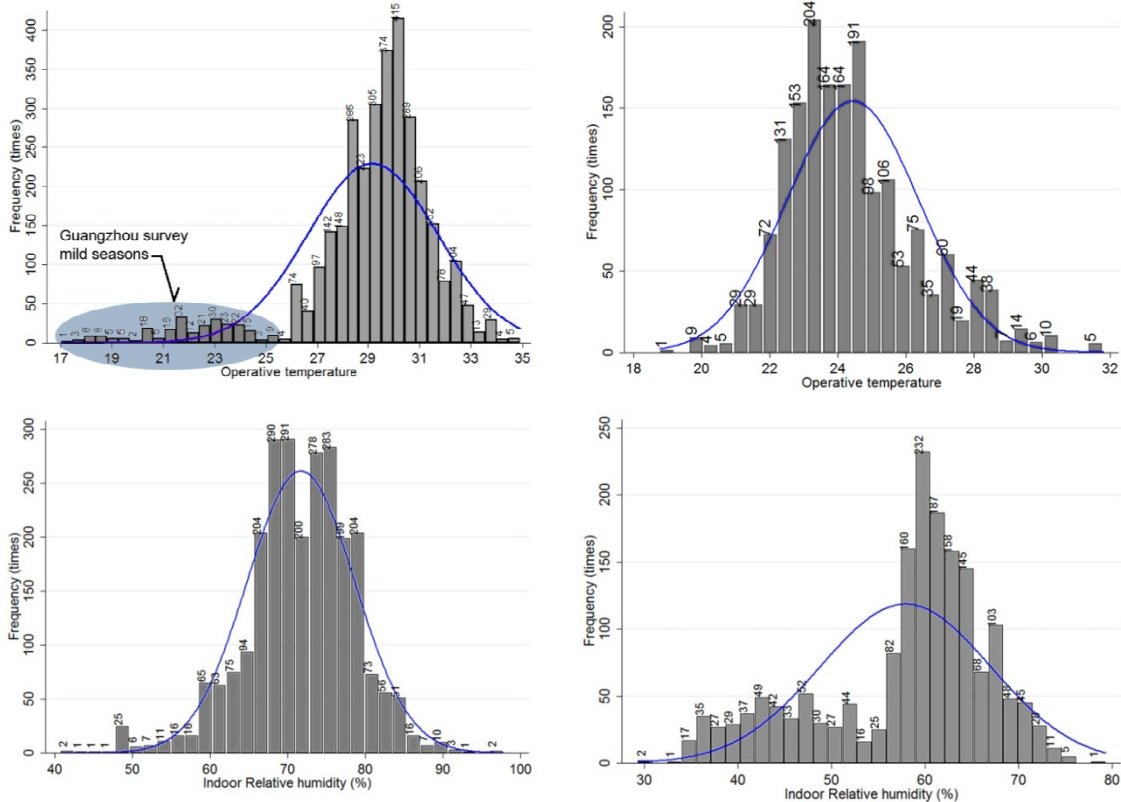


Figure 3-1: Distribution of indoor operative temperature and relative humidity in NV (left) and AC buildings (right) of all surveys

3.2.3.2 Mean neutral temperature

The weighted regression as described in detail in section 3.2.1 was performed to find mean neutral temperature (operative temperature, ET^* , SET^*). The results presented in this section have satisfied the statistical significance ($P < 0.01$). Traditional methods used to derive neutral temperature from field survey data are (Nicol & Humphreys, 2010):

- Probit analysis to find a comfortable temperature at which the largest proportion of subjects is comfortable (using Bedford thermal scale).
- Regression analysis to calculate a neutral temperature at which the average person votes neutral on the 7-point thermal sensation scale. This method is employed in this study.

Mean neutral operative temperature

The adaptive theory indicates that the neutral temperature changes as people adapt to the changing environment by modifying their clothing, activities as well as their expectation (Nicol & Humphreys, 2010) and thus the comfort temperature normally varies from month to month across the year. Neutral operative temperature calculated in this section is only a **mean value** corresponding to an indoor temperature range.

As shown in Figure 3-2, neutral $T_{i,o}$ in Guangzhou in mild seasons (25.5°C) is significantly lower than that (27.9°C) of other surveys in warmer climates. Neutral $T_{i,o}$ in AC buildings (Figure 3-2 – right) is 25.8°C , similar to the results of earlier studies conducted in climate chambers (Fanger, 1970; Rohles & Nevins, 1971). Interestingly, the regression slope gradually increases when the temperature range raises from 0.183 to 0.24 and to 0.41. It peaks in NV buildings instead of AC buildings. Since the regression slope reflects occupants' sensitivity to temperature changes, we argue that this regression slope does not reflect adaptation efficiency and opportunities. As being observed, it depends on temperature and humidity ranges. It is quite obvious that at high temperature and high relative humidity, adaptive actions (changing clothing, posture, activities...) will be less effective than at lower temperature because heat dissipation to the environment becomes difficult. Consequently, the occupant seems to be more sensitive to thermal changes. However, this phenomenon needs further investigations before drawing any conclusion.

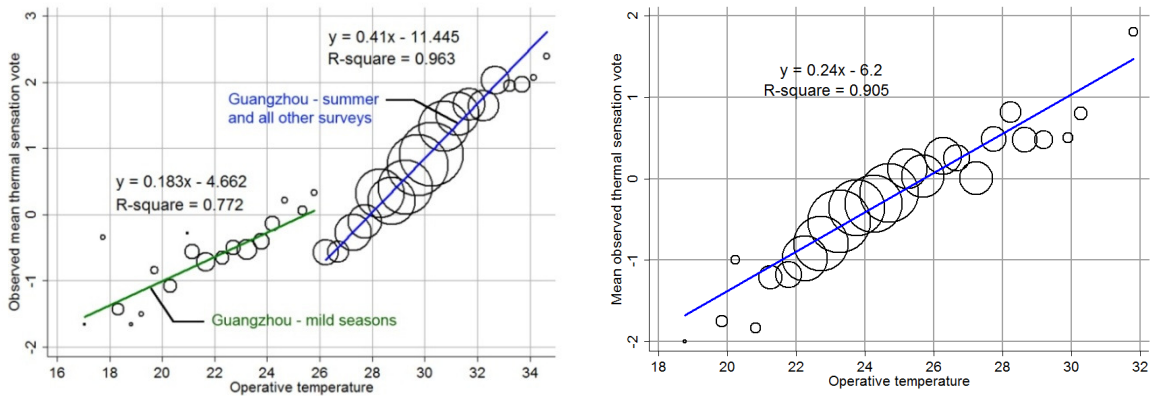


Figure 3-2: Weighted regression of mean $T_{i,o}$ versus mean TSV. Smallest and largest sample sizes in NV buildings (left) are 1 and 430, and in AC buildings (right) are 1 and 225.

Since the correlation coefficients R^2 of these regressions are very high and the number of observations is sufficiently large, this analysis gives very strong evidence that neutral temperature is a “moving target” instead of a fixed temperature as being found in the ‘steady-state’ experiments. The comfort temperatures found in climate chambers (around 25.5°C to 26.0°C) do not reflect the complex ways people interact with their surrounding environment in ‘real-world’ buildings.

Mean neutral effective temperature ET^*

As shown in Figure 3-3, mean neutral ET^* in NV and AC buildings are 27.1°C and 25.9°C, respectively. The regression equations of NV and AC buildings were nearly similar. The difference between mean neutral ET^* of NV and AC buildings still existed but it was smaller than the difference in neutral operative temperatures.

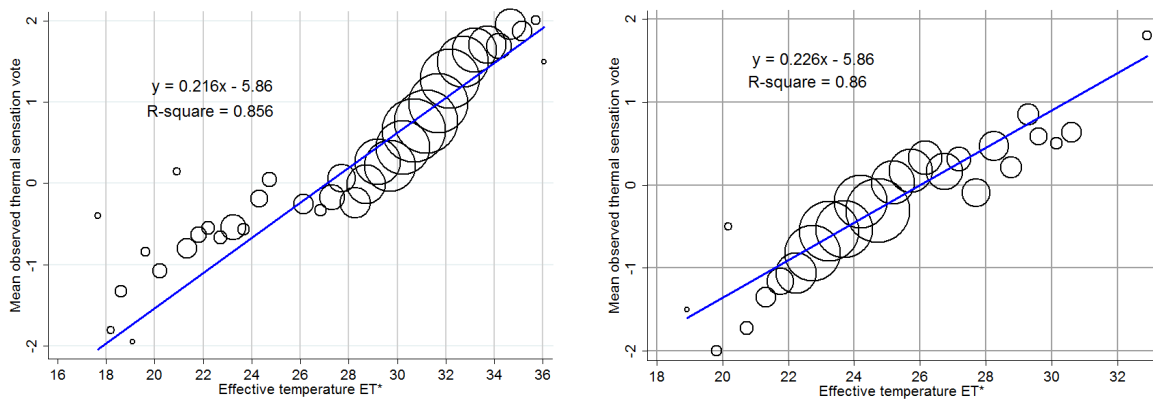


Figure 3-3: Weighted regression of mean ET^* versus mean TSV. Smallest and largest sample sizes in NV buildings (left) are 2 and 298, and in AC buildings (right) are 2 and 229.

Mean neutral Standard effective temperature SET*

Different from previous regressions in Figure 3-2 and Figure 3-3, Figure 3-4 shows that the regression equations of SET* versus TSV in NV and AC buildings are almost identical. Very high observed correlations (R^2) mean that there are strong relations between SET* and TSV. So the outcome, neutral temperature, calculated based on this analysis is more accurate. This analysis indicates that mean neutral SET* in both NV and AC buildings are about 25.5 - 25.7° SET*, very close to the neutral temperature found by Fanger (1970) and Rohles and Nevins (1971) in climate chamber experiments and by Fanger’s comfort equation. So it can be concluded that neutral SET* in AC and NV buildings are not different although the corresponding neutral operative temperatures deviate considerably, from each other.

Table 3-2: Mean observed neutral temperature in South-East Asia

Building type	Mean neutral operative temperature			Mean neutral Effective temperature			Mean neutral Standard effective temperature		
	$T_{i,o}$	R^2	RMSE**	ET*	R^2	RMSE	SET*	R^2	RMSE
NV buildings	27.9*	0.963	0.102	27.1	0.856	0.225	25.5	0.972	0.083
AC buildings	25.8	0.905	0.129	25.9	0.860	0.144	25.7	0.860	0.096

* Not take into account Guangzhou survey in mild seasons

** Root mean square error between actual TSV and predicted TSV by the regression equations in Figure 3-2, Figure 3-3 and Figure 3-4

Table 3-2 summarizes all mean neutral temperature observed from the above analysis. It can be seen that under hot and humid conditions, the majority of occupant feels comfortable when operative temperature is about 28 °C. This value is about 2 °C higher than that of AC buildings. This difference is mainly attributed to three adaptive actions of occupants: controlling window, varying activity levels and changing clothes (behavioral adaptation). When SET*, which takes all these adaptive actions into account and converts them into a ‘standard condition’, was used, the difference of neutral SET* between NV and AC buildings becomes minimum. SET* is a sub-set of ET* and is defined as equivalent temperature under standardized conditions (namely, pressure at sea level with 50% RH, still air at 0.1 to 0.15 m/s and standard clothing for a given activity) (Auliciems & Szokolay, 2007). SET* gives a rational basis for measuring the equivalence of any combination of environmental factors, clothing and metabolic heat production. Thus SET* strongly correlates with occupant’s thermal perception. The nearly similar neutral SET*s in both NV

and AC buildings have revealed that the role of expectation (psychological adaptation) and acclimatization (physiological adaptation) were very vague and human thermal adaptation mainly relies on behavioral actions. This result also proposes a new idea to implement SET* into building simulation tools to assess thermal comfort in buildings, regardless of building types - AC or NV. However, a specific thermal comfort experiment is needed to reconfirm the similarity of neutral SET* in AC and NV buildings.

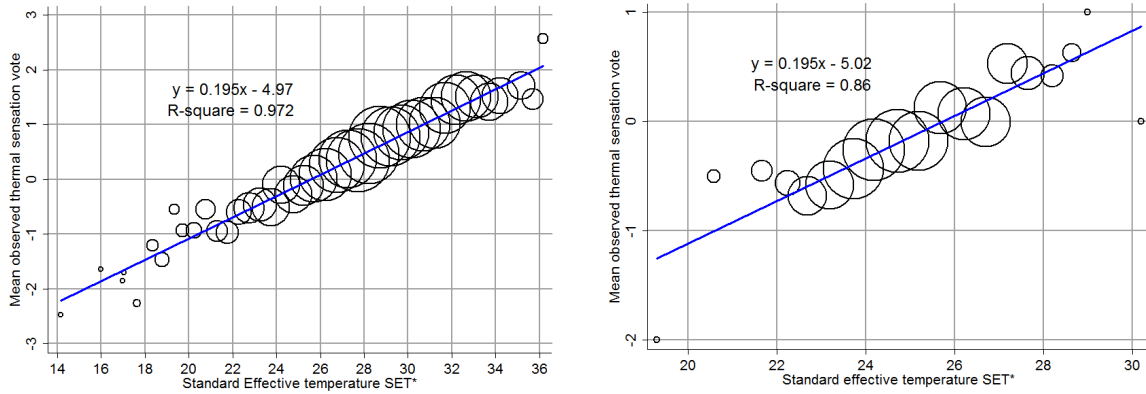


Figure 3-4: Weighted regression of mean SET* versus mean TSV. Smallest and largest sample sizes in NV buildings (left) are 1 and 118, and in AC buildings (right) are 1 and 93.

3.2.4 An adaptive thermal comfort model for South-East Asia

3.2.4.1 Sensitivity analysis and the choice of “Griffiths constant”

A traditional method to build adaptive thermal comfort models is linear regression in which mean comfort temperature of a group of subjects (or comfort temperature of each individual subject) is plotted versus an outdoor environmental parameter, e.g monthly mean outdoor temperature. Griffiths (1990) proposed a single standard value - namely Griffiths constant G_{cons} - to predict comfort temperature T_{conf} from a mean or an individual thermal sensation vote TSV and global temperature T_g using the equation defined as:

$$T_{conf} = T_g - TSV / G_{cons} \quad (3.2)$$

If TSV is equal zero, the comfort temperature is equal to the global temperature. The equation (3.2) indicates that individual comfort temperature is rather sensitive with the change of ‘Griffiths constant’. Using the database of this study, Figure 3-5 (left) graphically shows the sensitivity of adaptive comfort models derived from the present database if different Griffiths constants are applied. At 30°C, if Griffiths constants chosen are 0.33 and

0.5, predicted comfort temperatures will have a difference of 2.5°C. Figure 3-5 (right) indicates that the regression slope of adaptive comfort model is very sensitive within the range of Griffiths constants from 0.2 to 0.6. Therefore, the choice of Griffiths constant plays an important role in the derived adaptive model and must be made with care.

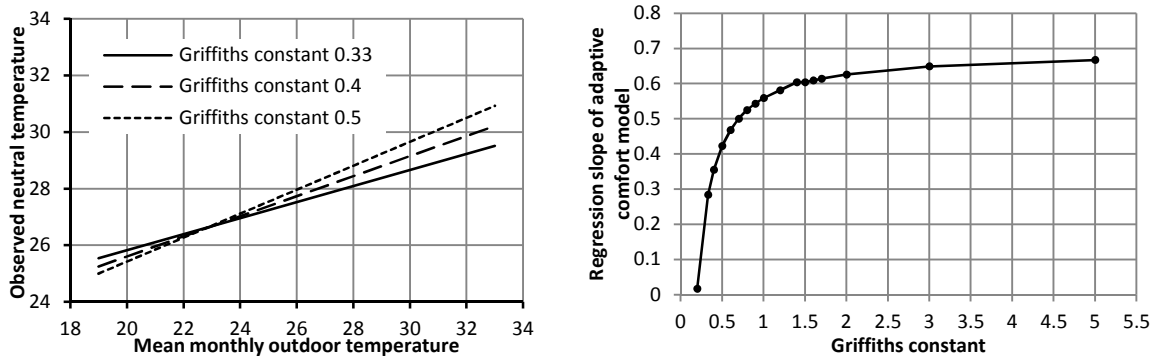


Figure 3-5: Sensitivity of resulted adaptive comfort model with different 'Griffiths constants' (left) and the relationship between Griffiths constant and regression slope of adaptive comfort equation (right)

Griffiths (1990) proposed a constant of 0.33 for use in adaptive comfort studies. de Dear and Brager (1998) extensively examined the ASHRAE RP-884 database to choose a 'Griffiths constant'. They proposed an appropriate 'Griffiths constant' of 0.5 for the relationship between thermal sensation votes and global temperature. Nicol and Humphreys (2010) examined the correlation R^2 of the linear regression between running mean temperature and observed comfort temperature with Griffiths constant at 0.4 and 0.5. They finally chose the value 0.5 for the SCATs project because it gave slightly higher correlation.

We examined the correlation coefficient R^2 of the adaptive comfort equation using the present database. The result is presented in Table 3-3 and Figure 3-6. Meta-analysis of different surveys conducted during a very long period consists of many input uncertainties and may produce inconsistencies among surveys. Consequently, low coefficients of correlation R^2 could be observed (lower than 0.7). It was observed that the higher Griffiths constant applied, the higher correlation yielded. This directly proportional relation is quite obvious because of the direct relationship among TSV , T_{comf} , $T_{i,o}$, T_{out} and G_{cons} . These analyses revealed that the correlation coefficient R^2 cannot be the criteria for the selection of Griffiths constant (As shown in the next sections, the weighted regression eliminated effects of bias observations by aggregating them into half-degree increments. Hence higher R^2 of all linear regressions were achieved and the scatter plots showed trends more clearly).



Figure 3-6: Relationship between Griffiths constant and correlation coefficient of adaptive comfort equation

Table 3-3: The role of Griffiths constant in the establishment of adaptive comfort equation and its correlation R^2

'Griffiths constant'	Adaptive comfort equation	R^2 – direct regression	'Griffiths constant'	Adaptive comfort equation	R^2 – direct regression
0.2	$T_{comf} = 0.017 T_{out} + 26.20$	0.00006	1.2	$T_{comf} = 0.581 T_{out} + 13.36$	0.499
0.33*	$T_{comf} = 0.284 T_{out} + 20.14$	0.0443	1.4	$T_{comf} = 0.604 T_{out} + 12.85$	0.531
0.4	$T_{comf} = 0.355 T_{out} + 18.50$	0.095	1.5	$T_{comf} = 0.607 T_{out} + 12.85$	0.534
0.5**	$T_{comf} = 0.423 T_{out} + 16.96$	0.180	1.6	$T_{comf} = 0.609 T_{out} + 12.72$	0.538
0.6	$T_{comf} = 0.468 T_{out} + 15.93$	0.262	1.7	$T_{comf} = 0.614 T_{out} + 12.61$	0.543
0.7	$T_{comf} = 0.500 T_{out} + 15.20$	0.331	2	$T_{comf} = 0.626 T_{out} + 12.33$	0.554
0.8	$T_{comf} = 0.525 T_{out} + 14.65$	0.385	3	$T_{comf} = 0.649 T_{out} + 11.82$	0.566
0.9	$T_{comf} = 0.543 T_{out} + 14.22$	0.426	5	$T_{comf} = 0.667 T_{out} + 11.41$	0.569
1	$T_{comf} = 0.559 T_{out} + 13.88$	0.457			

* This value was proposed by Griffiths

** This value was used in ASHRAE RP-884 and European SCATs project

We tried to predict the regression slope (Griffiths constant) from the standard deviation of indoor operative temperature (see Figure 3-7), as done previously by Humphreys et al. (2007). However, within our database, this correlation was very weak ($R^2 = 0.25$) and this low correlation failed to reach statistical significance using a chi-square test ($P = 0.0792 > 0.05$). It means that an appropriate Griffiths constant cannot be determined based on the basis of this standard deviation.

Finally, we decided to use the weighted mean of the regression coefficients of these surveys (the number of respondents was also taken into account as the weighing factor). The

weighted mean value of all regression coefficients was 0.384 (the extreme bias point of Guangzhou in mild seasons was excluded). This value is used to derive the comfort temperature from each thermal sensation vote and indoor operative temperature. As this value was obtained from a large number of surveys, it is also recommended for other similar adaptive comfort studies in hot humid climates.

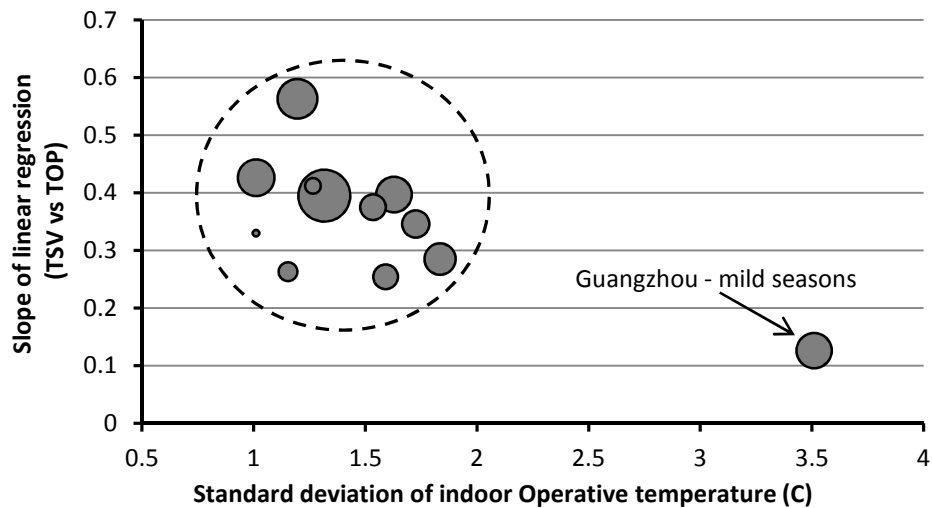


Figure 3-7: Slope of the regression in relation to the standard deviation of indoor operative temperature. Each point represents the slope of linear regression of a survey in a country, in NV or AC buildings. The survey in Guangzhou was divided into two surveys: hot season and mild seasons (Smallest and largest sample sizes are 97 and 762, respectively)

3.2.4.2 Adaptive comfort equation

Figure 3-8 presents the adaptive comfort equation developed for NV buildings. The correlation R^2 of this equation reaches 0.52. As being analyzed above, a raising Griffiths constant would raise the R^2 . If we used the Griffiths constant of 0.5 as being used by ASHRAE in the standard 55-2004, we would achieve the correlation R^2 of 0.698 which is almost equal to that (0.7) of the standard 55-2004 (de Dear & Brager, 2002). The comfort equation of EN15251 had much higher correlation since it only used the data of SCATs project which was specially designed for this standard. The 95% confidence intervals indicates that this adaptive comfort equation is highly reliable in the range of monthly mean outdoor temperature from 24 to 30°C (It would be 95% confident if the predicted comfort temperature has an accuracy of $\pm 0.5^\circ\text{C}$). The 95% confidence intervals also reveals that this model needs further investigations when monthly mean outdoor temperature drops below 24°C or exceeds 30°C.

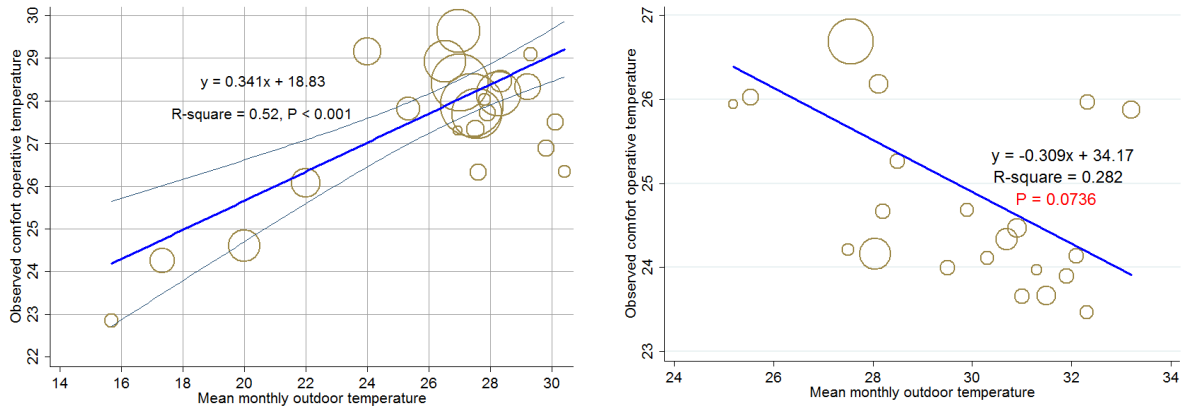


Figure 3-8: Predicted comfort temperature. Each bubble represents mean vote corresponding to a mean monthly temperature. For NV buildings (left): largest bubble size: 569, smallest bubble size: 14. For AC buildings (right): largest bubble size: 458, smallest bubble size: 21. 95% confidence intervals of the regression line were also shown.

The comfort equation for NV buildings achieved from this analysis is:

$$T_{conf} = 0.341T_{out} + 18.83 \quad (3.3)$$

The comfort model in equation (3.3) predicts slightly higher comfort temperature than the model of ASHRAE ($T_{conf} = 0.31T_{out} + 17.8$) and much closed to EN15251 ($T_{conf} = 0.33T_{o,rm} + 18.8$; free-running buildings). Although the methods and independent variables related to adaptive comfort temperature were different, it resulted in similar comfort equations showing a convergent trend of adaptive comfort studies with large databases.

Figure 3-8 also shows the model of predicted comfort temperature for AC buildings. In contrast with the case of NV buildings, it can be seen that P-value in this case is $P = 0.0736 (> 0.01)$, thus the correlation failed to reach statistical significance. This analysis shows that in AC buildings, occupant’s comfort temperature is almost independent of outdoor temperature.

3.2.4.3 Acceptability deviation around comfort temperature

There is a limited interval around ideal comfort temperature given by the adaptive comfort equation. This interval is called “acceptability range”. Based on the result of RP-884 project, de Dear and Brager (2002) found no climate-dependency for indoor thermal sensitivity and they stated that the acceptability range is unchanged across the entire range of outdoor climates. They proposed 7°C and 5°C as the widths of comfort range corresponding to 80% and 90% acceptability. However, the result of SCATs project

(McCartney & Nicol, 2002) reported that the acceptability range becomes narrower as the outdoor condition becomes warmer.

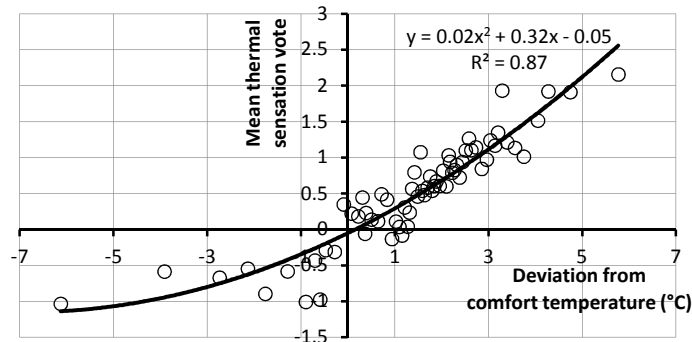


Figure 3-9: Change of mean thermal sensation vote corresponding to deviation from comfort temperature. Each point represents mean of 50 votes

This study defines the acceptability range by calculating the comfort temperature as well as the deviation of indoor $T_{i,o}$ from comfort temperature for each observation. Then we plot the TSV versus the deviation from comfort temperature using a scatter graph. The comfort range for 80% and 90% acceptability is assumed to correlate with mean TSV of ± 0.85 and ± 0.5 , as recommended by Fanger (1970). Figure 3-9 shows the result according to which the constant term of the regression equation is nearly zero as expected, and the correlation coefficient is fairly high. Figure 3-9 also reveals that subjects were less sensitive to the thermal change in the cooler side of comfort temperature. The comfort ranges for 80% acceptability (TSV from -0.85 to 0.85) and 90% acceptability (TSV from -0.5 to 0.5) are 5.7°C and 3.2°C, respectively. These comfort ranges are similar to what Nicol (2004) proposed for hot humid tropics, but lower than other standards (e.g. ASHRAE 55, EN 15251), indicating that people in South-East Asia are slightly more sensitive to temperature changes. As discussed previously, the high temperature range and relative humidity during the surveys might limit the efficiency of adaptive actions and narrow the comfort range.

For the regions where cool winter exists (e.g. Hanoi, Guangzhou), the winter comfort range may be extended to the value of 7°C as more adaptive actions become accessible such as changing clothes, adjusting openings and personal activities. This extension can be also found in ASHRAE standard 55 (ASHRAE, 2004), ISO 7730 (ISO, 2005) and EN15251 (CEN, 2007) where the winter comfort zone is always larger than the summer counterpart. Comprehensive analysis of ASHRAE project (de Dear & Brager, 1998) also indicated 6.9 K as the comfort range for 80% acceptability.

3.2.5 Other comfort-related issues

3.2.5.1 PMV and TSV, expectancy factor

Fanger and Tøftum (2002) proposed some corrections to make the PMV-PPD model applicable in non-AC buildings in warm climates. Their corrections adjust subject's metabolic rates by a reduction of 6.7% for every scale unit of PMV above neutral. A corrected PMV value is recalculated by using this reduced metabolic rate. The corrected PMV value is believed capable to predict occupants' thermal sensation in warm climates if it is multiplied by an appropriate expectancy factor e (e varies from 0.5 to 1 – depending on the climate and the popularity of AC buildings in the region).

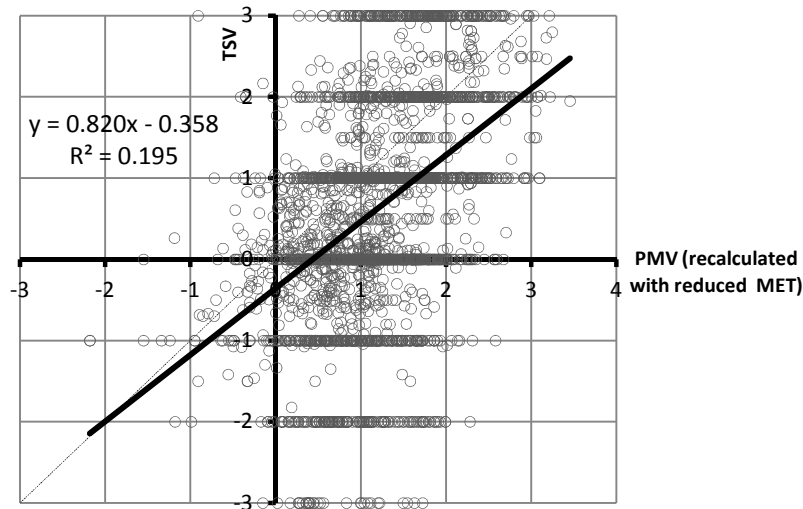


Figure 3-10: Corrected PMV versus thermal sensation vote in warm climate

The corrected PMV and its applicability were examined in the present study. Figure 3-10 shows the linear regression corrected PMV versus actual thermal sensation vote (TSV). In this analysis, 2708 observations of class I and class II surveys with $T_{i,o}$ greater than 26°C were included (these observations have all required variables allowing to recalculate PMV index). The achieved regression equation ($R^2 = 0.195$) is:

$$TSV = 0.82PMV - 0.358 \quad (3.4)$$

It can be seen that the constant term of the equation (3.4) is not small enough to be ignored and also the correlation is fairly low. Therefore an expectancy factor e cannot be derived. The author argues that human thermal response is a very complex phenomenon, continuously changed and governed by many objective and subjective factors, thus it cannot

be simply predicted by adding a corrected factor e to the PMV-PPD model. Thus the application of corrected PMV-PPD model in this climatic region is not recommended.

3.2.5.2 Other issues related to comfort temperature and adaptive mechanism

To clarify some other comfort-related issues, 7 statistical significance tests on the correlations of objective parameters and their attributes were done. The test results were reported in Table 3-4. It's worth noting that a statistically significant test does not confirm a strong correlation or a large difference, but only gives a proof of the existing correlation or difference.

Table 3-4: Results of some statistical significance tests of some parameters and variables' attributes in NV buildings

First variable	Second variable	Number of observations	Item to be tested	Statistical test method	Mean or observed value of the item to be tested	P-value*
Gender Male	Gender Female	Female: 1071 Male: 912	Difference of mean comfort temperature	Two independent samples T-test	Female: 27.39 °C Male: 27.24 °C	0.710
Operative temperature	Clothing insulation	3047	Correlation	Simple linear regression test	$Clo = -0.268T_{i,o} + 1.264$ ($R^2 = 0.1321$)	0.000
Relative humidity	Subject's comfort temperature	3054	Correlation	Simple linear regression test	$T_{comf} = 0.073RH + 22.77$ ($R^2 = 0.056$)	0.000
Air velocity	Subject's comfort temperature	2957	Correlation	Simple linear regression test	$T_{comf} = 0.670V_a + 27.666$ ($R^2 = 0.0029$)	0.003
Air velocity	Operative temperature	3058	Correlation	Simple linear regression test	$V_a = 0.006T_{i,o} + 0.081$ ($R^2 = 0.0037$)	0.001
Time taking questionnaire: before 12:00	Time taking questionnaire: after 12:00	Before: 416 After: 1574	Difference of mean comfort temperature	Two independent samples T-test	Before: 27.26 °C After: 27.40 °C	0.360
Subjects' age over 25	Subjects' age under 25	Over: 665 Under: 1308	Difference of mean comfort temperature	Two independent samples T-test	Over: 27.62 °C Under: 27.24 °C	0.004

* The significance threshold is 0.01

From Table 3-4, it can be seen that male and female subjects almost have the same comfort temperature since the difference was not statistically significant ($P = 0.71 > 0.01$).

Similarly, subjects' comfort temperature was not significantly different in the morning and afternoon ($P = 0.36 > 0.01$) that is quite consistent with the results from earlier studies (Fanger, et al., 1974; Nielsen, 1974 (result reported by Fanger P.O.)). This indicates that the same thermal comfort conditions can be applied from the morning to the evening. The analysis of subject's age and comfort temperature give evidence that older subjects tend to prefer slightly warmer environment.

Statistically significant correlations between clothing insulation, air velocity and operative temperature gave an evidence of subjects' adaptations. As temperature increases, subjects tend to turn on the fans or to open the windows along with wearing lighter clothing. Among these adaptive actions, changing clothing seems to be more common and more effective ($R^2 = 0.132$). Table 3-4 also shows statistically significant correlations between air velocity, humidity and comfort temperature although these relations are very weak (very low R^2). This reveals that air velocity and humidity played a minor role in subjects' comfort temperature.

3.3 Model validation under conditions of Vietnam

The adaptive thermal comfort model given by equation (3.3) based on field surveys around South-East Asia has a great potential to apply for Vietnamese since Vietnam locates in the center of this region and has a similar climate and cultural background. However, for scientific purposes this comfort model needs to be checked before applying for Vietnamese. In another way, this study will examine whether Vietnamese and people living in South-East Asia have similar thermal preference and comfort temperature.

3.3.1 The thermal comfort survey in Vietnam

A transverse comfort survey was conducted in April (spring), May and June (summer) 2012 in Danang, Vietnam. The survey was conducted in six independent days and was evenly distributed in 3 months, thus twice a month. As the aim of this comfort survey was to validate the adaptive thermal comfort model in (3.3), a large number of subjective comfort responses is needed. Therefore, the survey was designed to be conducted in NV classrooms and libraries where many students in the universities of Danang could take part in. Totally, there were over 1200 students who took part in the survey from which 1198 qualified responses were derived. All responses are independent as the students were from

different institutions and belong to different classes. Assuming that the thermal condition in a classroom was uniform, each classroom will give a unique mean thermal sensation vote corresponding to a specific indoor condition. This method is expected to be able to eliminate bias responses which might be observed in field surveys.

Class III protocols for a thermal comfort field study (de Dear, et al., 1997) were followed while measuring the indoor environment. Indoor variables measured were air temperature, surface temperature, relative humidity, and air velocity. Mean radiant temperature was calculated from the measured temperature of surrounding walls and surfaces and their angle factors with respect to the occupant's seat in the class. This method was recommended by ASHRAE (2009) and Fanger (1982). Operative temperature was then calculated from air and mean radiant temperature by the method of ASHRAE (2004). A set of hand held digital instruments was employed to measure indoor environmental variables as listed in Table 3-5 and in Figure 3-11.



Figure 3-11: Measuring equipments used and class room arrangement in the survey (The downward arrow indicates the position of the data logger in the middle of the classroom).

Although the Infrared thermometer HI 9950 and Anemometer LCA6000 were not calibrated due to limited local facilities, they were well preserved under the laboratory standard and still in good working order. HOB0 Data loggers were calibrated themselves as being preprogrammed and by comparing the recorded data among 3 Data loggers. The loggers were placed on the working table of students at the height of 0.85m above the floor in at least 45 minutes before delivering the questionnaires. They were preprogrammed to record data every 5 minutes and used values are the means of the records. Other measurements were taken place 3 times and average values were then calculated.

Table 3-5: Technical specifications of measuring instruments

Measuring variables	Name of instrument	Measurement range	Resolution	Accuracy	Country of origin
Temperature & Humidity	HOBO U12 External Data Logger	5 to 95% -20 to 70°C	0.03°C and 0.03%	±2.5% and ±0.35°C	U.S.A
Mean radiant temperature	Hanna Infrared thermometer HI 9950	-10 to 300°C	1°C	±2% of reading or ±2°C	Romania
Wind velocity	Air flow anemometer LCA 6000	0.1 to 20 m/s	0.01m/s	± 1% of reading or ± 1 digit	U.K.

A simple questionnaire was specifically designed for the validation purpose of the survey which needs a large number of respondents. Questionnaires were delivered by the author right after the courses and students were asked to carefully give their actual thermal sensation vote on the ASHRAE seven-point scale with ‘hot, warm, slightly warm, neutral, slightly cool, cool, cold’ (correspond to ‘nóng, ấm, hơi ấm, trung tính, hơi mát, mát, lạnh’ in Vietnamese) numbered from 3 to –3. They were then asked to provide some personal information such as their age, gender, weight and their location in the room. Figure 3-12 shows a sample of the original questionnaire in Vietnamese. Under this compact form, the questionnaire requires about 2 minutes to complete. As being expected, most students were pleased to fill the questionnaire with little effort for explanation.



Université
de Liège

PHIẾU ĐIỀU TRA CẢM GIÁC NHIỆT
của người Việt Nam trong công trình xây dựng



D BACH KHOA

Bạn hãy cho biết cảm giác nhiệt của bạn vào thời điểm này bằng cách khoanh tròn **một và chỉ một** trị số tương ứng với cảm giác nhiệt của bạn (một trong số bảy giá trị -3 ; -2 ; -1 ; 0 ; 1 ; 2 và 3)

-3 Lạnh (Cold)	-2 Mát (Cool)	-1 Hơi mát (Slightly cool)	0 Trung tính (Neutral)	1 Hơi ấm (Slightly warm)	2 Ấm (Warm)	3 Nóng (Hot)
-----------------------------	----------------------------	---	-------------------------------------	---------------------------------------	--------------------------	---------------------------

Bạn cung cấp thêm một số thông tin sau:

<ul style="list-style-type: none"> - Giới tính: <input type="checkbox"/> Nam <input type="checkbox"/> Nữ - Tuổi của bạn: tuổi - Cân nặng:..... kg (ước tính) 	<p>Vị trí tương đối của bạn trong lớp học (chấm tròn ● lên sơ đồ bên dưới):</p> <p style="text-align: center;">Bảng đen</p> <div style="border: 1px solid black; width: 100px; height: 100px; margin: 0 auto;"></div>
--	---

Cảm ơn bạn đã cộng tác với chúng tôi để hoàn thành công việc này.

Figure 3-12: Screen shot of the questionnaire (in Vietnamese) used in the survey

3.3.2 Survey data and validation results

Table 3-6: Statistical results of the survey

Date Time	Air temp. °C	Mean radiant temp. °C	Wind speed m/s	RH %	Operative temp. °C	Mean TSV	Sample size	Mean monthly outdoor °C
10 April 08h45	27.92	28.10	0.65	71.86	27.97	-0.164	67	28.7
09h50	29.14	27.88	0.20	64.32	28.55	0.286	70	28.7
13h50	33.02	32.79	0.20	59.53	32.91	1.488	90	28.7
15h05	32.30	32.05	0.18	63.13	32.18	1.396	89	28.7
23 April 08h00	28.54	28.21	0.30	75.25	28.41	0.228	57	28.7
09h50	31.50	30.72	0.15	68.99	31.11	1.432	81	28.7
13h49	32.88	32.35	0.15	65.43	32.62	1.505	95	28.7
14h49	29.66	29.10	0.25	72.78	29.41	0.400	45	28.7
10 May 08h10	31.85	30.85	0.20	64.00	31.40	1.000	39	30.2
09h25	32.30	30.80	0.20	63.50	31.55	1.431	65	30.2
13h40	31.15	31.56	0.45	65.43	31.31	1.195	41	30.2
14h25	31.3	31.75	0.50	52.50	31.48	1.206	68	30.2
21 May 09h20	32.65	31.08	0.20	56.00	31.89	1.489	47	30.2
10h17	33.40	30.99	0.30	53.00	32.32	1.800	40	30.2
14h32	32.60	31.52	0.35	62.00	32.17	1.222	27	30.2
16h05	32.10	31.08	0.15	62.00	31.59	0.375	32	30.2
11 June 08h25	32.92	31.75	0.30	57.00	32.42	0.730	37	30.7
09h55	34.41	33.00	0.30	51.00	33.81	1.342	38	30.7
14h35	34.05	32.46	0.30	55.00	33.37	2.216	23	30.7
15h27	35.24	33.92	0.20	54.00	34.60	2.167	42	30.7
21 June 09h22	31.77	30.06	0.25	59.00	30.96	1.067	15	30.7
10h50	33.21	32.24	0.10	55.00	32.72	1.900	10	30.7
14h27	32.67	31.50	0.20	64.00	32.09	0.300	30	30.7
15h25	32.76	31.28	0.25	69.00	32.06	1.160	50	30.7
Max	35.24	33.92	0.65	75.25	34.60	2.216	95.00	
Mean	32.24	31.13	0.26	61.82	31.73	1.132	49.92	
Min	27.92	27.88	0.10	51.00	27.97	-0.164	10.00	
Standard deviation	1.80	1.54	0.12	6.78	1.66	0.632	23.70	

During 3 months of the campaign, hourly outdoor temperature and humidity were obtained by recorded data from a National Meteorological Station and from a self-manufactured station in Danang city. From these data, the monthly mean outdoor temperature can be calculated easily.

Results in detail and related statistic of the survey are presented in Table 3-6. Due to space constraints, some details of the survey (e.g. room number; gender, age and weight of the subjects) were omitted. The mean monthly temperature in the table is calculated from mean daily maximum and minimum air temperature given by the National Meteorological Station. It can be seen that the survey was designed so that 8 classes were investigated each month and the surveys were conducted around the 10th and the 20th of each month. This design is aimed to yield both actual mean neutral temperature for the whole period and adaptive comfort temperature of each month.

3.3.2.1 Comparison of Neutral operative temperature

This comparison gives a general idea about the similitude or difference between the thermal preference of Vietnamese and that of people in South-East Asia. The weighted linear regression described in section 3.2.1 (the sample size was taken into account) between operative temperature and thermal sensation votes was used and the result was presented in Figure 3-13.

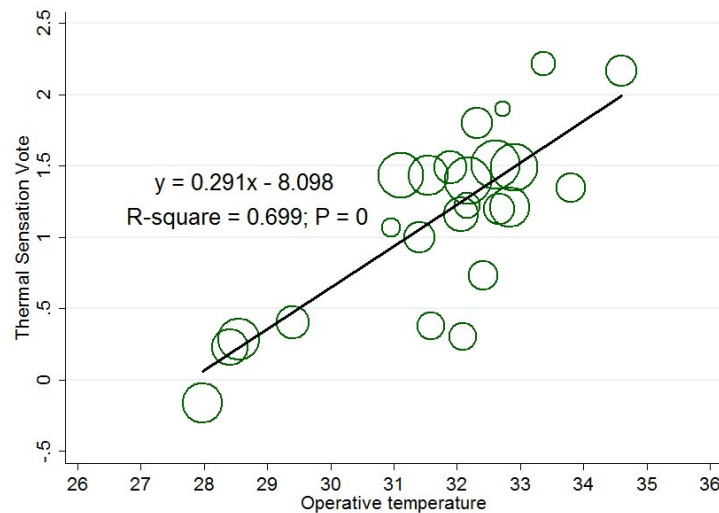


Figure 3-13: Weighted regression between Operative temperature and Thermal Sensation Vote in NV buildings in Vietnam. Each point represents mean thermal sensation vote of a class (Smallest and largest sample sizes are 10 and 95, respectively)

It can be seen that the correlation is significant ($P = 0$) and fairly robust ($R^2 = 0.7$). The coefficient of correlation R^2 was slightly lower than that of South East Asia. The reason may be that the survey in Vietnam was conducted on groups of people rather than on each individual; thus the responses were less precise. However, this method is suitable for the validation purpose as it allows researcher to collect numerous observations and mean thermal sensation votes of larger groups shortly. The neutral operative temperature obtained from the regression equation is 27.83°C . This neutral temperature is almost identical with that of South-East Asia (27.91°C), revealing that Vietnamese and people in South-East Asia almost have similar thermal preference.

3.3.2.2 Comparison of predicted and observed adaptive comfort temperature

Comfort temperature corresponding to each month was derived from regression analysis. Figure 3-14 shows the linear regressions of April, May and June. It can be seen that very small temperature ranges of May leads to low correlation R^2 of 0.26. Consequently, observed comfort temperature of May seems less reliable, compared with those of April and June.

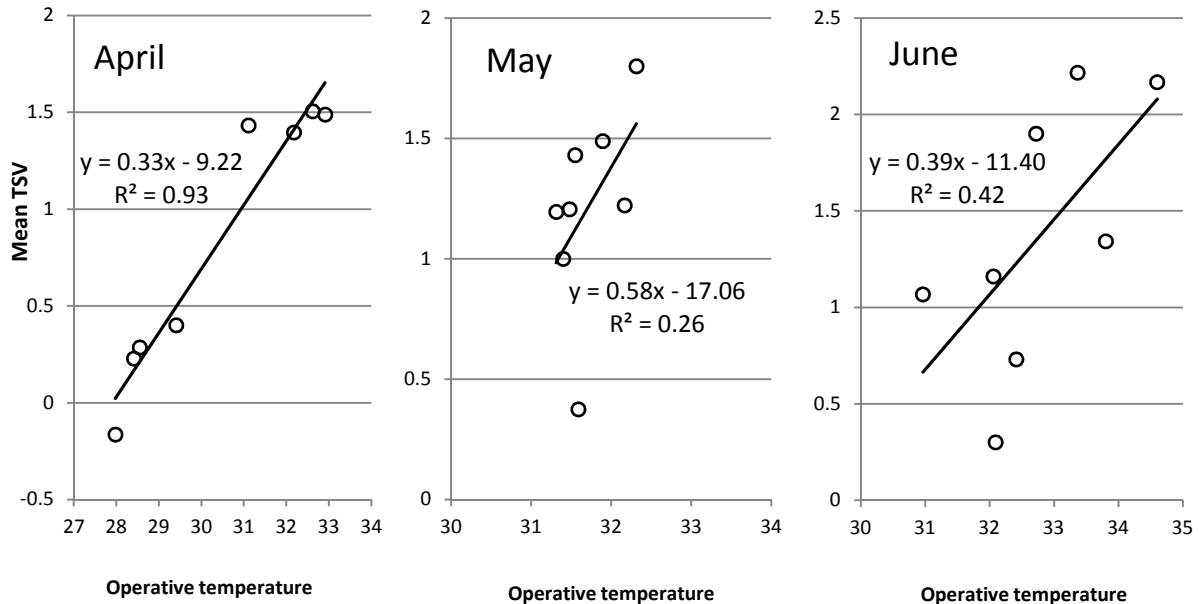


Figure 3-14: Observed neutral operative temperature corresponding to each month by linear regression. Each point represents mean vote of a class

Comparison between observed comfort temperature in Figure 3-14 and comfort temperature predicted by equation (3.3) is reported in Table 3-7.

Table 3-7: Comparison between predicted and observed comfort temperature

Month	Mean outdoor temperature °C	Predicted comfort temperature °C	Observed comfort temperature °C	Difference °C	Relative difference %
April 2012	28.7	28.6	27.9	0.7	2.4
May 2012	30.2	29.1	29.6	-0.5	-1.7
June 2012	30.7	29.3	29.3	0.0	0.0

It can be seen that the predicted and observed comfort temperatures were slightly different. Maximum deviations were only 0.7°C or 2.4%. So the adaptive model of South-East Asia successfully predicted comfort temperatures of Vietnamese in April, May and June.

Due to the limited time budget in Vietnam, this survey only achieves the adaptive comfort temperatures of April, May and June. For more reliable comparison, those of cold and cool periods from October to February should be obtained. Nevertheless, both similar neutral operative temperature and adaptive comfort temperature adequately proved that the adaptive model of South-East Asia is applicable in Vietnam.

3.4 Long-term evaluation of the general thermal comfort condition

Fanger's PMV-PPD comfort model is used to predict occupant's thermal sensation corresponding to an instantaneous thermal condition. The comfort indicators of Fanger's model are PMV and PPD indices. They have been proved to be satisfactory in predicting thermal sensation and comfort in AC buildings.

The adaptive comfort model for South-East Asia is, in fact, not used to predict thermal sensation, but to prescribe an operative temperature range within which most people will feel thermally acceptable. This temperature range is the basis of thermal comfort assessment in NV buildings.

In order to assess thermal conditions of a space during a period of time (e.g. a month, a year), the summation of these comfort indices should be used. This summation can be derived from calculations of long-term measured values or from the output of a thermal simulation tool. The standard ISO 7730 (ISO, 2005) recommends five methods for this purpose. Based on the requirements of this research, method A and D in ISO 7730 were chosen as follows:

- Method A: During the occupied period of the building, calculate the number of hours or percentage of time during which the operative temperature is outside a specified range of the adaptive comfort model.
- Method D: calculate the mean of hourly PPDs over the occupied period. The lower the mean PPD, the better the thermal condition.

Depended on the thermal comfort model applied in the building, method A or D will be employed. The simulation will be set at 20 time steps per hour to accurately calculate the input for the methods A and D.

3.5 Implementation of the adaptive model into a building simulation program

Recently, to assess thermal condition in a building by numerical simulation, the mathematical algorithm of a thermal comfort model is incorporated into a building thermal simulation program. This integration helps building scientists performing energy analysis and simultaneously determining whether an occupant feels thermally comfortable. As this thesis has to evaluate the thermal environment of both NV and AC buildings, appropriate comfort models must be selected and implemented in a simulation tool. EnergyPlus version 6.0 was selected as the primary building energy simulation tool for the thesis. The advanced features of EnergyPlus 6.0 are reported in section 5.3.1.

In EnergyPlus 6.0, three ‘steady-state’ thermal comfort models are available, including the model of Fanger. Hence PMV and PPD indices were integrated in EnergyPlus outputs. Consequently the assessment of thermal comfort in AC buildings is advantageous.

However, all adaptive comfort models were not ready in this version (adaptive model of ASHRAE 55–2004 and EN15251 are newly accessible in version 7.0); thus the assessment of NV buildings in Vietnam met an obstacle. To overcome this, the thesis used a small trick to implement the adaptive comfort model of South-East Asia into EnergyPlus. This trick is described as follows:

- In a NV thermal zone, an HVAC system was installed. This system was set at extremely low capacity so that its heating and cooling effects do not have any influences on the thermal environment and the amount of energy consumption of the zone.

- The thermostat of the HVAC system was established at upper and lower bounds of the comfort range given by the adaptive comfort model.
- ‘Time heating setpoint not met’ and ‘Time cooling setpoint not met’ were called from the output dictionary of EnergyPlus. These outputs are only available if the thermal zone is equipped with an HVAC system. These outputs will give total time (in hours) temperature of the zone is above or below the thermostat setpoints, corresponding to the total time thermal comfort is not satisfied.

With these techniques, EnergyPlus can solve all the questions that this research has to deal with. Tested simulation runs indicated that the results were quite satisfied.

3.6 Chapter conclusion

This chapter discusses the thermal comfort models for Vietnamese. These models are used to assess the thermal environment in AC and NV buildings in subsequent sections of the thesis. Both steady-state comfort model and adaptive comfort model were discussed and their applications were recommended. In section 3.1, the comfort model of Fanger (1970) was decided for application in AC buildings based on reliable scientific evidences.

Section 3.2 presents a full description of an adaptive comfort study for South-East Asia. Meta-analysis was performed on field observations collected from field surveys conducted around South-East Asia. While some studies assumed a minor role of “Griffiths constant” in the establishment of the adaptive comfort equation, this thesis gives proofs of its crucial role. Consequently, it must be chosen with much care. The adaptive equation obtained from the present study is rather similar to some other standards although the methods used were not identical. The resulted comfort equation is:

$$T_{comf} = 0.341T_{out} + 18.83$$

The study also found that at rather high temperature and humidity, adaptive actions do not seem very effective and the comfort range is, consequently, slightly smaller than that under more favorable conditions. The statistically significant correlation between temperature and wind velocity as well as clothing insulation gave strong proofs of occupant’s adaptation. Under hot and humid conditions, the neutral ambient temperature in NV buildings is nearly 2°C higher than that in AC buildings. However, the same neutral SET* in these buildings gave some proofs that this deviation mainly came from various

behavioral adaptations of occupants. Under favorable conditions, the difference between neutral operative temperature in NV and AC buildings might become minor, as the case of Guangzhou in mild seasons.

In the standard condition (pressure at sea level with 50% RH, still air at 0.1 to 0.15 m/s and standard clothing for a given activity), neutral SET* in NV and AC buildings was 25.5°C to 25.7°C. This indicates that people living in South-East Asia and around the world have the same neutral SET*; in other word, their thermal preferences are identical. Different neutral operative temperatures were possibly caused by various occupants' adaptive actions in NV buildings.

This thesis carefully examined the relationship between predicted PMV and actual TSV in NV buildings and did not recommend the application of PMV-PPD model for similar comfort studies, even if this model is adjusted by some corrections.

In section 3.3, the developed adaptive comfort model has been carefully validated by the result from the field survey in April, May and June 2012 in Vietnam. The study compared mean neutral operative temperature, adaptive comfort temperature of Vietnamese with those of people in South-East Asia. The validation result indicates that this model is quite satisfactory for applications in Vietnam. Finally, a special technique was successfully used to incorporate this adaptive comfort model into EnergyPlus 6.0 program for long-term thermal comfort evaluations in NV buildings.

Since our recorded observations in NV buildings mainly had the mean outdoor temperature range from 24°C to 30°C, the present results should be extended by other surveys in various conditions under 24°C or above 30°C. Such surveys would give more consistent proofs about subject's thermal sensitivity, its relationship to the temperature range and outdoor conditions.

CHAPTER 4

CLIMATE ANALYSIS

Since ancient times man has built his own shelter in different ways through observations of the climate and the innovation of diverse construction technologies. Architectural differences observed throughout the world are mainly originated from the diversities of the climate. The climate is therefore among the most influenced factors in building design and operation. Climate responsive architecture, of course, requires rich knowledge of the climate and other conditions of the site, e.g. available building materials, construction techniques. This chapter will provide an introduction about the climate in different regions of Vietnam. Some climate analysis methods are then employed to derive preliminary recommendations for building design. As an easy approach for architects, a simple method of climate-comfort analysis developed by the author will also be presented in detail in this chapter.

4.1 An overview about the climate of Vietnam

4.1.1 Climatic regions in Vietnam

The territory of Vietnam is located in the South-East edge of the Asian continent, bordering the East Sea (a part of the Pacific Ocean). It stretches from 23°22' to 8°30' North latitude and from 102° to 110° East longitude and covers an area of approximately 331210 km² (see Figure 4-1). The whole territory of Vietnam is located in the tropics (within 24° North and South latitudes), giving high annual average temperature and solar radiation throughout the territory.

Two-third of Vietnam is covered by mountains and highlands. The plains are narrow and stretch along the sea shore. These geographical natures combining with trade winds generate plenty of rain over the country. Rainfall of most regions well exceeds 1000 mm per

year. High rainfall and solar radiation also make the air very humid with an average humidity range of 77 - 87%.

The climate of Vietnam is strongly influenced by trade winds which often blows at low latitudes. In winter (December, January and February), the Northern part of Vietnam is often influenced by cold wind blowing from the Siberian region, creating fairly cold and dry weather. In the remaining period of the year, the wind mainly blows from the sea, bringing rain into the mainland.

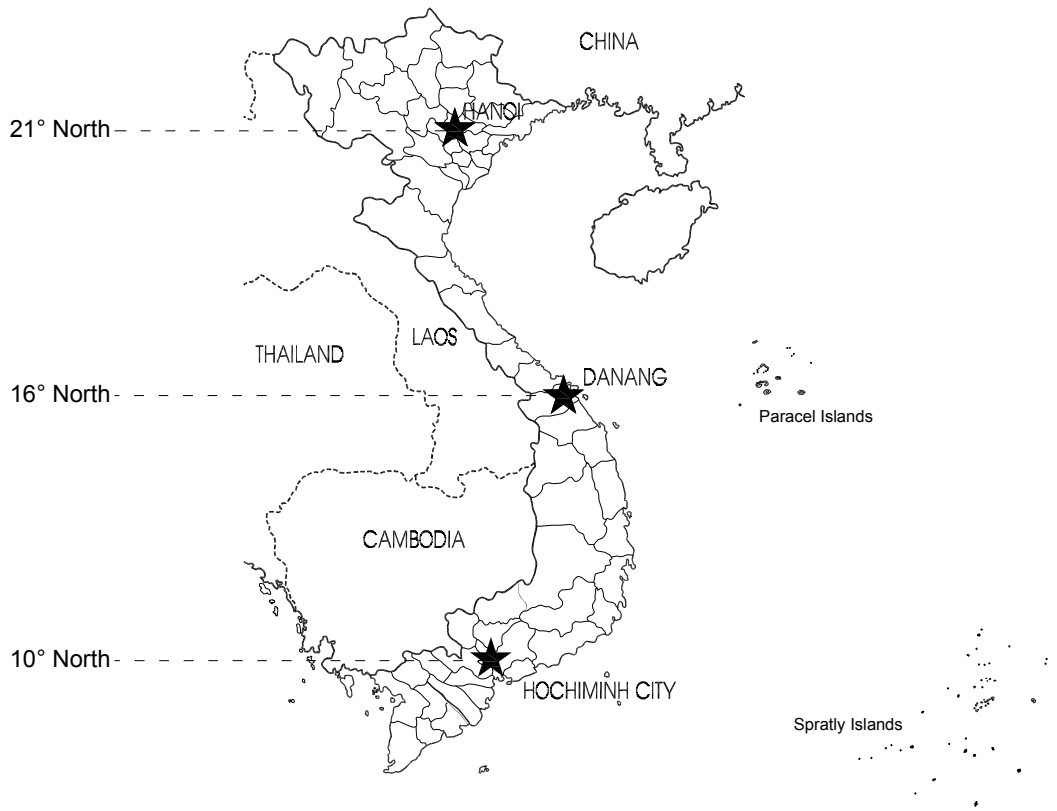


Figure 4-1: The map of Vietnam and three selected sites for this study

In general, Vietnam is considered having a tropical monsoon climate (Institute of Construction Science and Technology, 2009). The Vietnam Building Code (volume III) has divided Vietnam into two main climatic regions:

- The Northern climatic region (from 16° North latitude up): a tropical monsoon climate with cold winters.
- The Southern climatic region (from 16° North latitude down): a typical tropical monsoon climate with high temperature all year round. There are a rainy season (from May to October) and a dry season (from November to April).

These two climatic regions are even divided into smaller sub-climatic regions. However, according to Köppen – Geiger climate classification system (Köppen & Geiger, 1936) (updated version (Peel, et al., 2007)) Vietnam was divided into 3 separate climatic regions: C_{wa}, A_m, A_w in the North, Centre and the South, respectively (see Figure 4-2):

- The humid subtropical climate in the North: cold dry winter, hot wet summer,
- The tropical monsoon climate in the Centre: short dry seasons,
- The tropical wet and dry climate (or tropical savanna climate) in the South: hot and wet summer, hot and dry in remaining periods.

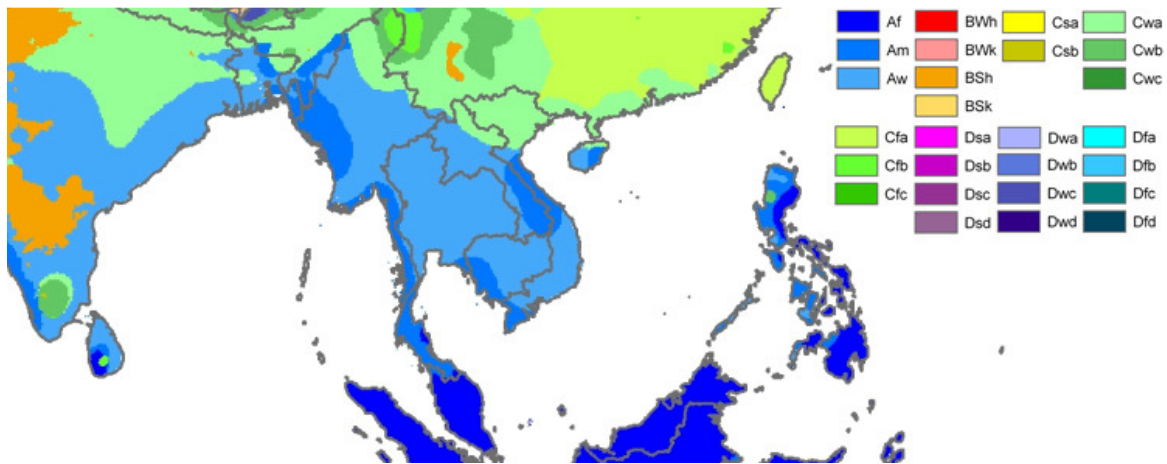


Figure 4-2: Köppen - Geiger climate classification map for Vietnam (see (Peel, et al., 2007) for the legend of other climatic regions)

The Köppen – Geiger classification seems more appropriate for the case of Vietnam because the territory of Vietnam is quite long. The Centre of Vietnam has a different climate pattern with which the rainy season drops into winter (in contrast with other regions) and hot dry Föhn wind and tropical storms often occur in summer. It should therefore be considered to be a separated climatic region. In his book, based on a detailed analysis, Pham (2002) also concluded that there were 3 climate types corresponding to 3 regions of Vietnam, as Köppen – Geiger proposed. Hence, in this work three typical sites, including Hanoi (21° North), Danang (16° North) and Hochiminh city (10° North) which represent three climatic regions in the North, the Centre and the South of Vietnam, have been selected (see Figure 4-1). These sites were selected because they are located at the centers of these climatic regions. Another more important reason of this selection is that detailed weather data (e.g. typical meteorological weather data, long-term statistical data) of these sites are readily available, making the next steps of the study feasible. Other choices hardly satisfy these requirements.

4.1.2 Characteristics of the climate of three climatic regions of Vietnam

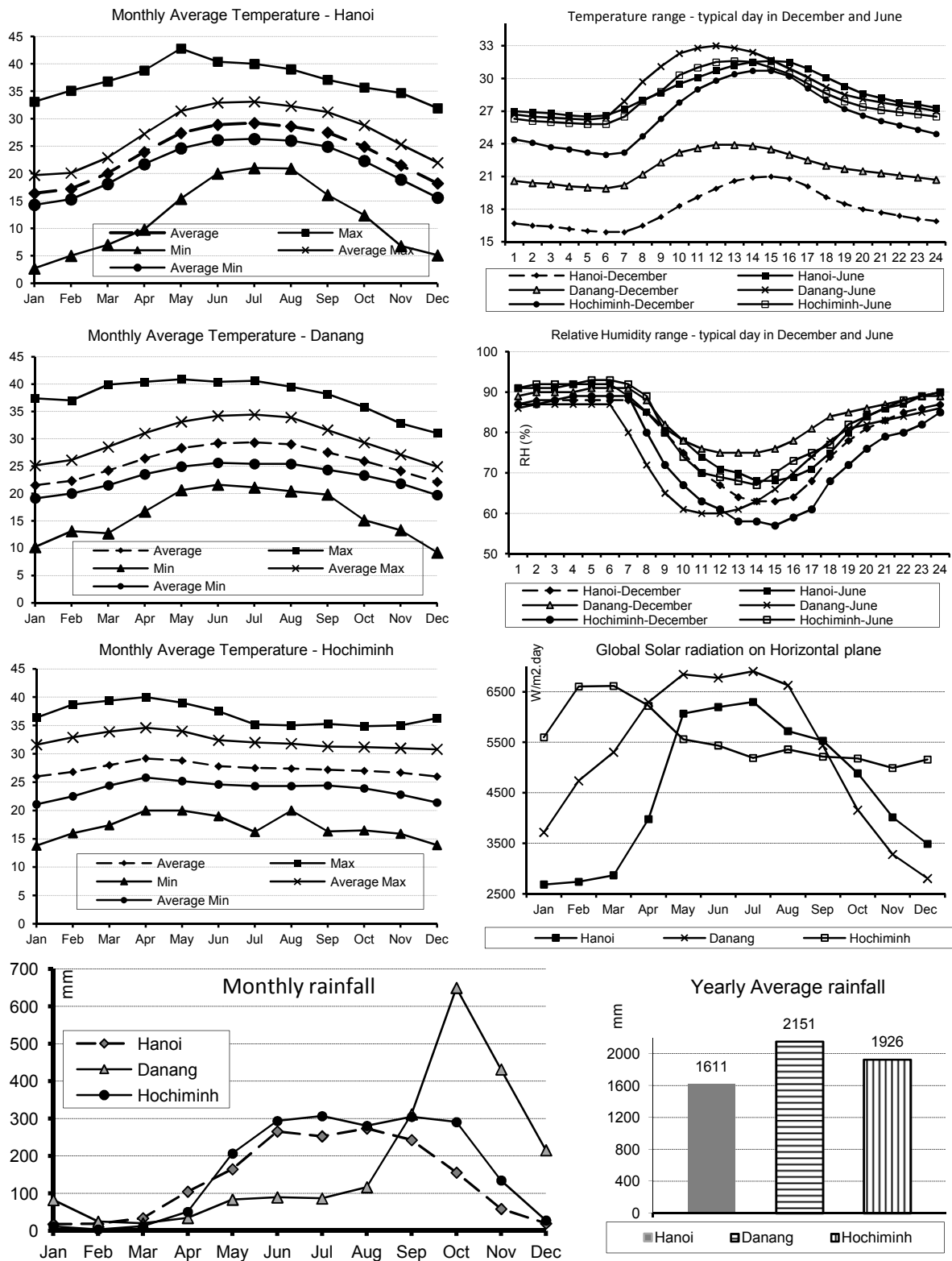


Figure 4-3: Statistical temperature, humidity, solar radiation and rainfall of selected sites

The climatic data of Hanoi, Danang and Hochiminh city were preliminary examined. All the data used in this analysis were derived from Vietnam Building Code 2009 (Institute of Construction Science and Technology, 2009). Data in this Code are based on monitoring records over several years from Meteorological stations of Vietnam General department of Hydrometeorology. Weather conditions in December and June, representing winter and summer periods, were chosen for the analysis and comparison.

Figure 4-3 shows statistical climatic data of three selected sites. It can be seen that that all locations have very high solar radiation, relative humidity and average yearly rainfall. Notably, Hanoi has three cold months during which average temperature drops below 20°C. Temperature in Danang and Hochiminh city is usually stable and high. Rainfall in Danang clearly differs from that of other locations as it reaches the peak value in October rather than in the mid-summer. In Hochiminh city, solar radiation peaks in February and March instead of in July. The strong solar radiation all year round makes temperature here always high and stable.

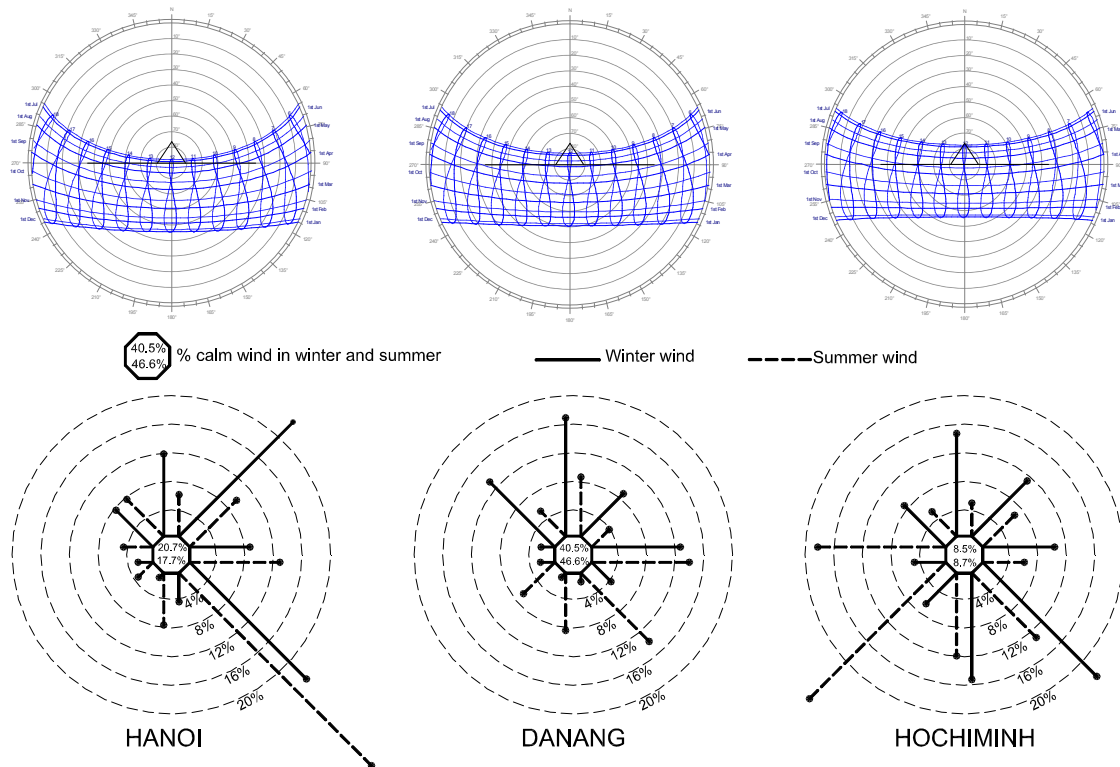


Figure 4-4: Sun chart diagram and wind regimes in the selected sites

In Vietnam, air relative humidity is always high and reaches around 90% at nights. The daily amplitude of temperature variation is quite small and almost below 7°C, even in

summer. This is because high relative humidity and the cloudy sky play the role of a "blanket", preventing radiation heat loss from the earth and consequently preventing air temperature from dropping much further.

The Sun path and wind regime in Vietnam are illustrated in Figure 4-4. It is clear that the Sun mainly moves on the South sky of the observation points, making South shading devices much more essential than North counterparts. Cold (winter) wind mainly blows from the North and North-East while cool (summer) wind comes from the East, South-East and South-West. As the wind regime is the most crucial factor in natural ventilation, the design of NV buildings should maximize the cool wind and avoid cold wind.

It is also necessary to emphasize the following climatic features of these sites:

- Hanoi has cold winters, but the lowest temperature hardly falls below 5°C. Protection from cold wind is required in winter. The highest temperature may reach 40°C. Temperature and humidity are generally moderate. Rainfall as well as rain intensity are significant, but Hanoi is rarely affected by tropical storms.

- In Danang, the climate is tropical with monsoons. The winter is not cold and the lowest temperature is often well above 15°C, thus protection from the cold is not essential. The highest temperature may exceed 40°C. Because of the impacts of the sea, daily and yearly temperature ranges are quite small. Coastal parts are directly influenced by strong tropical storms and rainfall often peaks in October, making appropriate roofing essential.

- Hochiminh city has a hot and humid climate with monsoons all year round. There are only two annual contrasting seasons; dry and wet, both consistent with two inhomogeneous monsoons in the region. Rainfall is quite high. Air temperature and solar radiation are constantly high all year which indicates that cooling is in demand. Wind is abundant all year round and this resource can be exploited for passive cooling purposes, especially during overheating periods.

4.2 Climate analyses using methods developed by some authors

Profound understanding of the local climate is the main requirement for the design of climate responsive architecture towards sustainable development. Statistical climatic data in the previous section only provide general information about the climates. Nevertheless, researchers, designers and engineers usually need much more detailed and helpful analysis

and guidelines for their specific tasks rather than relying completely on statistical climatic data from other providers. Climate analysis tools developed for this specific purpose are therefore essential. This section analyzes the climates of three climatic regions of Vietnam using two common methods developed earlier by other authors.

4.2.1 Climate analysis by Climate Consultant 5.3 program

Climate Consultant 5.3 (UCLA, 2011) is the analysis tool developed by UCLA Energy Design Tools Group. This program only accepts Typical Meteorological Year (TMY) weather files as the input and presents the output in form of graphical illustrations. The latest version of Climate Consultant evaluates a climate based on four thermal comfort models (ASHRAE standard 55 using the PMV index and the adaptive theory, ASHRAE Handbook 2005 comfort model, California Energy code Comfort model). The results given by these comfort models may be significantly different. Table 4-1 presents the most important results given by Climate Consultant 5.3 using the PMV comfort model (The adaptive comfort model in this program is not suitable for hot humid climates). The comfort periods predicted by this tool are significantly poor. The climates of Danang and Hochiminh city only provide comfort within 1% and 0.4% of a year. A little bit higher, the climate of Hanoi is comfortable during 4.9% of a year. As explained in section 4.3, these predictions are unacceptable, compared with the reality. This failure is caused by stringent humidity requirements of ASHRAE standard 55 which are more suitable for temperate climates.

Table 4-1: Comfort of the climates of Vietnam and corresponding design guidelines proposed by Climate Consultant 5.3

Regions	Comfort	Recommended design strategies in number (see legends below)
Hanoi	4.9%	14, 17, 18, 19, 32, 35, 37, 38, 39, 40, 42, 43, 46, 59, 65, 68, 4, 26, 30, 16
Danang	1%	14, 17, 18, 19, 32, 35, 37, 38, 39, 40, 42, 43, 46, 59, 65, 68, 25, 56, 57, 16
Hochiminh city	0.4%	14, 17, 18, 19, 32, 35, 37, 38, 39, 40, 42, 43, 46, 59, 65, 68, 25, 56, 57, 27
Legend		
4	Extra insulation (super insulation) might prove cost effective, and will increase occupant comfort by keeping indoor temperature more uniform.	
14	Locate garages or storage areas on the side of the building facing the coldest wind to help insulate.	
16	Trees (neither conifer nor deciduous) should not be planted in front of passive solar windows, but rather beyond 45 degrees from each corner.	
17	Use plant materials (ivy, bushes, and trees) especially on the west to shade the structure (if summer rains support native plant growth).	
18	Keep the building small (right-sized) because excessive floor area wastes heating and cooling energy.	
19	For passive solar heating face most of the glass area south to maximize winter sun exposure, but design	

- overhangs to fully shade in summer.
- 25** In wet climates well ventilated pitched roofs work well to shed rain and can be extended to protect entries, outdoor porches, and verandas.
 - 26** A radiant barrier (shiny foil) will help reduce radiated heat gain through the roof in hot climates.
 - 27** If soil is moist, raise building high above ground to minimize dampness and maximize natural ventilation.
 - 30** High performance glazing on all orientations should prove cost effective (Low-E, insulated frames) in hot clear summer or dark overcast winter.
 - 32** Minimize or eliminate west facing glazing to reduce summer and fall afternoon heat gain.
 - 35** Good natural ventilation can reduce or eliminate air conditioning in warm weather, if windows are well shaded and oriented to prevailing breezes.
 - 37** Window overhangs (designed for this latitude) or operable sunshades (extend in summer, retract in winter) can reduce or eliminate air conditioning.
 - 38** Raising the indoor comfort temperature limit will reduce air conditioning energy consumption (raise thermostat cooling setpoint).
 - 39** A whole-house fan or natural ventilation can store nighttime 'coolth' in high mass interior surfaces, thus reducing or eliminating air conditioning.
 - 40** High mass interior surfaces like stone, brick, tile, or slate, feel naturally cool on hot days and can reduce day-to-night temperature swings.
 - 42** On hot days ceiling fans or indoor air motion can make it seem cooler by at least 2.8°C thus less air conditioning is needed.
 - 43** Use light colored building materials and roofs with high emissivity to minimize conducted heat gain.
 - 46** High Efficiency air conditioner (at least Energy Star) should prove cost effective.
 - 56** Screened porches and patios can provide comfort cooling by ventilation and prevent insect problems.
 - 57** Orient most of the glass to the north, shaded by vertical fins, in very hot climates, if there are essentially no passive solar needs.
 - 59** In this climate air conditioning will always be required, but can be greatly reduced if building design minimizes overheating.
 - 65** Traditional homes in warm humid climates used high ceilings and high operable (French) windows protected by deep overhangs and porches.
 - 68** Traditional homes in hot humid climates used light weight construction with openable walls and shaded outdoor porches, raised above ground.

Considering the recommendations, it is found that design strategies for three climatic regions recommended by this tool are nearly identical. The differences, which are very minor, are highlighted by bold numbers in the Table. Moreover, the recommendations are rather unspecific and mostly common knowledge of architects. They are therefore not very useful for building design.

4.2.2 Climate analysis by Mahoney Tables

Mahoney tables refer to a set of reference tables used to predict preliminary climate responsive design strategies in architecture. Mahoney tables are developed on Spreadsheet without any code embedded and thereby can be reproduced by anyone. Mahoney tables only

require input data on monthly basis; thus facilitating the utilization of architects and engineers. Mahoney tables were first published in 1971 by the United Nations Department of Economic and Social Affairs. This tool consists of six elementary tables. Four of them need climatic data from users, for comparison with the requirements of a prescribed thermal comfort criterion. Appropriate design criteria are then read off from the remaining tables. An introduction of Mahoney tables can be found in (Koenigsberger, et al., 1973).

The author successfully reproduced Mahoney tables under useful instructions from Professor Carl Mahoney. This reproduction was not only aimed to use in the thesis but also to apply in teaching career of the author. The following parts report the analysis results for three climate regions of Vietnam from Mahoney tables. Climatic data imposed on the tables were derived from the reference (Institute of Construction Science and Technology, 2009).

TABLE 3: Recommended specifications					
Indicator totals from table 2					
H1	H2	H3	A1	A2	A3
6	4	12	0	0	2
Layout					
		0-10			X 1
		11, 12		5-12	1
				0-4	2
Spacing					
11, 12					3
2 -10					X 4
0, 1					5
Air movement					
3-12					X 6
1,2		0-5			7
		6-12			8
0	2-12				
	0-1				
Openings					
		0, 1		0	9
		11, 12		0, 1	10
Any other conditions					
					X 11
Walls					
		0 - 2			X 12
		3 - 12			13
Roofs					
		0 - 5			X 14
		6 - 12			15
Outdoor sleeping					
			2 - 12		16
Rain protection					
		3 - 12			X 17

small exceptions. It means that Mahoney tables may fail in providing more detailed information corresponding to a specific climatic region.

Table 4-2: Design strategies recommended by Mahoney tables

	Hanoi	Danang	Hochiminh city
Layout	Orientation North and South (long axis East - West)		
Spacing	Open spacing for breeze penetration, but protection from hot and cold wind		
Air movement	Room single banked, permanent provision for air movement		
Openings	Medium openings, 20 - 40% wall area	Large openings, 40 - 80% wall area	Medium openings, 20 - 40% wall area
Walls and floors	Light walls, short time-lag, low thermal capacity		
Roofs	Light, well-insulated roofs		Light, reflective surface, cavity roof
Outdoor sleeping	None	None	None
Rain protection	Protection from heavy rain necessary		
Position of openings	In North and South walls at body height on windward side		
Protection of openings	Provide protection from rain		
External features	Adequate rainwater drainage		

4.2.3 Discussions

The first method used in the above analysis relies on the climatic data of TMY weather files. The second one even requires more simple inputs in form of average statistics of the meteorological data. These climate tools are considered simple and may provide designers and researchers with useful information. Such information is helpful for educational purposes as well as for preliminary design stages of a project. However, by comparing the results of different climatic regions, it was found that the results were very similar or even nearly identical although these climatic regions are not in the same climate classification category. Another problem is that comfort predictions given by these tools seem incorrect and this failure cannot be fixed by users. These obstacles indicate that a new climate analysis tool developed for hot humid climates of Vietnam is essential.

4.3 An improved climate-comfort analysis method for hot humid climates using a graphical method and TMY weather data sets

It has generally been admitted that application of environmental support tool among design communities in hot humid climates seems rather limited. Wong et al. (1999)

conducted a survey on the application of environmental design tools among designers in Singapore. The results revealed that almost architects examined didn't employ such tools in their works and that architectural consultations accompanied with building scientists are rare. This means that designers are likely hesitant to use sophisticated tools or commercial tools which may impose a burden on their time and budget.

Recently there has been some weather tools developed for climate analysis (Autodesk, 2011; UCLA, 2011). Due to the criteria implemented, these tools are aimed to apply in temperate and cold climates where occupant tends to use HVAC systems more frequently. Under hot humid climates, NV buildings are very common and occupant's comfort criteria may differ significantly. For these reasons, an improved method was developed by the author. This method also allows users to modify the thermal comfort model and algorithms to meet specific requirements or conditions of a climate. The method consists of three steps: (1) proposal of an appropriate comfort zone on the Building psychrometric chart for people living in hot humid climates; (2) extracting and printing of climatic data on this chart; and (3) quantitative analysis and assessment of thermal comfort, heating and cooling potential of passive strategies. Three climatic regions in Vietnam, including Hanoi, Danang and Hochiminh city were investigated as case studies.

4.3.1 Comfort zone for people living in hot humid climates

The comfort zone on the Building psychrometric chart is well known as an important indicator in climatic analysis and in establishing design strategies. The earliest efforts to establish the comfort zone and the building climatic chart could be found in some publications (Yagloglou & Miller, 1925; Olgyay, 1963; Givoni, 1969).

However, it is still an argument that under a specific condition the comfort zone for different climatic regions is unchanged. Based on many comprehensive experiments carried out throughout the world (see section 2.2.3), ASHRAE (2009, p. 9.16) reported that under a steady-state condition, "*people cannot adapt to preferring warmer or colder environments, and therefore the same comfort conditions can likely be applied throughout the world*". However, the conventional comfort zone of ASHRAE (2004) seems inappropriate for Vietnamese because of the fact that it omits the effect of humidity adaptation of people living in hot humid climates. In this standard the upper comfort limit of $0.012 \text{ kg}_{\text{water}}/\text{kg}_{\text{dry-air}}$

is rather stringent because this requirement is hardly satisfied in hot humid climates where the relative humidity usually exceeds 80%.

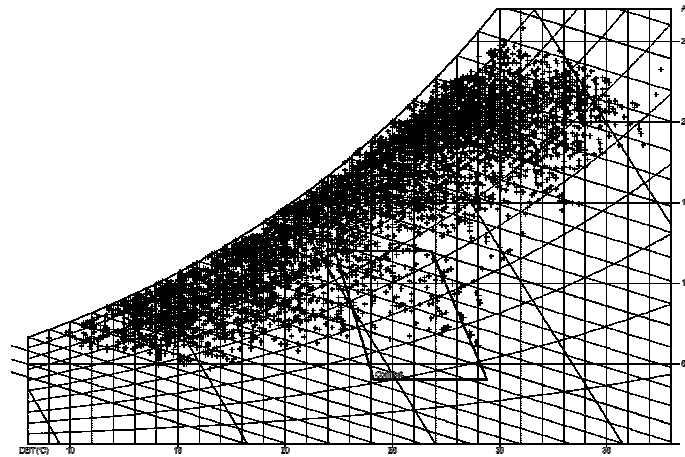


Figure 4-7: Incorrect prediction of the comfort zone for Hanoi by Ecotect (Autodesk, 2011)

Some computer weather tools have failed in predicting a comfortable period of the climates of Vietnam because they used inappropriate comfort boundaries. The comfort zone for Hanoi proposed by Climate Consultant 5.3 (UCLA, 2011) using the comfort model of ASHRAE standard 55 (ASHRAE, 2004) indicates that only 4.9% of total time of a year should be comfortable. Also in Hanoi, Figure 4-7 shows the comfort prediction of another weather tool (Autodesk, 2011) in which method of Szokolay (2004) was adopted. The significant weakness of this method is that a ‘steady-state’ condition was imposed (clothing = 0.57 clo, metabolic rate = 1.25 met), but the ‘adaptive comfort model’ of Auliciems (1981) - $T_{conf} = 17.6 + 0.31T_{out}$ - was employed to find neutral temperature. According to this prediction, only 2.5% of total time in a year is considered to be comfortable. Actual observed percentage of satisfied people is still in question due to the lack of outdoor comfort surveys in Vietnam. However based on the data of 7 comfort surveys in NV buildings in hot humid South-East Asia (Nguyen, et al., 2012), we found that 2113 of 3271 (64.6%) votes were on [-1, 1] and 961 of 3271 (29.4%) votes were on [-0.5, 0.5] of the ASHRAE seven-point scale. These actual percentages of satisfied people of South-East Asia reveal that the predictions given by these computer weather tools (Autodesk, 2011; UCLA, 2011) may significantly underestimate the actual comfort potential of the climates of Vietnam.

In Vietnam air humidity hardly falls below 60% which is around the upper limit of the ASHRAE comfort zone. This indicates that it is essential to create appropriate thermal

comfort boundaries for Vietnamese as well as other people living in the tropics, considering their adaptation to very humid environment. This thesis therefore proposes a revised thermal comfort zone on the psychrometric chart for Vietnamese based on the ‘steady-state’ heat balance theory of Fanger (1970) as shown in Figure 4-8. Field surveys on thermal comfort have pointed out that Fanger’s comfort model worked fine in ‘steady-state’ thermal environment such as that of AC buildings (de Dear & Brager, 2002). In NV buildings, human thermal adaptations and fluctuating thermal stimulus may generate some deviations of occupants’ thermal perception. Hence, the condition for comfort may be extended well beyond the conventional comfort boundaries. This study makes some modifications on the conventional comfort zone by implementing some Control Potential Zones (CPZs). These CPZs are aimed to take human adaptations into account, including: expanding upper humidity limits, varying clothing insulation, cooling by natural ventilation and water evaporation, heating by solar energy. The revised comfort zone and its CPZs may therefore be applied in both NV and AC buildings.

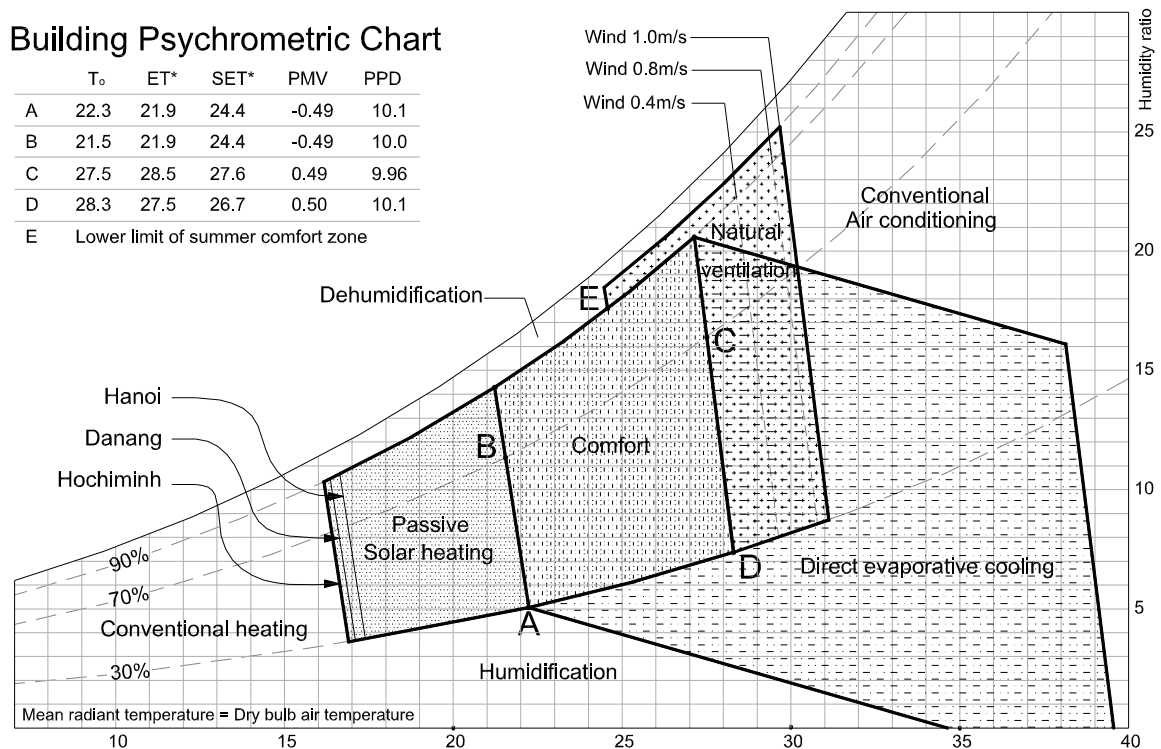


Figure 4-8: Comfort zone proposed for Vietnamese and its control potential zones

The comfort zone in Figure 4-8 is established for a normal person in sedentary work (60 W/m^2) under a still air condition (0.15 m/s). Clothing insulation varies from 0.5 clo to 1

clo, reflecting the change of clothing styles to suit seasonal weather. The environmental condition inside this comfort zone is expected to satisfy 80% of occupants, based on 10% of predicted whole-body dissatisfaction given by the PMV-PPD model and 10% possible dissatisfaction caused by local discomfort, e.g. draught, cold floor, radiant temperature asymmetry.

The cooler and warmer boundaries of the comfort zone - lines AB and CD in Figure 4-8 - are defined by the PMV-PPD indices. Points inside these boundaries would satisfy $-0.5 \leq \text{PMV} \leq 0.5$ and $\text{PPD} \leq 10\%$ correspondingly. Points B and C rely on the 70% RH curve because the PMV-PPD model becomes a little inaccurate at relative humidity higher than 70% (ISO, 2005). These lines nearly coincide with constant effective temperature ET^* lines.

The lower humidity level of the comfort zone in Figure 4-8 was set at 30% relative humidity because it hardly falls below this threshold in humid climates. On the other hand, Vietnamese are not acquainted with the discomforts caused by dry air such as dry nose, throat, eyes, skin, and lip cracks.

The upper humidity limit is more complicated due to the lack of specific studies on this issue. ASHRAE standard (ASHRAE, 2004) specifies the upper humidity ratio limit at $0.012 \text{ kg}_{\text{water}}/\text{kg}_{\text{dry-air}}$. This limit is mainly based on the requirements for hygiene and for avoiding condensation - mold growth in the ducts of HVAC systems (Legacy Resources Management Program, 1990) rather than on human thermal comfort. In fact, in a hot humid climate building surface temperature is normally closed to or higher than ambient air temperature due to solar heat gain, thus the climate itself reduces the potential of condensation and mold growth on building surfaces, allowing a higher acceptable humidity limit.

Olgay (1963) proposed around 78% relative humidity as the upper limit for U.S. inhabitants living in moderate climatic regions. In his book, Givoni (1969) suggested that this upper limit could be enlarged to 90% relative humidity and up to 93% with ventilation. Pham (2002) conducted a small comfort survey in Vietnam in 2002; his results revealed that over 80% of subjects found to be thermally comfortable at $28.5 - 29.5^\circ\text{C}$ and 90% relative humidity. The adaptive comfort theory and standards (Brager & de Dear, 2000; ASHRAE, 2004; CEN, 2007) do not indicate any humidity limit for thermal comfort, provided that adaptive opportunities are allowed. Based on 3054 thermal sensation votes of people living

in hot humid South-East Asia, the correlation and the regression coefficient between relative humidity and comfort temperature was found very low ($T_{comf} = 0.073RH + 22.77$, $R^2 = 0.056$) (Nguyen, et al., 2012), revealing a minor effect of relative humidity on thermal perception. Based on above-mentioned studies and findings, the upper limit of the revised comfort zone was established at 90% relative humidity. During hot weather, this humidity limit may be even extended to 95% under the effect of wind of 0.8 – 1m/s because air movement can eliminate stuffiness and accelerate evaporation of sweat and heat diffusion.

4.3.2 Extended comfort zones using passive cooling and heating strategies

In this study, **indirect** passive cooling and heating strategies (e.g. **indirect** evaporative cooling, thermal mass and night purge, indirect solar heating) were not included as they are related to other building parameters, occupancies and equipments. Hence, only **direct** passive cooling and heating measures which are directly related to the climate were examined in subsequent sections.

4.3.2.1 Passive cooling by natural ventilation

The convective - evaporative heat exchange between a person and surrounding environment is partly influenced by air movement. Extensions of the comfort zone by air movement depends on occupant's clothing, activity and different between skin/clothing and the air temperature. Both ASHRAE standard (ASHRAE, 2004) and ISO 7730 (ISO, 2005) recommend a maximum wind speed of 0.82 m/s for sedentary activity. However, this limit is mainly based on the requirement of stabilization of loose clothing and paper rather than human discomfort caused by draught. A recent field survey on occupants' wind preference in a hot humid climate indicates that the minimal air velocity value obtained based on 80% and 90% acceptability was close to or above 0.8 m/s (Cândido, et al., 2010). It is not difficult to create thermal comfort for a person exposed to wind velocity of 1 m/s (Fanger, 1970) and under overheated conditions air velocity up to 2 m/s may be welcome (Szokolay, 2004). The air movement of 1 m/s is therefore adopted in the CPZ by natural ventilation shown in Figure 4-8. Temperature offset above the warmer limit of the comfort zone by elevated air velocity simply followed the calculation method recommended by these two standards (ASHRAE, 2004; ISO, 2005). Point E lies on the lower summer comfort

boundary corresponding to clothing insulation of 0.5 clo. This extension neglects the effect of humidity on cooling potential of air movement because this effect is rather minor.

4.3.2.2 Passive cooling by Direct evaporative cooling

Direct evaporative cooling is a process where water evaporates directly into the airstream, reducing the air's dry-bulb temperature and raising its humidity, but wet-bulb temperature is always unchanged. In Vietnam, relative humidity usually drops to within 60% - 70% at noon during summer periods (around June, July and August), enabling greater use of evaporative cooling. Particularly, much harsh conditions can be found in some provinces located between Danang and Hanoi where very hot and dry conditions (42 °C and 30% relative humidity) may occur during summer months due to the Föhn wind from Laos. In fact, this cooling method has been widely used for outdoor or industrial environment in Vietnam; thus, its potential should also be investigated.

In direct evaporative cooling, the total heat content of the system does not change, therefore it is said to be adiabatic. Cooling performance of a cooler may be determined:

$$T_{LA} = T_{DB} - (T_{DB} - T_{WB}) * \psi \quad (4.1)$$

where

T_{LA} = Leaving air dry-bulb temperature, °C; T_{DB} = Inlet Dry-bulb temperature, °C; T_{WB} = Inlet wet-bulb temperature, °C; ψ = Efficiency of the evaporative cooler.

A direct evaporative cooler can be completely passive (e.g. water pool, hand sprayer system, water-evaporative wall system, evaporative cooler driven by solar energy), partly passive (e.g. evaporative electric fan) or active (e.g. swamp cooler). The cooler efficiency usually runs between 80% and 90%. Under a typical operating condition, an evaporative cooler will nearly always deliver the air cooler than 27°C. A typical residential swamp cooler in good working order should cool the air to within 3°C – 4°C of the wet-bulb temperature (The Philippine builder, 2012). Primarily based on previous experiments of other authors, Givoni (1994) stated that ambient air can be cooled by 70–80% of the dry-bulb - wet-bulb difference. This observation led him to a comfort limit of ambient dry-bulb temperature of 42°C controlled by direct evaporative cooling. Based on an experimental investigation of porous ceramic evaporators for building cooling, Ibrahim et al. (2003) found that dry-bulb temperature easily dropped of 6–8°C at a mean air velocity of 0.08–0.10 m/s, accompanied by a 30% increase of relative humidity. It is impractical to lower dry-bulb

temperature more than 11°C by direct evaporative cooling (Szokolay, 2004). The upper comfort limit was therefore extended 11°C along the wet-bulb temperature line.

4.3.2.3 Passive heating using solar energy

The basic principle of passive solar heating involves allowing solar irradiation into building through solar apertures (e.g. Trombe wall system, massive masonry wall, south-facing glazing façade, and sunspace), then using this energy to warm up the internal environment. It is quite sophisticated to precisely quantify the periodic heat flows between the Sun, the building and its surrounding. To get a very approximate idea of how effective a passive solar system is, the steady-state heat transfer model is used. Assume a typical south-facing space (e.g. an apartment or an office) in a building of a 100 m² floor area (10 m x 10 m x 3.3 m) with a 33 m² external south-facing wall; direct solar gain is controlled by a 10 m² south-facing window (small window is to prevent overheating), no heat exchange with adjacent spaces and no internal heat gains.

The energy flow through the window Q_w can be estimated on the following basis (ASHRAE, 2009):

$$Q_w = (SHGC) * I_s * A_w - U_w * A_w * (T_i - T_o) \quad (4.2)$$

The energy flow through the external wall Q_c is calculated as (Koenigsberger, et al., 1973):

$$Q_c = U_{ew} * A_{ew} * (T_i - T_{sol-air}) \quad (4.3)$$

In the above equation, the concept sol-air temperature is used to include the heat flux from the Sun and sky on the wall surface. Assuming no difference between outdoor air temperature and sky mean radiant temperature, sol-air temperature is defined as:

$$T_{sol-air} = T_o + \frac{I_s * \alpha}{h_o} \quad (4.4)$$

The energy flow caused by air infiltration through cracks and openings Q_v is calculated as:

$$Q_v = 1004 * 1.204 * \frac{N * V}{3600} * (T_i - T_o) \quad (4.5)$$

where

Q_w , Q_c , Q_v = instantaneous energy flow through window, wall and ventilation, W; $SHGC$ = Solar heat gain coefficient, dimensionless; I_s = solar irradiance on south-facing surface, W/m²; U_w = window overall coefficient of heat transfer (U-factor), W/m².°C; A_w = total projected window area, m²; T_i = indoor air temperature, °C; T_o = outdoor ambient temperature, °C; $T_{sol-air}$ = sol-air temperature, °C; U_{ew} = external wall thermal transfer value (U-value), W/m².°C; A_{ew} = external wall area, m²; α = solar absorbance of the external wall, dimensionless; h_o = conductance of the air film on the wall surface, W/m².°C, taken as 10 to 20 at wind speed of 1 m/s (Koenigsberger, et al., 1973); 1004 = volumetric specific heat of the air, J/kg.°C; 1.204 = density of air at 20 °C and standard pressure, kg/m³; N = number of air changes per hour; V = volume of the space, m³.

Assume that the external wall is 220mm light yellow cavity brick wall with $U_{ew} = 1.6$ W/m².°C and $\alpha = 0.3$; the window is 5mm single glazing - vinyl frame with U-factor = 5.2 W/m².°C and average $SHGC = 0.45$; $h_o = 15$ W/m².°C; air change rate $N = 0.8$ ACH; indoor temperature at the lower limit of the comfort zone $T_i = 22.3$ °C at $RH = 30\%$ (see Fig. 4); average solar irradiance (I_s) on south-facing walls in the coldest month of Hanoi, Danang and Hochiminh city are 166, 175 and 184 W/m² (Institute of Construction Science and Technology, 2009), respectively.

The space achieves energy balance at T_i and T_o (evaporation heat loss can be omitted), thus:

$$Q_s - Q_c - Q_v = 0 \quad (4.6)$$

From this balance, T_o for Hanoi, Danang and Hochiminh city are 17.4°C, 17.1°C and 16.9°C. These are lowest outdoor temperature at which the heat delivered by a passive solar system can compensate to maintain indoor comfort temperature.

It is necessary to mention that the efficiency of a passive solar system strongly depends on building design, solar system types and many design variables of the system. The above model considers a typical design in a standard condition and some assumptions; the given result is therefore simply a reference.

4.3.3 Plotting weather data on the Building psychrometric chart

In this step, hourly temperature and humidity of Hanoi, Danang, and Hochiminh city were plotted on the psychrometric chart (see Figure 4-9). The comfort zone and its CPZs in Figure 4-8 were then superimposed. All analyses and statistics were carried out on this two-layer psychrometric chart from which comfortable, potentially comfortable and uncomfortable periods can be determined.

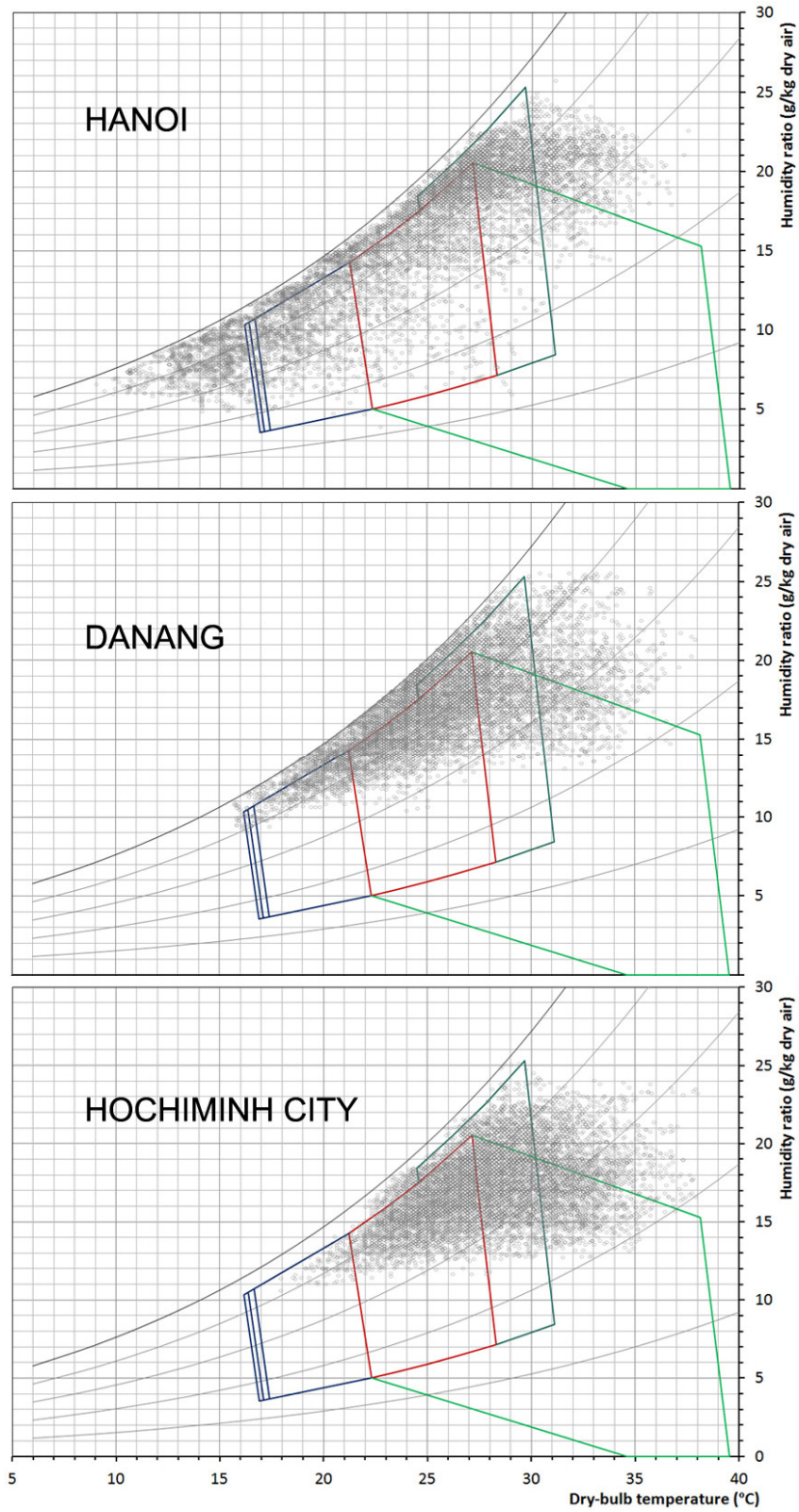


Figure 4-9: Hourly plot weather data on Building psychrometric chart at standard atmospheric pressure (101.325 kPa)

A Typical Meteorological Year (TMY) data set provides users with a reasonably sized annual data set that holds hourly meteorological values for a 1-year period that represent typical conditions of a specific location over a longer period of time (usually 30 years). TMY files of more than 2100 locations of the world can be obtained from the opened database of the U.S. Department of Energy (2012). TMY files of more than 1000 other locations, distributed under the license of Meteotest¹³, can also be found in TRNSYS thermal simulation package¹⁴. Some computer weather tools can create TMY files with acceptable accuracy by interpolating monthly weather data provided by users. With a TMY file, hourly weather data of any season, any month or any day can be separately extracted.

In Figure 4-9, hourly temperature and humidity of a year are presented by the scattered cloud on the Cartesian coordinate system. Each point is presented by its x-coordinate (temperature) and y-coordinate (humidity ratio). Hourly temperature and relative humidity are always available in TMY files. Hourly relative humidity is then converted into hourly humidity ratio. Following steps can be followed, giving an acceptable accuracy of conversion.

At standard atmospheric pressure (101.325 kPa), water vapor saturation pressure p_{ws} of saturated air is derived by the equation of Hyland and Wexler (1983).

$$\ln p_{ws} = C_1 / T + C_2 + C_3 T + C_4 T^2 + C_5 T^3 + C_6 \ln T \quad (4.7)$$

For higher accuracy, the method of International Association for the Properties of Water and Steam (2007) should be used. After that, the partial pressure of water vapor p_w is calculated by the definition of relative humidity:

$$RH = \frac{p_w}{p_{ws}|_{t,p}} \quad (4.8)$$

Then humidity ratio W_h is given by (in (ASHRAE, 2009) – chapter 1):

$$W_h = 0.621945 \frac{p_w}{p_s - p_w} \quad (4.9)$$

where

¹³ Meteotest, Fabrikstrasse 14, 3012 Bern, Switzerland

¹⁴ University of Wisconsin Madison. TRNSYS energy simulation software package. Available at <http://sel.me.wisc.edu/trnsys/index.html> [Last accessed 13 Feb 2012]

p_{ws} = pressure of saturated pure water, Pa; p_s = standard atmospheric pressure, Pa; p_w = partial pressure of water vapor in moist air, Pa; W_h = humidity ratio, $\text{kg}_{\text{water-vapor}}/\text{kg}_{\text{dry-air}}$; T = absolute temperature, $\text{K} = ^\circ\text{C} + 273.15$; RH = relative humidity, %; $C_1 = -5.8002206 \text{ E}+03$; $C_2 = 1.3914993 \text{ E}+00$; $C_3 = -4.8640239 \text{ E}-02$; $C_4 = 4.1764768 \text{ E}-05$; $C_5 = -1.4452093 \text{ E}-08$; $C_6 = 6.5459673 \text{ E}+00$.

These calculations are automated by a spreadsheet (e.g. Microsoft Excel[®]), providing hourly humidity ratio of a whole year.

The next step is to identify whether a point is located inside or outside a zone on the building psychrometric chart and to calculate number of points inside the boundaries. First, the mathematical function of each boundary is defined ($f(x)$:temperature \rightarrow humidity ratio). Each zone, e.g. the comfort zone, normally consists of 4 boundaries. Points and number of points inside these boundaries are then identified and calculated by an IF-THEN-ELSE logic in the Spreadsheet. This process has to be done only once and later can be employed many times with a single mouse click.

4.3.4 Results of the method

4.3.4.1 One-year analysis of the climates of 3 regions

All year weather data of each site were plotted on the building psychrometric chart. For all sites, the air is always very humid and sometimes saturated (see Figure 4-9). Figure 4-10 shows all year cumulative comfort potentially achieved by using various passive cooling and heating strategies and their combinations. The weather in Hanoi is found to be naturally comfortable in only 23.0% of a year whereas in Danang and Hochiminh city this value was around 37%, revealing that the climate of Hanoi seems more severe than the others. It is worthy of note that Hanoi experiences both cold-humid and hot-humid weather patterns. This type of climate is really a challenge to every designer because of the fact that the building must be both ‘opened’ using lightweight materials in summer and ‘closed’, well-insulated in winter. Very high humidity in winter also raises the possibility of water condensation on building surfaces, resulting in mold growth and structure damages. On the contrary, both Danang and Hochiminh city have warm-humid winters and hot-humid summers where only overheating periods should be taken into account in building design.

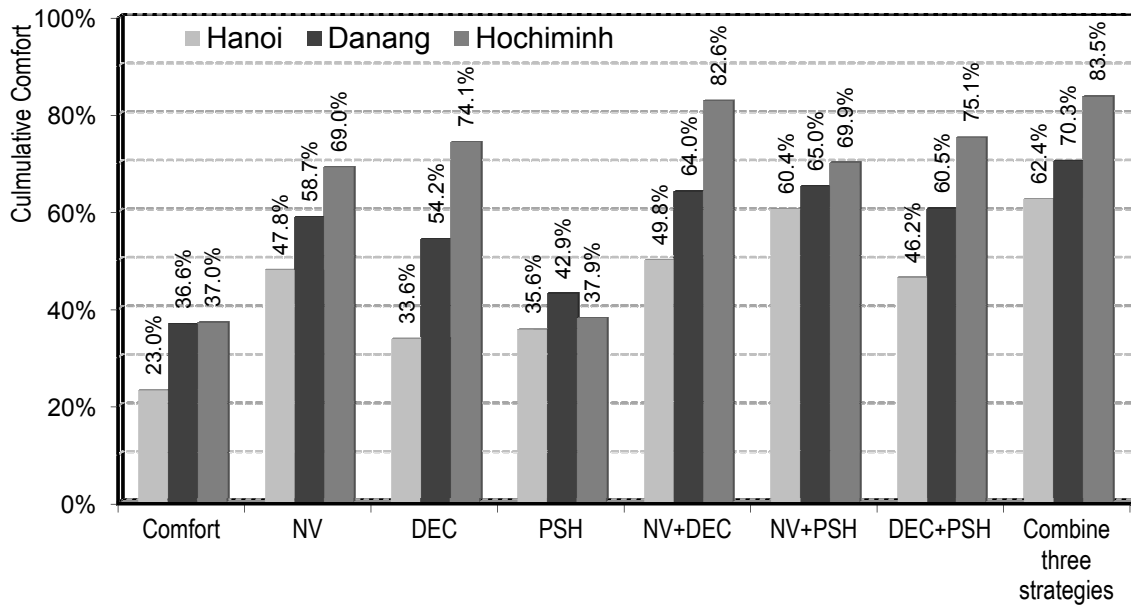


Figure 4-10: All year cumulative comfort using passive heating and cooling strategies (NV: natural ventilation; DEC: direct evaporative cooling; PSH: passive solar heating)

Table 4-3: Potential comfort improvement by each strategy

Passive strategies applied	Comfort improvement (%)		
	Hanoi	Danang	Hochiminh
Natural ventilation (NV)	24.8	22.1	32.0
Direct evaporative cooling (DEC)	10.6	17.6	37.2
Passive solar heating (PSH)	12.6	6.3	0.9
NV + DEC	26.8	27.4	45.6
NV + PSH	37.6	28.4	32.9
DEC + PSH	23.2	23.9	38.1
Combine all strategies	39.4	33.65	46.6

The percentage of comfort improvements by each passive strategy are separately listed in Table 4-3. In Hanoi, natural ventilation proves to be the most effective strategy for comfort improvement (24.8% of a year). The comfort improvement by passive solar heating (12.6% of a year) is considerable, compared with the short heating season. Total comfort potential of a year is only 62.4%, revealing that Hanoi mainly relies on many other solutions to yield all year comfort. In Hochiminh city, natural ventilation is a very effective solution by which the comfort period can be nearly doubled. Direct evaporative cooling is also a good promise because it may provide comfort for over 74% of total time. Nearly 84% of total time would be thermally acceptable if all strategies were combined, revealing that

passive solutions must be considered as the first choice in building design in Hochiminh city. Danang geographically locates in the centre of Vietnam; consequently the climate characteristics in Figure 4-10 show a transitional comfort improvement between Hanoi and Hochiminh city. It can be seen that passive solar heating is not important in Danang (improvement of 6.3%) and nearly meaningless in Hochiminh city (improvement of 0.9%).

The discomfort period shown in Figure 4-9 helps designers determine appropriate design solutions to modify the climate. It also reveals hints to select heating, cooling and dehumidification systems for buildings and to size these systems preliminarily. For the sites where data of extreme years such as Design Summer Years or Design Winter Years are available, further analysis on these data using this method may offer more useful inputs.

4.3.4.2 Four-season and 12-month analysis of the climate of Hanoi

A further analysis was carried out to examine the potential of comfort improvement of these strategies in each season and each month in Hanoi. The weather data of each month and each season were plotted on the building psychrometric chart. The results are shown in Figure 4-11 and Figure 4-12.

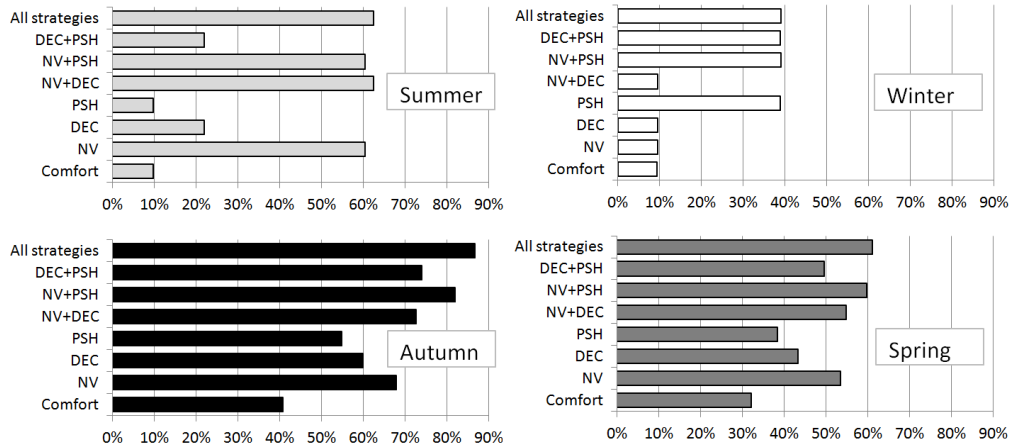


Figure 4-11: Cumulative comfort during 4 seasons in Hanoi by passive strategies (NV: natural ventilation; DEC: direct evaporative cooling; PSH: passive solar heating)

Figure 4-11 shows that in winter, comfortable time occupies only 10% of the season and only passive solar heating would be effective. In other seasons, natural ventilation may provide comfort for at least 54% of the total time. Under humid conditions, natural ventilation offers many advantages, e.g. improving of IAQ, preventing mold growth. Other strategies as well as a combination of various strategies are not recommended because

comfort improvement is not noticeably higher. This analysis reveals that natural ventilation and passive solar heating are among the most important passive solutions for Hanoi and should be the greatest concern of designers.

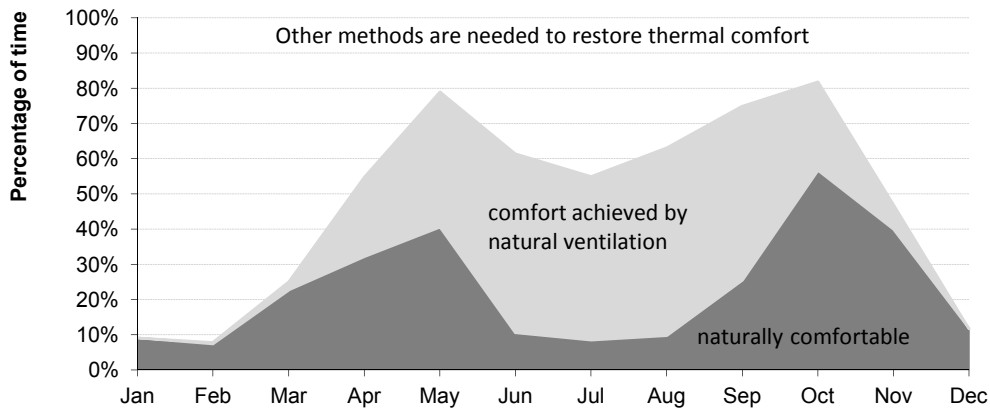


Figure 4-12: Natural comfort and cumulative comfort by natural ventilation during 12 months in Hanoi

Natural comfort and cumulative comfort during 12 months by natural ventilation is presented in Figure 4-12. According to this, natural ventilation is effective from April to the end of September. The most effective period falls within summer (from June to the end of August), confirming that natural ventilation may significantly reduce the building cooling load and energy consumption. Maximum comfort occurs in mid-spring and mid-autumn. Figure 4-11 and Figure 4-12 also reveal that during winter natural comfort is extremely low (below 10%) due to cold weather and that passive solar heating would be able to raise comfort up to 40%. Further heating solutions and design strategies are therefore needed to keep indoor environment comfortable.

4.4 Climate analysis using the adaptive comfort model

As discussed in CHAPTER 3, it is quite reasonable that thermal environment in NV buildings should be evaluated by adaptive comfort models. Adaptive comfort standards are able to provide a comfort temperature range throughout the year corresponding to mean outdoor conditions. A simple principle of comfort evaluation is that indoor temperature above or below this comfort range is considered uncomfortable.

By implementing an adaptive comfort model into a building energy simulation program (see section 3.5), the comfort and discomfort period in a building can be derived

from simulation outputs. To evaluate thermal performance of a building, we need to see how effective the building successfully modifies the climate. In other words, we need to compare comfort (discomfort) periods given by the building with those naturally given by the climate. For this reason, *natural comfort and discomfort period given by the climate itself must be known*. There are at least two simple methods proposed by the author to obtain these values.

In the first method, hourly weather data of a TMY weather file is plotted on the adaptive comfort model by a Spreadsheet program (e.g. Microsoft Excel[®]). The comfort and discomfort periods are then easily determined and calculated using the boundary functions and IF-THEN-ELSE statements. Figure 4-13 shows an example of this method. A small drawback of this method is that, as hourly data is used, the result is accurate to within one hour. Higher accuracy requires higher resolution of climatic data.

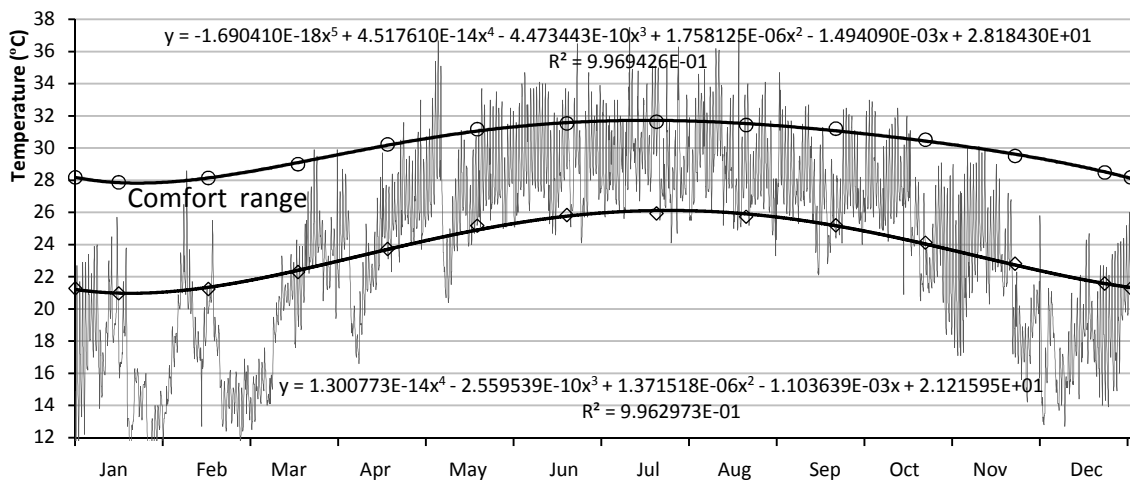


Figure 4-13: The climate of Hanoi on the adaptive comfort model of South-East Asia

In the second method, instead of directly evaluating the climatic data, indoor temperature of a very well-ventilated space is simulated by a building energy simulation program. The ventilation flow rate of this space must be set at an extremely high value, say 2000 ACH, so that indoor temperature and outdoor temperature are completely identical. Then the method introduced in section 3.5 is employed to determine comfort and discomfort periods. As the simulation program predicts the indoor temperature, the result is accurate to within one simulated time step (e.g. 30 minutes, 15 minutes or even smaller). The results reported in Table 4-4 is calculated by this method using 20 simulation time steps per hour. The results are the “comfort performance” of the climates.

Table 4-4: Results of climate analysis by the adaptive comfort model

	Hanoi		Danang		Hochiminh city	
	Discomfort cause by the cold	Discomfort cause by overheating	Discomfort cause by the cold	Discomfort cause by overheating	Discomfort cause by the cold	Discomfort cause by overheating
By categories	3515	602	2892	649	1560	1542
Total	4117		3541		3102	
Percentage of a year	47.0%		40.4%		35.4%	

As can be seen, the climate of Hochiminh city is most favorable with only 35.4% discomfort, followed by the climate of Danang and then Hanoi. In Hanoi, 3515 hours of discomfort caused by the cold really challenge architects in finding an appropriate solution. The discomfort periods of a year shown in Table 4-4 should be considered as the “lowest performance” that every building must overcome.

In fact, the adaptive comfort model is not really a climate analysis tool. Instead, it provides a glance at a climate and gives a reference comfort zone for building performance analysis. The method recommended in this section is useful if thermal performance of the building is assessed by adaptive thermal comfort models.

4.5 General conclusions about the climates of Vietnam

This chapter describes the climates of Vietnam in detail. Some simple methods to evaluate a climate for climate responsive design were used. This thesis also developed an improved analysis method applied to hot humid climates. The climates of three regions of Vietnam were evaluated by this method as case studies. In Vietnam, the climate of Hanoi is the most severe one with only 23% of a year comfort while the comfort periods of Danang and Hochiminh city are approximately 37%. Both heating and cooling measures are necessary in Hanoi, while in other regions only the cooling demand should be taken into account. For all sites, the air is always very humid and sometimes saturated. It is found that natural ventilation and direct evaporative cooling almost have similar cooling effectiveness. Direct evaporative cooling often requires sophisticated equipments and may raise the air humidity and mold growth on walls and clothes. Natural ventilation is low-cost, easy to apply and provides good IAQ, but it strongly relies on natural wind and building configurations as well as the building location. Since Vietnam generally has a hot and

humid climate, natural ventilation in most cases would be the better choice for passive cooling because the increase of air humidity due to direct evaporative cooling is not expected in humid conditions. Passive solar heating should only be employed in Northern Vietnam, giving a noticeable benefit.

Under the climates of Vietnam, relying completely on these three passive solutions to maintain thermal comfort is not feasible, but there is a significant potential of comfort improvement. Estimated total comfort achieved by three main passive strategies was 62%, 70% and 84% for Hanoi, Danang, and Hochiminh city, respectively. In bioclimatic design, buildings must be capable to modify the climate through passive design strategies. Through profound climate understanding, architects play a key role in creating climate responsive shelters without using modern energy dependant systems. A wise building occupancy and management would also contribute to this target.

The method developed in section 4.3 has its own limitations as hourly weather files are required for the analysis and currently these data resources are only available for a limited number of locations in the world (about 3100). For a certain location, a corresponding weather file can be manually created using computer aided tools (e.g. weather tools or commercial Meteonorm) with acceptable accuracy, provided that sufficient input data exist. This method is rather simple and can provide reliable results. The graphical presentation of the result may help architects and engineers to get familiar with this tool quicker. This method can be used and modified by any user... without much computational effort. It can be refined and applied by software programmers who focus on computer weather analysis tools and thermal comfort assessment in building simulation.

CHAPTER 5

THERMAL PERFORMANCE OF TYPICAL HOUSING TYPOLOGIES

An overview about thermal performance of the current housing stock in Vietnam will provide useful hints for further improvements. This task was done by using dynamic thermal simulation. First, the most common housing styles in Vietnam were identified. Case-study houses of these housing styles were selected for an in-situ monitoring campaign. The simulation models were then calibrated by comparing simulated results with the in-situ monitoring data and then whole-year simulations were performed. Finally, thermal performance during a year of each house was therefore evaluated.

5.1 Identifying typical housing prototypes in Vietnam

Housing styles and their corresponding proportions in the total housing stock of Vietnam are still rather vague due to the lack of surveys. The latest national survey in 2009 does not provide such information. Instead, the survey offered detail statistics about housing quality and corresponding income of the owners. Ly et al. (2010) reported that there were various housing types in Vietnam; but there are only 3 major common types, including urban **row houses** (terraced houses or town houses), **detached houses** (or single-family houses) and low-rise or high-rise **apartments** (or flats). Other housing types (e.g. semi detached houses, student or worker dormitories) still exist in Vietnam, but their proportions are not significant and their roles are modest. Consequently, this research will be focused on these three most popular housing types.

A row house is a typical unit among a series of houses, located in a narrow and long parcel of land with the main façade facing the street, often of similar or identical design, situated side by side and may have common walls or not. Developed from the 17th century, row houses occupy a dominant portion of the current housing stock in Vietnam, accounting for about 75% of the total number of houses (Ha, 2002), especially in urban areas. The row

house is a certain result of the increase of population in urban areas. Nowadays, under the pressure of population boom, this housing typology has even spread out to many rural areas. In spite of its advantages and disadvantages, the row house will continue playing a significant role in urban planning and management in at least a few decades.

A detached house is a single-family residential building that is located on a large parcel of land and is isolated from the other houses by its surrounding garden. As this housing style requires much land and urban infrastructure, they usually appear in suburban and rural areas. There is no statistical number about the percentage that this housing style occupies; it is believed that the detached house is the second most popular style in Vietnam and can be found easily in the rural regions.

A low-rise or high-rise apartment indicates a self-contained residential unit that occupies only part of a building and such a building is called the “apartment building”. Each apartment is usually occupied by a household or a family. According to the National survey in 2009 (CPHSC, 2010), apartment housing accounts for about 16.64% number of houses in Hanoi, 6.13% in Hochiminh city and only 4% for the whole country. Nevertheless, the rapid urbanization process which is booming in big cities of Vietnam has raised the importance of apartment buildings in urban planning. It is now considered as the major housing typology for new housing projects. As an example, according to article 7 of the decree No. 123/QĐ-UB on 6th Dec. 2001 of Hanoi People Committee, in new housing projects 60% area of the land must be used for high-rise apartment buildings; 40% for detached houses and row houses are strictly forbidden. It can be seen that in a near future, apartment buildings will become more popular and more important in urban areas in Vietnam.

5.2 The monitoring campaign

5.2.1 The selections of case-study houses

Three houses representative of the three styles were selected for the study, thus one row house, one detached house and one apartment in a 7-storey building. These selected houses are situated in Danang city, central Vietnam so as to facilitate the measuring process; to share the data of outdoor weather and to compare the performances of these houses. As

the styles of these houses are very common, houses with similar design can be found in any regions of Vietnam.

Figure 5-1 shows the map of Danang city in which the locations of these houses are indicated. In this figure, the location of the National Meteorological Station which provided information of outdoor weather during the survey period is also indicated, on the right side of Danang International airport. All the three houses were built after the year 2000 and are in good conditions.

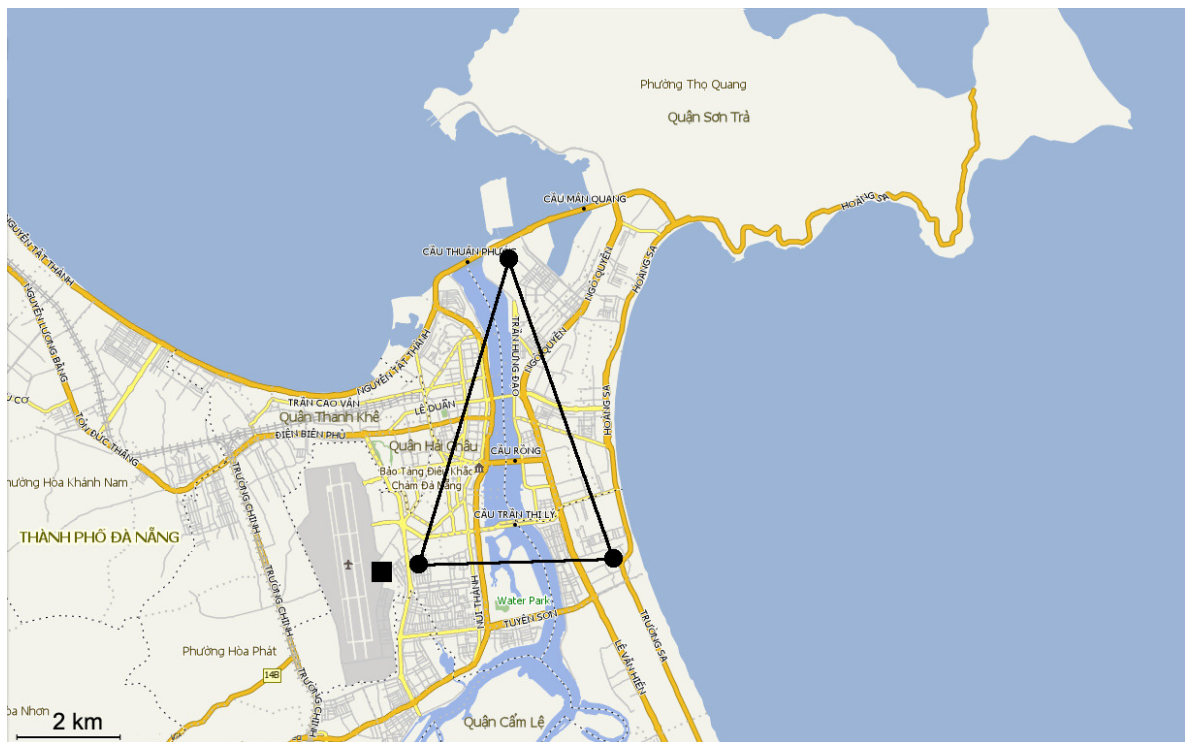


Figure 5-1: Locations of the 3 case-study houses (black round dots) and the Meteorological station (square dot) in Danang city

The row house (the lower left one in Figure 5-1) was built about 10 years ago with an average budget and occupied by a household. This 2-storey house is located in a dense urban area and adjacent houses are almost similar in style and size. During the measuring period, this house was unoccupied until 20th May and from 20th to 31st May, it was occupied by a family of 3.

The detached house (the lower right one in Figure 5-1) situated near the seashore is being occupied by a family of 4. Although the house was equipped with local AC units, it

was in free running mode during the measurement. This house is surrounded by a garden; thus it is completely isolated from other buildings.

The apartment (the top one in Figure 5-1) is situated on the 4th floor of a low-cost 7-storey apartment building in the North of Danang city. This building represents the typical design for low income residents who have been evacuated for urban slum clearance and planning elsewhere. The building was newly constructed in 2010, but during the survey period, it was occupied by two persons. The apartment in consideration has the gross floor area of 53 m² with two small bedrooms. The position of this apartment ensures that it is always subject to solar irradiation in both the morning and afternoon.

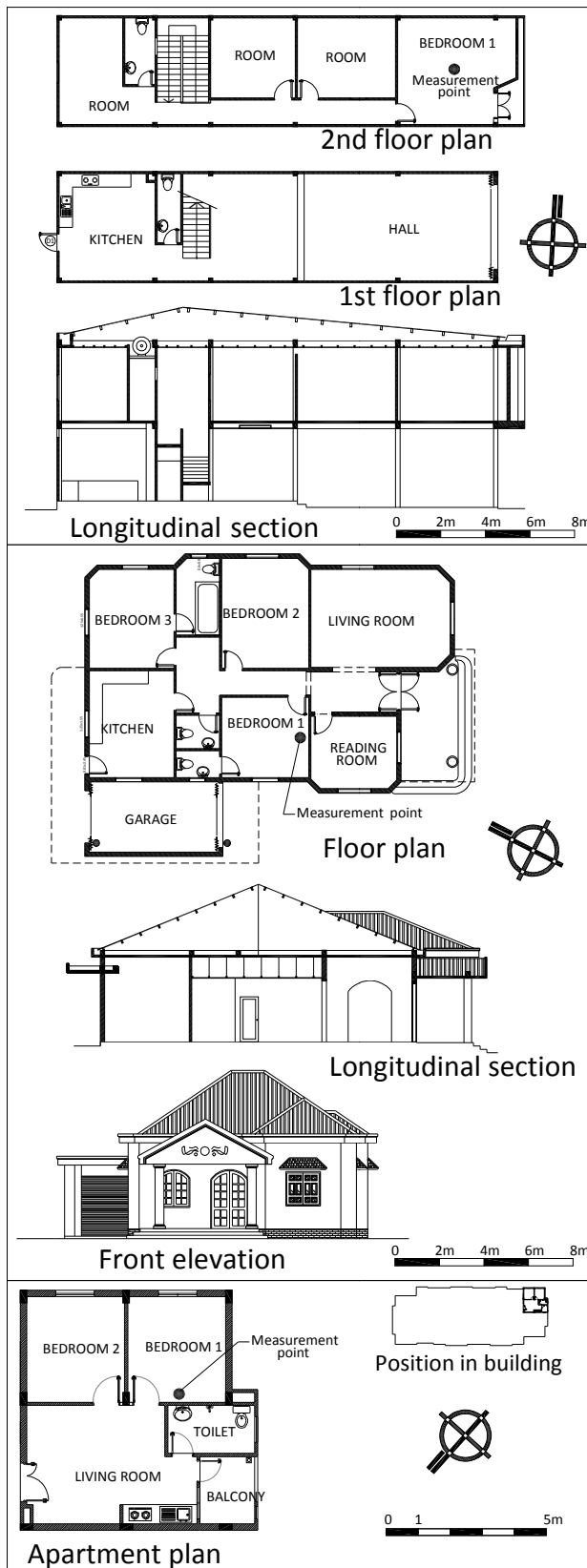
Architectural configurations of these houses were directly measured at the sites. All details of the houses as well as their orientations are presented in Figure 5-2. Table 5-1 summarizes some basic features of these houses.

Table 5-1: Basic features of the case-study houses

Type	Foundation	External wall	Structure	Roof	Floor	Openings
Row house	Reinforced concrete	110mm solid brick wall	Reinforced concrete frame	Metal color sheet – PVC ceiling panel	Reinforced concrete	Single glazing-steel frame
Detached house	Reinforced concrete	220mm solid brick wall	Reinforced concrete frame	Metal color sheet – Reinforced concrete ceiling	Wooden floor or granit floor	Single glazing-wooden frame
Apartment	Reinforce concrete piles	220mm solid brick wall	Reinforced concrete frame	Reinforced concrete	Reinforced concrete	Single glazing-aluminum frame

5.2.2 Monitoring protocol and monitoring results

The monitoring period was conducted in 31 days (a full month), beginning from the 1st May 2012. In principle, this baseline period for the calibration purpose should include the seasons and phases of the most unfavorable weather, e.g. winter or summer. The period selected is considered to be acceptable because summer in Vietnam normally starts from May and extend to the end of September. From the beginning of May 2012, the weather became rather hot and uncomfortable as being reported in the monitoring result.



The row house – street view



The detached house – front façade



The building and selected apartment

Figure 5-2: Three case-study houses and the locations of measuring equipments

Monitoring equipments are calibrated Hobo data loggers as described in section 3.3.1. These loggers are able to record air temperature, relative humidity and light intensity simultaneously. They were attached on the walls of occupied houses or fixed at center of the room of unoccupied houses, at height of 1.1m (see locations in Figure 5-2). The selected monitoring room in each house was the most critical zone that is subject to solar radiation and wind. The data loggers were programmed to record data at every 1-hour interval.

As the apartment and the detached house were occupied during the monitoring period, their occupancies were gathered by questionnaires. Openings of occupied houses were freely controlled by the occupants and were almost opened as being observed. On the contrary, as the row house was completely unoccupied until 20th May, its openings were definitely controlled by the author, and May was divided into 3 sub-periods. From the 1st to 9th May all openings and doors were closed. From the 10th to 19th May, all openings and doors (except entrance doors) were opened. From 20th to 31st May, all openings and doors were manually controlled in correspondence with outdoor conditions by occupants. All facilities which consume energy were also noted for modeling.

Hourly outdoor conditions of May 2012, including temperature, relative humidity, wind speed, wind directions, global horizontal, direct and diffused solar irradiance were ordered from the National Meteorological Station in Danang city in early April and were obtained in mid – June. These data were carefully checked for errors before being implemented into the TMY weather file of Danang. This process was done by the weather tool in EnergyPlus program. In the newly generated weather file of Danang, weather conditions of 10-day periods before and after May (20th April - 1st May and 1st June - 10th June) were modified and interpolated so that the transitions between original data of the weather file and monitoring data are smooth. After this modification, the new weather file was able to represent the weather of Danang in May 2012.

5.2.3 Discussions on the monitoring results

The monitoring results as well as outdoor conditions of the monitoring period are shown in Figure 5-3. The light grey band is the comfort range for 80% acceptability calculated by the adaptive comfort model developed in CHAPTER 3, corresponding to the mean outdoor temperature of May 2012 - 30.2°C. As can be seen, the outdoor temperature is rather high and sometimes becomes very hot (the 1st, 2nd, 3rd, 4th, 18th, 19th, 20th and 21st of May). The indoor temperature of the apartment and detached house were almost roughly acceptable, but they have failed under extreme conditions. The row house performed worst among these houses as discomfort frequently occurred during the monitoring period. After the 10th May when the openings were controlled, the row house slightly improved its performance. Notably, the indoor temperature of these houses always followed the warmer side of the comfort range, thus the mean indoor temperature deviated considerably from the optimal comfort temperature.

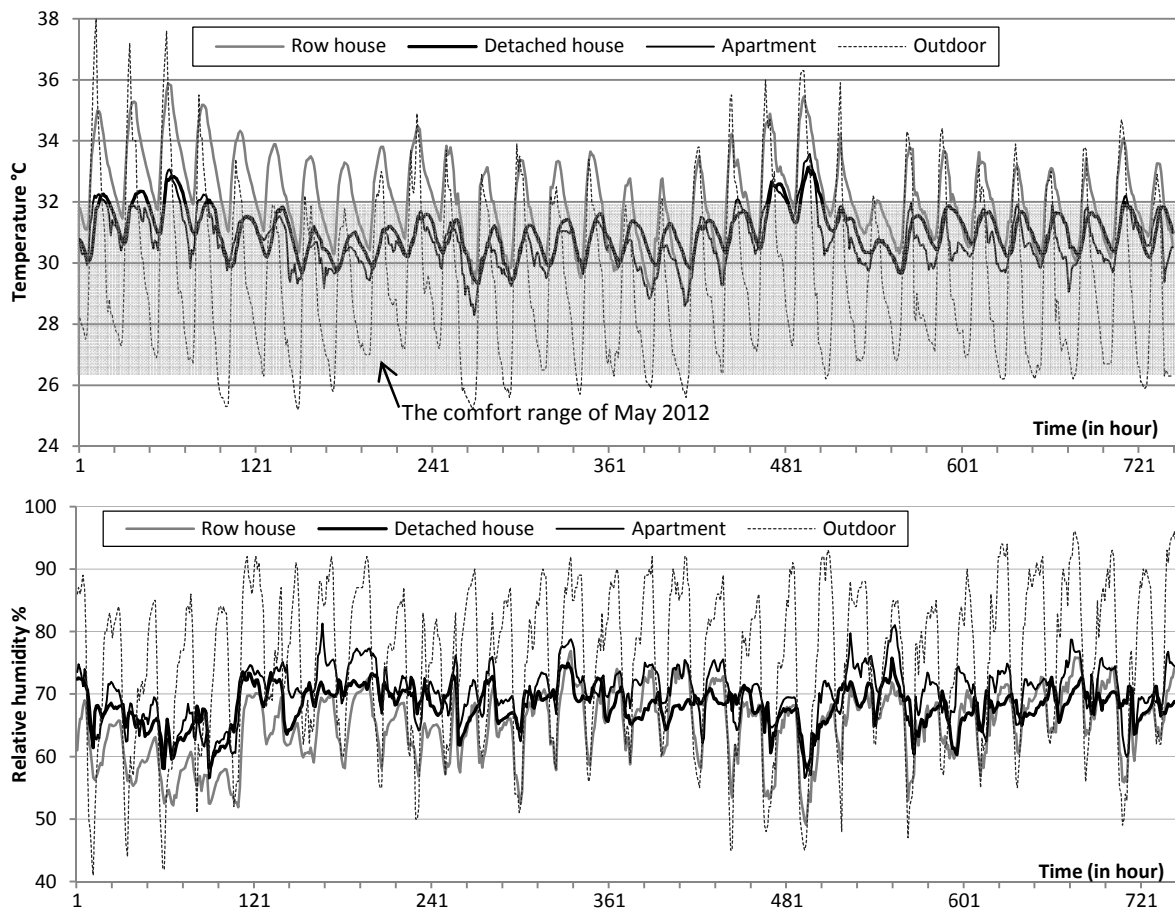


Figure 5-3: Indoor - outdoor temperature and humidity during 31 days of May

In Figure 5-3, the variation of temperature in the apartment was not as smooth as those of other houses. This phenomenon may indicate that the apartment was well-ventilated by natural wind and consequently its indoor temperature fluctuated more often and followed outdoor conditions. Generally, the apartment was the best dwelling among the surveyed houses while the row house was completely uncomfortable. Nevertheless, all houses need further improvements so as to perform better under extreme conditions and to shift the mean indoor temperature close to the comfort temperature.

Indoor humidity of these houses was rather stable and varied around the threshold of 70%. This threshold is considered acceptable for thermal comfort and for avoiding condensation, compared with the outdoor humidity which was very high during nighttime.

5.3 Numerical modeling and simulation of buildings performance

The measurement campaign was conducted in one month; hence the monitoring results only present short-term performances of the case-study houses. Long term thermal comfort assessment (e.g. seasonal or annual assessment), energy consumption as well as improvement strategies for the houses are still in question. The method relied on numerical modeling and simulation of buildings performance was selected to deal with this challenge.

Since late 1990s, along with the rapid growth of computational sciences, building performance simulation (BPS) has emerged as a fast and accurate method of assessment during the building design process. With increasing complexity in building design and higher requirements on energy performance and environmental protection, the use of building simulation tools during the design process and building retrofits becomes inevitable. The subsequent sections give brief discussions on computer simulation programs used in this thesis, their characteristics and capabilities, and validation results of these tools.

5.3.1 Building energy simulation programs and EnergyPlus

There are currently around 400 building energy simulation tools¹⁵ which are almost commercial products. Each of them can only perform some specific tasks as being programmed and the reliability of numerical results still remains the biggest concern of the simulation community. The choice of building simulation tools and validation methods is therefore very important in building research.

¹⁵ http://apps1.eere.energy.gov/buildings/tools_directory/alpha_list.cfm [accessed 10th August 2012]

Before going to the final choice, the author has carefully experienced some well-known building simulation programs, including: Pleiades-Comfie (Izuba energies, 2010) (licensed by author's Laboratory), Autodesk Ecotect 2011 (Autodesk, 2011) (student license), Virtual Environment 6.0 (IES, 2010) (trial license), EnergyPlus™ 6.0 (Crawley, et al., 2001) (free license). It is obvious that each program has its own strengths and weaknesses thus some of them were sometimes used in this thesis when needed. It was also found that capabilities of EnergyPlus 6.0 completely satisfied most criteria and requirements of this research; it is therefore employed as the main building energy simulation program.

EnergyPlus is used to model energy and water flows in a building. EnergyPlus has been developed by inheriting most popular features and capabilities of BLAST and DOE-2 under the supervisor of U.S. Department of Energy. Although the first version of EnergyPlus was released in 2001, its age should date back to 20 years before when BLAST and DOE-2 appeared. Figure 5-4 presents the structure of EnergyPlus program. As can be seen, EnergyPlus program combines many program modules which work together to estimate the energy required for a building implementing a variety of systems and energy sources. EnergyPlus is capable to model heating, cooling, lighting, ventilation, other energy flows, and water use in buildings. Many advanced simulation capabilities were implemented in EnergyPlus: time-steps less than an hour, modular systems and plant integrated with heat balance-based zone simulation, multi-zone Airflow network, thermal comfort, water use, natural ventilation, photovoltaic systems and life cycle analysis¹⁶. EnergyPlus offers advanced users maximum flexibility and modeling details. EnergyPlus reads inputs and produces outputs in form of ASCII files that facilitates the coupling of EnergyPlus with third party programs such as GenOpt, Dakota, SimLab, etc. The only challenge of this program is that users have to interact with EnergyPlus through a text-based interface rather than a user friendly graphical user interface.

EnergyPlus performs calculations by solving a series of energy balance equations of the building systems and surrounding environment. All details about algorithms used within EnergyPlus are carefully described in EnergyPlus documentations (Ernest Orlando Lawrence Berkeley National Lab, 2010a) and it is of course not necessary to further discuss these algorithms in this document.

¹⁶ <http://apps1.eere.energy.gov/buildings/energyplus/> [accessed 10th August 2012]

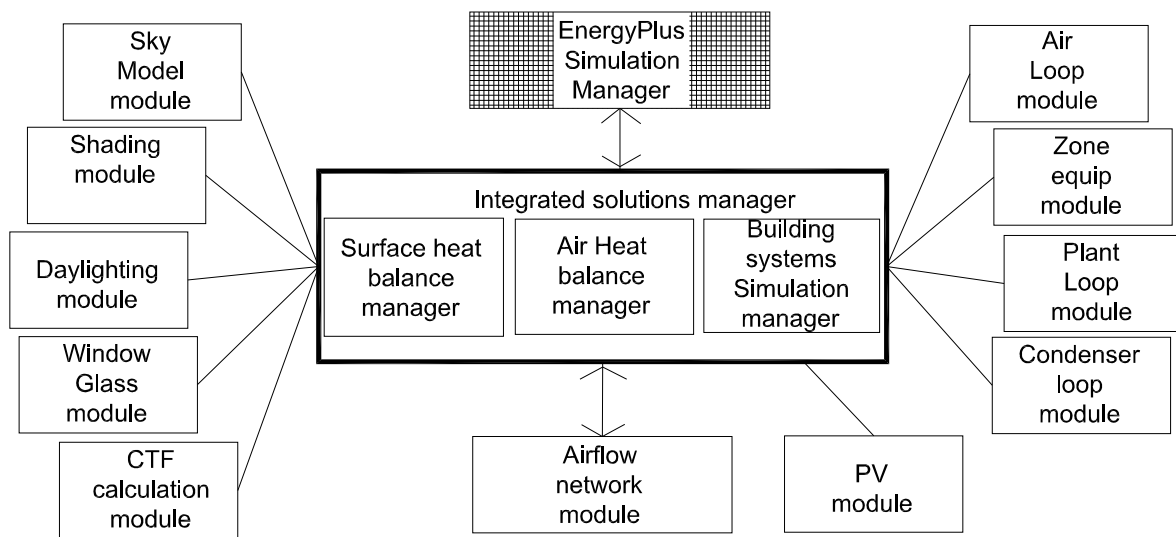


Figure 5-4: EnergyPlus program schematic, its modules and capabilities (Ernest Orlando Lawrence Berkeley National Lab, 2010a)

To make EnergyPlus free from bugs, all versions of EnergyPlus were extensively tested before release using industry standard methods. Major types of tests that have been performed are (Office of Energy Efficiency and Renewable Energy, 2012):

** Analytical tests:*

- HVAC tests, based on ASHRAE Research Project 865
- Building fabric tests, based on ASHRAE Research Project 1052

** Comparative tests:*

- ANSI/ASHRAE Standard 140-2007
- International Energy Agency Solar Heating and Cooling Program (IEA SHC) BESTest (Building Energy Simulation Test) methods not yet in ANSI/ASHRAE Standard 140-2007. These tests compare the results of multiple Building Energy Simulation tools for a series of load-related attributes
- EnergyPlus HVAC Component Comparative tests
- EnergyPlus Global Heat Balance tests

** Release and executable tests*

Most of test results proved that EnergyPlus is stable and qualified enough for academic purposes as well as practical applications. All test results are now available on the World Wide Web (Office of Energy Efficiency and Renewable Energy, 2012). In this thesis, EnergyPlus settings and simulated results of the case-study houses will be subsequently

validated and calibrated by measuring data before performing official simulation runs and analyzing simulation outputs. This task will be reported in section 5.5.

5.3.2 Airflow prediction in and around buildings using Computational Fluid Dynamics

The movement of the air plays an important role in building research. As air movement strongly affects human thermal sensation and energy balance of a building, knowledge of characteristics of the airflow in and around buildings is very necessary for thermal comfort assessment and energy calculations. Chen (2009) carried out a review study on the methods of ventilation prediction for buildings. Seven models of prediction were pointed out, including:

- Analytical models,
- Empirical models,
- Small-scale experimental models,
- Full-scale experimental models,
- Multi-zone models,
- Zonal models, and
- Computational Fluid Dynamics (CFD) modeling.

He also emphasized that CFD modeling has accounted for 70% of the ventilation performance studies published in recent years. A full review of these models was introduced by Allard (1998) or Vickery, et al. (1977). In this study, we analyzed naturally driven air motion measured around and inside buildings by using a CFD model.

5.3.2.1 A brief introduction about the CFD approach

Wind is a natural physical phenomenon characterized by random fluctuations of its physical properties. However, the wind or the motion of the air can be numerically represented on computers by a flow field where velocity vectors, temperature, pressure and other scalar species are averaged out and identified. These variables are unknown, but can be numerically predicted using some fundamental physical principles of a fluid flow and the CFD technique.

CFD is a generic term used to designate a family of numerical methods which is used to calculate the properties (e.g. velocity, pressure, temperature, and other scalar

species) of a fluid flow (e.g. water, wind). In building engineering, CFD can provide designers detailed information about the airflow outside and inside a building under specific boundary conditions.

The physical properties of any fluid flow are governed by three fundamental principles: (1) mass of the fluid is conserved; (2) conservation of momentum $\vec{F} = m\vec{a}$ (according to the Newton's second law of motion); and (3) energy is conserved (Wendt, 2009). These principles are represented by some **partial differential equations** (e.g. at least 5 equations for a 3-D problem). Successfully solving these equations will give the solution to the fluid flow.

The number of unknown variables is normally higher than the number of the partial differential equations. Furthermore, the partial differential equations (containing unknown variables of the flow field) are highly nonlinear and coupled; thus they therefore cannot be solved by analytical mathematics. In CFD, these partial differential equations are solved using a method known as Finite Volume Method (or maybe Finite Difference Method, Finite Element Method, Spectral Method) (Heisenberg, et al., 1998). To do that, all initial conditions must be imposed on the boundaries of the flow field. The study domain is then discretized into a set of non-overlapping adjoining rectilinear cells (or finite volume grid cell). At each grid cell (control volume), the governing partial differential equations mentioned above are still correct. To solve these partial differential equations, they are re-arranged and converted into a set of algebraic equations using a Taylor series expansion. The algebraic equations can be solved by the basic numerical method. The unknown (or dependant) variables are iteratively or simultaneously calculated at each grid cell by the numerical method until the convergence criteria are satisfied or predefined number of iterations reaches.

The fundamental partial differential equations of CFD are classical, rather long and sophisticated; they are therefore not necessary to present in this thesis. Details about CFD fundamental equations and principles can be found in many references (Versteeg & Malalasekera, 1995; Heisenberg, et al., 1998; Allard, 1998; Wendt, 2009). The governing equations of RNG k- ϵ turbulence model will be presented in detail in the subsequent sections as a substitution. A brief explanation of how these equations are solved can be found in (Bakker, 2012).

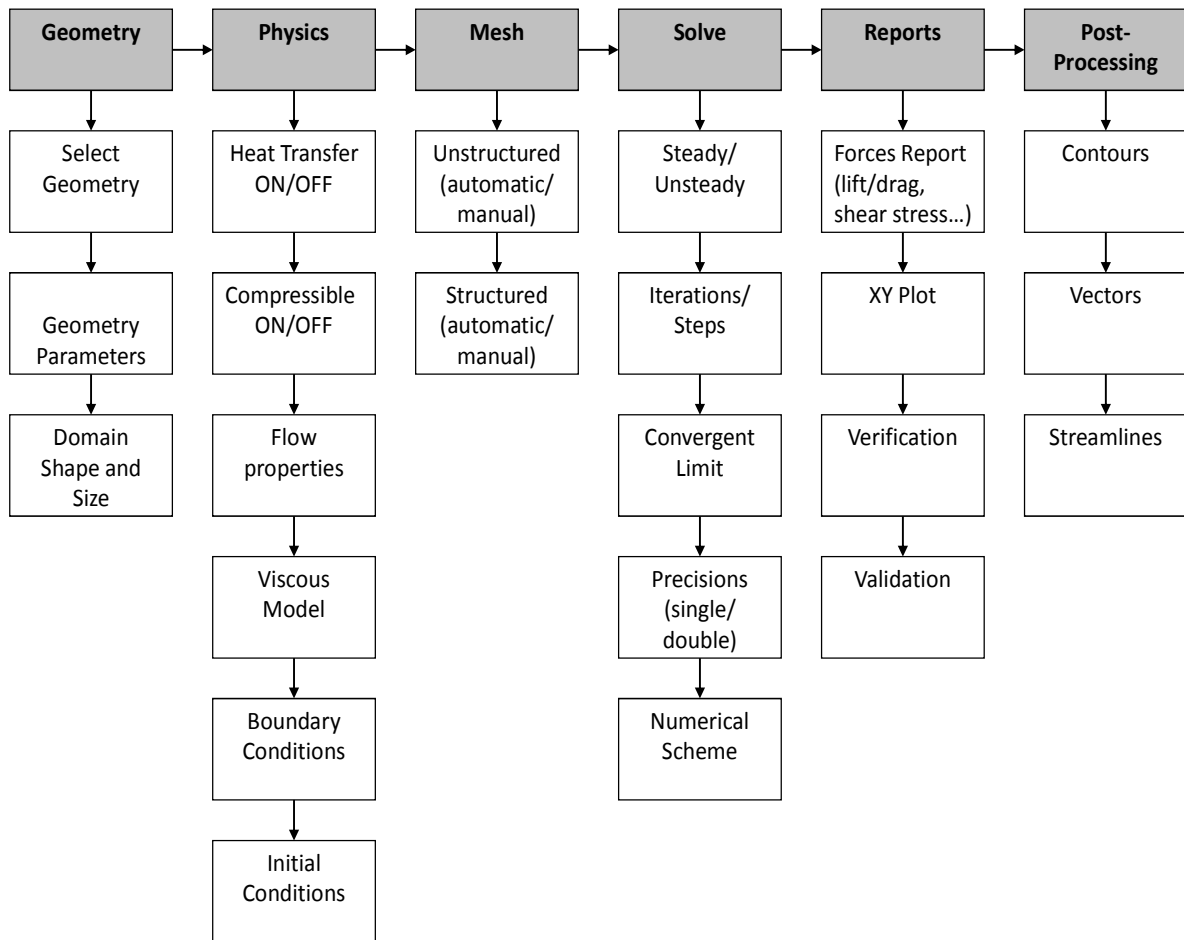


Figure 5-5: Typical steps of a CFD study (Xing & Stern, 2010)

A typical CFD simulation usually consists of 6 steps as described in Figure 5-5. Three first steps generate CFD inputs for a Solver (step 4) in which the governing equations of CFD are solved. Step 5 and 6 use specific tools to read the outputs and illustrate them in form of graphs, contour, streamlines, vectors, etc. These six steps can be done by some separated modules or integrated into a unique simulation package. Generic instructions and requirements for each step were given in ASHRAE Handbook (ASHRAE, 2009).

Benefits of the CFD technique are numerous (see (Versteeg & Malalasekera, 1995)).

In building sciences, CFD provides the following benefits:

- Significant reduction of time and cost of studies on natural ventilation and HVAC systems, compared to those of experiments in wind tunnels.
- Unlimited level of detail of results.

- Ability to perform studies on very large or complex buildings where experiments are impossible or too expensive to perform.

Nowadays, the CFD technique becomes stronger and spreads into many industrial applications. In the building engineering, CFD was used to predict the wind flow inside and around buildings (Jiang, et al., 2003; Takahashi, et al., 2004; Murakami, et al., 2004; Glória Gomes, et al., 2005; Reiter, 2010), air distribution systems (Ladeine & Nearon, 1997; Li, et al., 2009), contaminants concentration (Emmerich, 1997; Barbason & Reiter, 2011), thermal comfort (Gebremedhin & Wu, 2003; Sevilgen & Kilic, 2011), fire safety (Huang, et al., 2009)... Although CFD requires high expertise of users and fundamental knowledge of aerodynamics, it is the most frequently used among ventilation prediction methods (Chen, 2009). Results given by CFD are considered as the most accurate among numerical methods. The CFD technique also allows users to perform a series of parametric simulation with reasonable cost of time. For these reasons, the CFD method was chosen in this thesis for most studies related to the wind.

5.3.2.2 The choice of RANS approach, turbulence model and CFD solver

Records of the time variation of wind have shown that wind velocity and directions randomly fluctuate and that wind is an irregular physical phenomenon (Vickery, et al., 1977; Allard, 1998). The term “TURBULENCE” is used to designate such a random phenomenon. Consequently, modeling “turbulence” of the wind is the main challenge of wind engineering.

There are three main approaches to model “turbulence” in CFD: Direct Numerical Simulation (DNS), Reynolds-Averaged Navier-Stokes (RANS) and Large Eddies Simulation (LES).

DNS method is very accurate, sometimes more accurate than experimental methods. In reality, DNS does not model turbulence, but it uses a very fine grid system to catch the Kolmogorov microscale¹⁷ (of order 1mm) - the concept given by Kolmogorov’s experiments on turbulence. This method may need a grid system of 10^{14} cells for the airflow in a room. Current supercomputers can solve a grid resolution of 10^7 (Murakami, 1998; Zhang & Chen, 2000); the DNS method is therefore not feasible for any studies on indoor

¹⁷ Kolmogorov microscales are the smallest scales in turbulent flow within which viscosity of the fluid is dominant and the turbulent kinetic energy is dissipated into heat

and outdoor airflows. It is only used to study spatially and temporally simple geometries, e.g. flows over an isolated cube or flows in a duct. DNS cannot be used to study natural ventilation due to the limitation of available computer memory and speed at present. To overcome this obstacle, many other methods have been developed.

LES is used to calculate the time-dependant large eddy motion for a simple building geometry that RANS fails to resolve. It is a technique in which the smaller eddies of the flow field are filtered and modeled using a sub-grid scale model, while the larger energy carrying eddies are explicitly simulated. When the grid size is as small as the Kolmogorov length scale, the LES turns into a DNS. However, LES still requires enormous computing resources and time (ASHRAE, 2009).

In the RANS approach, three main families of modeling were retained: the Spalart-Allmaras model (one equation model, which only solves one transport equation for a viscosity-like variable $\tilde{\nu}$), the k-epsilon (k- ϵ) and the k-omega (k- ω) models. The k- ϵ models are based on two equations: one for the turbulent kinetic energy (k) and one for the rate of dissipation of turbulent kinetic energy (ϵ). The k- ω is also based on two transport equations to represent turbulent properties of the flow: the first transported variable is turbulent kinetic energy (k) and the second is the specific dissipation (ω). RANS is generally the most popular approach in industrial applications, mostly for simulating steady mean flows and scalar species transport that are relatively suitable for architectural research. Consequently, RANS is selected and applied in this work.

Another less-mentioned method is Detached Eddy Simulation (DES) which is a hybrid form of RANS-LES models. Detailed reviews of these approaches can be found in (Murakami, 1998; Zhang & Chen, 2000; ASHRAE, 2009).

The standard k- ϵ model has been proven effective for various engineering applications and it has widely been used in the industrial sector. Barbason and Reiter (2010) compared performances of various turbulence models and reported that the choice of k- ϵ was a good compromise except for natural ventilation with significant indoor thermal loads. However, certain characteristics of an air flow, such as the creation of regions with very low velocities and thus low Reynolds numbers, particularly in near-wall regions, could not be accurately predicted by standard k- ϵ . This requirement led to the formulation of a modified k- ϵ turbulence model, which is expected to be more effective and more accurate for such

regions. These models are the low-Reynolds number $k-\epsilon$ model (LR $k-\epsilon$), the RNG $k-\epsilon$ model and Reynolds stress model (RSM) (Stamou & Katsiris, 2006). A basic characteristic of the RNG $k-\epsilon$ (Yakhot & Orszag, 1986) turbulence model is that it involves an analytically derived differential formula for effective viscosity that accounts for low-Reynolds number effects. This feature of the RNG $k-\epsilon$ model combined with appropriate treatment of the near-wall region gives better prediction of indoor airflow applications than that of the standard $k-\epsilon$ model (Stamou & Katsiris, 2006).

Gebremedhin and Wu (2003) examined five RANS models (the standard $k-\epsilon$, the RNG $k-\epsilon$, the LR $k-\epsilon$, the $k-\omega$ and the RSM) using Phoenics code for a space occupied by 10 cows. Based on the convergence and computational stability criteria, they stated that the RNG $k-\epsilon$ model was the most appropriate model to characterize the flow field in a ventilated space.

Glória Gomes et al. (2005) carried out some experiments and numerical simulations on Phoenics code to see effects of different irregular-plan shapes on the air flow. They reported that the RNG $k-\epsilon$ model results were in good agreement with the experimental results.

Chen (1995) compared five different $k-\epsilon$ models, including a standard $k-\epsilon$ model, a low-Reynolds-number $k-\epsilon$ model, a two-layer $k-\epsilon$ model, a two-scale $k-\epsilon$ model, and a renormalization group (RNG) $k-\epsilon$ model. Corresponding experimental data from relevant literature on the subject were used for validation. He found the RNG $k-\epsilon$ model is slightly better than the standard $k-\epsilon$ model and is therefore recommended for simulations of indoor airflow. He also stated that the performance of the other models was not stable.

The results mentioned above show that the RNG $k-\epsilon$ model gives fairly good results and is an appropriate turbulence model for the simulation of indoor airflow. Therefore, RNG $k-\epsilon$ turbulence model was chosen for this work.

There are many CFD codes written recent years. Most of them are free codes (e.g. Code_Saturne, COOLFluid, NaSt2D-2.0, Edge...) while some others are commercial codes (e.g. MicroFlo in VE 6.1 software package, Fluent, Flovent, Turbo CFD...). This thesis used the commercial code Phoenics 2010 (CHAM Co., 2010) to solve the governing equations of the airflow. Phoenics 2010 allows architects and engineers to simulate a 3-D flow field and gives simultaneously results of various parameters by solving the continuity,

momentum and energy equations. With Fluent code, Phoenics is currently one of the mostly-used codes in academic CFD research (Zhang & Chen, 2000; Gebremedhin & Wu, 2003; Glória Gomes, et al., 2005; Stamou & Katsiris, 2006).

5.3.2.3 Validation of the selected turbulence model in predicting indoor and outdoor airflows in a simple cross ventilation case

Experimental settings of the wind tunnel experiment:

Validation demonstrates the ability of both users and the CFD code in accurately predicting representative indoor environmental applications for which some forms of reliable data are available. In this thesis, the CFD results of a simple cross ventilation case were compared with the experimental data performed by Jiang et al. (2003) to validate the reliability of the RNG k- ϵ turbulence model.

Jiang et al. (2003) carried out a wind tunnel experiment at Cardiff University to study the flow field in and around a cubic model which allowed cross ventilation. The wind tunnel had a cross section dimension of 2 m in width and 1 m in height. The maximum wind speed in the tunnel was about 12.0 m/s and its variation between measurement runs was within 2%. A 6.0 m upstream fetch in the tunnel used a combination of blockage, fences and surface roughness (Lego Duplo blocks) to simulate the lower part of an urban atmospheric boundary layer. The cubic model was 250 mm x 250 mm x 250 mm in dimension with an 84 mm x 125 mm opening in both windward and leeward wall. The wall thickness was 6 mm evenly. Wind velocities were measured along 9 vertical lines at the center section of the model with 18 measurement points on each line (see Figure 5-6).

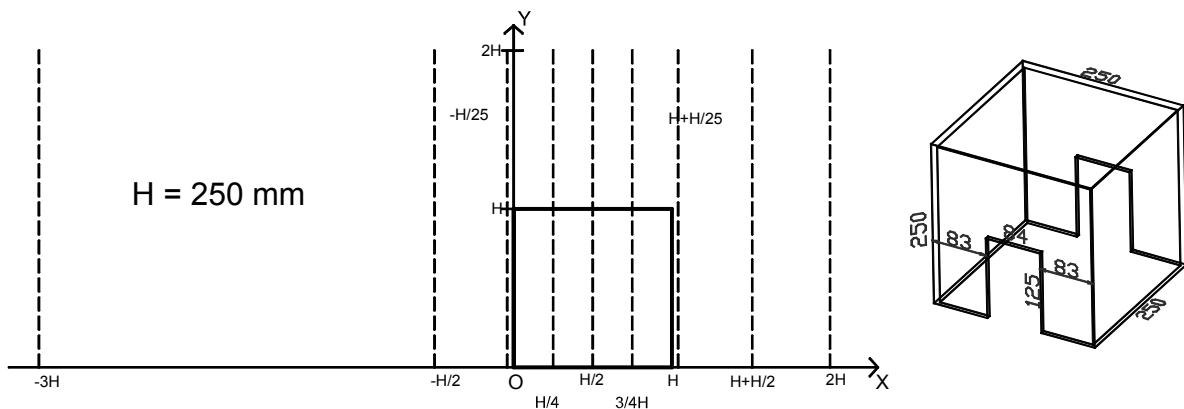


Figure 5-6: Locations of wind velocity measurement on the symmetrical section of the model (thick dark block) and model configurations (all dimensions in mm)

Governing equations of the RNG k-ε turbulence model:

The RNG k-ε model (Yakhot, et al., 1992) is a two-equation turbulence model, similar to the standard k-ε model, which is derived by using Renormalization Group methods. This model differs from the standard k-ε model only due to the modification of ε to the equation. As this simulation was assumed isothermal, the equation of energy conservation is excluded. The remaining governing equations are the time-averaged continuity (5.1), momentum (5.2) and transport equations for k (5.3) and ε (5.4), as follows:

$$\frac{\partial u_i}{\partial x_i} = 0 \quad (5.1)$$

$$\frac{\partial}{\partial x_j} (u_i u_j) = \frac{\partial}{\partial x_j} \left[(v + v_t) \frac{\partial u_i}{\partial x_j} \right] - \frac{1}{\rho} \frac{\partial p}{\partial x_i} \quad (5.2)$$

$$\frac{\partial}{\partial x_j} (k u_j) = \frac{\partial}{\partial x_j} \left[\left(v + \frac{v_t}{\sigma_k} \right) \frac{\partial k}{\partial x_j} \right] + v_t S_{ij} \frac{\partial u_i}{\partial x_j} - \varepsilon \quad (5.3)$$

$$\frac{\partial}{\partial x_j} (\varepsilon u_j) = \frac{\partial}{\partial x_j} \left[\left(v + \frac{v_t}{\sigma_\varepsilon} \right) \frac{\partial \varepsilon}{\partial x_j} \right] + c_{\varepsilon 1} \frac{\varepsilon}{k} v_t S_{ij} \frac{\delta u_i}{\delta x_j} - c_{\varepsilon 2} \frac{\varepsilon^2}{k} - \frac{C_\mu \eta^3 (1 - \eta / \eta_0) \varepsilon^2}{1 + \beta \eta^3} \frac{\varepsilon^2}{k} \quad (5.4)$$

where

u_i, u_j are the mean and fluctuating velocity components in the x_i, x_j direction, respectively; p is the mean pressure; ρ is the fluid density; k and ε stand for the turbulence kinetic energy and its rate of dissipation, respectively; $v_t = C_\mu k^2 / \varepsilon$ (isotropic eddy viscosity), $\eta = kS / \varepsilon$, $S = (2S_{ij}S_{ij})^{1/2}$ and $S_{ij} = (\partial u_i / \partial x_j + \partial u_j / \partial x_i) / 2$ (mean rate of strain tensor). The turbulence constants are: $\sigma_k = 0.7179$; $\sigma_\varepsilon = 0.7179$; $C_\mu = 0.085$; $c_{\varepsilon 1} = 1.42$; $c_{\varepsilon 2} = 1.68$; $\eta_0 = 4.38$; $\beta = 0.015$.

Solution for the flow field in near-wall regions:

The k-ε model is not able to predict the flow in the near-wall region (the thin air layer near the hard surface such as wall, floor, etc) due to the viscous effect of the air at low velocity and low Reynolds number within this region. Very dense grid is therefore needed for accurate prediction, thereby significantly increasing simulation time. Two methods were

proposed for near-wall modeling: the Low-Reynolds-number model (Patel, et al., 1985) and the wall-function method (Launder & Spalding, 1974).

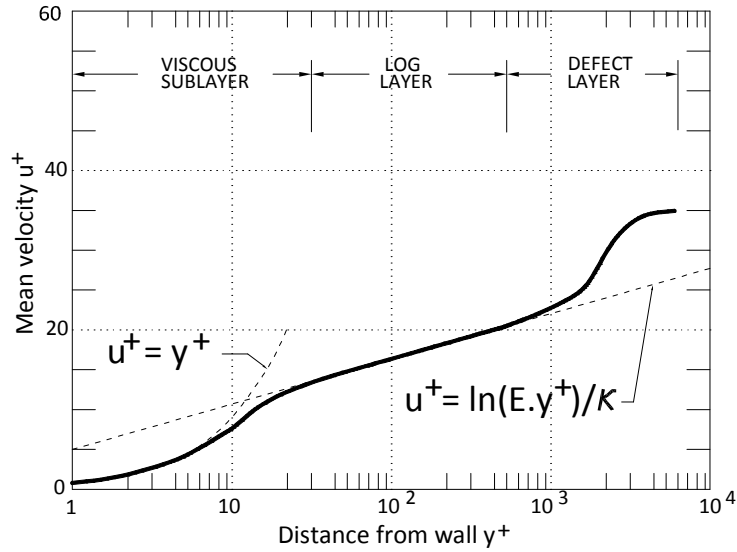


Figure 5-7: Typical velocity distribution in near-wall region (after (Wilcox, 1998))

In this study, the near-wall boundary layer was treated by employing the *equilibrium Logarithmic wall-function method*: for the viscous (laminar) sublayer and log-law sublayer (ASHRAE, 2009). These layers are presented in Figure 5-7. This method is the most suitable solution for isothermal simulation (Spalding, 2009) and may be written as follows:

$$u^+ = \frac{u_r}{u_\tau} = \frac{1}{\kappa} \ln(Ey^+) \quad (5.5)$$

Strictly this law should be applied to a point whose $30 < y^+ < 130$, and

$$u^+ = y^+ \quad (5.6)$$

if y^+ value is in the range $0 < y^+ < 5$. Turbulent kinetic energy and its dissipation rate within near-wall regions:

$$k = \frac{u_\tau^2}{\sqrt{C_\mu}} \quad (5.7)$$

$$\varepsilon = \frac{C_\mu^{3/4} k^{3/2}}{\kappa y} \quad (5.8)$$

where:

u^+ is dimensionless velocity;

u_r is the absolute value of the resultant velocity parallel to the wall at the first grid node;

u_τ is the resultant friction velocity $u_\tau = \sqrt{\tau_w / \rho}$; τ_w is wall shear stress;

y is the normal distance of the first grid point from the wall;

y^+ is the dimensionless wall distance $y^+ = \rho u_\tau y / \mu$;

C_μ is a constant equal to 0.085 in the RNG k- ϵ model;

\mathcal{K} is the von Karman constant equal to 0.42;

E is a function of the wall roughness parameter (in Phoenics, for smooth wall, $E = 8.6$).

Discretization technique:

The finite volume method was implemented for the spatial discretization of the research domain by applying 3-D structured Cartesian mesh. As reported by Loomans (1998) and Spalding (2009) as well as by grid testing, grid distribution must be continuous to reduce the rate of change of grid size across region boundaries. The size of adjacent cells should be equal or as close to equal as possible to avoid serious numerical errors during simulation. Besides, grid merge tolerance must be less than or equal to the thickness of the smallest component. Power-law distribution method (Spalding, 2009) was exploited to ensure high grid density around the object without increasing the total number of cells in the domain. A finer mesh was imposed in the near-wall regions in order to accurately resolve the high-gradient regions of the flow field. After some grid dependency tests to verify the influence of grid discretization on numerical results, the final simulation used a non-uniform structured grid of 97 x 47 x 55 cells with the domain dimension of 12L (length) x 4L (height) x 8L (width), where L is the reference size of the cubic model (see Figure 5-6).

Time step, iteration number, and convergence criteria:

In this validation simulation, 1st-order Upwind scheme was selected to discretize the convection term in the governing equation. The SIMPLEST (Spalding, 2009) (Semi-Implicit Method for Pressure-Linked Equations - Shortened) algorithm which is a variant of SIMPLE algorithm was used for the solution of the systems of algebraic equations for velocity components and pressure. The iteration uses the false-time-step relaxation for the velocities u , v and w and linear method for all other variables.

The simulation achieved convergence when the mass balance was accurate within 1% of the mass flow rate for the whole domain. Furthermore, the variation of flow variables (u , v , w) at specified positions in the flow field had to be less than 1% over the last 100 time steps for absolute values larger than 0.01. Convergence was controlled by three simultaneous factors: spot monitor (unchanged values) at a probe location, variables' error

(under 1%), and mass conservation (mass in – mass out = 0). In the validating simulation, the solution achieved convergence after 2270 iterations, equal to 7h47' CPU time (2x1.46 Ghz, 2Gb RAM).

Other boundary conditions:

We ensured the homogeneity between numerical simulation conditions and those of the wind tunnel experiment. The variation of wind velocity with the height of the inlet follows logarithmic law, which was the case in our experiment, and the effective roughness height was 0.003 m. The building model in the simulation was placed at the same location as in the experiment conducted by Jiang et al. The model surface roughness was assigned to be zero as the experimental model was made of Perspex. At the ground wall boundary, the wall function method was adopted with a roughness of $5 \cdot 10^{-5}$ m. At the side and upper boundaries, the full-slip velocity condition was adopted. The simulation was assumed to be isothermal. Details of boundary conditions are reported in Table 5-2.

Table 5-2: Details of the boundary conditions and computational parameters

	P	u	v	w	k	ε
Inflow	--	$U_{ref}=10\text{m/s}$ $\frac{u_z}{U^*} = \frac{1}{\kappa} \ln\left(\frac{z}{z_0}\right)$	0	0	$k=3U_{ref}^2 i_t^2 / 2$	$\varepsilon = C_\mu k^{3/2} / l$
Outflow	Zero external ambient pressure	$u, v, w, k, \varepsilon: \partial/\partial x = 0$				
Upper and side surfaces of computational domain	--	$(u_n) = 0; (u_t), k, \varepsilon: \partial/\partial x = 0$				
Solid wall	--	0	0	0	$\partial k/\partial n = 0$	Equation (8)
Relaxation method	Linear	False-time step	False-time step	False-time step	Linear	Linear
Relaxation factor	0.5	1	1	1	0.5	0.5
Convergence criterion	1%	1%	1%	1%	1%	1%

where: U_{ref} is reference inflow velocity at height 500mm; i_t is turbulence intensity; l is characteristic length; C_μ is constant equal 0.085, u_z is wind velocity at height z ; z_0 is aerodynamic roughness length; U^* is the friction velocity [$U^* / U_{ref} = \kappa / \ln(z_{ref} / z_0)$]; (u_n) , (u_t) are normal and tangential velocity component at 1st grid cell adjacent to upper and side wall; n is local coordinate normal to the wall.

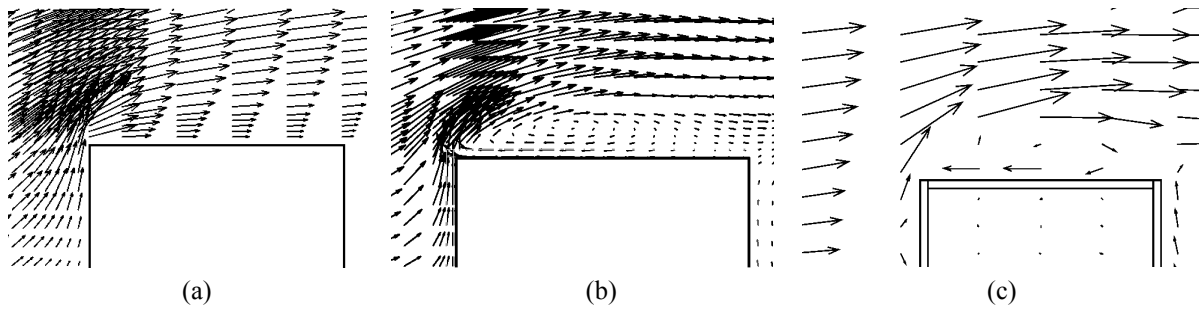


Figure 5-8: Incorrect prediction of recirculation above a cube by the $k-\epsilon$ model (a); the correction by the method of Gao and Chow (b) and wind tunnel experiment (c)

A further problem needed to be resolved. The results of many studies (Murakami, 1998; Tsuchiya, et al., 1997; Thomas & Williams, 1999) have pointed out that the $k-\epsilon$ turbulence model does not accurately predict the flow field above a cube due to an incorrect prediction of turbulence kinetic energy k at the frontal sharp edge, that might interfere with the pressure distribution behind the object. To obtain a better prediction of the recirculation flow at the top of the cube, this study adopted the suggestion of Gao and Chow (2005) by limiting the longitudinal velocities in the first cell adjacent to the sharp edge of the cube, and setting appropriate wall functions at the intersection cells for the velocity components (see Figure 5-8).

Validation of the numerical results:

This section compares the results of the numerical simulation from this thesis with those given by the wind tunnel experiment of Jiang et al. (2003). First, the mean velocity distributions outside and inside the model will be analyzed and then the wind flow pattern on the model will be discussed.

Figure 5-9 and Figure 5-10 show comparisons of the mean velocity U/U_{ref} and V/U_{ref} distributions on 9 vertical lines at the center section of the model (U , V are mean velocities on x and y axes, respectively). With the same inlet wind profile at $x = -3H$, it is clear that results generated by the RNG $k-\epsilon$ model generally matched those from the experiment. It is notable that this agreement is even better inside the model ($0 < x < H$, $y < 0.25$).

Figure 5-11 illustrates the wind flow pattern around the model generated by the CFD simulation and the corresponding experiment. Similar wind distribution was obtained, especially inside the model where the velocity vectors' distribution was almost the same.

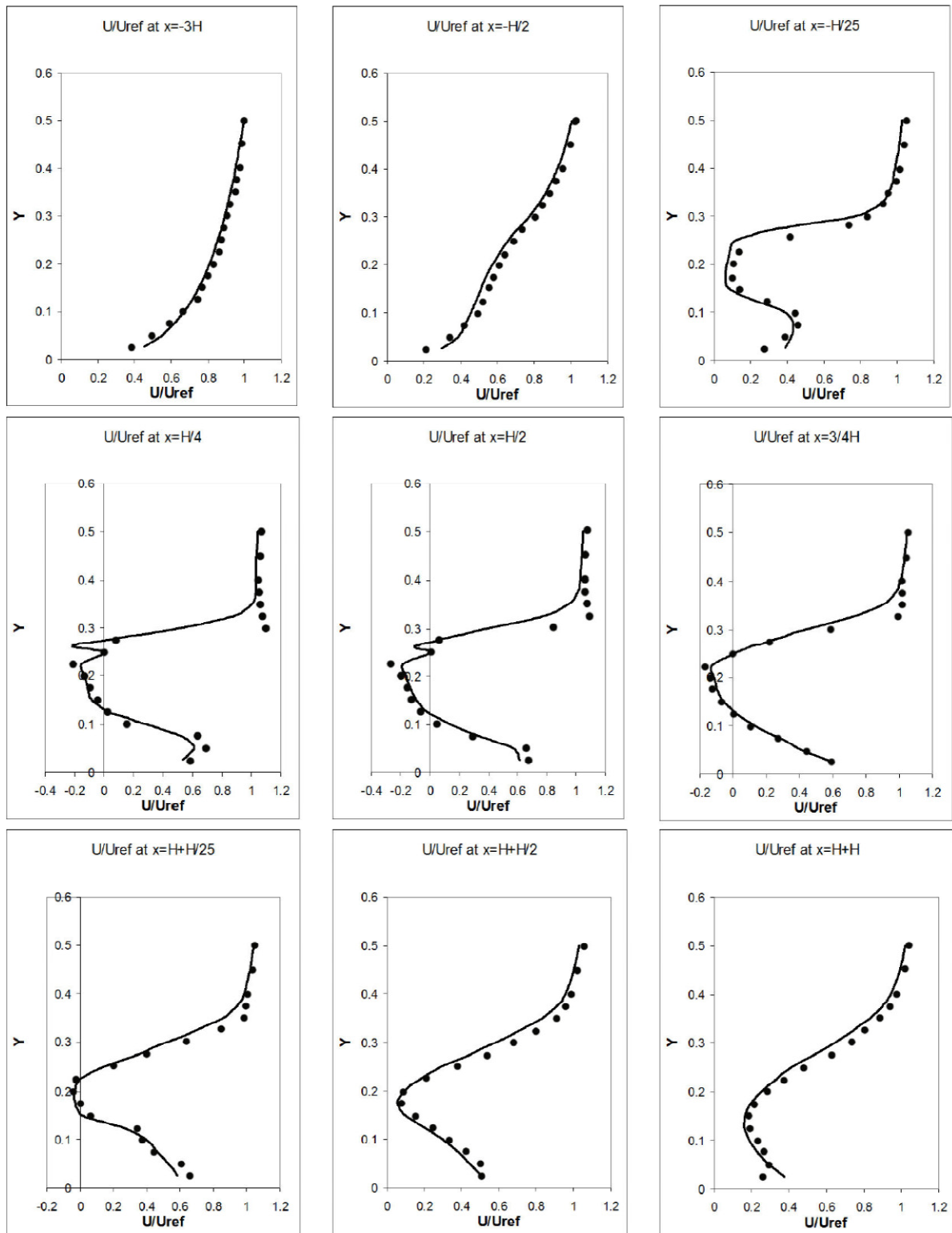


Figure 5-9: Mean velocity U/U_{ref} on 9 vertical lines at center section of the model (Black dots: experiment; solid line: numerical results)

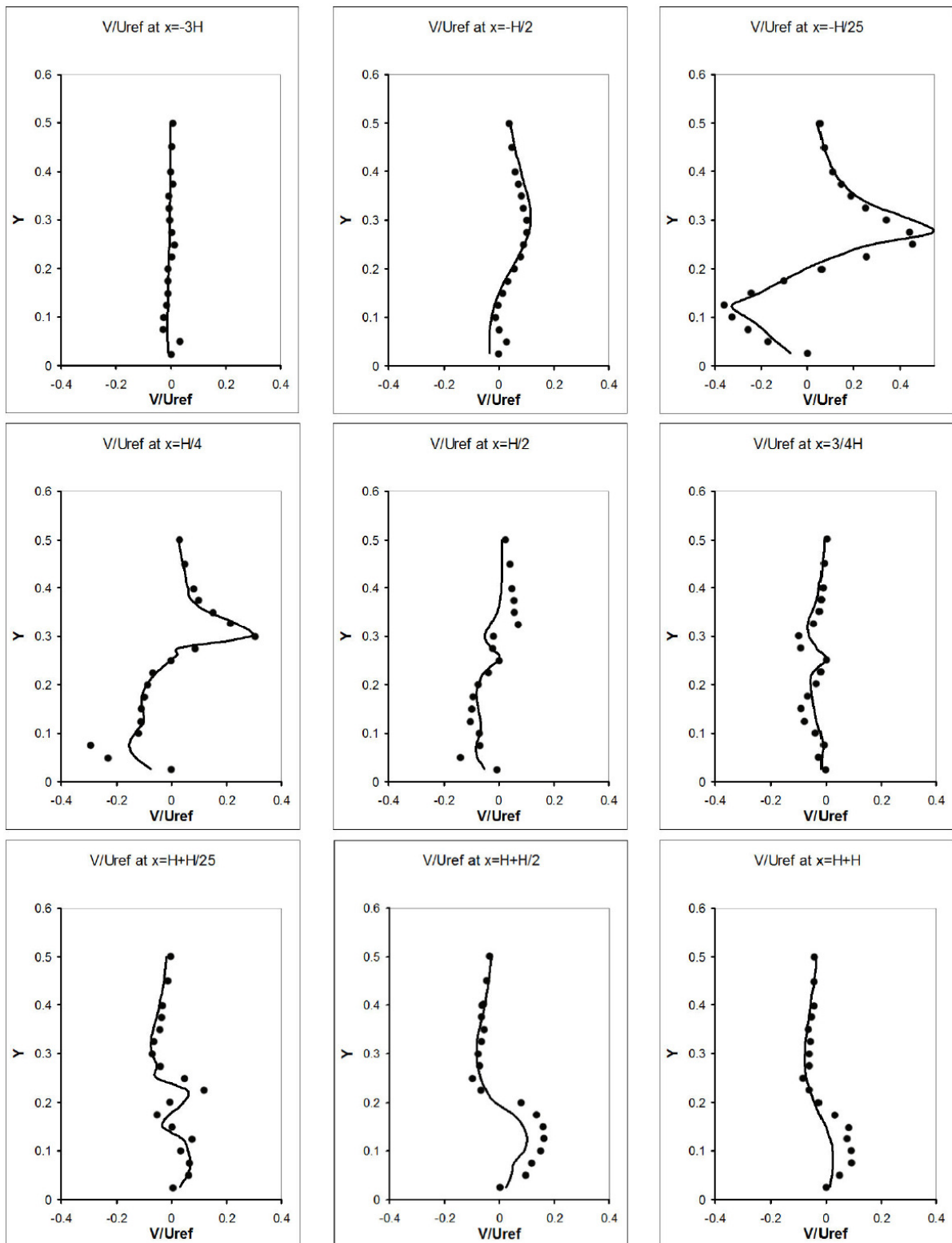


Figure 5-10: Mean velocity V/U_{ref} on 9 vertical lines at center section of the model (Black dots: experiment; solid line: numerical results)

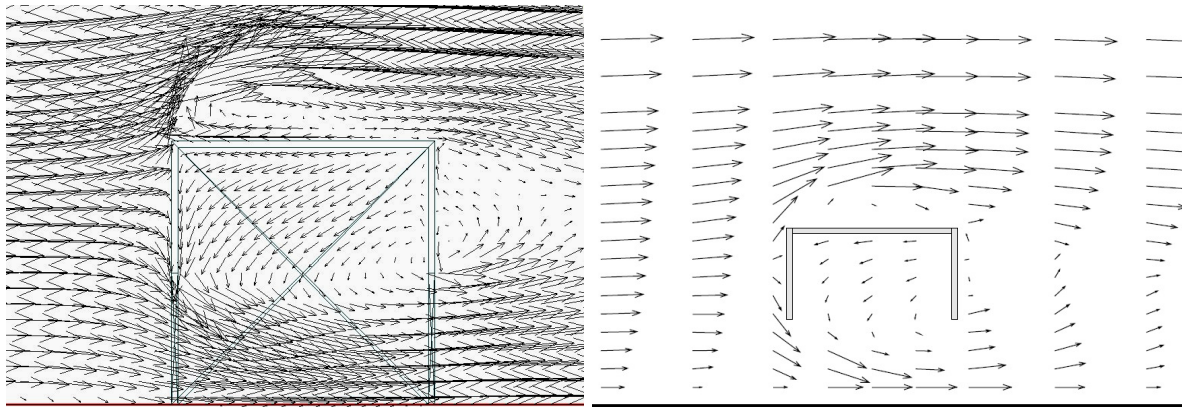


Figure 5-11: Wind velocity distribution around the model by RNG $k-\epsilon$ simulation in this study (left) and in the practical experiment (right)

Even so, some discrepancies between experimental and numerical results exist. The simulation generally seems to underestimate the wind speed above the top of the model in both x and y directions ($y > 0.25$). As can be seen from Figure 5-11, the recirculation area above the roof of the model is higher and a little bigger in the simulation which leads to the underestimation of the wind velocity. As reported above, the $k-\epsilon$ model does not accurately predict the flow field above the cube although a correction of the boundary condition was established. Near the ground boundary, small discrepancies may be attributed to coarseness of the mesh dividing near the floor. Discrepancies might also come from the differences in boundary conditions present during the two studies that are very difficult to eliminate such as inlet turbulence intensity, the effect of heat transfer, errors in measurement during the experiment, etc.

Generally the comparisons correlated, confirming the reliability of the RNG $k-\epsilon$ model in accurately predicting the airflow field in and around the building. Therefore, the RNG $k-\epsilon$ model can be used for other simulations of similar configurations with confidence.

5.4 Modeling the case-study houses in EnergyPlus

The in-situ measuring data of the case-study houses was used to build the computer thermal models for EnergyPlus simulation program. As EnergyPlus does not have any user interface, these 3D CAD models were first built in Autodesk Ecotect[®] Analysis software (Autodesk, 2011) and then converted into the file format readable by EnergyPlus. Autodesk Ecotect[®] Analysis is able to graphically display the models; hence it helps reduce errors during the modeling process. Figure 5-12 shows these 3D models in EnergyPlus. As can be

seen, nearby buildings and other obstacles such as trees were also included in the models for solar irradiation calculations. Walls adjacent to other thermal zones of adjacent houses or apartments (in cases of the row house and apartment) were assumed adiabatic; thus only thermal inertias of those walls were taken into account. In EnergyPlus, building materials, components, systems and occupancies were assigned. Building materials and components are almost readily available in EnergyPlus library. Building occupancy and openings control were scheduled following the daily habits as being observed.

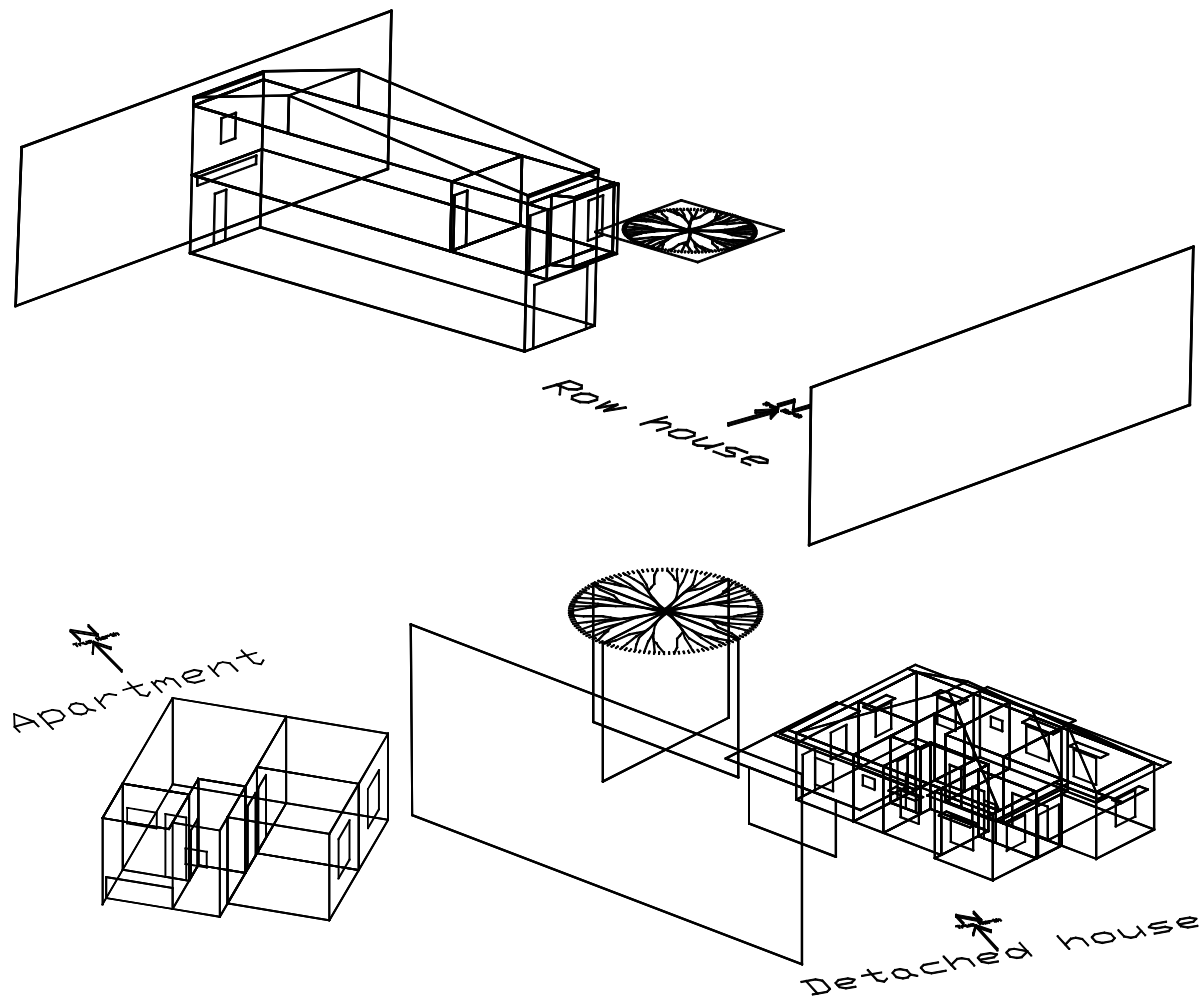


Figure 5-12: 3D housing models in EnergyPlus. Rectangular planes around the houses represent adjacent buildings and trees. Adjacent buildings of the apartment are not shown.

The simulations were set at 20 time-steps per hour to ensure the complete convergence although this will almost double simulation time. The heat balance algorithm selected was Conduction Transfer Function. Inside and outside surface convection heat transfer algorithms were TARP and DOE-2, respectively. The solar distribution calculation

was Full Interior and Exterior algorithm. Details about these settings can be found in EnergyPlus Documentations accompanying with the simulation package.

5.4.1 About Airflow Network model and its role in modeling NV buildings

In NV buildings, the airflow rate has a great influence on indoor thermal environment. However, it is not easy to model the effect of wind in thermal dynamic simulation. Allard (1998) reported that most thermal simulation models applied a very simplistic approach to calculate the ventilation and air infiltration rates. In AC buildings where ventilation is completely governed by a mechanical system, such approach can be acceptable. Conversely, if the building is fully or partly ventilated by natural mechanisms, such an approach is possibly inadequate and simulation models may result in questionable thermal predictions (Allard, 1998).

Results of sensitivity analysis in BPS also show that the air flow rate is among the most sensitive parameters which have maximum effects on the output (Hopfe, et al., 2007; Hopfe & Hensen, 2011). To accurately predict the airflow rate of each simulated time step using hourly outdoor wind conditions, the Airflow network model in EnergyPlus was used. An Airflow network consists of a set of nodes (thermal zones) linked by airflow components through the openings and voids. The variables are node's pressures and the linkage between nodes is the airflow rate. Further detailed descriptions of airflow network model can be found in (Walton, 1989) and his related works. More sophisticated models, e.g. CFD or zonal modeling, are currently available, but out of scope of this task. Inputs of the Airflow network model includes hourly wind speed and direction; building location, building azimuth and shape; window sizes and positions, discharge coefficient, window crack infiltration, control schedule and wind pressure coefficients (WPC) on the openings corresponding to each wind direction.

5.4.2 Calculation of wind pressure coefficient using CFD

WPC is a dimensionless number represents the relative pressure throughout the flow field. It is defined as:

$$C_p = \frac{p_{st} - p_{\infty}}{0.5\rho_{\infty}V_{\infty}^2} \quad (5.9)$$

where

C_p is WPC, dimensionless;

p_{st} and p_{∞} are static wind pressure at the point in question and free stream static pressure, respectively, Pa;

ρ_{∞} is free stream air density, kg/m³ (this thesis takes 1.189 kg/m³ at 20°C and standard atmospheric pressure);

V_{∞} is free stream velocity at reference height (opening height), m/s.

WPC is required for the calculation of airflow rates through an opening caused by natural wind. WPCs on an opening can be obtained by a few methods, e.g. from in-situ measurements, from published pressure coefficient data sets (Allard, 1998; ASHRAE, 2009) or from CFD simulation. In this thesis, WPCs of each opening of the houses were calculated for each wind direction using the CFD method. In BPS, this approach offers great advantages that WPCs of any building geometries and sites' topographies corresponding to any wind directions and wind speeds can be accurately predicted. However, this method requires much time and effort because CFD simulation must be run for every wind direction as well as strong knowledge of fluid mechanics.

As three case-study houses are located in different urban areas of Danang and three houses have different sizes and typologies, three series of CFD simulation corresponding to three houses must be conducted. The boundary conditions applied in these series of CFD simulations slightly differed from each other as described below.

The building models in the simulation were placed at the center of a square domain so that wind can reach the building from any directions in the same manner. The model surfaces were considered as a solid wall with smooth friction and wall roughness were assigned to be 0.5m to reproduce rough building façades. The surrounding buildings and obstacles were also included in the CFD simulation.

The inlet wind velocity followed the power-law function of height with exponent values of 0.17 to 0.22 - similar to terrains category 2 and 3 in ASHRAE handbook (ASHRAE, 2009). The reference wind speed at height of 10m is equal to annual average wind speed of Danang - 1.85m/s (Institute of Construction Science and Technology, 2009). The effective roughness heights of the ground were varied from 0.1 to 0.5 m. Other sides and upper boundaries of the domain were considered as opened sky where the pressure and velocity field were assumed identical between inside and outside of the boundaries.

The finite volume method was implemented for spatial discretization of the simulation domain by using a 3-D structured Cartesian mesh. The power-law method (Spalding, 2009) was applied to ensure high grid density around objects without increasing the total number of cells in the domain. A finer mesh was imposed in the near-wall regions so as to accurately resolve the high-gradient regions of the flow field. After some grid dependency tests to verify the influence of grid discretization on numerical results, the final setting used a non-uniform structured grid of around 78 x 78 x 28 cells. The domain dimension of 200m (length) x 200m (width) x 50m (height) was imposed on the row house and detached house. As the surrounding buildings of the apartment are taller and spread on a large area, the simulation domain of the apartment was much larger (350m x 350m x 100m).

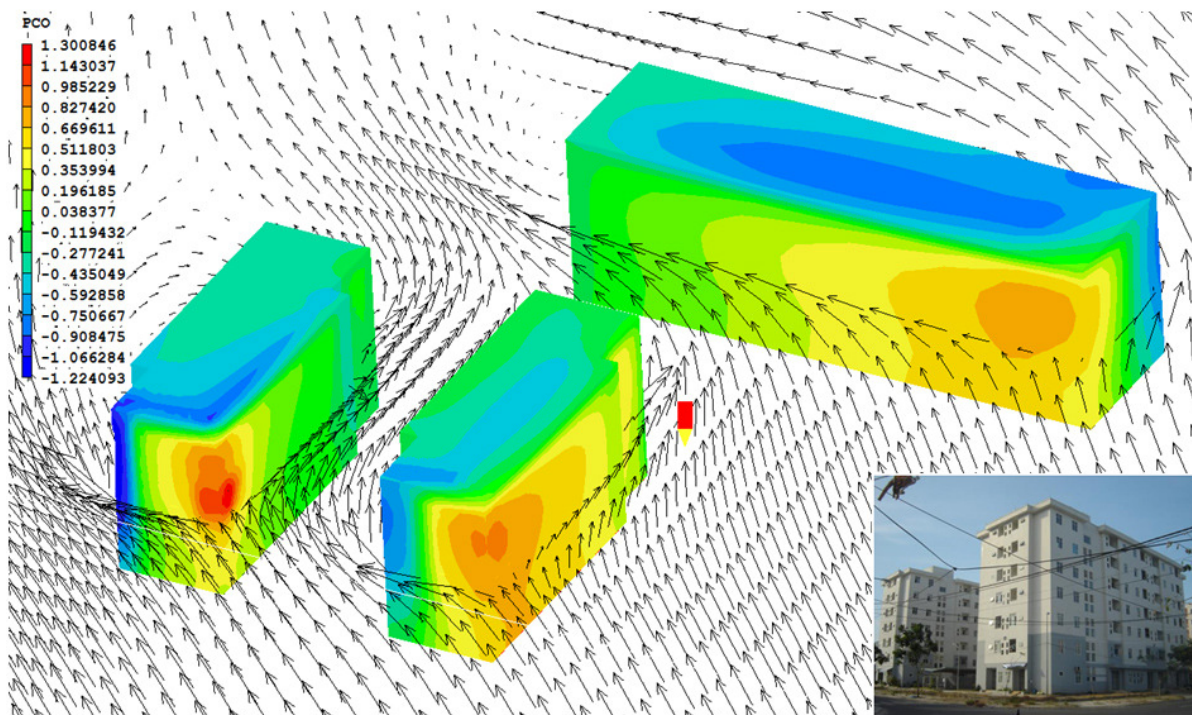


Figure 5-13: Simulated WPC surface contours of the wind from the South (180°) – the apartment is on the 4th floor of the building on the left.

The RNG k- ϵ turbulence model (Yakhot, et al., 1992) was chosen for these simulations because the accuracy of its predicted results were satisfied as reported in the validation study in section 5.3.2. All simulations were assumed isothermal. The CFD Phoenics code (version 2010) was used to solve partial differential equations for all grid cells in the domain iteratively until convergence criteria were satisfied. For each house, a series of 12 CFD simulations were conducted, corresponding to 12 wind directions (from 0°

to 330° in 30-degree steps). Totally, 36 simulations were launched. Each simulation completed after around 60 minutes CPU time.

Figure 5-13 shows a representative WPC distribution on the apartment buildings given by a CFD simulation under the South wind. This figure indicates that the nearby buildings had great impacts on the pressure distribution on building façades; thus their presence in the simulations was really relevant and necessary. The probe (red - yellow pointer) of the CFD code helps identify exact values of WPCs at its location. Detailed WPCs of each house, at each opening are listed in Table 5-3, Table 5-4 and Table 5-5. All simulated WPCs from CFD simulation were implemented into the Airflow network module of EnergyPlus.

Table 5-3: Wind pressure coefficient of the row house

Wind direction (true North is 0 degree)		Front façade			Backward façade		
		Openings at Height 2m	Openings at Height 5.2m	Openings of the attic	Openings at Height 3.2m	Openings at Height 5.2m	Openings of the attic
North	0	0.007	0.002	-0.002	0.001	0.001	-0.002
	30	-0.063	-0.070	-0.183	-0.099	-0.125	-0.191
	60	0.001	0.038	-0.090	-0.108	-0.109	-0.127
East	90	0.138	0.100	-0.187	-0.060	-0.061	-0.059
	120	-0.010	-0.039	-0.254	-0.145	-0.147	-0.167
	150	-0.053	-0.058	-0.196	-0.105	-0.123	-0.167
South	180	-0.016	-0.012	-0.026	-0.011	-0.011	-0.015
	210	-0.106	-0.131	-0.162	-0.080	-0.102	-0.119
	240	-0.110	-0.113	-0.129	-0.060	-0.073	-0.002
West	270	-0.095	-0.098	-0.104	-0.130	-0.133	-0.111
	300	-0.104	-0.107	-0.112	-0.115	-0.123	-0.072
	330	-0.114	-0.158	-0.139	-0.052	-0.074	-0.057

Table 5-4: Wind pressure coefficient of the detached house

Wind direction (true North is 0 degree)		South façade			North façade		
		Reading room window	Entrance door	Living room window	Kitchen door	Kitchen window	bedroom3 window
North	0	-0.040	-0.030	-0.020	0.096	0.150	0.078
	30	-0.005	-0.005	0.050	0.240	0.200	0.185
	60	0.058	0.067	0.090	0.225	0.197	0.198
East	90	0.110	0.110	0.070	0.115	0.135	0.130
	120	0.003	0.007	-0.015	0.048	0.059	0.068
	150	-0.137	-0.125	-0.125	-0.147	-0.150	-0.140

Wind direction (true North is 0 degree)		South façade			North façade		
		Reading room window	Entrance door	Living room window	Kitchen door	Kitchen window	bedroom3 window
South	180	-0.178	-0.142	-0.231	-0.285	-0.275	-0.285
	210	0.180	0.300	-0.300	-0.380	-0.380	-0.290
	240	-0.140	-0.106	-0.225	-0.355	-0.355	-0.369
West	270	-0.245	-0.191	-0.156	-0.410	-0.400	-0.400
	300	-0.148	-0.130	-0.130	-0.342	-0.366	-0.204
	330	-0.080	-0.080	-0.097	-0.097	-0.005	0.026

Wind direction (true North is 0 degree)		East façade			West façade		
		Living room window	Bedroom2 window	Bedroom3 window	Kitchen window	Bedroom1 window	Reading room window
North	0	-0.027	-0.025	0.000	-0.034	-0.040	-0.053
	30	0.105	0.142	0.178	0.179	0.142	0.070
	60	0.138	0.164	0.198	0.243	0.210	0.145
East	90	0.145	0.145	0.145	0.148	0.250	0.147
	120	0.063	0.060	0.060	0.071	0.090	0.035
	150	-0.125	-0.117	-0.110	-0.125	-0.137	-0.144
South	180	-0.275	-0.255	-0.285	-0.290	-0.270	-0.320
	210	-0.350	-0.354	-0.327	-0.400	-0.430	-0.210
	240	-0.293	-0.334	-0.346	-0.355	-0.374	-0.460
West	270	-0.170	-0.224	-0.295	-0.415	-0.415	-0.415
	300	-0.158	-0.170	-0.168	-0.337	-0.330	-0.313
	330	-0.085	-0.115	-0.050	-0.147	-0.110	-0.145

Table 5-5: Wind pressure coefficient of the apartment

Wind direction (true North is 0 degree)		Window bedroom 1	Window bedroom 2	Window Balcony and toilet
North	0	-0.363	-0.394	-0.380
	30	-0.249	-0.298	-0.245
	60	-0.102	-0.158	-0.141
East	90	-0.240	-0.254	-0.255
	120	-0.403	-0.402	-0.362
	150	0.377	0.138	-0.079
South	180	1.300	0.734	0.477
	210	-0.964	-0.274	1.046
	240	-3.020	-1.275	1.079
West	270	-1.568	-0.952	0.464
	300	-0.422	-0.425	-0.491
	330	-0.333	-0.337	-0.410

At a glance, it can be seen that the absolute WPCs of the apartment were much higher than those of the row house and detached house. This can be explained by the fact that huge physical dimensions of the apartment building strongly block the wind, thus creating higher static pressure and consequently increasing the WPCs on building façades. On the other hand, the apartment is located on the 4th floor (10.2m height), being exposed to higher wind velocity. Consequently, the airflow rate in the apartment was expected much higher as observed in section 5.2.3.

5.5 Calibration of the three EnergyPlus housing models

5.5.1 Introduction to the calibration approach

The calibration of a numerical building model by measured data has been recognized as an important factor in substantiating how well the model fits the data from the actual building. In this case, to analyze the overall thermal performance of the case-study houses, the simulated indoor temperature during the baseline period was compared against the average measured temperature to judge how successful the simulation was. The calibrated model will be then used to evaluate long-term building thermal performance without the need of performing so many in situ measurements (Nguyen & Reiter, 2012c).

A calibration procedure normally includes several stages. First, site specific hourly data of a baseline period must be carefully collected to create relevant weather inputs. The weather data are then joined into a single datafile and packed onto a weather tape (Bronson, 1992) for use by EnergyPlus simulation program. Second, the calibration procedure requires an EnergyPlus input model based on information obtained from site visit and architectural as-built plans. The simulated results are finally extracted and compared with measured values to assess the "goodness-of-fit". During the calibration, the "goodness-of-fit" is gradually improved by adjustments made on the input model. Input variables that include uncertainty can be varied within their possible ranges. These inputs usually consist of physical properties of building materials, building compositions, opening control, HVAC details and performances, occupancy schedules, calculation algorithms... The input model is declared "calibrated" if the residual reaches an acceptable threshold defined in some standards (ASHRAE, 2002; ASHRAE, 2009). An overall summary of the present calibration is illustrated in Figure 5-14.

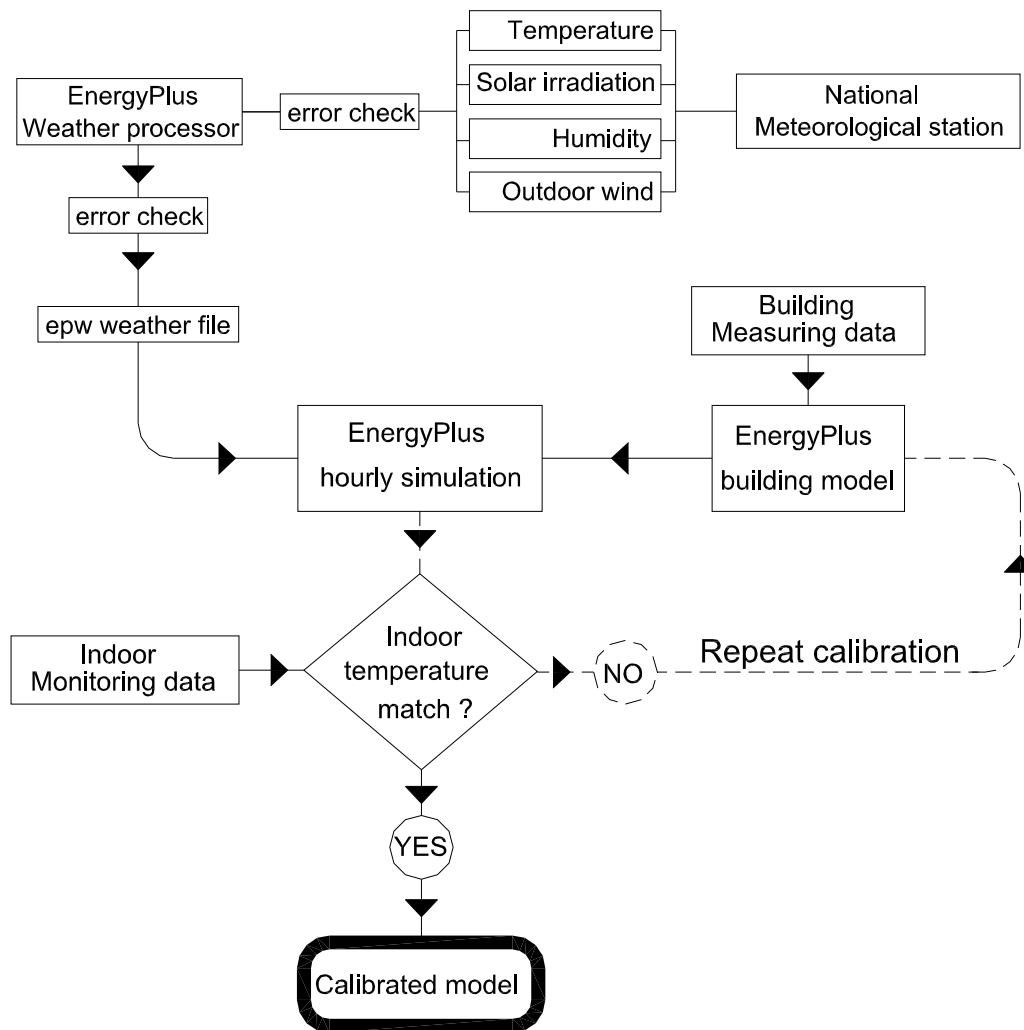


Figure 5-14: The creation of a weather file for EnergyPlus and calibration procedure

In the thermal simulation of NV buildings, the opening control and the ventilation flow rate are very important input variables which crucially influence the indoor thermal environment. However, these items are strongly dependent on natural wind, occupants, building configurations; thus they are difficult to identify. In such a case, the calibration approach will produce reasonably relevant inputs which significantly improve the accuracy of the whole year simulation (Nguyen & Reiter, 2012c).

5.5.2 Criteria to assess the agreement between simulated and measured data

As summarized by Bou-Saada and Harberl (1995), in many previous studies some methods have been proposed to verify the "goodness-of-fit" between simulated and measured data. For example, the graphical method was useful for determining where

simulated results differ from measured data and which appropriate modifications can be applied to the model.

So far, it is generally accepted that the statistical approach which applies two statistical indicators - Normalized Mean Bias Error (NMBE) and Coefficient of Variation of Root Square Mean Error CV(RMSE) - has become the most reliable measure to verify the calibration. The statistical approach has been adopted in some calibration guidelines, e.g. ASHRAE guideline 14 (ASHRAE, 2002) and ASHRAE Handbook of Fundamentals (ASHRAE, 2009) and can be defined as follows:

NMBE (Normalized Mean Bias Error):

$$NMBE(\%) = \frac{\sum_{i=1}^n (t_{ip} - t_{im})}{n-1} \frac{1}{t_m} 100\% \quad (5.10)$$

where t_{ip} is the i_{th} predicted temperature by the simulation; t_{im} is the i_{th} measured temperature; t_m is the arithmetic mean of the sample of n measurements and n is the number of data points (temperature) in the measurement.

A positive value of NMBE shows an over-estimate while a negative value indicates an under-estimate by the model. Ideally a zero value of NMBE should be obtained.

CV(RMSE) (Coefficient of variation of Root square mean error):

$$CV(RMSE)(\%) = \sqrt{\frac{\sum_{i=1}^n (t_{ip} - t_{im})^2}{n-1}} \frac{1}{t_m} 100\% \quad (5.11)$$

CV(RMSE) is a frequently-used measure of the differences between values predicted by a model or an estimator and the values actually observed from the thing being modeled or estimated. The CV(RMSE) is always positive and a zero value is ideal.

The value of NMBE represents the systematic error or bias while the CV(RMSE) is a strong indicator of accuracy. A simulation with a small CV(RMSE) accompanied with a significant NMBE, might indicate an error in simulation inputs. A simulation with a large CV(RMSE) but a small NMBE, might have no errors in simulation inputs, but building performance may reflect some other unmodeled behaviors (such as occupant behaviors) that are difficult to simulate (Claridge, et al., 2003).

In this work, the above-mentioned statistical approach was combined with linear regression analysis as discussed in the next section to fully assess the changes made after each calibration run.

5.5.3 Calibration runs

5.5.3.1 Calibration runs of the row house

The monitoring temperature in the bedroom on 2nd floor was used for the calibration purpose. Calibration simulations began with Run #1. In reality, about 30 ‘trial and error’ runs were completely done. Due to space constraints, only nine most significant runs were reported. Table 5-6 summarizes the results of the entire calibration process, from the first run to the final calibrated run where simulated temperature relatively matched with measured temperature. The major changes made to the EnergyPlus input file were also reported, along with their associated NMBE and CV(RMSE).

Table 5-6: Row house calibration runs

Run	Observations from previous run	Adjustments made for current run	NMBE	CV(RMSE)
Run#1	No Airflow network, ventilation simulation by fixed ventilation flow rate and infiltration rate.		-4.21	4.16
Run#2		Use Airflow network.	-3.8	4.14
Run#3	Air change rates were high in all zones	Reduce air mass flow coefficient when openings are closed kg/s-m ; most from 0.01 to 0.001 Adjust discharge coefficient for opening factor 1 (when open) by reduce nearly a half.	-2.32	2.76
Run#4	Ventilation rate level 1 (large volume) is rather high 0.382 ACH Bedroom ventilation rate was low (0.067 ACH) when openings are closed and high when opened (2.29 ACH) Ventilation rate attic was high (0.305 ACH)	Reduce air mass flow coefficient of front door level 1 when openings are closed to 0.002 and raise discharge coefficient for opening factor 1 to 0.41 Increase air mass flow coefficient of other openings when they are closed to about 3 times Reduce sizes of opening level 2 when opened to 70% due to effect of the tree Reduce discharge coefficient of the attic	-1.87	2.42
Run#5	Too low vent. rate of the attic and Level 2-zone 2 The model underestimated indoor temperature of the bedroom	Adjust thermal properties of PVC sheet for ceiling by changing double layer ceiling → single-layer Adjust thermal properties of brick, plaster by increase thermal absorbance Reduce height of the front tree	-1.40	2.14

Run	Observations from previous run	Adjustments made for current run	NMBE	CV(RMSE)
		Increase ventilation coefficient for attic by 3 times		
Run#6	Night temperature of the bedroom dropped too much; predicted temperature from the 1 st to 5 th May rather low	Little reduce of ventilation coefficient of the attic and the zone in level 1 Increase thermal density of the house by increasing concrete slab thickness 0.08-0.09m	-1.16	1.97
Run#7	Night temperature still dropped much after 19 th May	Add one people for all thermal zones the house during the 3 rd sub-period of May	-1.09	1.92
Run#8	Night temperature still dropped much	Add two small concrete columns in the bedroom that were ignored before Increase the thickness of the flooring mortar from 0.03 to 0.04m Increase concrete slab density from 2400 → 2700 kg/m ³	-0.85	1.80
Run#9	Night temp. still dropped much	Adjust equipment schedule during the night Increase equipments' power from 100 → 160W in the bedroom	-0.06	1.35

The improvement of the "goodness-of-fit" between the simulated and the measured temperature in the apartment after each run was graphically presented in Figure 5-15 (For reason of clarity, only runs #1, 6, 9 were presented). This figure was very helpful in determining where the difference occurs and which modifications to the model should be applied. Figure 5-15 demonstrates that almost no difference existed after the run #9 and that the accuracy of predicted temperature was considerably improved.

The tuning progress of seven calibration runs was illustrated in Figure 5-16 using statistical indicators and a linear regression. Figure 5-16 (left) demonstrates that as the calibration proceeded, the total residual in terms of the CV(RMSE) was gradually reduced and the average deviation from the mean (NMBE) approached zero. Runs #1, 2, 3, 4 and 5 significantly reduced the CV(RMSE). Runs #6, 7 and 8 had a small improvement in both the NMBE and CV(RMSE). At the final run, the CV(RMSE) was reduced to 1.35%, and the NMBE reduced to -0.06%. These figures are statistically excellent, comparing with some guidelines. ASHRAE (2009) recommends an empirical validation using the normalized mean square error (NMSE) which is similar to the CV(RMSE) and this should be less than 0.25 (or 25%).

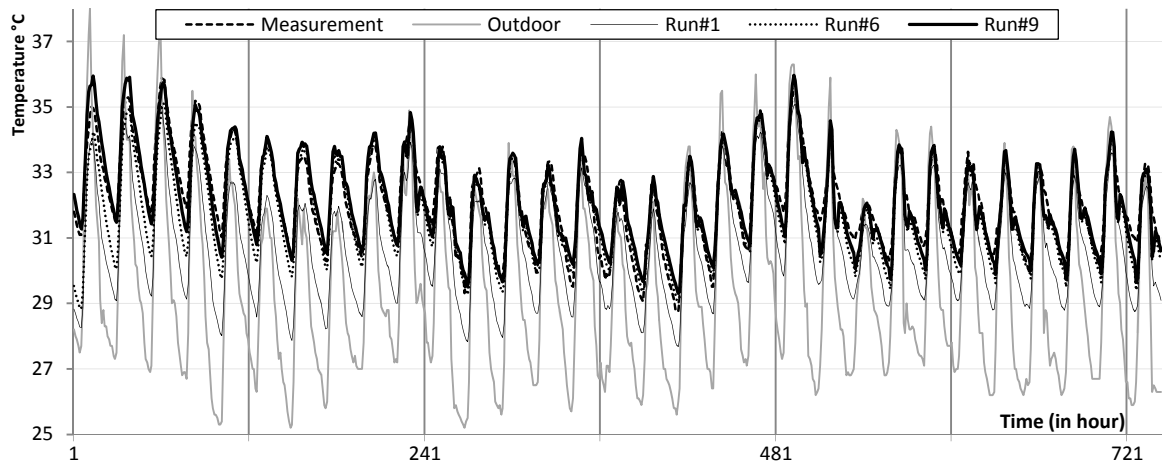


Figure 5-15: Comparison between simulated and measured temperature in the bedroom – row house

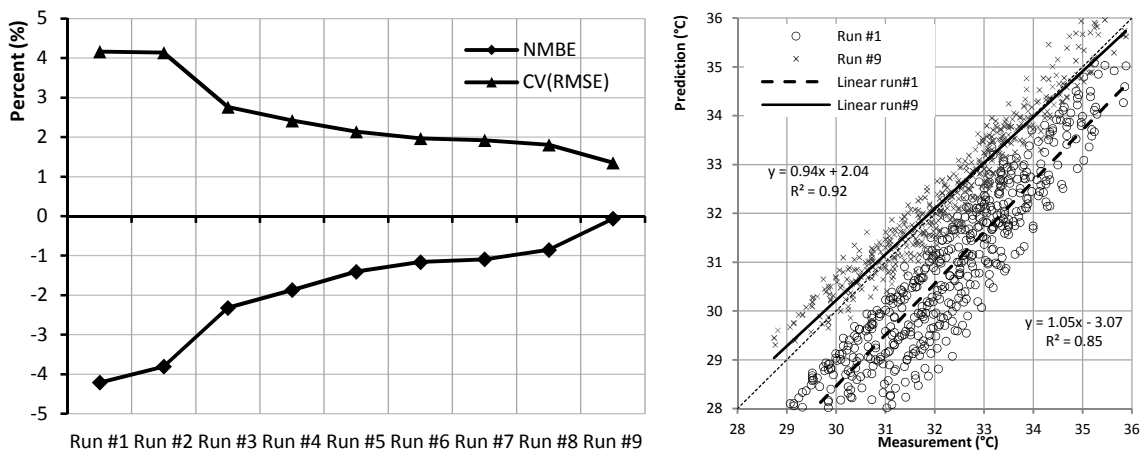


Figure 5-16: Tuning progress with input modifications (left) and linear regression analysis of run #1 vs. run #9 (right) - row house.

Another method is to use the linear regression analysis to graphically assess the accuracy and correlation, which was also presented in Figure 5-16 (right). It can be seen that in the first run, the predicted results underestimated the measured results by about 1.5°C and the coefficient of correlation R^2 was only 0.84. But the final model really overcame this shortcoming. The correlation coefficient R^2 of the final prediction versus the measurement of 0.924 and the linear slope of 0.939 were quite good, compared with the recommendation of ASHRAE (2009) (R^2 of 0.9 or greater, slope between 0.75 and 1.25).

To assess indoor thermal conditions, the relative humidity is sometimes needed. Hence, this study compared the predicted and measured relative humidity in the bedroom.

The result is presented in Figure 5-17. As shown in this figure, the final model slightly over-predicted relative humidity at night, but during daytime, it worked fine. The CV(RMSE) of the run #9 is 5.84% and the absolute error of relative humidity is about 3.85%. These figures are considered to be satisfactory because the initial measuring accuracy of the HOBO data loggers was about 2.5% (see Table 3-5).

The good agreement of the predicted and measured results shown in this section indicates that the EnergyPlus model successfully reproduced the actual building. The simulated temperature and humidity are ready for thermal comfort assessment.

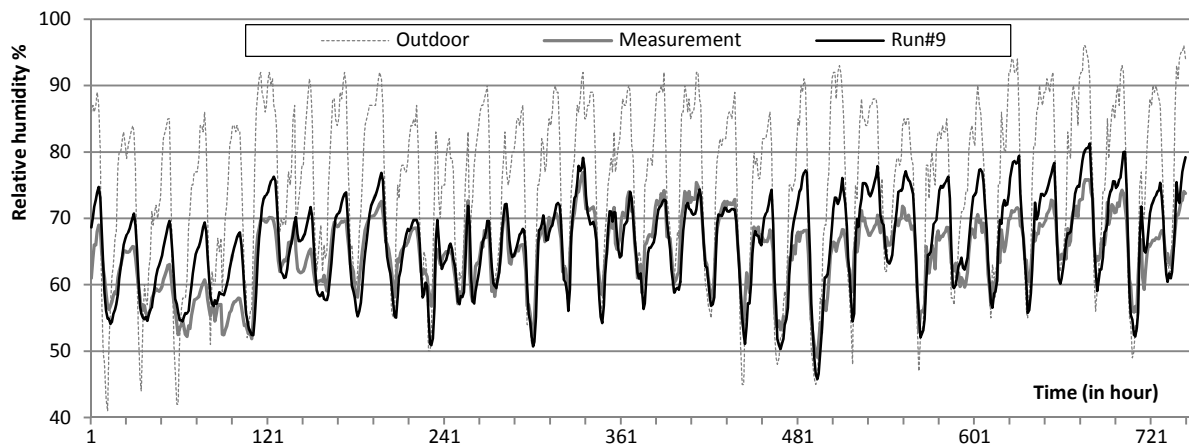


Figure 5-17: Measured versus predicted relative humidity in the bedroom – row house

Both statistical indices and linear analysis indicates that the calibration process achieved success and significantly improved the numerical thermal model. The model after run #9 is declared ‘calibrated’ and is ready for further simulations.

5.5.3.2 Calibration runs of the detached house

There are 3 bedrooms in the house and this section reports the calibration process by the temperature observed in the bedroom No. 1. The calibration of the detached house was much more complicated than the row house calibration because the detached house has many thermal zones and it was occupied during the monitoring period. Another reason was that the house is completely isolated, thus its indoor thermal environment was strongly affected by outdoor environment and the Sun. Three main groups of inputs considered in the calibration process were: opening configurations, thermal properties of materials and solar design. In reality, about 50 ‘trial and error’ simulations were completely done. Table 5-7 summarizes the results of the entire calibration process. The calibration results are presented

in a compact report of the 6 most significant runs. After the final run, the NMBE was nearly zero, indicating that the model is fairly balanced. The CV(RMSE) was acceptable (1.13%). Further calibration runs could not help improve these indices and the calibration was therefore completed.

Table 5-7: Detached house calibration runs

Run	Observations from previous run	Adjustments made for current run	NMBE	CV(RMSE)
Run#1	Use Airflow network model for natural ventilation prediction		-2.94	4.29
Run#2	Air change rates were high in all zones Air change rates were too low in roof zone and toilet	Increase air mass flow coefficient of the roof and toilet; most from 0.001 to 0.008 kg/s-m for roof, from 0.004 to 0.0055 for the toilet Adjust discharge coefficient for opening factor 1 (when open) of door and window by reduce nearly a half. Reduce air mass flow coefficient of the doors and bedroom windows by 0.5 times	-2.10	2.95
Run#3	Ventilation rates kitchen, Reading room when opened rather high about 5 ACH Ventilation rates bedroom1 when closed high about 1.5 ACH Ventilation rates attic low about 0.021 ACH	Reduce real sizes of bedroom window when open to 70% Reduce discharge coefficient of the bedroom window by a half Double crack flow rates of the roof from 0.008 to 0.015 kg/s under pressure 1Pa Reduce vent. Flow rates of the door when open slightly.	-1.02	1.72
Run#4	Vent. rates in the bedroom1 were slightly high 0.5 ACH Time lag of Bedroom1 temperature was smaller than measurement → thermal mass must be considered Ventilation rates attic low about 0.021 ACH Vent. rates of the corridor was still high 5 ACH	Adjust specific heat capacity and density of Brick and concrete. Adjust the thickness of the roof slab Increase vent. rates of the attic by 4 times Change the control schedule of the entrance doors from open to closed to reduce ventilation rates of the corridor	-0.54	1.61
Run#5	Time lag of Bedroom1 temperature was smaller than measurement Night temp. dropped much	Adjust the control schedule of the door of bedroom1 Reduce discharge coefficient of window bedroom1 to 0.15 Add thermal mass in the roof zone (the concrete beams)	-0.32	1.49
Run#6	Under predicted temperature	Increase thermal and solar absorbance of the roof to 0.345 Modify Sensible Heat Capacity Multiplier by 12	-0.16	1.13

Figure 5-18 shows the temperature in bedroom 1 and outdoors during May 2012. As can be seen, the first run under-predicted the measurement and the results were quite inaccurate. Both daily temperature range and mean daily temperature were incorrect. If these results are used to evaluate thermal comfort in the bedroom 1, they may draw incorrect conclusions. The final run closely caught the measurement and significantly improved the predicted results. The result shown here indicates that the calibration process is very important and nearly compulsory for a thermal simulation of NV buildings.

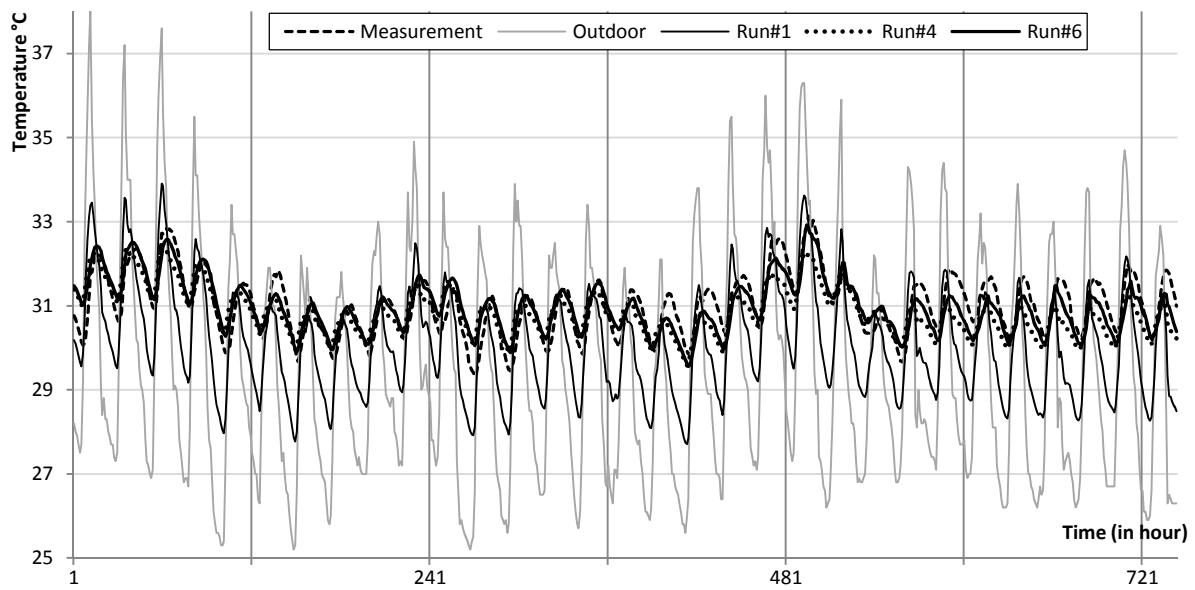


Figure 5-18: Comparison between simulated and measured temperature in the bedroom 1-detached house

The improvement of statistical indices during the calibration is shown in Figure 5-19. This figure shows that NMBE nearly reached zero while CV(RMSE) couldn't reach 1%. It means that the model slightly overestimated the indoor temperature in the first half of May and underestimated in the remaining half, but the mean error was zero. Figure 5-19 (right) shows a great improvement of the model after run #6, compared with the first run. Nevertheless, the R^2 of 0.82 and the regression coefficient of 0.78 were not really excellent, compared with the calibration of the row house.

As the house was occupied by a household during the calibration period, uncertainty of simulation inputs caused by the human occupancy was inevitable. Such uncertainty is not easy to reproduce using deterministic models; and consequently the calibrated model was not a perfectly convergent solution.

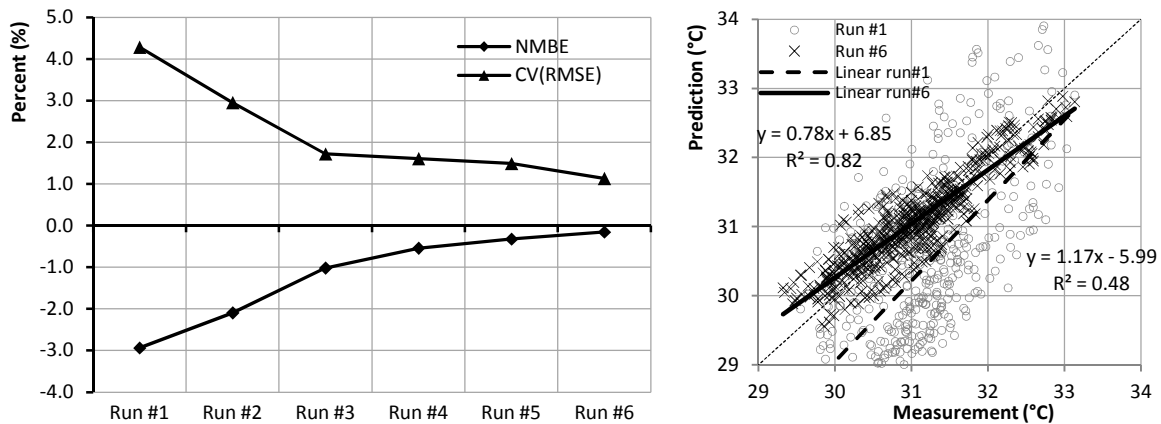


Figure 5-19: Tuning progress with input modifications (left) and linear regression analysis of run #1 vs. run #6 (right) – detached house

During the monitoring period, the bedroom 1 was nearly unoccupied; the variation of its water vapor content was therefore simply the result of exchanged air and the thermodynamic process of moist air. Predicted relative humidity in the bedroom 1 after calibration was compared with the measured counterpart and presented in Figure 5-20. As can be seen, the observed and predicted humidity was in good agreement. Largest different were about 6%, coinciding with the disagreement in the temperature. This error may produce a deviation of about 0.05 units PMV (Fanger, 1970) at 30°C operative temperature; thus the prediction of humidity won't create notable errors in thermal comfort predictions.

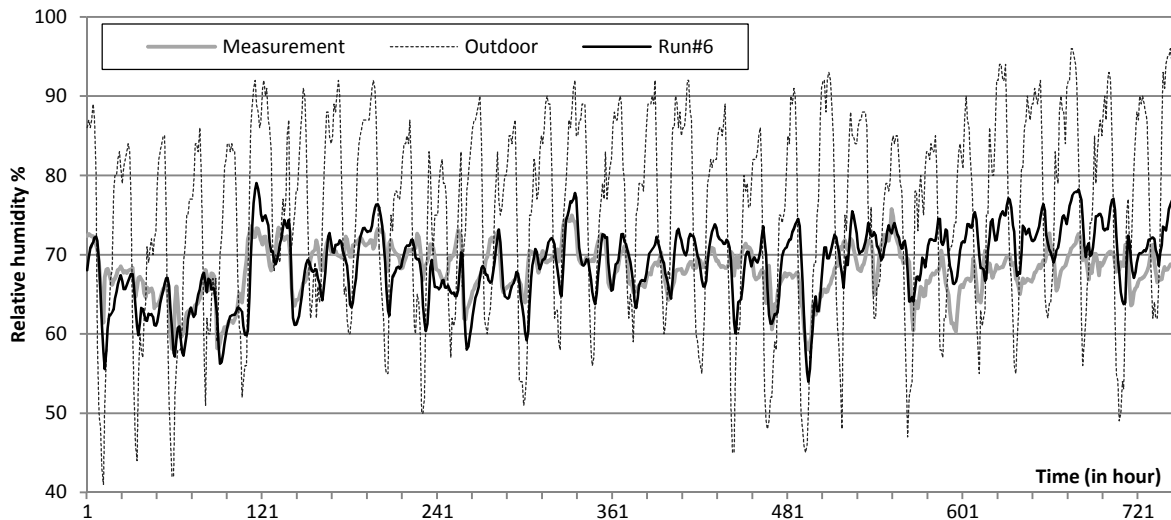


Figure 5-20: Measured versus predicted relative humidity - bedroom 1, detached house

In conclusion, the calibrated model of the detached house can produce reliable predictions that are ready for thermal comfort assessment.

5.5.3.3 Calibration runs of the apartment

There are 2 bedrooms in the apartment and this section reports the calibration process by the temperature observed in the bedroom No. 1. The calibration was a little difficult because the apartment was subject to unstable occupancy and ventilation control. During the monitoring period, as observed by the author, the number of people living in the apartment varied from 0 to 5 and the openings were opened / closed randomly. In addition, the apartment is frequently subject to rather high outdoor wind speed at the height of 11 m. These processes were not easy to reproduce in EnergyPlus and may cause a certain bias between predicted and measured values.

Table 5-8 and Figure 5-21 report the calibration process and modifications made on the model. As the calibration proceeded, the “goodness-of-fit” between predicted and observed results was gradually improved. The calibration process prevents the model from underestimating / overestimating because NMBE reached 0% after run #8. The absolute error was reduced to 1.41%. In the linear regression, the coefficient of correlation R^2 of 0.79 is acceptable. The calibration was considered as “converged” after run #8 as no further improvement was recorded.

Table 5-8: The apartment - calibration runs

Run	Observations from previous run	Adjustments made for current run	NMBE	CV (RMSE)
Run#1		Use Airflow network model for natural ventilation prediction	-2.80	3.8
Run#2	The model underestimated indoor temperature, temperature range was too large RH was extremely high and usually saturates; completely different from measuring RH	Use Airflow network	-2.09	3.54
Run#3	Temperature fluctuated significantly, daily temperature range is also too large, up to 6°C Air change rates were high in all zones The model underestimated indoor temperature Predicted RH was significantly improved	Reduce air mass flow coefficient when closed of bedroom windows from 0.004 to 0.002kg/s-m; Reduce discharge coefficient of door and window Reduce high and wide factor of doors and windows (assume that they are not opened completely).	-1.47	2.27
Run#4	Air change rates were slightly high in all zones Temperature fluctuates considerably.	Reduce discharge coefficient, width and height factor of openings (take the window curtain into account)	-1.16	1.95

Run	Observations from previous run	Adjustments made for current run	NMBE	CV (RMSE)
	Peak temperature from 1st to 3rd and 22nd May is too high.			
Run#5	The model slightly underestimated indoor temperature Predicted RH was still high	Increase solar absorbance and visible absorbance of external wall materials	-0.76	1.72
Run#6	The model slightly underestimated indoor temperature Predicted RH was still high Low vent. rates in bedroom 2	Increase width and height factor of window bedroom 2 Reduce thermal specific capacity of inside wall mortar Slightly Increase solar and visible absorbance of outside wall mortar	-0.65	1.68
Run#7	The model still slightly underestimated indoor temperature Time lag of Bedroom1 temperature was smaller than measurement High vent. rates in living room	Add thermal mass in the living room (the kitchen) Increase specific heat capacity of concrete from 650 to 750 J/kg.K Brick from 820 to 900 J/kg.K Slightly reduce vent. factor of door balcony; slightly increase width and height factor of bedroom 1 window Slightly increase solar gain of external walls	-0.36	1.6
Run#8	Predicted temperature in some days was significantly lower than measurements	Slightly modify window control of the bedroom Slightly modify air mass flow coefficient when closed of bedroom windows from 0.002 to 0.004kg/s-m Slightly reduce the solar absorbance of external walls from 0.3 to 0.285 Modify Sensible Heat Capacity Multiplier and Humidity Capacity Multiplier by 15 and 12, respectively	0.00	1.41

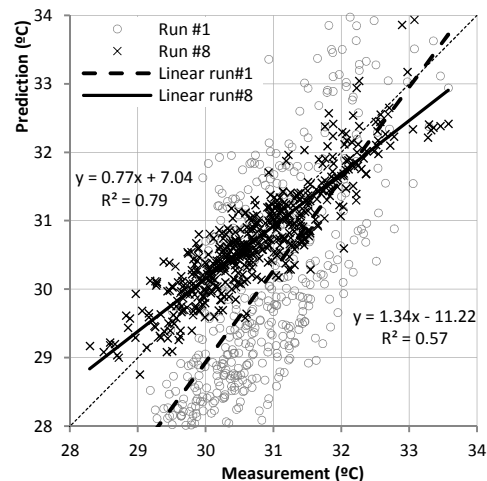
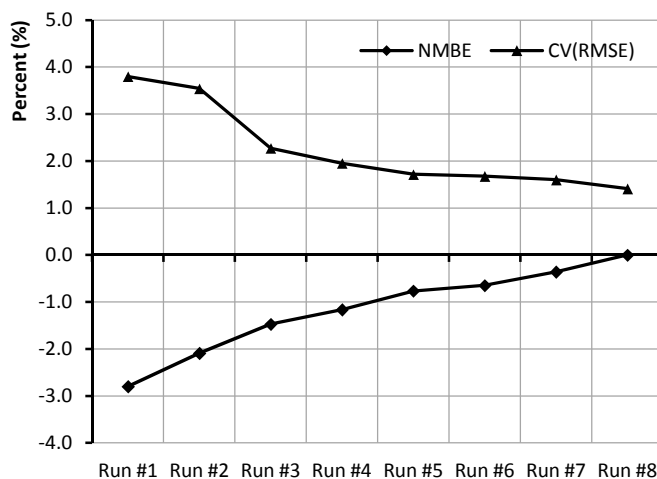


Figure 5-21: Tuning progress with input modifications (left) and linear regression analysis of run #1 vs. run #8 (right) – apartment

Figure 5-22 shows the comparison between predicted and measured temperature / humidity. As can be seen, the predicted and measured temperatures were in fairly good agreement after run #8. Temperature prediction of run #8 showed a significant improvement, compared with run #1. The calibrated model is capable to predict accurately the thermal condition of the apartment.

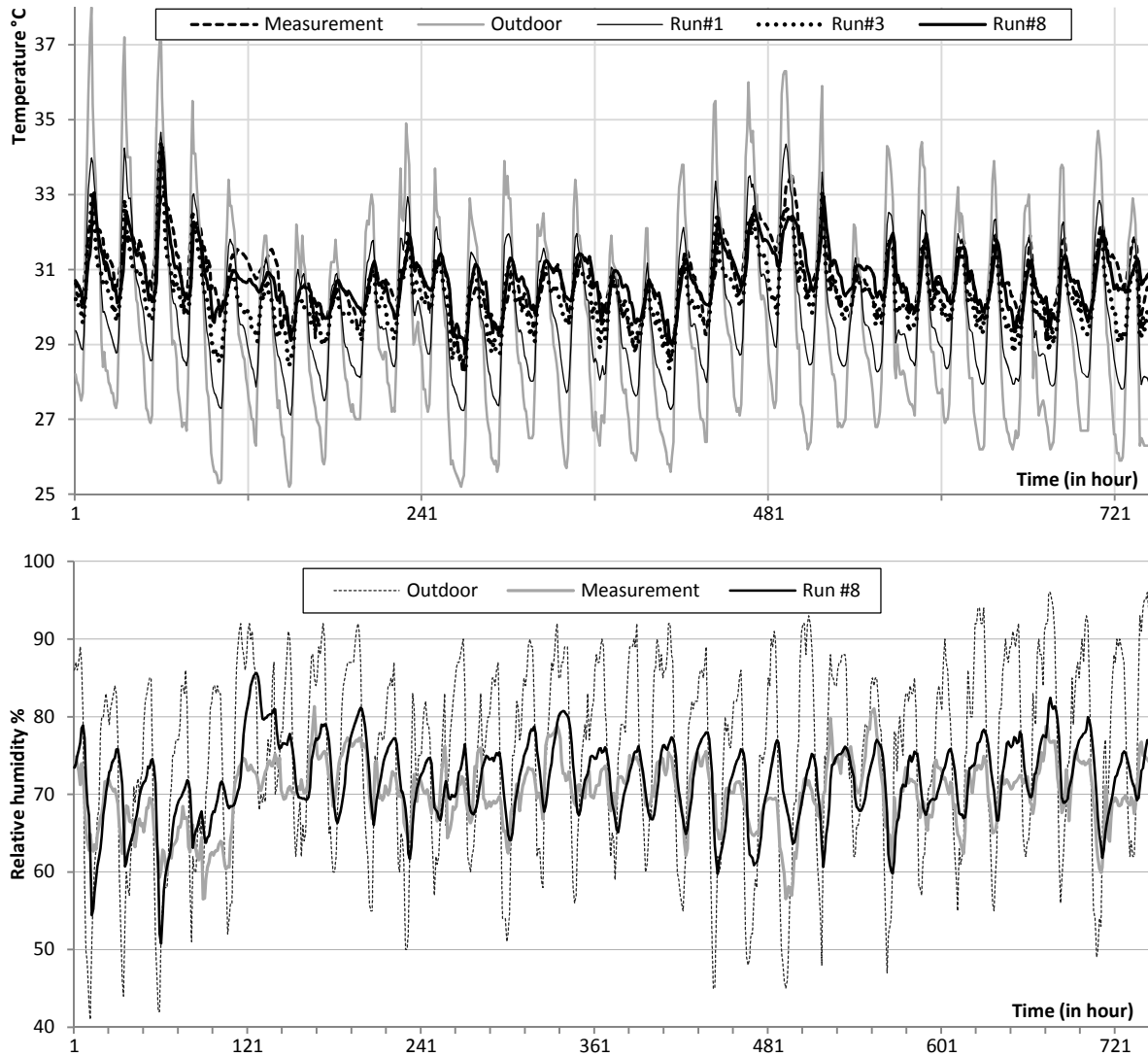


Figure 5-22: Comparison between simulated and measured temperature / humidity in the bedroom 1- apartment

However, many differences were detected between the predicted relative humidity and its measurement. The linear correlation R^2 of 0.42 and the CV(RMSE) of 6.3% were not really persuasive. These disagreements were possibly caused by one of two following reasons:

- The presence of occupants and the ventilation rate in the bedroom 1 were not correctly reproduced (scheduled) in this EnergyPlus model.
- The Conduction Transfer Function algorithm of EnergyPlus has failed in predicting zone's humidity if human occupancy is assigned. It is worthy of note that other advanced algorithms to calculate humidity using the finite element method are available in EnergyPlus, but they requires too many unknown inputs; and the simultaneous calibration of both temperature and humidity would be quite sophisticated and well beyond the scope of this research.

The author is slightly in favor of the first hypothesis because the good humidity predictions in unoccupied bedrooms of the row house and detached house (see section 5.5.3.1 and 5.5.3.2) were obtained earlier. The above analysis indicates that thermal comfort assessment using the PMV-PPD model in occupied zones by simulated results should be done with much care. In contrast, the comfort assessment using the adaptive approach is nearly independent from air humidity and seems more reliable.

5.6 Thermal performance of the case-study houses during a year

Long-term thermal comfort conditions in these case-study houses were examined using full-year simulations of calibrated EnergyPlus models of these houses. A full calendar year can successfully reflect the climatic characteristics of a region. In the next series of simulations, the TMY weather files (described in section 4.3) of Danang, Hanoi and Hochiminh city were used, instead of the weather files of May 2012. Calibrated EnergyPlus models of these houses were adjusted to adapt themselves to a one-year scenario. Following assumptions were proposed:

- All the houses are NV. All windows are always opened to allow natural ventilation (except that they are closed during November, December, January and February in Hanoi). All doors are normally opened during day time and closed during nighttime.
- The row house and detached house are occupied by 4 people while a family of 3 occupies the apartment.
- The clothing insulation of people living in Hanoi and Danang is slightly higher during winter (0.85 clo) and reduces to 0.45 clo at peak summer while that of

people living in Hochiminh city is always kept at 0.5 clo. These clothing insulation levels reflect actual changes of clothing habit of Vietnamese.

This study also examines another operating scenario according to which these houses are equipped with HVAC systems and the indoor environment is mechanically controlled. In this scenario, the initial Construction cost and the 50-year Operation cost are objectives of the assessment. The purpose of this scenario is to generate reference performances of these houses for the comparative studies as discussed in detail in CHAPTER 8.

5.6.1 Thermal comfort analysis

Thermal comfort conditions in these houses were assessed by two comfort criteria mentioned in section 3.4 and 3.5. Methods A and D for long-term comfort assessment in the standard ISO 7730 (ISO, 2005) were used.

The ‘steady-state’ comfort criterion was evaluated by the mean PPD of a year (Fanger, 1970) which should be smaller than 20% (80% occupants are thermally satisfied). The adaptive comfort criterion was based on the model of South-East Asia (Nguyen, et al., 2012) discussed in CHAPTER 3 which defines the indoor comfort temperature T_{comf} as a linear function of the monthly mean outdoor temperature T_{out} as follows:

$$T_{comf} = 0.341T_{out} + 18.83 \quad (5.12)$$

The comfort range for 80% acceptability is from ± 2.85 °C to ± 3.45 °C around T_{comf} depending on prevailing mean outdoor temperature (higher mean outdoor temperature, smaller the comfort range). This adaptive comfort criterion provides a basis to calculate the Total Discomfort Hours (TDH). The TDH of a thermal zone is defined as total time in a year (in hours) during which indoor temperature of the zone is beyond the comfort range of equation (5.12). The TDH of a building is the mean of the TDHs of all thermal zones. Due to the random nature of the use pattern in residential buildings, both the PPD and the TDH were calculated throughout the year, regardless of whether the house is occupied or not.

As the best knowledge of the author, acceptable thresholds of the TDH for NV spaces have not been well defined. The standard EN15251 (CEN, 2007) recommends a very detailed assessment method which is unrealistic for most engineering applications. Van der Linden et al. (2002) proposed a classification system of building performance based on

adaptive criteria and indoor temperature as shown in Table 5-9. This classification system will be used to classify the case-study houses based on their thermal performances.

Table 5-9: Classification system of thermal performance for NV buildings

Classification	% of time comfort limits are exceeded (% of TDH)	Exceeding amount (average)
Excellent	0%	-
Good	0-10%	< 1 °C
Moderate	0-10%	> 1 °C
Poor	> 10%	-

Table 5-10: Thermal performance in a year of the row houses

	Total discomfort hours in a year (hour)			Mean PPD during a year (%)		
	Hanoi	Danang	Hochiminh city	Hanoi	Danang	Hochiminh city
Level 1	2777	1290	681	34.89	34.62	44.77
Level 2 - other zones	3457	1957	1767	44.96	45.04	60.04
Bedroom level 2	3508	2118	2155	44.84	46.03	62.82
Average	3247	1788	1534	41.56	41.90	55.88
Discomfort of the house	37.1%	20.4%	17.5%	-	-	-
Discomfort of the climate	47.0%	40.4%	35.4%	-	-	-
Discomfort reduction	9.9%	20.0%	17.9%	-	-	-

Table 5-11: Thermal performance in a year of the detached house (only 5 major thermal zones of the house were considered)

	Total discomfort hours in a year (hour)			Mean PPD during a year (%)		
	Hanoi	Danang	Hochiminh city	Hanoi	Danang	Hochiminh city
Bedroom1	2460	1208	865	41.10	42.05	55.33
Bedroom2	2654	1408	1064	42.86	45.31	57.85
Bedroom3	2825	1507	933	40.14	41.17	53.92
Living room	2591	1281	878	39.62	40.06	51.47
Reading room	2639	1384	1005	41.20	40.11	53.50
Average	2634	1358	949	40.98	41.74	54.41
Discomfort of the house	30.1%	15.5%	10.8%	-	-	-
Discomfort of the climate	47.0%	40.4%	35.4%	-	-	-
Discomfort reduction	16.9%	24.9%	24.6%	-	-	-

The simulation outputs for these comfort criteria are the mean PPD (if Fanger's comfort model is used) or the TDH (if the adaptive comfort model is used). The results of

this section will show how well these houses adapt to different climates of Vietnam, their comfort performances (or occupants' thermal satisfactions) and possible weak points that need to be improved. Table 5-10, Table 5-11 and Table 5-12 show the details of simulated results of each house, in each climatic region. The thermal condition of each thermal zone was reported. In these tables, the percentages of discomfort hours of the climates were imported from the analysis in section 4.4.

Table 5-12: Thermal performance in a year of the apartment

	Total discomfort hours in a year (hour)			Mean PPD during a year (%)		
	Hanoi	Danang	Hochiminh city	Hanoi	Danang	Hochiminh city
Bedroom1	2304	940	1293	43.36	46.12	62.65
Bedroom2	2262	955	1354	44.44	47.84	64.19
Living room	2269	965	1207	40.98	41.9	55.91
Average	2278	953	1285	42.92	45.29	60.92
Discomfort of the apartment	26.0%	10.9%	14.7%	-	-	-
Discomfort of the climate	47.0%	40.4%	35.4%	-	-	-
Discomfort reduction	21.0%	29.5%	20.7%	-	-	-

As can be seen from these tables, the performances strongly depend on the housing types, the climates, the thermal zone examined and even the assessment criteria (comfort criteria). The relations between thermal performances and these factors were non-linear and not easy to explain.

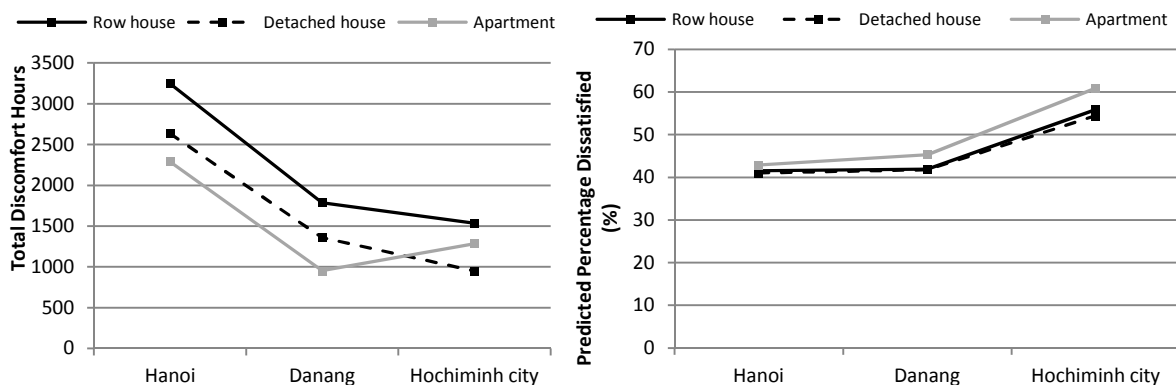


Figure 5-23: The contradictory of predicted results given by the two comfort criteria

Figure 5-23 illustrates the results in line charts. It can be seen that the predicted results given by two comfort criteria were almost contradictory. In most case, the better the house performs with the TDH, the worse it achieves with the PPD. As an example, all the

houses performed worst with the TDH criterion under the climate of Hanoi, but it showed the best performance with the PPD criterion under the same climate. *This contradictory raises a question of whether the TDH or PPD model should be used for thermal comfort evaluation in NV dwellings.*

It can be seen that the warmer the climate is (Hanoi - Danang - Hochiminh city), the higher mean PMV (thus higher PPD) value is predicted. The PMV-PPD indices were stated by many authors that they **overestimate the warm sensation** of occupant's in NV buildings in warm climates (Fanger & Tøftum, 2002). It should be important to stress that the PMV-PPD model implemented in EnergyPlus does use fixed clothing insulation, metabolic rate, air velocity as empirically prescribed by users; thus it omits occupants' adaptive actions occurring in NV buildings. Many researchers have pointed out the failures of the PMV-PPD model in NV buildings (Nicol, 2004; Nguyen, et al., 2012), and even its own inventor - Fanger (Fanger & Tøftum, 2002). The PMV-PPD model can be modified to be used in warm climates by extended PMV-PPD model as recommended by Fanger and Tøftum (2002), but the research of the author (Nguyen, et al., 2012) has proved that extended PMV-PPD model is not valid for NV buildings in hot humid South-East Asia (see section 3.2.5.1). For these reasons, the adaptive model is believed to produce more reliable results than the PMV-PPD model. Here after, the TDH index of the adaptive comfort model is therefore used to assess thermal conditions in NV buildings.

As can be seen from the above analyses, the apartment generally performs best among the case-study houses, followed by the detached house and the row house respectively. The TDH varies from 3247 to 949 hours per year (from 37% to 10.8% of a year). Ideally the TDH should be zero, but it is practically difficult to reach this threshold because the houses are NV. According to the classification shown in Table 5-9, thermal performances of these houses are classified as "POOR" and therefore they need further improvements. As shown in Figure 5-23 (left), the design of the case-study houses are completely not adequate under the climate of Hanoi.

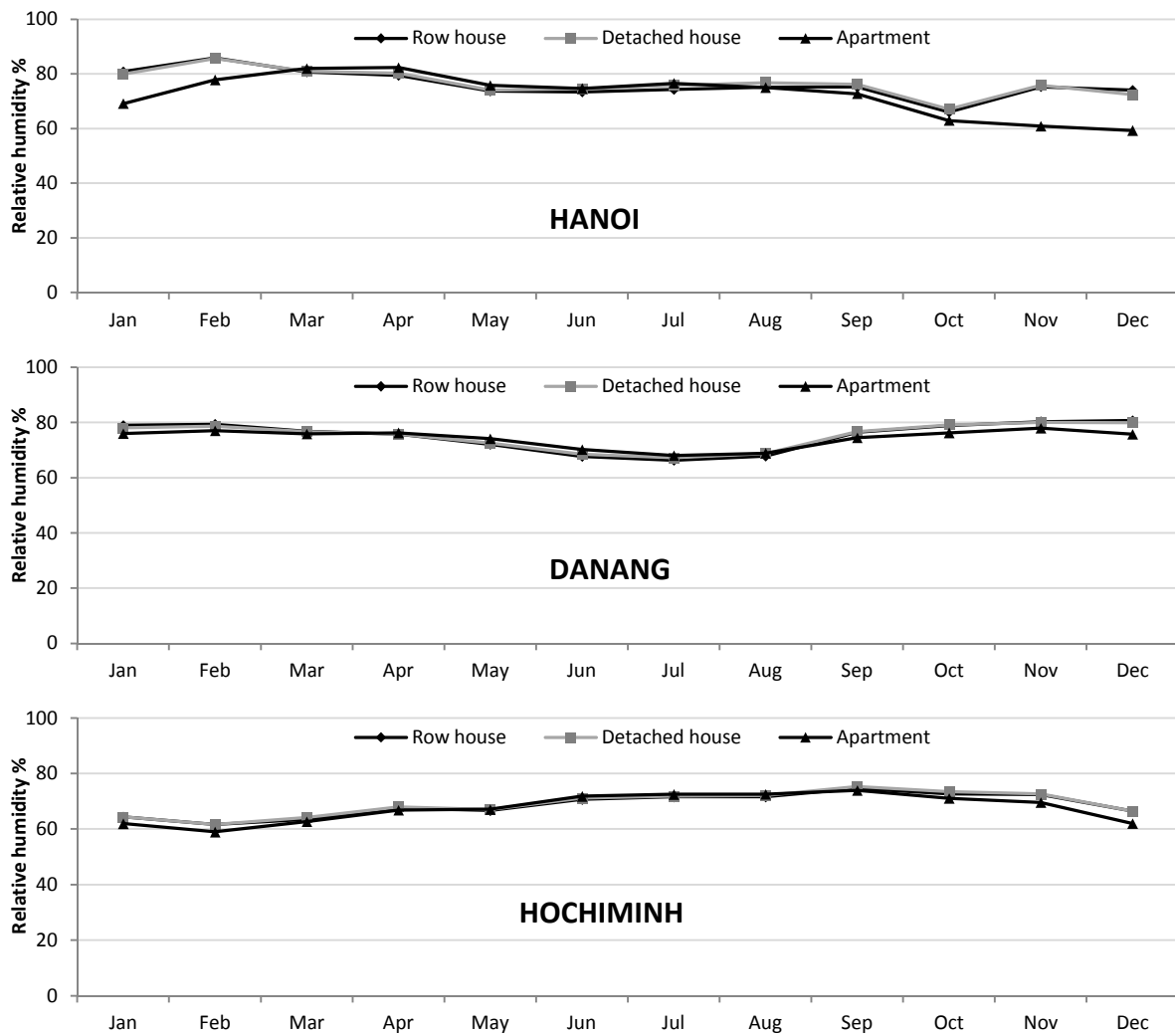


Figure 5-24: Monthly mean indoor relative humidity of major thermal zones through the reference year

Under high temperature, relative humidity plays a greater role in thermal perception of occupants. Damp air might cause mold growth and some health problems. Thus humidity control is necessary in Vietnam. The humidity in these houses was examined by monthly mean relative humidity of all major thermal zones in each house as shown in Figure 5-24. As can be seen, mean indoor relative humidity rarely exceeds 80% and varies between 60% and 80% thresholds. These variations almost follow the mean of outdoor relative humidity. As these houses are NV, such an indoor relative humidity is considered to be acceptable. A slightly increase of relative humidity was observed in winter in Hanoi (all openings were closed), but the apartment still performed well because it may have higher infiltration rates (caused by higher wind pressure on its building façades).

5.6.2 Identifying strong and weak points and potential improvements

In order to identify strong and weak points of these houses, hourly temperature of each thermal zone was plotted on the adaptive comfort model of each climatic region. By this graphical method, the discomfort period will be detected and possible useful hints for improvement may be derived. Figure 5-25, Figure 5-26 and Figure 5-27 compare the indoor temperature of each house with the adaptive thermal comfort band, corresponding to each climate. Three most important thermal zones of each house were simultaneously plotted. Many observations were obtained:

- Indoor thermal conditions of these three houses were not satisfied in summer (or hot periods) and in winter. During mild seasons, they perform better. The thermal performances of these dwellings need to be improved much further to satisfy thermal comfort requirements. If the indoor temperature is up to 2°C above the comfort boundary, short-term human thermal comfort may still be restored by the wind of 0.6 m/s or higher (ASHRAE, 2004; ISO, 2005) with can be created by an electric fan or by natural ventilation. When the indoor temperature is above this limit (about 34°C), it is not possible to restore thermal comfort by wind movement because air temperature is nearly equal or higher than skin temperature and only mechanical cooling will be feasible.
- For Hanoi (North of Vietnam): As discomfort periods caused by the cold and overheating were detected, improvements of the houses should be concentrated on both strategies for hot and cold weather. It is important to note that the indoor temperature dropped very far from the lower comfort boundary during a long period in winter (up to 8°C) and may cause serious discomfort.
- For Danang (Central Vietnam): Design strategies for hot weather play a dominant role in housing design while that for cold weather is a secondary matter.
- For Hochiminh city (South of Vietnam): The houses were only experienced overheating all year round; thus only design strategies for passive cooling are necessary. Discomfort caused by the cold is rare and can be completely eliminated by simply controlling openings of the house.

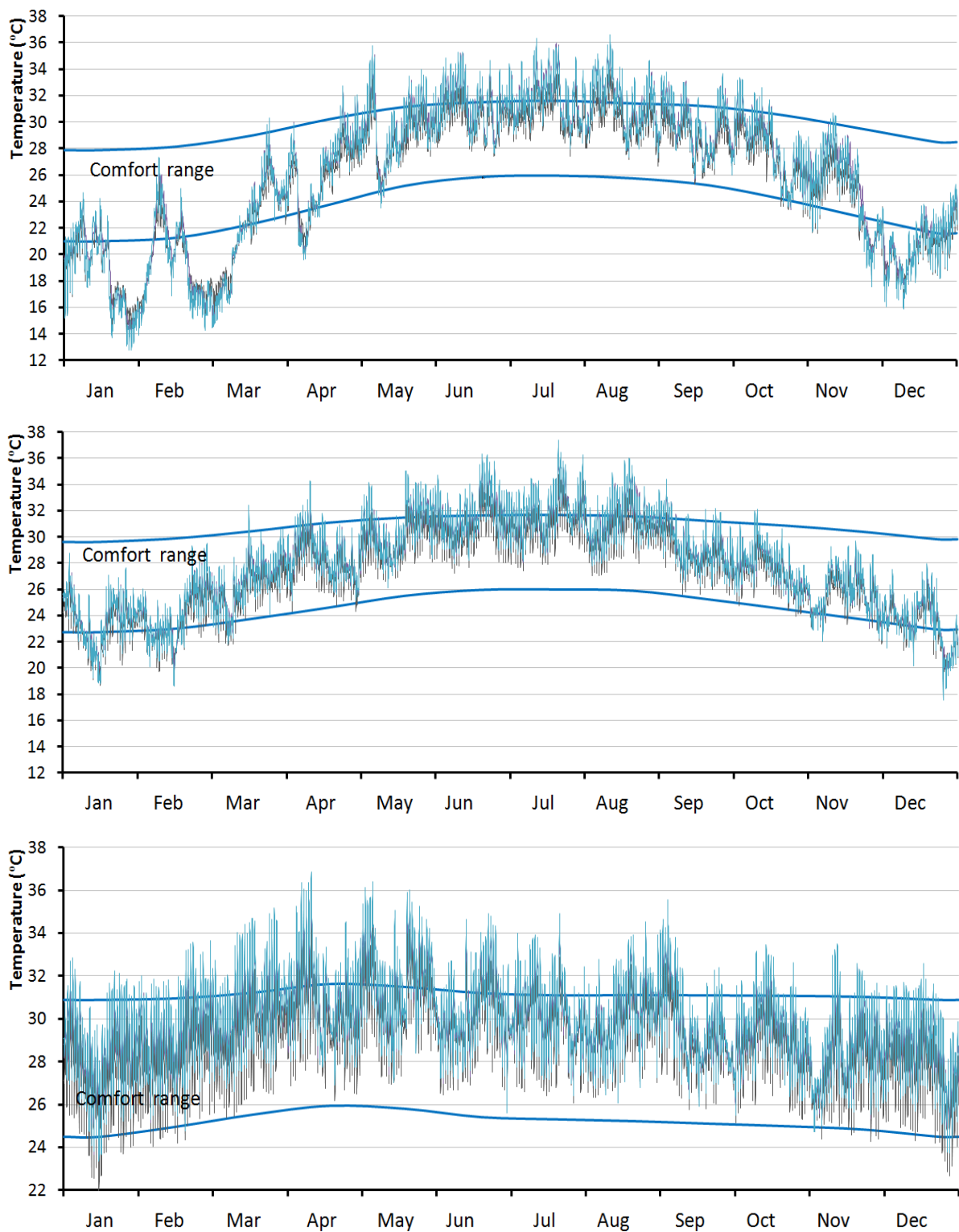


Figure 5-25: From top to bottom: hourly temperature of the row house under the climate of Hanoi, Danang and Hochiminh city respectively (all thermal zones are presented)

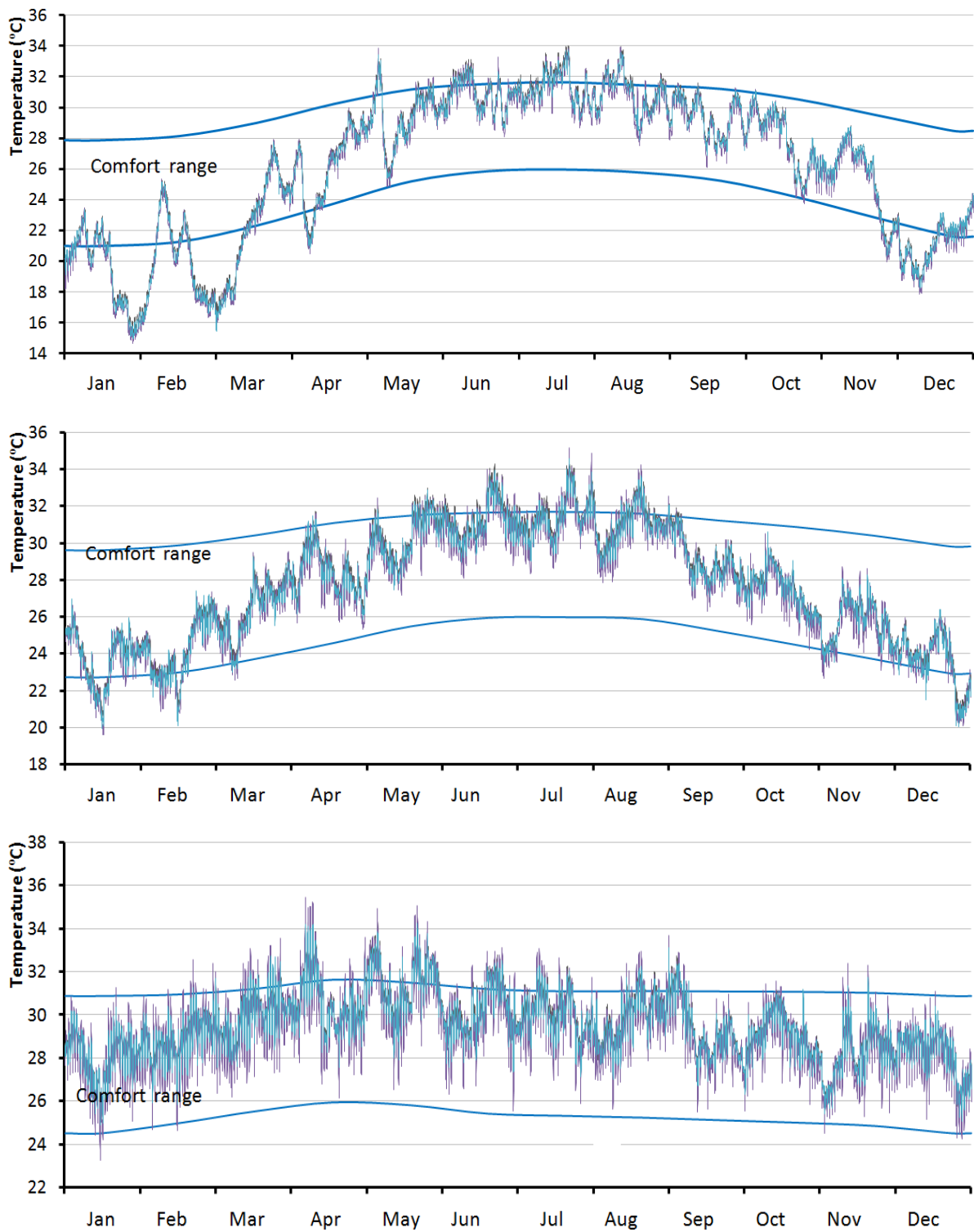


Figure 5-26: From top to bottom: hourly temperature of the detached house under the climate of Hanoi, Danang and Hochiminh city respectively (for clarity, temperature of the bedroom 1 + 2 and living room are shown)

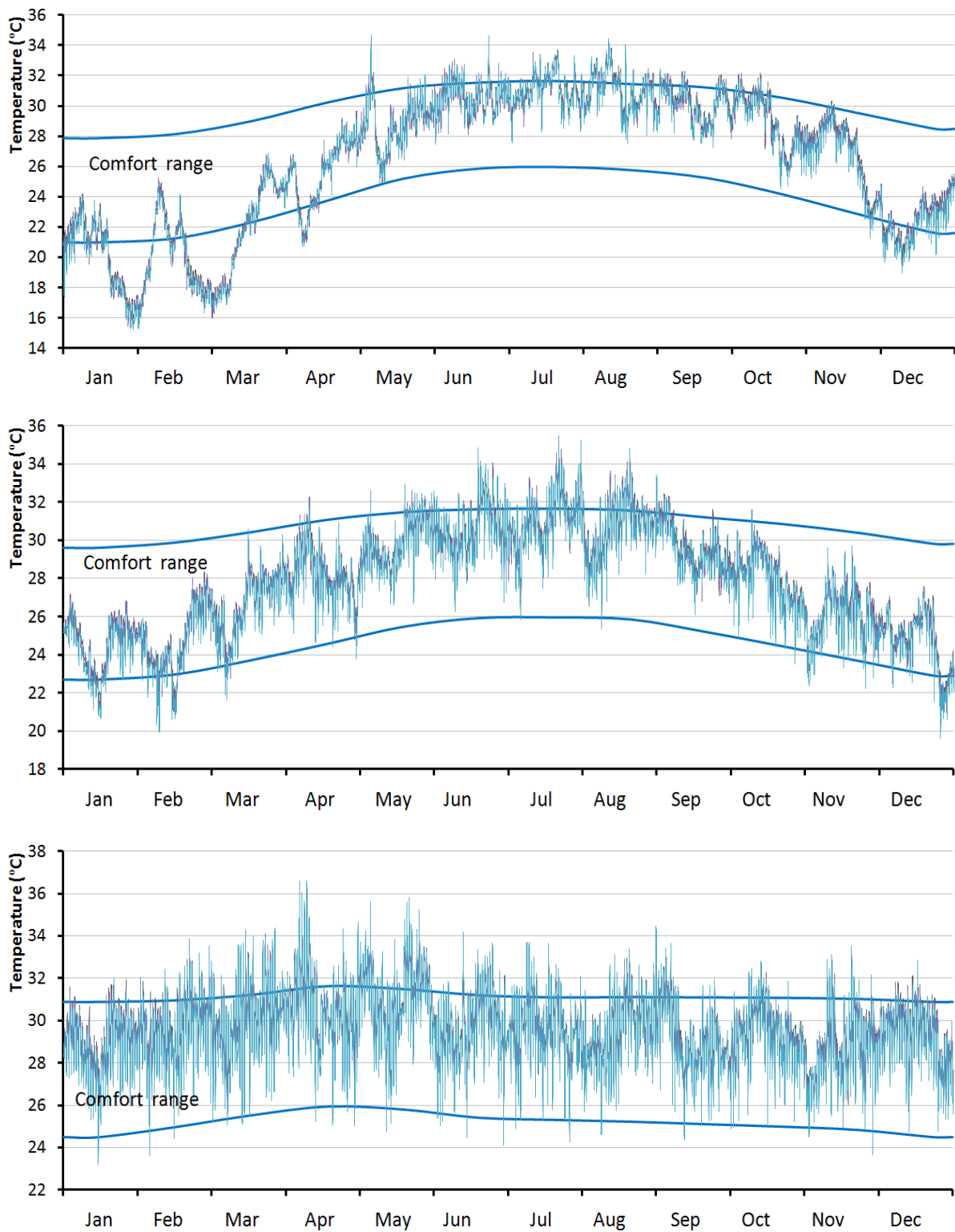


Figure 5-27: From top to bottom: hourly temperature of the apartment under the climate of Hanoi, Danang and Hochiminh city respectively (all thermal zones are presented)

5.7 Chapter conclusion

This chapter discusses the procedure through which thermal performances of the case-study houses were evaluated. The process was conducted through 4 steps:

- Selecting typical case-study houses and monitoring indoor conditions in one month,
- Modeling these houses in EnergyPlus energy simulation program,
- Calibrating these numerical models in EnergyPlus using measured data,
- Full-year simulations and thermal performance evaluations.

Following findings were derived from the analysis in this chapter:

- The case-study detached house and the apartment thermally performed better than the row house during the monitoring period in May 2012.
- This chapter uses the CFD method to calculate WPCs on building façades. These WPCs were then transferred to the Airflow Network in EnergyPlus to model wind driven natural ventilation. By comparing the CFD and experimental results, it can be said that the RNG k- ϵ turbulence model of Phoenics code can produce satisfied predictions of the airflow inside and around the building with simple configuration.
- The numerical models of these houses were calibrated using industrial standards. Statistical indicators - Normalized Mean Bias Error (NMBE) and Coefficient of Variation of Root Square Mean Error CV(RMSE) - have been employed to assess the calibration of the housing models in EnergyPlus.
- Simulated results of calibrated numerical models indicate that thermal performances of these dwellings were not identical and that none of these dwellings could completely satisfy thermal comfort requirements.
- The detailed analysis indicates that thermal performances of these houses need some improvements to prevent the cold in Hanoi (North of Vietnam) and overheating in all regions of Vietnam.

Thermal performances of these houses are considered as reference thresholds for all renovations and improvements that will be discussed in the next chapters.

CHAPTER 6

CLIMATE RESPONSIVE DESIGN STRATEGIES OF VERNACULAR HOUSING

6.1 Introduction and background of the study

In recent years, facing the risk of global warming and of the depletion of fossil fuels, reduction in energy consumption along with sustainable development is a priority for many countries, including Vietnam. Today, we generally acknowledge that the building sector consumes about one-third of the total energy consumption worldwide and this figure may vary according to building types and locations. In 2010, the building sector in Vietnam occupied between 20% and 24% of the total national energy consumption and this portion is expected to increase significantly (MOC, 2010). Reducing energy use, especially energy used by occupants of buildings, is an important issue in Vietnam as the country is constantly in the state of energy crisis. Research to reduce building energy consumption through climate responsive strategies without compromising human comfort is essential. In this context, vernacular architecture is widely recognized as a practical and effective solution.

Vernacular architecture is a term used to categorize methods of construction which use locally available resources to address the local needs (Coch, 1998). Vernacular architecture results from long-term growth and is part of traditional popular culture; therefore vernacular architecture is considered well adapted to the natural and social conditions of a specific location in which it exists.

In Vietnam, many detailed studies have shown that Vietnamese vernacular architecture is multiform and valuable. Unfortunately, due to many fierce wars, the impact of state policies (for example the land reform from 1953 to 1956) and natural disasters, much vernacular architecture in Vietnam has been destroyed or has disappeared altogether. Today, those remaining are very modest in scale and form, but the architectural and environmental lessons that they provide are still considerable.

The principal purposes of this chapter are to: (1) search and discover the underlying climate responsive strategies conceived in vernacular architecture in Vietnam; (2) recommend appropriate solutions for current design and construction, aiming towards sustainable development and (3) assess the importance of preserving the vernacular housing remaining in Vietnam. The content of this chapter mostly relies on the works of the author published in (Nguyen, et al., 2011).

Six old houses in rural and urban areas spread over the 3 regions of Vietnam, representing vernacular architecture, traditional architecture and old architecture, were thoroughly investigated to understand the climatic design strategies employed and their effectiveness in maintaining human comfort and health.

6.2 Materials and methods

To comprehensively and systematically review architectural strategies in Vietnam, both scientific methods and respect for the natural and social context was essential. Various approaches were employed in the literature. Dili et al (2010) used **long-term in-situ measurement method** to evaluate the thermal environment in a traditional building in Kerala, India. Cañas and Martín (2004) employed a **statistical method** to gather data about vernacular Spanish buildings and categorized them into different bioclimatic strategies based on their locations. By doing so, they found the mostly frequently used strategies which correspond to the building locations and local climate. Vissilia (2009) conducted a study to evaluate a sustainable Greek vernacular settlement by using **subsequent analysis**, based on two major steps: (1) a study concerning the evolution of the built environment (typological analysis, site planning, construction materials and techniques), and (2) an evaluation of specific vernacular dwelling types and their response to climate, based on passive design principles. She has made it clear that the vernacular settlement demonstrates an economical use of local building resources, adapting to climatic conditions without using much energy and providing human comfort.

Manioğlu and Yılmaz (2008) studied energy saving design strategies employed in ancient housing in Mardin, Turkey. They made a simplified thermal evaluation and **comparison of a traditional house with a contemporary house** by using **in-situ measurement method and questionnaires** which were carried out for 100 buildings. They

found traditional houses performed better than their counterparts in providing human comfort and energy saving.

In an intensive study in Japan, Yoshino et al (2007) researched four traditional farmhouses using both **in-situ measurement and computer simulation** on a model house. Their findings revealed that cooling technologies of traditional buildings, such as solar shading by thatched roof, earthen floor and natural ventilation... are effective for interior cooling.

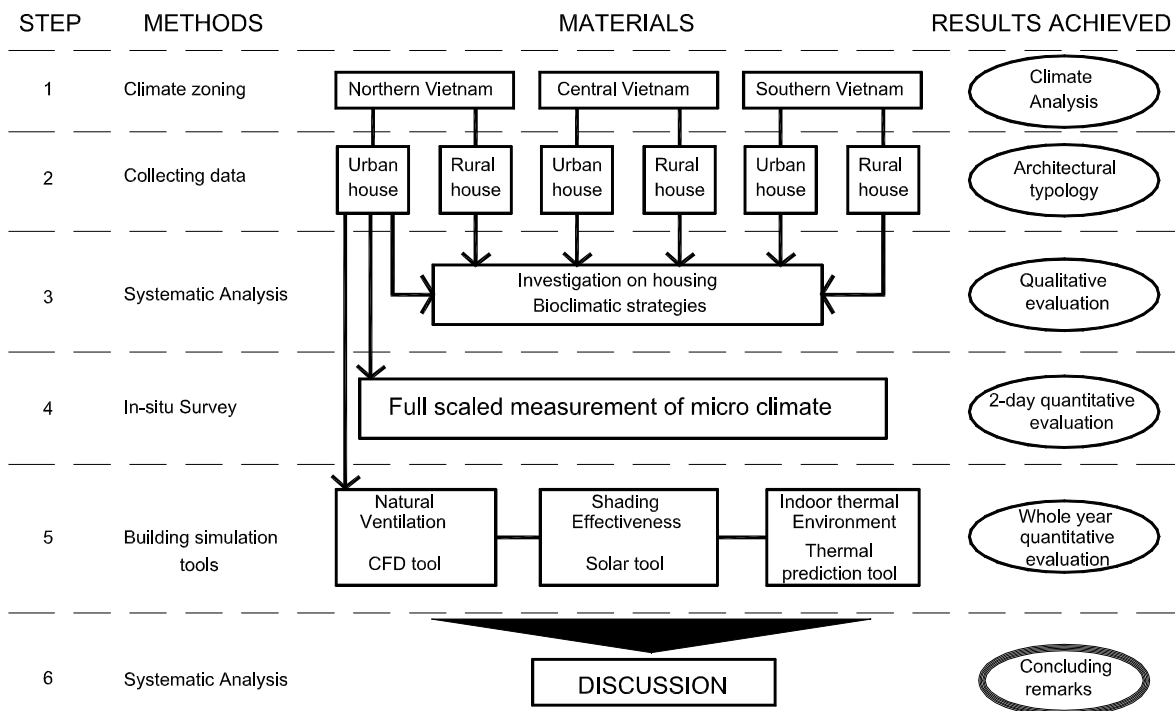


Figure 6-1: The innovative approach proposed and applied to this research

The territory of Vietnam stretches from the North to the South and along the country the complex social background differs. Based on these geographical and social characteristics and referring to all the above-mentioned methods (in-situ measurement, statistical method, comparative study and computer simulation), this study proposes a new approach for analyzing and evaluating vernacular dwellings in Vietnam in terms of building physics. This approach includes six subsequent steps as clearly described in Figure 6-1. It is expected that both qualitative and quantitative analysis included in this method will reinforce the findings from this study.

6.3 Theory, measurement, calculation and results

6.3.1 Step 1: Climate zoning and selected sites of the survey

In this step three typical sites, including Hanoi (*latitude: 21° N*), Danang (*latitude: 16° N*) and Hochiminh city (*latitude: 11° N*), which represent the three climatic regions in the North, Centre and South of Vietnam, were selected (see Figure 4-1). The climatic features of these locations were carefully discussed in section 4.1.2.

6.3.2 Step 2: Collecting data

Vietnam is a country of rivers. Its origins can be traced from two big deltas established in the valley of Hong river (in the North) and Cuu Long river (in the South). In ancient times, Viet people travelled on boats, and then lived in stilt houses which have influenced current communal houses (see Figure 6-2). Today, in many parts of Vietnam, people still live in stilt houses like their ancestors did.

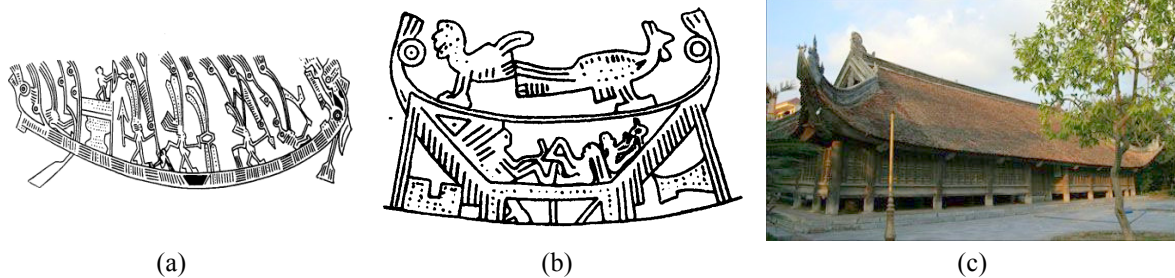


Figure 6-2: Traditional life on boats affected the housing style of Viet people: (a) ancient boat and (b) ancient house found on Dong Son bronze drum 6th century BC; (c) current Viet communal house

Most traditional buildings and vernacular houses in Vietnam have been destroyed or have completely disappeared due to damage caused by wars, natural disasters and even the policies of both feudalism and the government. Those remaining, among which the most ancient house (property of the Nguyen Thac family) was built in 1734 (Tran, 2005), are often modest in size and age. This study investigated six typical vernacular houses in three climatic regions mentioned in section 6.3.1 (see Figure 6-3). Each region is represented by two case-study houses: one in an urban area and the other in a rural area, since many significant differences between these two housing styles exist. Urban houses are typically large, multi-functional, and influenced by foreign architectural styles whereas rural houses are smaller, purely vernacular and are only used for living purposes.

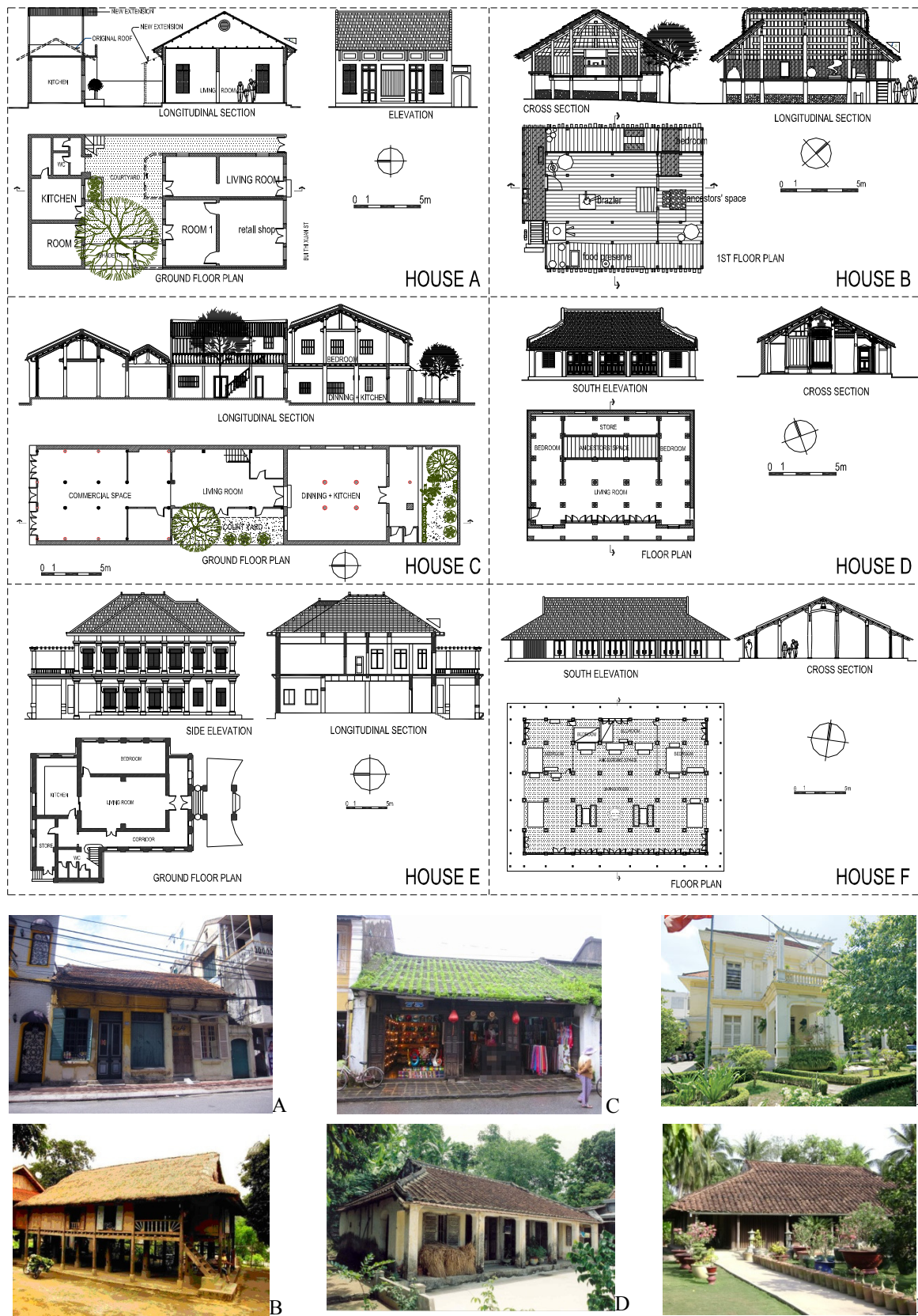


Figure 6-3: Architectural details of the selected houses A, B, C, D, E, and F

All six houses are typical in terms of style and size and are in good state of repair. Specific data of these houses are listed in Table 6-1. The purpose of this selection is to find the climate responsive design strategies corresponding to the three climate types in Vietnam.

Table 6-1: General information about the houses in question

	Location	Climatic region	Built in	Architectural style	Function	Construction method
House A	102 Bui Thi Xuan st, Hanoi city	North	1920	Traditional urban style	Commercial and living space	Traditional methods - Workers were employed from adjacent trade villages
House B	Hoabinh province	North	NA ^b	Vernacular style	Living space	Mainly by owners with wisdom of their ancestors.
House C	75 Tran Phu, Hoian city	Central	1860	Traditional - Japanese influence	Commercial and living space	By local skilled workers of traditional carpenter bands Kim Bong
House D	Tien Canh ward, Tienphuoc district, Quangnam province	Central	1890	Vernacular style	Living space	Traditional methods - By local skilled workers of traditional carpenter bands Van Ha
House E	32 Tran Quoc Thao st, Hochiminh city	South	1920 ^a	Colonial style	Living space	By French design and local builders
House F	Tan LyTay ward, Chauthanh district, Tiengiang province	South	1901-1904	Traditional style	Living space	By local skilled workers of traditional carpenter bands from Central Vietnam

^a year of construction estimated

^b Not available (housing style has existed for centuries, but the life span of each house is not very long)

It is well-known that vernacular housing all over the world makes use of materials found locally which reduces energy consumption for material extraction and fabrication, reducing its environmental impact. Local materials also encourage local characteristics which is also the case of the houses studied (see Table 6-2).

Table 6-2: Types of materials used in the houses investigated

	Foundation	Wall	Structure	Roof	Floor	Openings
House A	Normal solid fired clay brick	Solid brick wall with plaster on both sides	Load bearing wall and timber	Fired clay tile on timber frame	Cement tiled floor	Timber and glass
House B	No foundation	Bamboo lattice or wooden panel	Bamboo and wooden frame	Thatch (rice straw, thatch, reeds, palm leaves...)	Broken neohouzeau ^c	Bamboo lattice
House C	Stone or burned clay brick	Fired – clay bricks with plaster on both	Hard timber	Fired clay tile on timber frame	Fired clay brick - Wooden	Wooden panel

	Foundation	Wall	Structure	Roof	Floor	Openings
		sides			floor	
House D	Laterite stone ^a	Mixture of clay and straw on bamboo lattice ^b	Hard Timber	Two layers: Thatch roof (upper) and ramped earth (lower) ^d	Ramped earth	Wooden panel
House E	Stone	Fired clay brick with plaster on both sides	Load bearing wall	Fired clay tile on timber frame	Reinforced concrete + cement tiles	Wooden panel
House F	No foundation	Wooden panel - vertical bars	Hard timber	Fired clay tile on timber frame	Fired clay brick	Wooden panel

^a A special porous stone naturally formed from laterite soil (in Vietnamese: “đá ong”), exploited by local inhabitants. Laterite blocks connect together with mortar made from lime, resin of “boi loi” tree and molasses.

^b It was replaced by a fired clay brick wall about 20 years ago.

^c A kind of small bamboo.

^d The thatch roof was replaced by fired clay tiles about 20 years ago.

Among the above mentioned materials, some types were widely used in housing construction in Vietnam, especially in rural areas, until the end of the 20th century. These materials have certain advantages and positive characteristics as described in Table 6-3.

Table 6-3: Most used materials and their properties

Materials' name	Advantages ^a	Notes
Bamboo	High durability ^b , local availability, easy fabrication, multi-purpose usage, high tensile strength (up to 200 MPa), compressive strength up to 70 MPa, light - weight material (about 630 kg/m ³)	Fire prevention
Laterite stone	Very high durability, local availability, high moisture absorption, suitable for walls (compressive strength 20 – 30 MPa) ^c	Only available in some regions
Ramped earth	Available in most regions, multi-purpose usage, easy fabrication, low compressive strength (0.84 - 0.92 MPa)	Humidity control
Clay-straw mixture	Available in most regions, easy fabrication, low thermal conductivity (0.18 W/m.K)	Low compressive strength (< 4.6 MPa), erosion by rain
Thatch	Extremely low thermal conductivity (0.07 W/m.K), local availability, light - weight material (240kg/m ³), easy fabrication	Insect and fire prevention (about 180 J/kg.K), durability

^a Physical properties of these materials were obtained from references (Hammond & Jones, 2008; Berge, 2001; Spence & Cook, 1983; Bui & Morel, 2009; Walker, 2010).

^b According to vernacular experience, bamboo will have long life-expectancy and remain free from insects if it is soaked in water, under a layer of mud for 2 - 3 months before use.

^c Value proposed by the author.

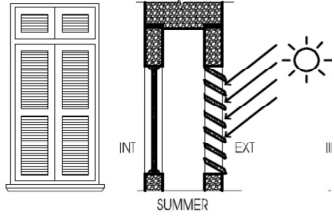
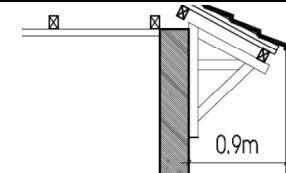
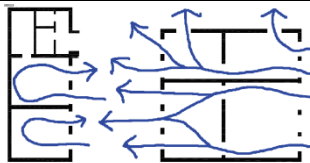
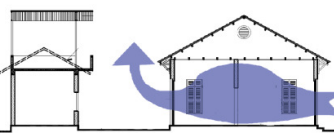
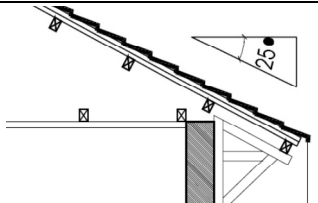
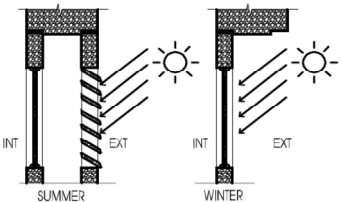
6.3.3 Step 3: Investigation of housing climate responsive design strategies

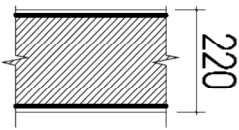
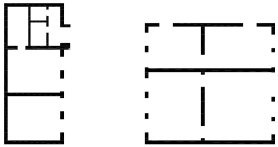
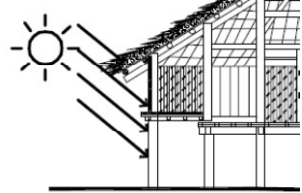
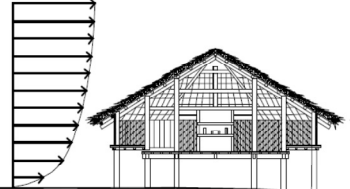
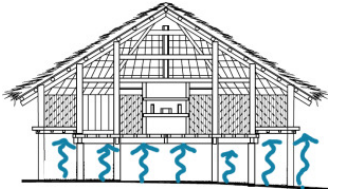
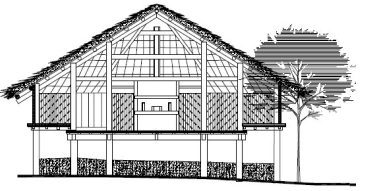
Popular climatic strategies used in the built environment in hot humid regions were categorized and numbered as 17 architectural solutions proposed by the author as follows:

- 1- Building orientation and shape
- 2- Solar shading
- 3- Natural ventilation: (a) cross ventilation, (b) stack ventilation, (c) single-side ventilation
- 4- Natural lighting techniques
- 5- Light weight construction
- 6- High thermal mass
- 7- Evaporative cooling
- 8- Earth sheltering (Use thermal inertia of the earth to stabilize indoor temperature, e.g. underground dwellings)
- 9- Passive cooling by using color
- 10- Thermal insulation by material
- 11- Thermal insulation by design (e.g. well ventilated attic, double-skin façade...)
- 12- Passive solar energy
- 13- Storm prevention
- 14- Flood prevention
- 15- Rainwater discharge
- 16- Moisture and condensation prevention
- 17- Others

These 17 strategies applied in these selected houses were qualitatively investigated and evaluated using the “*Description and Image*” approach. In this approach, the criteria of assessment is that if there is at least one climate responsive solution which corresponds to each of the local climatic features, the house is considered completely adapted to its local climate. Conversely, if no adaptation measures are found, the house is regarded as completely unadapted. In practice, most of the houses are neither completely adapted nor completely unadapted and are usually within this range. Subsequently, the following points were carefully examined: the advantages and disadvantages of local climatic features were identified; the drawings and photos of the buildings were analyzed to show climate responsive solutions and their effectiveness; qualitative assessment was then derived based on the criteria and analysis illustrated in Table 6-4.

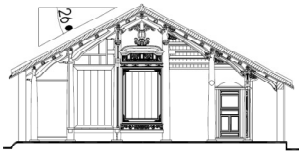
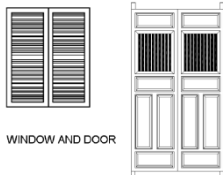
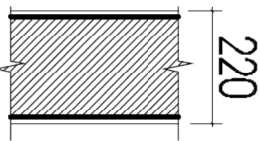
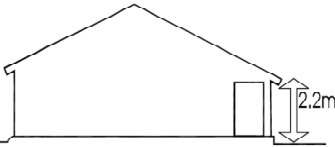
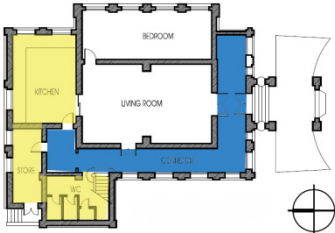
Table 6-4: Qualitative investigation of bioclimatic design strategies used in traditional architecture in Vietnam

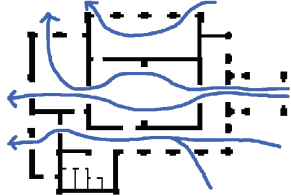
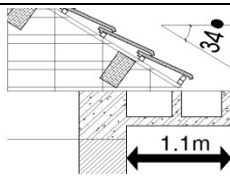
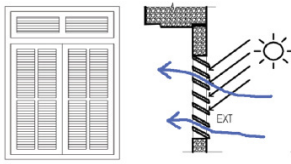
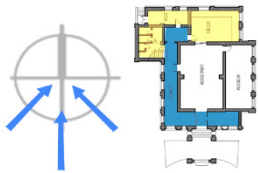
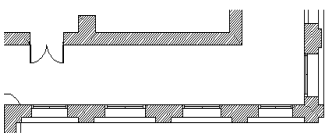
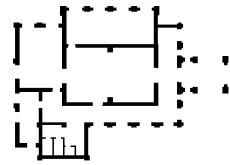
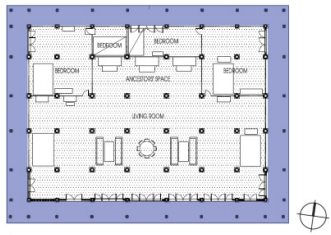
Climatic features	Description of strategies used	Image	Category
Ancient house in Hanoi center (house A)			
High solar radiation, especially on West and horizontal surfaces	Openings with wooden louvers shades the glazing well		2
	- Large, well ventilated attic acts as a well insulated roof		11
	- Deep eaves (0.9m) provide shading for walls. Shade tree in the courtyard provides more shade - Minimization of heat absorption by the facades by painting them white or light colors		2, 9
High average temperature and humidity	- Room height is 3.9m – 4.2m and many large openings improve ventilation		3a
	- Large and long courtyard helps enhance natural ventilation and reduces humidity. Side corridor induces wind into the courtyard.		3a
Heavy rain	- Steeped roof (25°) and deep eaves (0.9 m from the wall) - High bases of the wall prevent humidity from the ground		15
Sun path on the South sky	Strategies NOT clear due to its location in city center		
Two different seasons (hot and fairly cold)	- Two layered window (French window) provides flexible and operable control of openings during hot and cold periods		17
North cold wind, South-East cool wind	Building orientation strategy for prevailing wind is NOT available due to its location in the city center		

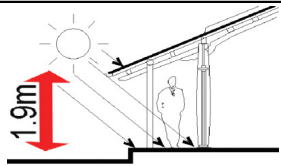
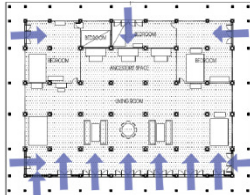
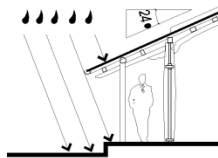
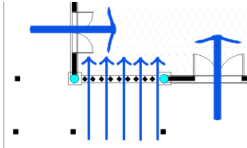
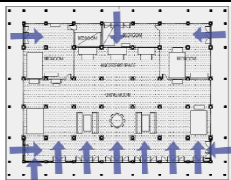
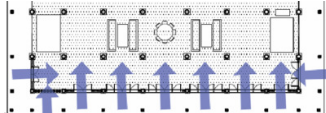
Climatic features	Description of strategies used	Image	Category
Low diurnal temperature – humidity range	- Light weight construction (thin load bearing wall – 220mm) has average time lag (about 6 - 7 hours) - Insulation was not used		5
Others	Indoor lighting is fairly good due to many large openings and light from the courtyard		4
Traditional stilt house of small ethnic groups in Hoabinh province - North of Vietnam (house B)			
High solar radiation, especially on West and horizontal surfaces	Thick thatch roof (about 200mm) provides ideal insulation (U-value 0.25 – 0.35 W/m ² K). Thatch roof absorbs moisture which reduces overheating by evaporative cooling effect		10, 7
	- Deep eaves shade short walls, protecting all walls and openings from direct sun		2
	- Well ventilated attic by funnel-shaped holes at the gables		11
High average temperature and humidity	Stilt house easily meets airflow at higher speed. Wind speed at height 2m can be 2 times as high as that at 1m. The air near the ground is often stagnant		3
	The house is raised 1.6m above ground to prevent moisture entering from the ground		16
Heavy rain	- Steeped roof (32°) and deep eaves (1m from the wall) enhance rainwater discharge		15
Sun path on the South sky	Not highly influential because of the deep eaves around the house		

Climatic features	Description of strategies used	Image	Category
Two different seasons (hot and fairly cold)	<ul style="list-style-type: none"> - Cooking (brazier) is done right at the middle of the house to keep warm in winter. - Openings on the gables enhance stack effect and release smoke from the brazier 		17, 3b
North cold wind, South-East cool wind	Windows are oriented to the South; cross ventilation through door, windows, and openings on the gables. When there is no wind, stack effect increases airflow		1, 3a
Low diurnal temperature – humidity range	Light weight building components: thatch roof, bamboo lattice enclosure with high porosity, bamboo floor and wooden column	See Figure 6-3	5
Others	House on stilts adapts well to floods (from high mountain) and prevents wild animals (snakes, centipedes, insects etc.) from entering		14
Traditional urban house in Hoian – Central Vietnam (house C)			
High solar radiation, especially on West and horizontal surfaces.	Thick porous roofing materials absorb moisture at night and release it during daytime cooling the roof.		7
	Creepers in front of the house, shade trees in the courtyard and backyard (see Figure 6-3).		2
High average temperature and humidity	On outdoor walls, there are 17 windows in total (19.7 m ²) and 8 doors (23.42 m ²). $S_o/S_f = (19.7 + 23.42) / 293.92 = 14.7\%$ effectively enhances airflow		3
East and South-East cool wind	<ul style="list-style-type: none"> - Building orientation strategy is NOT available due to its location in city center. - Front street, large courtyard and backyard improve cross ventilation. - Lighting condition is improved by the courtyard. 		3, 4
Heavy rain	- Pitched roof (25°) and deep eaves along with special roof tiles at the end of the roof help to drain away the rain.		15

Climatic features	Description of strategies used	Image	Category
Sun path on the South sky	Strategies NOT clear due to the location in city center		
Hot and a mild season, no cold season	<ul style="list-style-type: none"> - Louvers window allows natural wind to go through. - “lattice above – panel below” door style allows wind to go through during operation. 	<p>WINDOW AND DOOR</p>	3
Small diurnal and seasonal temperature – humidity range	<ul style="list-style-type: none"> - Light and porous wooden partitions, providing airflow path - Load bearing wall (220mm and 330mm) on two sides - No insulation. 	<p>220, 330</p>	5
Strong tropical storm, wind speed up to 220km/h)	- Low, thick and heavy roof (height 3.15m from the ground)	<p>3.15m</p>	13
Flood - up to 2.5m (in 1966)	Due to its location very close to the river mouth by the sea, building a two-storey house helps to minimize inconvenience caused by annual floods as the second floor level was always higher than the peak flood.	<p>FLOOD FLOOD FLOOD</p>	14
Others	The front part served as commercial space, facing the crowded street while the living space was separate towards the back and isolated from the front part by a large courtyard	<p>COMMERCIAL SPACE buffering SPACE LIVING SPACE COURT YARD</p>	17
Traditional house in Quangnam province – Central Vietnam (house D)			
High solar radiation, especially on West and horizontal surfaces.	Thick and porous roofing materials absorb moisture at night and release it during daytime cooling the roof.	<p>Vapor Temperature Porous mortar and fired clay tiles</p>	7
	Main building is oriented to the South to avoid East - West solar radiation.		1
	Front corridor covered by the roof protects inner space from the Sun and heavy rain.		2
	<ul style="list-style-type: none"> - Many shade trees, fruit-trees (e.g. jackfruit, plum...) on the West. - Heat absorption of the facades is minimized by its light color. 	See Figure 6-3	2, 9
High average temperature and humidity	Many large openings facing South include: 2 windows (1x1.2m), 3 grand doors (1.9 x1.9m), enhancing natural ventilation.		3

Climatic features	Description of strategies used	Image	Category
East and South-East cool wind	<ul style="list-style-type: none"> - The house is oriented to the South to catch the prevailing wind. Building blocks were separately distributed - Banana trees behind the house block cold wind. Front yard enhances wind induced ventilation 		1, 3
Heavy rain	<ul style="list-style-type: none"> - Pitched roof (26°) but no deep eaves (to stabilize the house from strong wind since the building site is uncovered). 		15, 13
Sun path on the South sky	South shading device is dominant. North, East and West counterparts are very short to avoid strong winds.		--
Hot and a mild season, no cold season	<ul style="list-style-type: none"> - Louvers window allows natural wind to go through - “lattice above – panel below” door style allows wind to go through during operation. 		3
Small diurnal and seasonal temperature – humidity range	<ul style="list-style-type: none"> - Light weight construction (thin load bearing wall – 220mm) - Insulation was not used 		5
Strong tropical storm, wind speed up to 220km/h)	<ul style="list-style-type: none"> - Low, thick and heavy roof (only 2.2m from the ground), short eaves on other sides of the house - Strong wind (from the East) can only attack side walls of the house 		13, 1
Flood - up to 2.5m (in 1966)	Not flooded because of its location on a midland region		
Others	Except the front yard, shade trees have been planted around the house, providing effective shading and cooling down the air temperature		17
Old urban house in Hochiminh city (house E)			
High solar radiation, especially on West and horizontal surfaces.	Wide corridors on the west and south façade protect the house from high solar radiation.		2
	Room arrangement: Stair, WC and store facing West. Main rooms are protected from direct Sun. Main façade is oriented to the South to avoid East - West solar radiation.		1
	Minimization of heat absorption by painting the facades light colors.		9

Climatic features	Description of strategies used	Image	Category
	- Large and well ventilated attic acts as well insulated roof.		11
High average temperature and humidity all year round	Many large openings in all directions including windows (1.34mx2.10m) and grand doors (1.85mx3.40) enhance natural cross ventilation.		3
	Ceiling height is significant: 4.8m on ground floor & 4.0m on second floor.	See building section in Figure 6-3	17
	Ground floor is raised 0.75m above the ground to prevent humidity		16
Heavy rain	- Pitched roof (34°) and deep eaves (1.1m from walls) with large gutter		15
No cold season, only dry and rainy season	- All louvers windows and doors create an “open” architecture, connecting the indoor and outdoor environment		3
South East to South West cool wind	- South orientation and window positioning allows airflow from the prevailing wind. WC and kitchen windows were positioned at the end of the wind flow		1
Small diurnal and seasonal temperature – humidity range	- Thick load bearing wall (400mm on average), combined with many large openings and transitional space (corridor), provide flexible control of the indoor environment.		6
Others	The many openings provide enough natural light for occupied rooms		4
Traditional house in Tiengiang province – South of Vietnam (house F)			
High solar radiation, especially on West and horizontal surfaces.	Corridor and deep eaves around the house protect it from direct sunlight.		2
	Main façade is oriented to the South.		1

Climatic features	Description of strategies used	Image	Category
	Height of the front roof is minimized, producing an effective solar shading solution.		2
High average temperature and humidity all year round	12 large openings on all the façades allow effective natural ventilation		3
	Ceiling height is significant (max 5.7m)		17
Heavy rain	<ul style="list-style-type: none"> - Corridor and deep eaves around the house protect it from wind driven rain. - Pitched roof (24°) and gutter operate well under heavy rain 		15, 15
No cold season, only dry and rainy season	- Vertical wooden bars replace the wall panel, allowing wind to pass through 12 large openings 24/24h.		3
South East to South West cool wind	- Building is oriented to the South to catch the prevailing wind and has 9 large openings on the south façade.		1, 3
Small daily temperature – humidity range	- Light weight construction (wooden walls and partitions) quickly releases heat at night (night cooling).		5
Others	More openings on the south façade obtain more natural light as the Sun mainly moves in the South sky		4

Comprehensive analysis in Table 6-4 indicates that vernacular housing in different regions of Vietnam has adapted relatively well to the climate as well as adverse weather conditions. Though the solutions employed are considered simple, inexpensive and easy to apply, they proved to be very effective, demonstrating a deep understanding of the ancestors about the building and its surrounding environment.

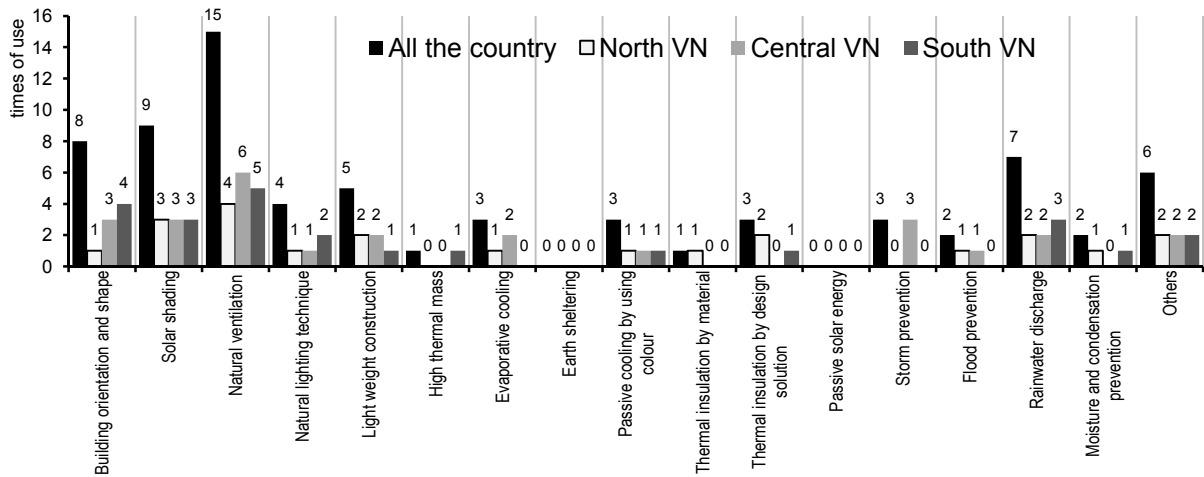


Figure 6-4: Frequency of use of different climatic responsive strategies

Other findings were also obtained. All strategies used were numbered and their usages were listed in Table 6-4. Consequently, the frequency of use of each strategy in these houses was found and illustrated in Figure 6-4. This graph shows that in all regions natural ventilation was the most used strategy whereas earth cooling and passive solar energy were not employed. Sophisticated technical requirements may be the main reason that passive solar energy was not employed for heating in vernacular housing, but solar heating has a potential to be applied in Vietnam and needs to be investigated further. Other findings are that it is suitable and effective to employ natural ventilation, building orientation - building shape and solar shading strategies in Vietnamese climatic conditions while earth cooling, thermal insulation and high thermal mass are inappropriate. Storm prevention was only found in central Vietnam where tropical storms usually hit. Due to time and resource limitations, this preliminary investigation included only six buildings. These findings can be consolidated by larger investigations.

6.3.4 Step 4: Full-scale measurement of micro-climate in a vernacular house

In order to have a more accurate assessment than the qualitative one mentioned above, an in-situ survey and measurement was carried out in Hanoi. Since investigations on all six houses would not be feasible, this thesis targeted the house at №102 Bui Thi Xuan street in Hanoi as the unique vernacular building for the full-scale measurement. The survey was continuously conducted from 8h to 21h on a typical summer day and winter day in Hanoi (16 December and 22 August).

All measurements were in relation to four physical climatic indices: air temperature, relative humidity, wind velocity and natural illuminance. The results shown here are the averaged values of ten-minute measurements (for mean wind velocity) and of three-minute measurements (for other variables). The measuring points were distributed as shown in Figure 6-5. The indoor air temperature, humidity, wind velocity and natural illuminance were measured at head level of a sitting person (height of 1.1 m) as recommended by ISO 7726 (ISO, 1998). During measurement periods, openings of the house were operated by the occupants, adapting to outdoor conditions.

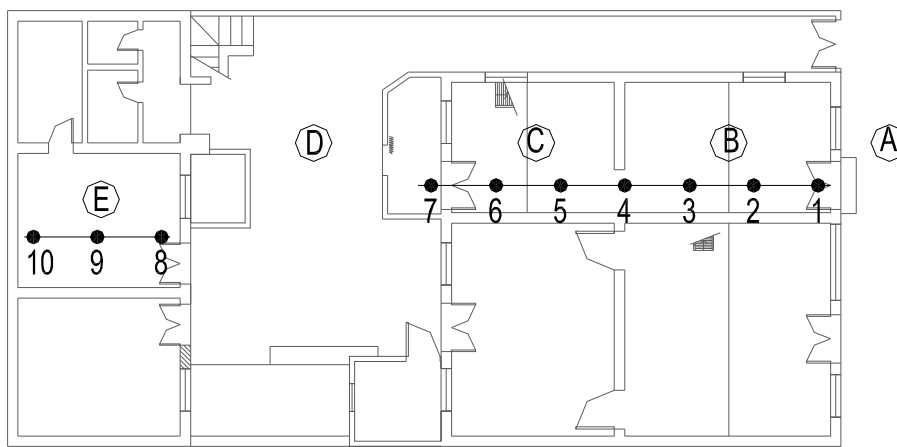


Figure 6-5: Distribution of measuring points (1, 2, ..., 10 are illumination measuring points; A, B, ..., E correspond with measuring points of other variables)

Measuring instruments consists of 3 hygro-thermometers, 2 anemometers and 3 photometers as listed in Table 6-5. The results for illumination were compared with a Vietnam building code (MOC, 1991) as shown in Table 6-6.

Table 6-5: Measurement instruments and their properties

Environmental indicator	Instrument	Quantity	Accuracy	Response time
Temperature	Asman	3	$\pm 0,2^{\circ} \text{C}$	60 seconds
Illumination	Testo	3	$\pm 1\%$	1 second
Wind velocity	Kata	2	$\pm 2\%$	Depended on the wind
Humidity	Asman	3	$\pm 3\%$	60 seconds

Table 6-6: Vietnam building code of natural illumination for residential facilities

Measurement variable	Main room	Toilet and store
Illumination coefficient	0.5%	0.3%
Minimum illumination	50 lux	30 lux

Results of the measurement:

Average air temperature, humidity and wind velocity at survey points were plotted on a combined diagram shown in Figure 6-6. As can be seen from Figure 6-6, there are no significant disparities between indoor and outdoor temperature as well as humidity except humidity at point E (in the kitchen) which was a little higher because of its earthen floor. This demonstrates that good ventilation of indoor space was achieved. However, daytime ventilation in summer was not appropriate since outdoor temperature was rather high. This corresponds to the study carried out by Kubota et al. (2009) in which they reported that in a hot humid climate, night ventilation effectively reduces indoor operative temperature and improves thermal comfort, but the majority of occupants tend to apply not night ventilation but daytime ventilation mainly due to insects, security risks and rain. Figure 6-6 also reveals that indoor wind velocity achieved in the survey was not sufficient to remove heat and humidity in summer, but a little high in winter. High indoor wind velocity in winter could be easily reduced by an appropriate openings control. Natural ventilation performance and humidity at point E was worst since this room uses single side ventilation.

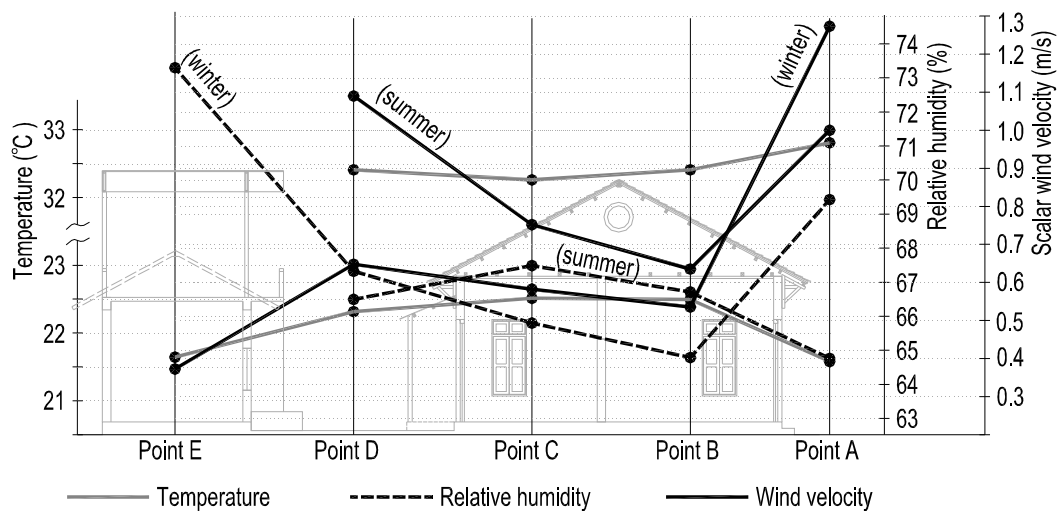


Figure 6-6: Average air temperature, relative humidity and scalar wind velocity at surveyed points in a typical summer and winter day (measurement at point E in summer was unavailable due to construction work being done there)

Indoor and outdoor hourly temperature, humidity and wind velocity were also compared as shown in Figure 6-7. It is clear that indoor parameters were similar to those measured outdoors. The fluctuation of indoor humidity might be caused by occupants’ activities (cooking, washing, etc.). These confirm the “open” characteristics of this house

which is generally recommended for hot humid climates. Another finding is that the wind velocity at point D (in the courtyard) was independent of wind conditions at point A (in front of the house). This improves natural ventilation of the rooms facing the courtyard.

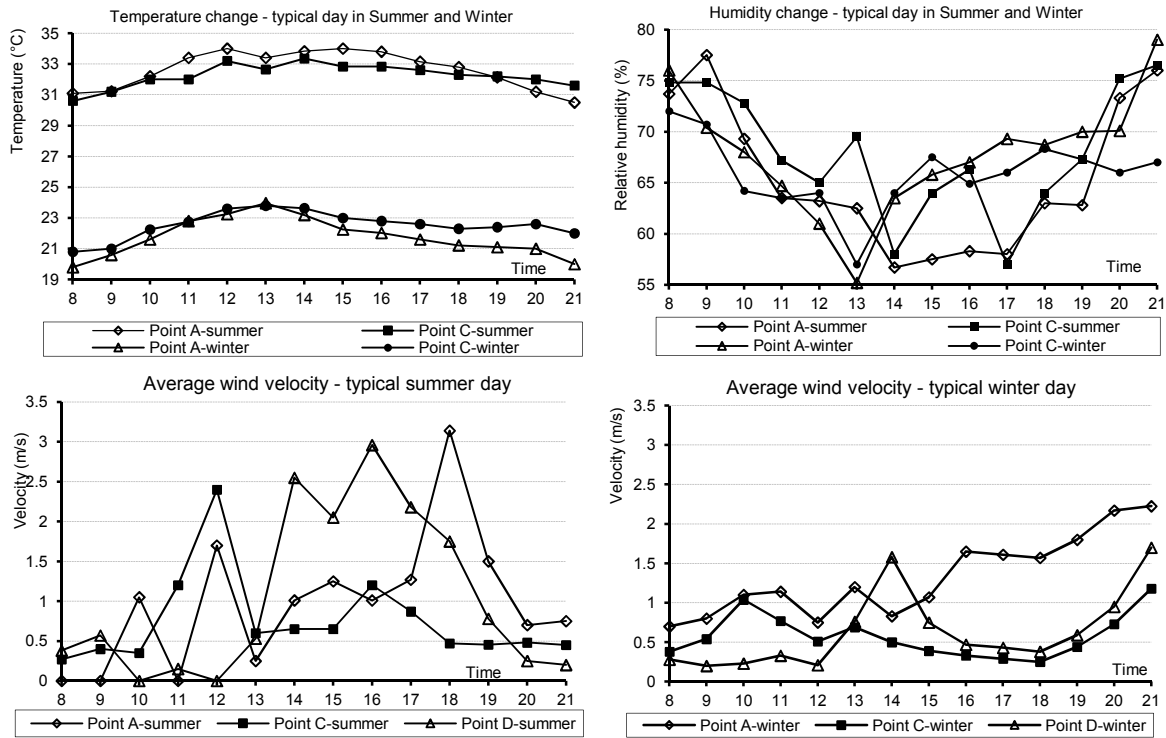


Figure 6-7: Change of temperature, humidity and wind velocity at some survey points during a typical summer and winter day

In order to evaluate indoor thermal comfort, indoor thermal conditions should be evaluated by a relevant thermal comfort model. As reference temperature (running mean outdoor or mean monthly outdoor) was not available, adaptive comfort models could not be used. Hence, measuring temperature and humidity at points B, C and outdoor in the summer and winter days were simultaneously plotted on the building psychrometric chart using the method of the author in CHAPTER 4 (Nguyen & Reiter, 2011b). As the house is completely passive, mean radiant temperature is assumed to be equal to air temperature.

As shown in Figure 6-8, indoor conditions of the winter day were mostly within the comfort zone and could be further improved by appropriate control of openings or passive solar heating. However, these of the summer day were well above the comfort range and the extended comfort zones, revealing that the house was not satisfactory in the summer day investigated. The similarity between indoor and outdoor conditions shown on the graph indicates that the house was well ventilated. According to this analysis, the house performs

fairly well in winter, but it needs other strategies to maintain human comfort in summer. This thesis proposes two control measures for summer period: (1) combining better thermal insulation and structural mass of building envelopes with nocturnal ventilation or (2) employing mechanical control methods during extreme conditions.

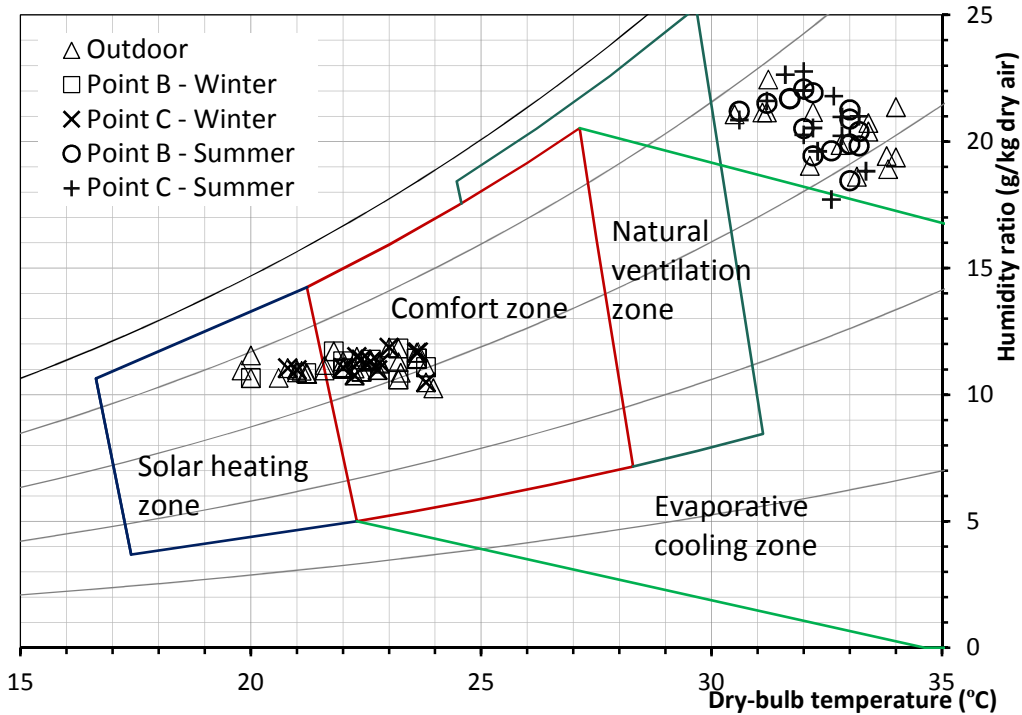


Figure 6-8: Indoor thermal comfort evaluation by the building psychrometric chart developed for hot humid climate (Nguyen & Reiter, 2011b)

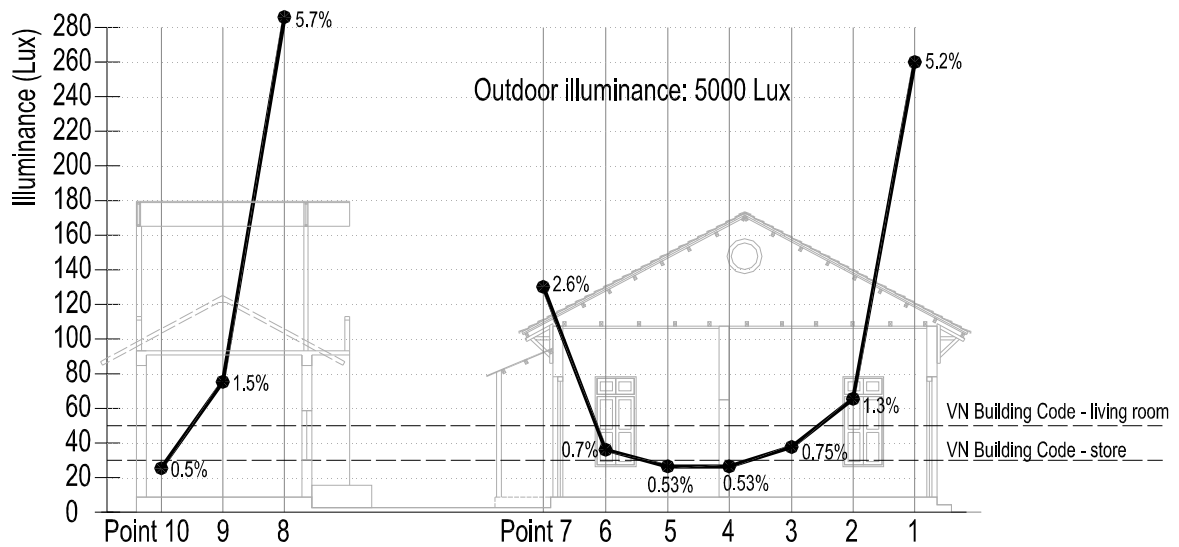


Figure 6-9: Indoor illuminance compared with Building code (15h, 16th December)

Natural illuminance of the 10 survey points on the winter day (16 December, 15h) is illustrated in Figure 6-9. During the measurement period, the sky was completely obstructed by the cloud cover and outdoor illuminance was around 5000 lux. Although the house has many openings, it is a little surprising that some indoor points did not have enough light according to the current Building code of Vietnam while others exceeded. This suggests that many openings should be appropriately distributed to achieve better lighting.

6.3.5 Step 5: Whole – year simulation of building performance

In recent years, building simulation has become an effective method to predict building performance and save time and resources. It also gives predictions for numerous different cases and can simulate extremely complicated circumstances which are rarely examine by experimental methods. Nevertheless, it is recommended that the reliability of simulation results would be carefully validated before use. The present study employs three simulation tools, including a CFD tool, a solar tool and a thermal prediction tool which will be presented in the following sections.

6.3.5.1 Study on natural ventilation performance of the house

Natural ventilation of various situations of house A was examined using Computational fluid dynamics (CFD) method. RNG k- ϵ turbulence model in conjunction with Phoenics code was used as it was reported to be one of the most reliable two-equation turbulence models for indoor and outdoor airflow applications (Gebremedhin & Wu, 2003; Glória Gomes, et al., 2005). RNG k- ϵ turbulence model was also proved to be effective in predicting cross ventilation by the authors (Nguyen & Reiter, 2011a).

The following boundary conditions were applied: power-law wind velocity profile with exponent $\alpha=0.22$; zero external ambient pressure; no heat transfer; structured grid distribution: 106, 72, and 39 in the x-, y- and z-axes, respectively; Hybrid convection schemes; equilibrium Logarithmic wall-function, SIMPLES algorithm (Spalding, 2009), global convergence criteria of 0.01, converged iteration of around 3500. Average wind velocity of 1m/s at height of 1.1m which was obtained from the measurement was adopted in all simulations. All windows were assumed to be opened while doors were closed, reflecting normal operating conditions of the house. Urban context was included into the model by adding neighboring houses and creating a street canyon. Air flow field in the

living room, retail shop and courtyard in five cases as well as their simulation results were examined as shown in Table 6-7.

Table 6-7: Characteristics of air flow field through the model

Case	Wind angle of attack ^b	Ventilation flow rate (m ³ /s)		Average wind velocity on working plane 1.1m above floor level (m/s)					
		Living room	Retail shop	Living room		Retail shop		Courtyard	
				Velocity	STDV ^a	Velocity	STDV ^a	Velocity	STDV ^a
A	0°	0.264	0.147	0.047	0.036	0.022	0.030	0.202	0.065
B	30°	0.204	0.229	0.075	0.077	0.079	0.082	0.234	0.084
C	45°	0.188	0.258	0.070	0.083	0.132	0.130	0.234	0.090
D	90°	1.272	1.567	0.331	0.219	0.300	0.285	0.324	0.173
E ^c	90°	1.370	1.619	0.366	0.253	0.323	0.304	0.181	0.152

^a Standard deviation

^b Prevailing wind direction of Hanoi in summer (90° wind direction is perpendicular to the front façade)

^c Side corridor was closed by the front door.

In cases A, B, and C, ventilation flow rates were low due to the “slide-effect” caused by inertial force of the wind and the row house (wind slides on building surface without entering the room). This detailed CFD analysis found that in these cases, courtyard-facing windows sometimes played a more important role than street-facing windows did. The “slide effect” can be reduced by providing each of two front windows with vertical wing walls. Case D and E had significantly higher flow rates since “slide-effect” did not occur. Table 6-7 shows the indoor and outdoor wind conditions associated with 5 wind directions. It was observed that the wind motion in the Living room was more homogeneous than that in the Retail shop, and also that the outdoor wind was generally more homogeneous than its indoor counterpart.

* Effects of side corridor:

Comparison between case D (side corridor open) and case E (side corridor closed) shows that ventilation flow rate and average indoor velocity increased noticeably when the side corridor was closed (case E). Another effect was that average velocity in the courtyard dropped significantly in this case. These phenomena can be explained by employing the principle of static pressure drop. Figure 6-10 illustrates pressure and velocity filed in these two cases. It is clear that case E had a larger static pressure drop between the windward and

leeward wall than that of case D. According to Bernoulli's equation of flow rate: $Q = C_d * A * \sqrt{2 * \Delta P / \rho}$ (where ΔP is pressure difference across the openings, other variables are constant in this case), this higher pressure drop leads to higher flow rate in case E. Average velocity in the courtyard in case D (0.324 m/s) was, in contrast, far higher than that of case E (0.181 m/s), proving that the side corridor played the role of a wind tunnel which induced more wind into the courtyard.

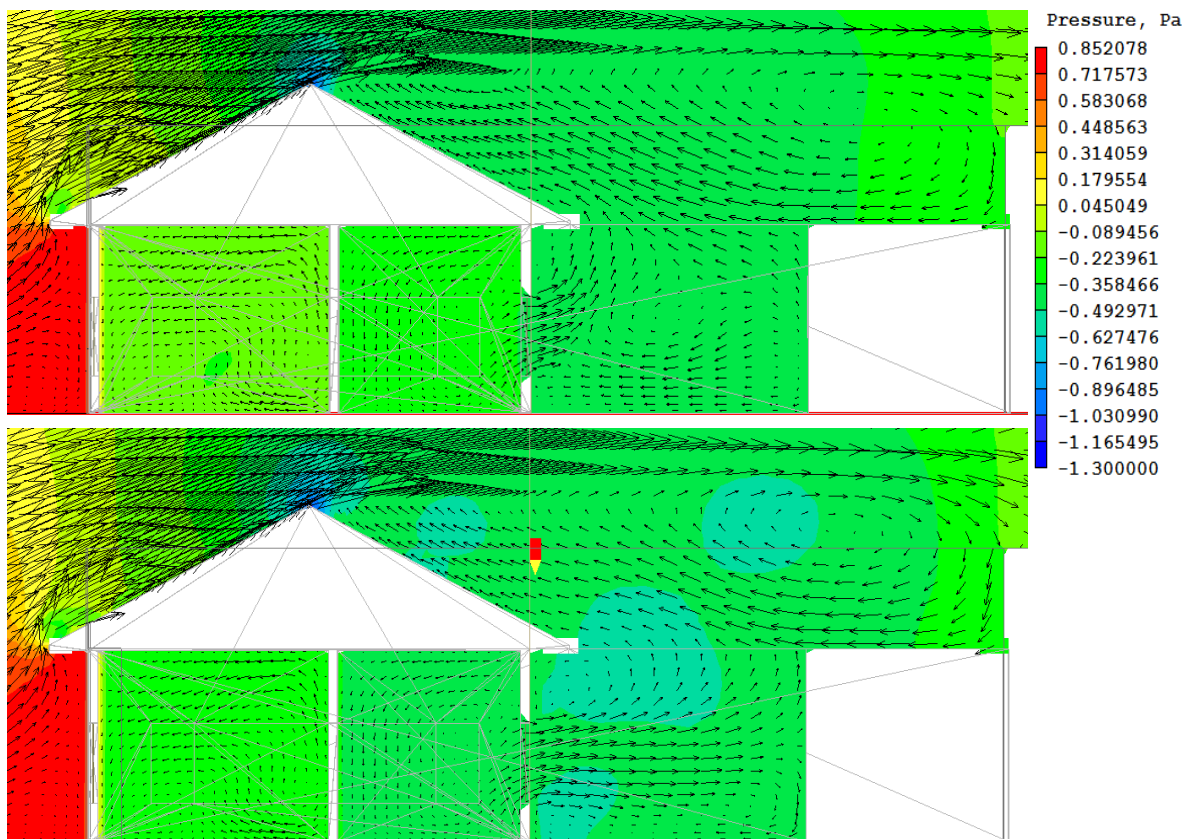


Figure 6-10: Distribution of static pressure and time-averaged velocity in case D with side corridor opened (above) and case E with side corridor closed (below)

Since natural ventilation conditions in the front and back part of this house is a function of wind conditions in the courtyard, the side corridor and the courtyard are a good way to control natural ventilation. Closing the side corridor gives better ventilation in the front part while opening the side corridor improves wind induced ventilation in the back part.

* Comparison with standards and codes:

ASHRAE standard 62.1 (ASHRAE, 2004b) recommends that in residential facilities Air change rates should be higher than 0.35 ACHs and 7.5 l/s.person to ensure IAQ. Flow rates shown in Table 9 were far higher than these requirements (the minimum air change rate occurred in case A and was 3.01 ACHs). However, the average indoor wind velocity of case A, B and C were lower than the minimum wind speed - 0.2 m/s (ASHRAE, 2004) - needed to improve human thermal sensation.

6.3.5.2 Simulation of shading effect by solar shading devices

Shading effectiveness of the shading devices was examined by using the solar tool of Ecotect analysis[®] program (Autodesk, 2011). Three cases are presented in Figure 6-11. Case B reflects the current context in which the house exists whereas case A and case C are the control case and comparative case, respectively.

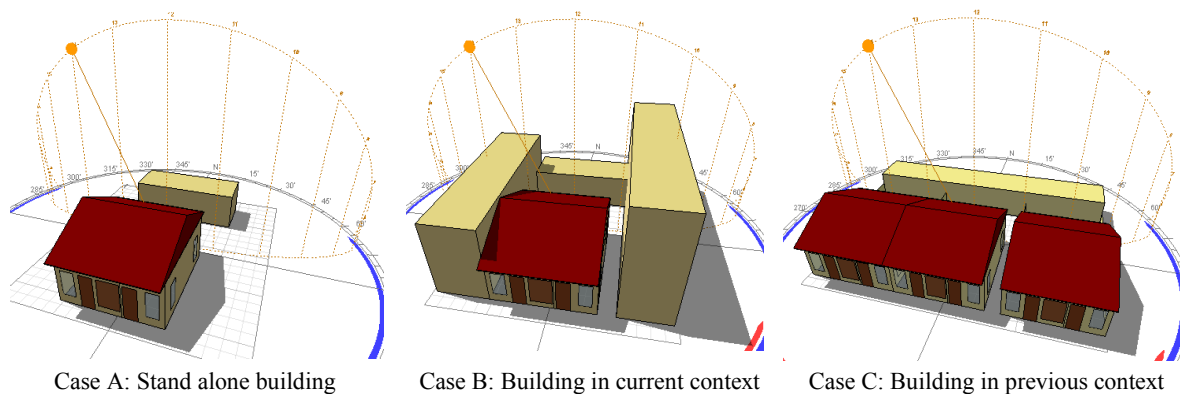


Figure 6-11: Three cases in the study of solar shading effectiveness (14h; 11th July)

Percentages of the shaded area on different vertical surfaces are compared in Figure 6-12. It can be seen that in the current context (case B), the house is currently suitably protected by its shading system since all walls achieved very high shaded percentages (over 90%) in summer and much of the sunlit area in winter. In its previous context (case C), the shading system also performed well with over 80% average shading area in summer. Certainly, case A performed worst among these cases although north and south walls were protected well in summer. In brief, the shading system of the house almost satisfies the shading requirement, especially in the current context.

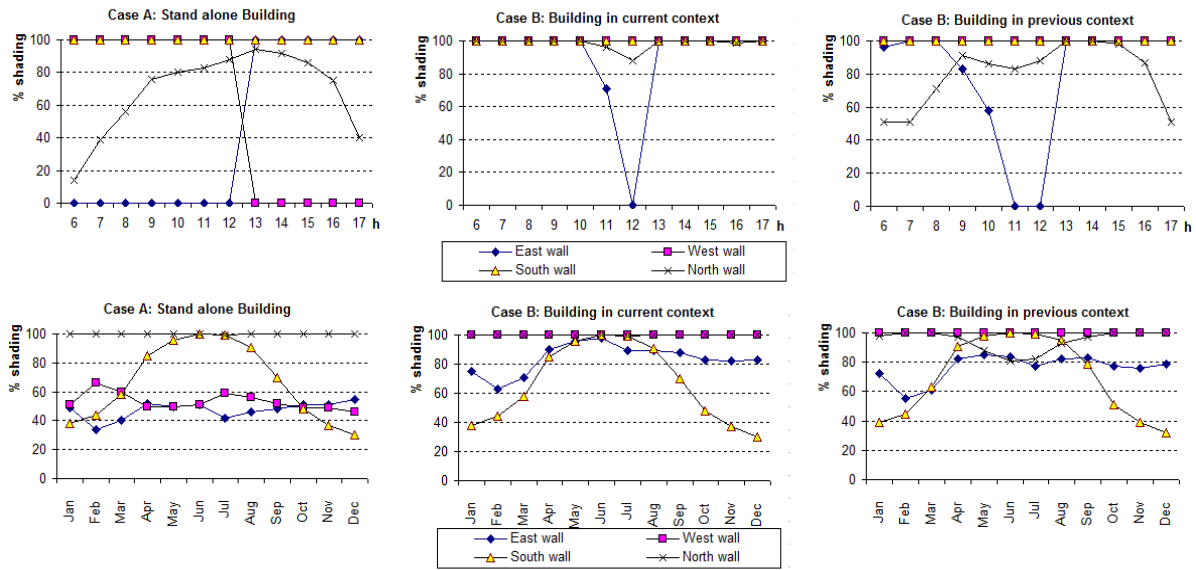


Figure 6-12: Shading effectiveness on the hottest day - 11th July (above) and monthly average shading percentage of the vertical façades (below)

6.3.5.3 Simulation of thermal performance

This study employed COMFIE program (Izuba energies, 2010) for thermal simulation of the house. This program requires information regarding global characteristics of the buildings in question: materials, composition, building finishes, ventilation schedules, surrounding conditions and so forth. COMFIE’s performance was validated by Peuportier (2005) by comparing simulation results with those of similar tools like DOE2, TRNSYS, TAS, SIMULA, CODYBA, confirming that COMFIE successfully predicted the building thermal environment. However, the calibration for this case which helps improve the accuracy of simulation results was overlooked because there is no experimental data available. Therefore, the following scenarios were assumed: operating scheme reflects the activity of a typical Vietnamese family (maximum of 4 occupants during night time); three natural ventilation strategies (night, daytime and full-day ventilation) with different flow rates were separately applied for summer, winter and the mild season using a maximum flow rate of $0.258\text{m}^3/\text{s}$ obtained from the CFD simulation; the attic was ventilated at 1 ACH during daytime and 0.5 ACH during night time; the average internal heat gain was $25\text{ W}/\text{m}^2$ and varied according to the house’s occupancy; the weather data was exploited from a Typical Meteorological Year (TMY) weather file of Hanoi, then converted into Test

Reference Year (TRY) format for COMFIE. All building parameters were reproduced in the model as shown in Figure 6-13.

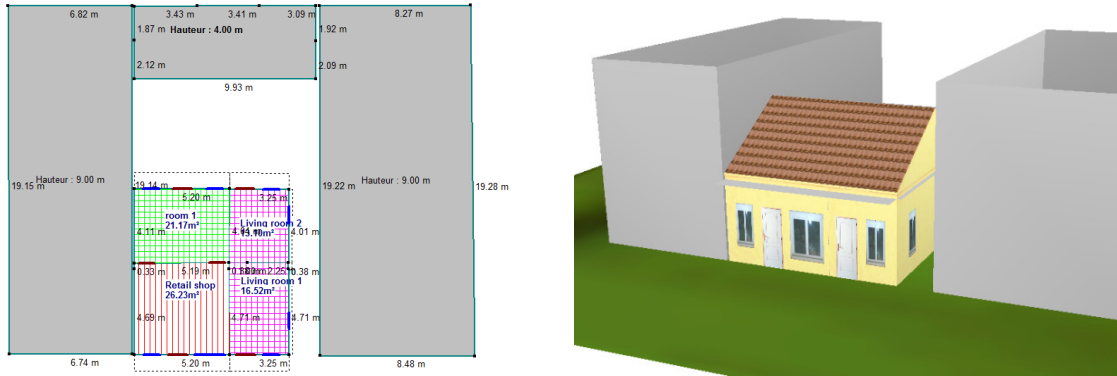


Figure 6-13: Building model for the simulation on thermal performance

Temperature variation during a year shown in Figure 6-14 indicates that indoor temperature was relatively stable, regardless of the fluctuation of outdoor temperature. However, the house failed to protect indoor environment from extreme outdoor conditions although these conditions did not last very long (see highlighted points in Figure 6-14). For the rest of the year, the indoor environment was almost thermally acceptable.

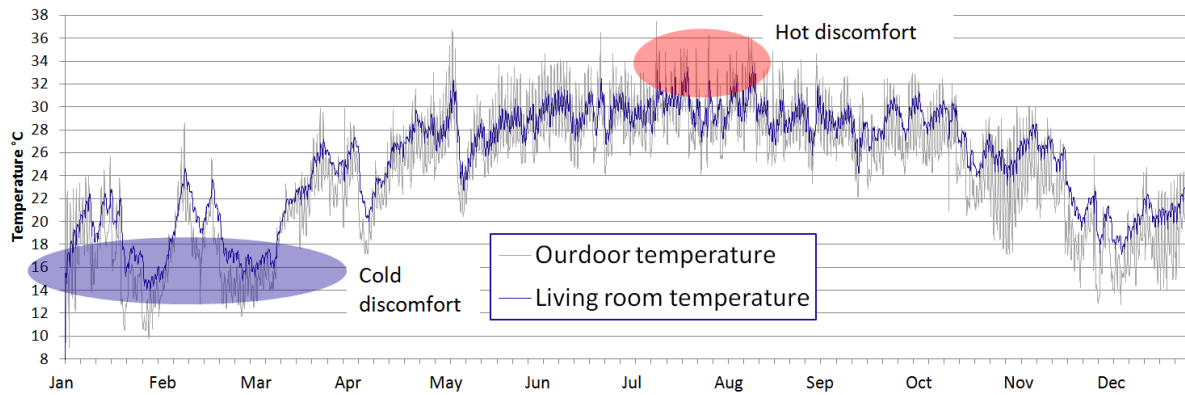


Figure 6-14: Temperature variation in the living room over one year

Thermal comfort in the living room was examined by plotting hourly temperature on the adaptive comfort model (Nguyen, et al., 2012) developed in CHAPTER 3. The optimum comfort temperature underlined in this model is as follows:

$$T_{conf} = 0.341T_{out} + 18.83 \quad (6.1)$$

where: T_{conf} is comfort temperature and T_{out} is monthly mean outdoor temperature.

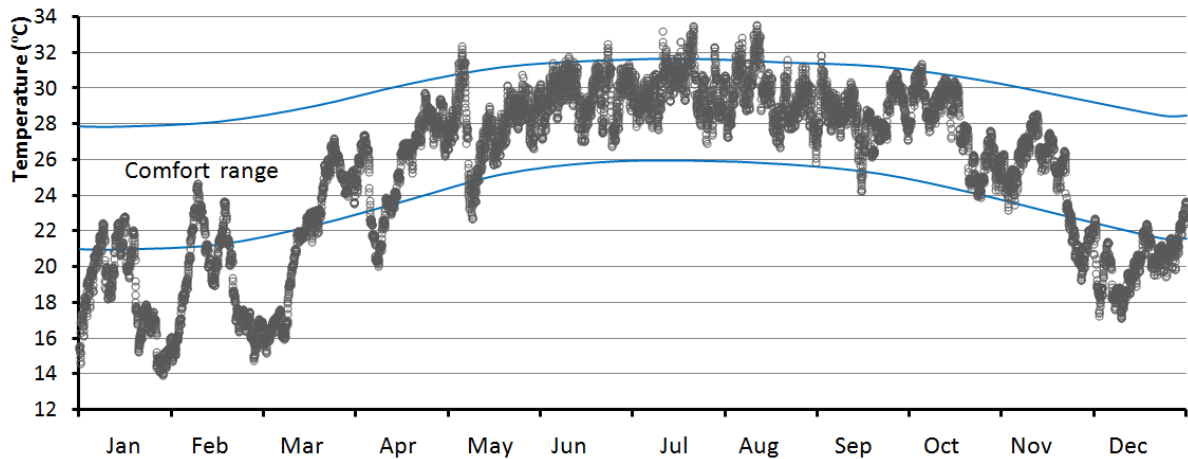


Figure 6-15: Hourly plot of living room air temperature on the adaptive comfort model during a year

This plot was executed by Microsoft Excel[®]. The upper and lower boundaries first established. Points lie above and below the comfort range were then calculated directly in Excel by IF-THEN-ELSE logics. The plotting result in Figure 6-15 reveals that about 68% of the year was found to be thermally acceptable, complying with 80% acceptability. About 92% of the uncomfortable period dropped into the cold zone, showing that the house needs further thermal insulation and improving air tightness against the cold in free running mode.

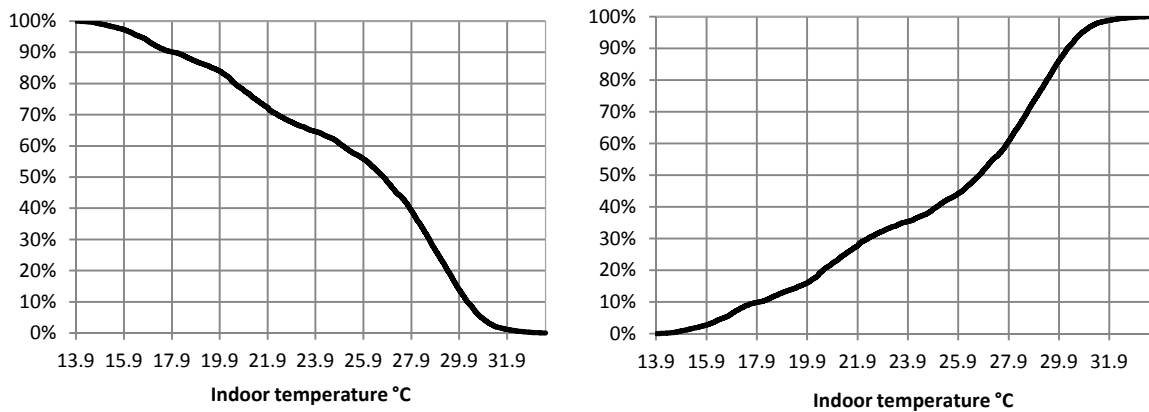


Figure 6-16: Cumulative percentage of living room temperature over base temperature 13.9°C (left) and below base temperature 32°C (right) during TMY

Figure 6-16 shows that there was only about 5% of a year when indoor temperature exceeded 31°C while 29% of a year temperature was below 22°C, proving that the house performed much better in hot weather. According to some standards (ASHRAE, 2004; ISO, 2005), this warm sensation (about 1°C higher than comfort temperature) can be completely eliminated by a wind speed of 0.4m/s, e.g. created by a ceiling fan.

Notably, better performance in summer found by this simulation is contrary to the result in section 6.3.4, indicating that a short-term in-situ survey cannot always provide a good evaluation about building performance.

6.4 Step 6: The lessons given by vernacular architecture - Conclusions

This thesis thoroughly assessed the design principles employed in simple, durable and eco-friendly vernacular dwellings in Vietnam and their effectiveness by qualitatively and quantitatively assessing their performance. The new approach launched in this study to evaluate vernacular architecture proves to be effective and adequate and may be employed in research of vernacular housing in other regions. Nevertheless, necessary modifications would be strongly recommended due to the differences in climates, geographical features and so forth.

The results of this study clearly indicate that not all vernacular buildings have perfect building physics. Through this study, the advantages and disadvantages of these buildings were thoroughly investigated, with the aim to effectively exploit their positive attributes for current developments. The evaluation of a vernacular building should employ suitable objective methods; otherwise the process leads to incorrect or inaccurate findings as described in section 6.3.5.3. Since the weather might change from day to day, in some cases short-term in-situ measurement cannot give an accurate overview of building performance. It would be better to combine short-term in-situ measurements with other long-term prediction tools, such as building simulation.

Generally, vernacular housing in Vietnam has adapted fairly well to climatic conditions in different locations by using low-energy design principles that basically ensure human comfort and health. Natural ventilation, building orientation - building shape and solar shading were the strategies the most commonly employed whereas earth cooling and high thermal mass seemed inappropriate. Although thermal insulation was not used in the six investigated dwellings, the previous analysis suggested that thermal insulation would improve indoor thermal comfort during the cold weather in the Northern areas of Vietnam. The survey on a house in an urban area indicated that the shading devices performed quite well, but the distribution and configuration of the openings should be adjusted to improve

natural lighting and ventilation. Building courtyard played a significant role on ventilation flow rate of the rooms facing the courtyard.

In the hot and humid climate of Vietnam, relying entirely on traditional design strategies to maintain thermal comfort is not completely possible. Therefore, under extreme conditions the building would benefit from low-energy mechanical systems, such as mechanically assisted ventilation, evaporative cooling, passive solar heating... or occupants' adaptive responses such as clothing insulation, activities, opening control and the use of fans.

The present study has limitations as the quantitative assessment of only one house was carried out. A larger investigation is therefore needed. Besides, further studies to include comparative assessment between vernacular and more modern architecture are necessary to better evaluate their performance and provide recommendations for sustainable housing design in Vietnam.

In conclusion, this work has emphasized the importance of climate conscious appropriate building design for the living environment without excessive use of natural resources. Vernacular housing in Vietnam gives evidence that humans can live in harmony with nature, without consuming energy. The vernacular housing in Vietnam has provided valuable social, cultural and scientific values, confirming the need to preserve vernacular architecture there.

CHAPTER 7

CLIMATE RESPONSIVE DESIGN STRATEGIES TO IMPROVE THERMAL COMFORT

7.1 Improving the thermal performance by a parametric simulation method

In CHAPTER 5, the results of 1-year simulations revealed that the comfort requirements of the 3 case-study houses were not satisfied because the discomfort periods extend more than 10% of a year. This section therefore looks for climate responsive design strategies and building control with an aim of improving these performances. The analysis method, commonly known as “parametric analysis” or “parametric simulation”, is used to perform this task. Following a trial-and-error procedure of numerical simulations, this method allows users to explore the effect of each design variable on the simulation outputs; hence it is able to provide improved solutions to the problem. Because of the simplicity of parametric simulations, this method has been widely used in the literature (Axley, et al., 2002; Wang & Wong, 2007; Nguyen & Reiter, 2012c). Results of parametric analysis, however, cannot give a complete insight of variables’ sensitivity as well as very complex interaction among them. This section will present impacts of design variables given by parametric simulations and then quantify the global effectiveness of this approach.

7.1.1 The effects of various external wall types

By varying the composition of external walls of the calibrated EnergyPlus models, thermal comfort conditions in the three case-study houses were examined using full-year simulations. The Total Discomfort Hours (TDH) was the criterion of assessment. Thermal resistance of the external walls of these houses was improved by changing the wall thickness and then adding a central layer of thermal insulation (expanded polystyrene - EPS). The alternative solutions of the external walls are shown in Table 7-1.

Table 7-1: Retrofit choices for the external walls and their corresponding U-values

	Reference case	Option 1	Option 2	Option 3	Option 4	Option 5
Row house	110 mm brick wall	220 mm brick wall	+ 1 cm insulation	+ 2 cm insulation	+ 3 cm insulation	+ 4 cm insulation
Detached house - apartment	220 mm brick wall	-	+ 1 cm insulation	+ 2 cm insulation	+ 3 cm insulation	+ 4 cm insulation
U-value* (W/m ² .K)	2.69 and 1.90	1.90	1.15	0.82	0.64	0.52

*U-value is calculated with an assumption that internal and external surface thermal resistances are fixed at 0.12 m².K/W and 0.06 m².K/W, respectively (Szokolay, 2004).

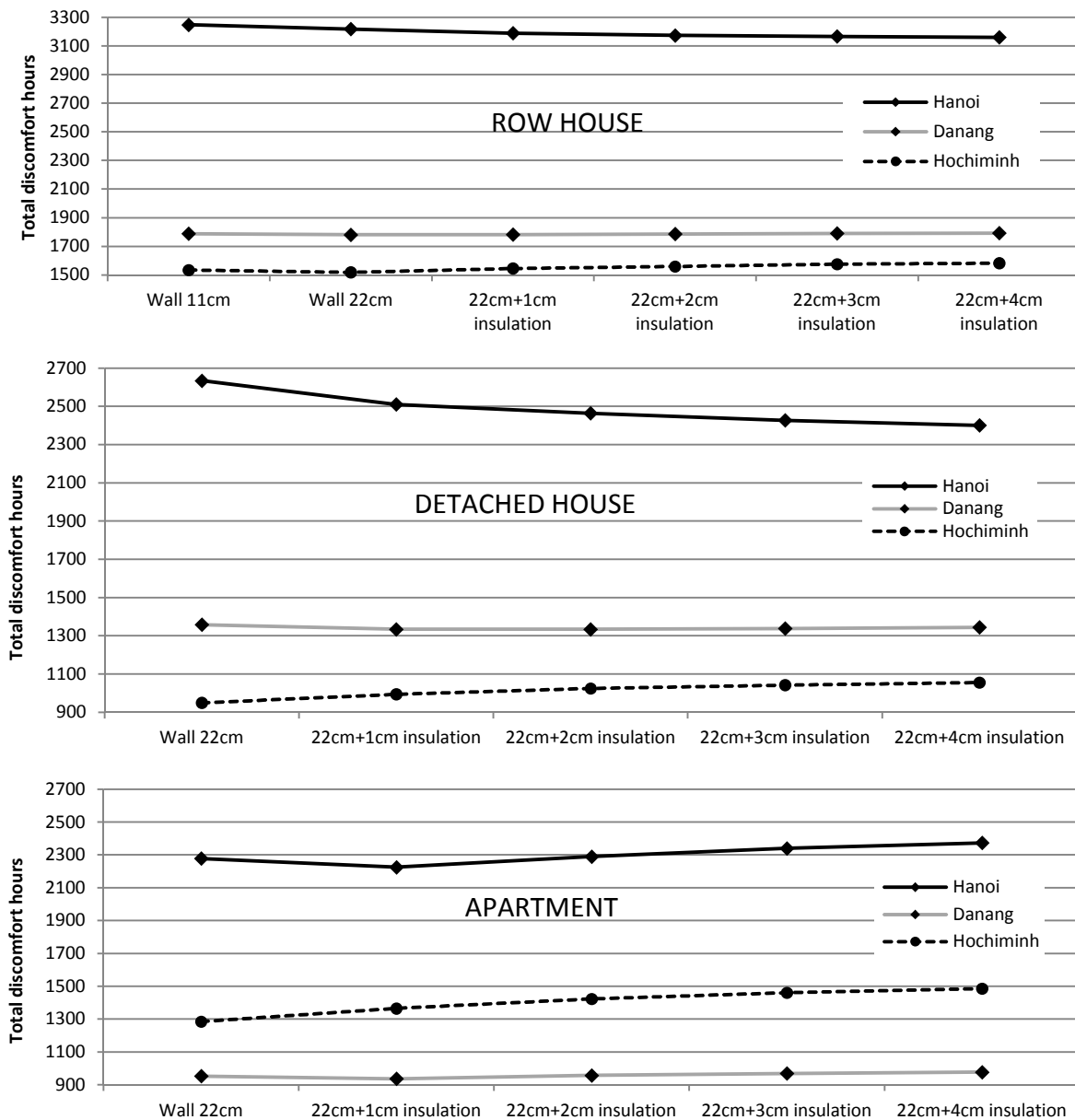


Figure 7-1: Thermal performance of the houses with various types of the external walls

As can be seen from Table 7-1, by changing the composition of the wall the U-value changes significantly. The U-value reduces nearly a half as the first insulation layer of 1 cm is added. However, when the thickness of the insulation layer increases, the U-value is slowly reduced. This indicates that the first insulation layer has the maximum effect on the thermal resistance of the wall.

Totally, 48 successful simulations were executed. Total time needed to complete this task was about 6 hours. Thermal performances of the three houses before and after modifications of the external walls are shown in Figure 7-1. It can be seen that in Danang and Hochiminh city (the climates are warm and humid) the role of thermal insulation was insignificant. Even in some cases the thermal insulation layer produced negative thermal effects on the houses. *It is therefore important to stress that the use of thermal insulation for external walls can be omitted in Danang and Hochiminh city.*

In Hanoi, the situation was more complicated. As the climate of Hanoi has a fairly cold winter, the role of thermal insulation is larger. While the row house and the detached house well profited from the insulation added, it seems that heavy wall insulation was not suitable for the apartment. Detailed analysis of the simulation output reveals that the wall insulation reduced cold discomfort, but significantly increased overheating in the apartment. It was possibly because the insulation restricted the heat transfer process through external walls, thus it helped reduce heat loss in winter, but it also slowed down the cooling effect of wind on the building. On the other hand, the profit given by thermal insulation is rather limited. The external wall with 4 cm insulation may offer the reductions of TDH of only 2.7% and 8.8% in the row house and detached house, respectively. The increase of insulation will anyway strongly influence construction cost of the houses. *The use of thermal insulation in Hanoi is therefore very sensitive and should be carefully determined.*

7.1.2 Thermal insulation for the roof and thermal performance of the houses

Compared with other building components, the roof receives the majority of the solar radiation distributed on a building. Thus, it is obvious that the roof must achieve a certain level of thermal resistance to prevent overheating, especially in hot climates. Additional thermal insulation in the roof also prevents heat loss during cold weather or reduces cooling load in AC buildings. This section discusses the influence of the thermal insulation implemented into the roof on global thermal performance of the house.

In the present form, the roofs of the row house and detached house consist of only a layer of pre-painted corrugated steel sheets. A new insulation layer (expanded polystyrene - EPS) is installed right below the steel sheets. Thickness of the insulation layer is 1 cm, 2 cm, 3 cm, 4 cm and 5 cm. U-values of the reinforced roof are listed in Table 7-2. Totally 36 simulations were completed and this task took about 2.5 hours.

Table 7-2: Retrofit choices for the roof and their corresponding U-values

	Reference case	Option 1	Option 2	Option 3	Option 4	Option 5
Thickness of insulation layer	0 cm	1 cm	2 cm	3 cm	4 cm	5 cm
U-value* (W/m ² .K)	5.52	1.90	1.15	0.82	0.64	0.52

*U-value is calculated with an assumption that internal and external surface thermal resistances are fixed at 0.14 m².K/W and 0.04 m².K/W, respectively (Szokolay, 2004).

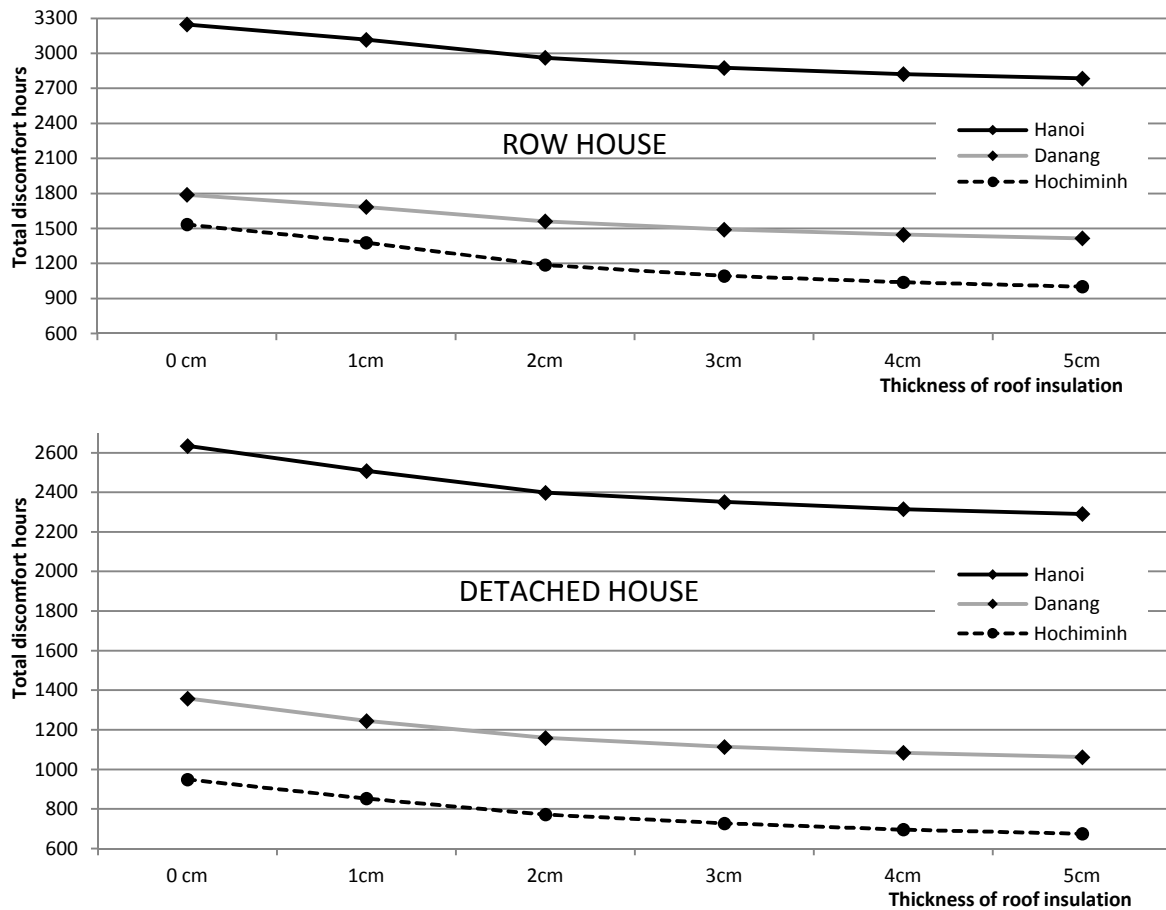


Figure 7-2: Thermal performance of the houses before and after installing thermal insulation into the roof

Table 7-2 shows that U-value of the roof drops sharply from 5.52 to 1.90 by the installation of a 1 cm insulation layer. Increasing thickness of the insulation layer only

produces small reductions of U-value. Figure 7-2 reveals that the thermal performance of the houses with a well insulated roof was remarkably improved, regardless of the climates or the housing types. Remarkable decreases of the TDH were obtained with the average of maximum reduction of 334 hours. Sharp decreases occurred if thickness of the insulation layers was 1 cm, 2 cm and 3 cm.

The above findings lead to a rule of thumb that thermal insulation should be installed below the roof with poor thermal resistance (e.g. steel sheet roof), even if a ceiling has already existed. Furthermore, if the construction cost is an important constraint, thickness of the insulation layer should not exceed 3 cm to obtain a good balance between performance and cost.

7.1.3 The effect of color of the external walls

Color of the external walls determines its solar absorptance factor, thereby the amount of solar heat received by the walls. Because the case-study houses in the present form are painted very light yellow, estimated solar absorptance of the external wall is about 0.3 (Henninger, 1984). Three other scenarios were assumed. These houses were repainted green or blue (solar absorptance of 0.5), dark brown (0.7) and very dark color (0.9). This study then executed another series of 36 simulations which took approximately 2.5 hours to complete. As expected, thermal performances of these houses changed considerably as shown in Figure 7-3. Under the climates of Vietnam, the TDH is almost proportional to the solar absorptance; thus external walls (and building envelopes – in general) should be painted light color (e.g. white, light yellow) to reduce solar heat gain through walls.

Figure 7-3 also shows that the detached house and the apartment were very sensitive to the change of solar absorptance while the row house was not. These sensitivities can be explained by the fact that the row house has a small external wall area and it is well shaded by adjacent houses and trees. Meanwhile, the apartment is completely exposed to the Sun and its external walls are large, compared with its floor area. The detached house also has large external walls, but they are shaded by roof overhangs, window overhangs, trees and other buildings. This analysis indicates that the color of apartment buildings should be chosen with much care because they are generally much more exposed to the solar radiation (in Vietnam, apartment buildings are almost isolated and high-rise blocks).

7.1.4 The effect of ventilation schemes on thermal performance of the houses

Technical measures to enhance natural ventilation will be studied in 7.2. This section only discusses the control of openings of the houses by occupants and its effects on thermal comfort. Five ventilation schemes which are very common in Vietnam were subsequently applied to the case-study houses to examine their capability in improving comfort. All the openings' configurations were not changed, but the openings were opened and closed during the year using different schemes. To facilitate the interpretation of result, each ventilation scheme was assigned to a notation, in turn from A to E. Details of these ventilation schemes are described in Table 7-3.

Table 7-3: Description of the ventilation strategies

	Full open	Full close	Day summer + mild seasons vent.	Night summer + mild seasons vent.	Full vent. summer + mild seasons
Description	Openings never close	Openings never open	Openings open during <i>day time</i> of summer and mild seasons	Openings open during <i>nighttime</i> of summer and mild seasons	Openings open during summer and mild seasons
Ventilation period	All the year	None	1 st March to 31 st October	1 st March to 31 st October	1 st March to 31 st October
Notation	A	B	C	D	E

This analysis required 45 simulations and 4.5 working hours. Simulated performances of these ventilation schemes were compared with that of the reference case as shown in Figure 7-4. Thermal performance of the houses fluctuated considerably as the ventilation schemes changed. No ventilation scheme could produce the best result for all housing types and climates. For the row house, scheme E produced the best performance. For the detached house and the apartment, scheme D generally resulted in better effects. Very low internal thermal mass and low level of thermal insulation in the row house is possibly the reason of this difference because night ventilation (scheme D) is more effective in buildings with high thermal mass. One exception occurred with the apartment in Hochiminh city where scheme A (Full open) was the optimal choice for thermal comfort. In Hochiminh city it is worth to note that schemes A, D and E resulted in rather similar performances. Hence, all of them can be used in this climate. In all cases, schemes B (Full close) and C (Day summer + mild seasons vent.) did not show competitive results; thus they are not recommended.

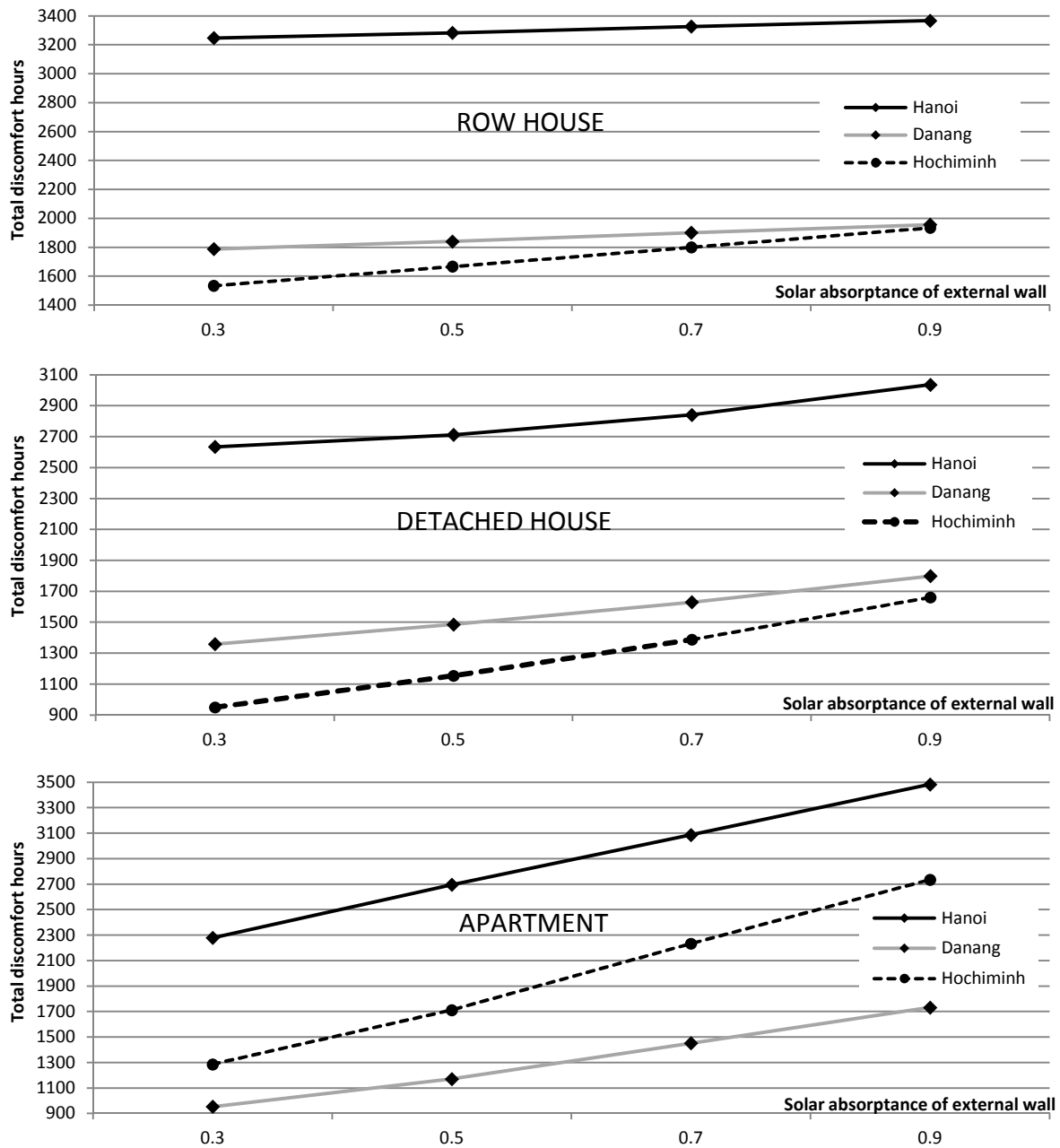


Figure 7-3: Thermal performances of the case-study houses with various external wall colors

To conclude, schemes D and E are generally recommended for all climate regions of Vietnam. In most cases scheme D will perform better. Nevertheless, for better IAQ and lower humidity scheme E seems more favorable. The choice of ventilation scheme therefore depends on how and when the house is occupied and its thermal characteristics. As an example, night ventilation (scheme D) can be applied if the occupants go out during day time and only come back home at night.

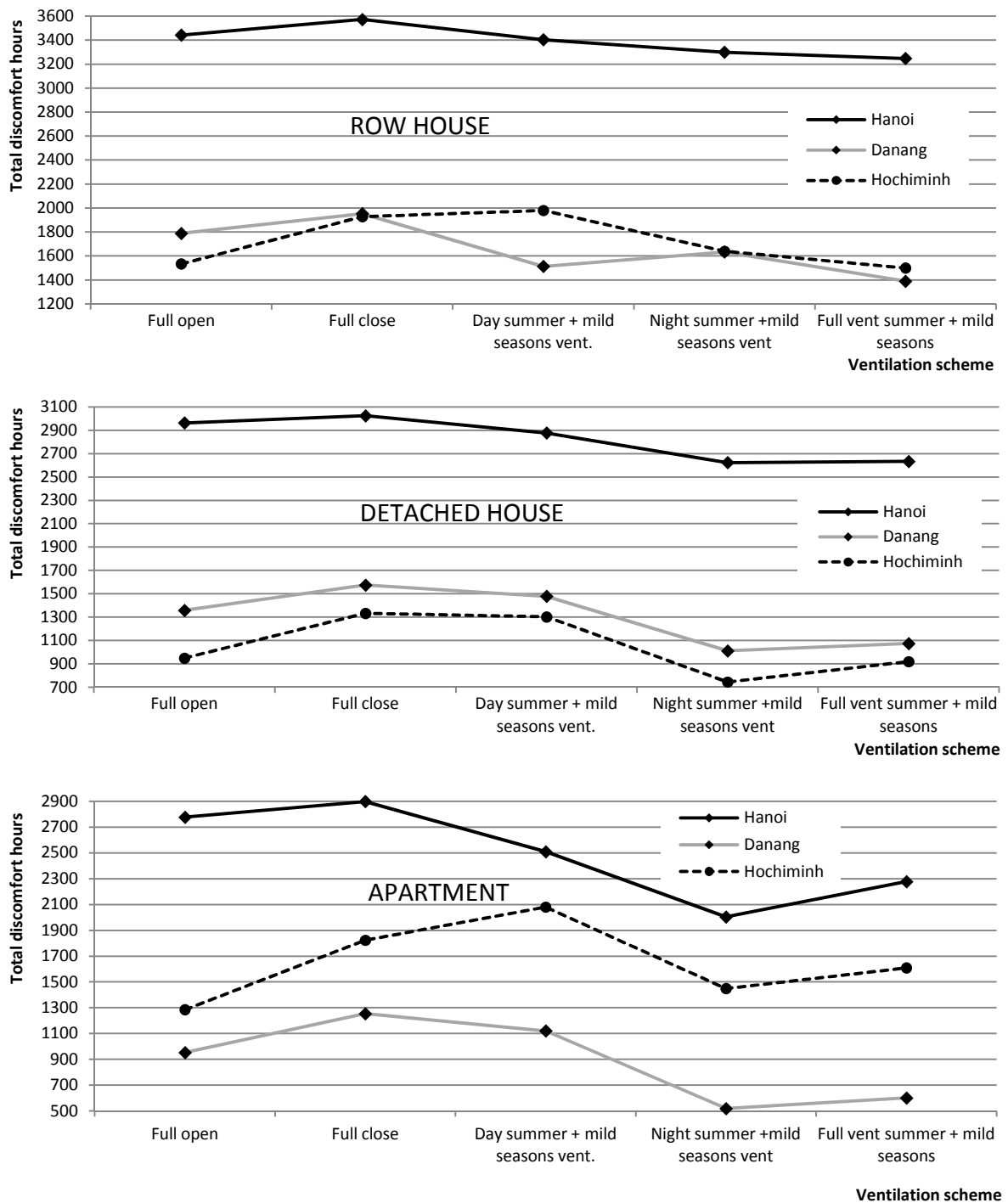


Figure 7-4: Thermal performances of the case-study houses with different ventilation schemes

7.1.5 Other design strategies to improve thermal performance of the houses

Five other common design strategies were selected for the parametric analysis. These strategies and their assigned notations were as follows:

- F: the use of a 0.8 m overhang above window and other external glazing area
- G: the window area was doubled
- H: the single glazed (6 mm) windows were replaced by the double glazed windows with a central air gap of 6 mm
- I: the rate of air leakage through window cracks were reduced by half
- J: the thickness of internal walls was doubled (increase internal thermal mass)

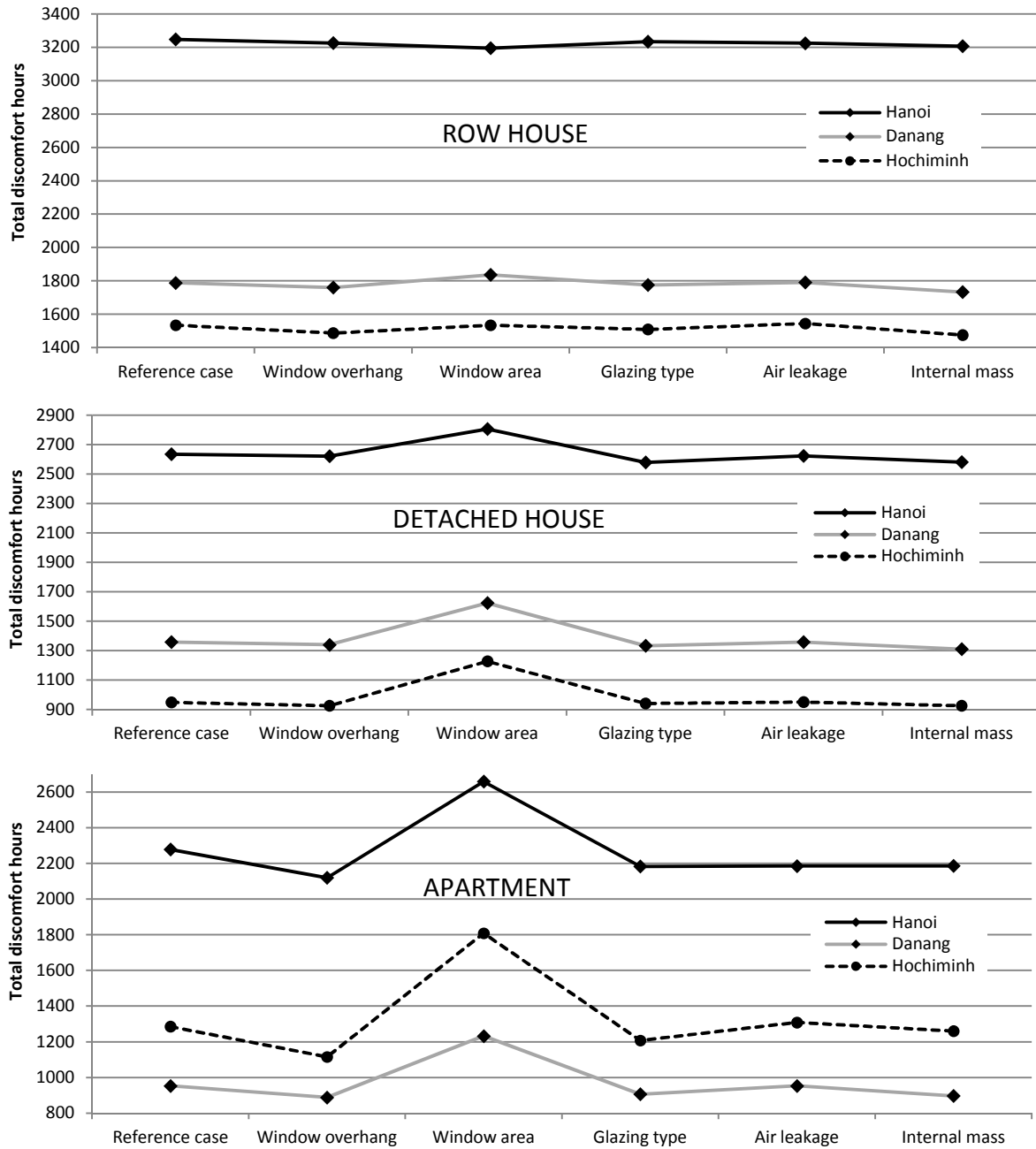


Figure 7-5: Effects of other strategies on thermal condition of the case-study houses

The simulated results of the TDH are presented in Figure 7-5. To achieve these results, 54 simulations were executed in about 4 working hours. Strategy G (doubling window area) alone resulted in severe negative thermal effects in most cases and therefore should be avoided. In the apartment, strategy F (window overhang) gave considerable comfort improvement. The houses were not very sensitive to other strategies as minor changes were observed. However, the trend of improvement was explicit. Strategies F, H, J consistently gave positive changes on thermal conditions of these houses. Strategy G can be used in order to promote natural ventilation and lighting, provided that sufficient solar shading devices are installed. Strategy I (air leakage) slightly gave positive effects in Hanoi where winters are usually cold, but these effects were too small to take into consideration.

7.1.6 Efficiency of the combination of all positive strategies

Table 7-4: Recommended changes for the houses to obtain improved performances

	Hanoi	Danang	Hochiminh
Row house	External wall 4 cm insulation Roof 5 cm insulation Window overhang 0.8 m Double window area Double glazed window Reduce air leakage Increase thermal mass	Wall 220 mm no insulation Full ventilation in summer and mild seasons Roof 5 cm insulation Window overhang 0.8 m Double glazed window Increase thermal mass	Wall 220 mm no insulation Full ventilation in summer and mild seasons Roof 5 cm insulation Window overhang 0.8 m Double glazed window Increase thermal mass
Detached house	External wall 4 cm insulation Night ventilation in summer and mild seasons Roof 5 cm insulation Window overhang 0.8 m Double glazed window Reduce air leakage Increase thermal mass	External wall 1 cm insulation Night ventilation in summer and mild seasons Roof 5 cm insulation Window overhang 0.8 m Double glazed window Increase thermal mass	Night ventilation in summer and mild seasons Roof 5 cm insulation Window overhang 0.8 m Double glazed window Increase thermal mass
Apartment	External wall 1 cm insulation Night ventilation in summer and mild seasons Window overhang 0.8 m Double glazed window Reduce air leakage Increase thermal mass	External wall 1 cm insulation Night ventilation in summer and mild seasons Window overhang 0.8 m Double glazed window Increase thermal mass	Window overhang 0.8 m Double glazed window Increase thermal mass

Strategies which resulted in positive effects on the thermal conditions of each house in each climate were combined together. These combinations were expected to produce higher improved performances of the three housing types in 3 climatic regions in Vietnam.

Table 7-4 summarizes the necessary changes for the present houses. Other design variables of the case-study houses were unchanged if they are not mentioned in this Table.

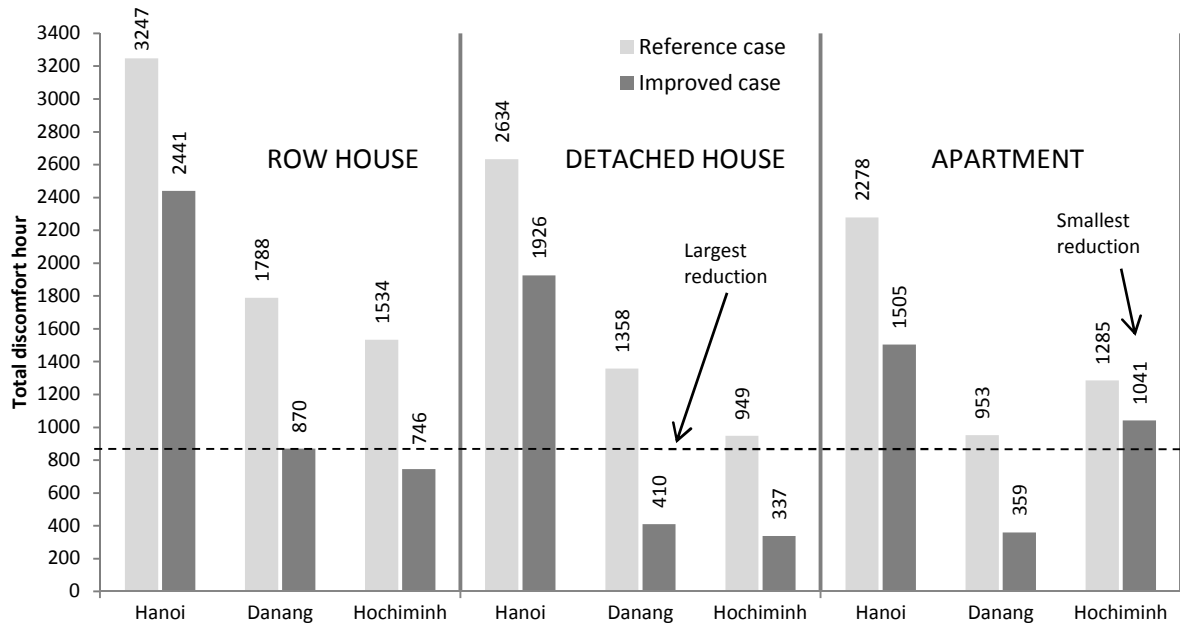


Figure 7-6: Thermal performances of the houses if combined strategies are used. The horizontal line indicates the acceptable threshold of TDH.

The thermal conditions in the reference houses and the improved houses using the combined strategy were compared as shown in Figure 7-6. In all cases, the TDHs were effectively reduced. The largest reduction of 70% was observed in the detached house under the climate of Danang. The smallest reduction was 19%, observed in the apartment in Hochiminh city. In average, a 44.9% reduction of the THD was obtained, providing a solid proof that the parametric approach was really effective.

Total time used for setting and then running parametric simulations was roughly 22 working hours. There were totally 9 cases (three housing types and three climatic regions), thus each case would need approximately 2.44 hours to complete. This time cost is not expensive, compared with time needed for the whole design process of a dwelling.

Thermal performances of the improved houses using the combined strategy were classified by the criteria of Van der Linden et al. (2002) prescribed in Table 5-9. Results of the classification are shown in Table 7-5.

Table 7-5: Thermal classification of the improved houses

	% of time comfort limit is exceeded	Average of exceeding amount	Classification
Row house - Hanoi	27.9	-	Poor
Row house - Danang	9.9	0.73°C	Good
Row house – Hochiminh city	8.5	0.77°C	Good
Detached house - Hanoi	17.0	-	Poor
Detached house - Danang	4.7	0.47°C	Good
Detached house – Hochiminh city	3.8	0.42°C	Good
Apartment - Hanoi	17.2	-	Poor
Apartment - Danang	4.1	0.46°C	Good
Apartment – Hochiminh city	11.9	-	Poor

It is worth to note that the performances of the reference houses in all climates were classified as “poor” (see section 5.6.1). It is easy to find that in 5/9 cases after being improved the performances were classified as “good”. The remaining cases were considered to be “poor”, but the TDHs were decreased noticeably. 3/4 cases of which thermal performances were “poor” belong to Hanoi. This means that the climate of Hanoi seems more severe than those of Danang and Hochiminh city and that special techniques are required to maintain indoor thermal comfort throughout the year.

7.2 Design strategies to enhance passive cooling by natural ventilation

7.2.1 Theory of passive cooling by natural ventilation

Natural ventilation is the process of air exchange between an indoor and outdoor space by natural mechanisms. According to CIBSE (1997), besides mechanically assisted ventilation, there are three types of natural ventilation in buildings: cross ventilation; single-side ventilation and stack ventilation. Cross ventilation and single side ventilation are wind driven ventilation while stack ventilation is driven by the increased buoyancy of air as it warms up. The majority of buildings employing natural ventilation rely mainly on wind driven ventilation. However, stack ventilation has many advantages, especially in moderate and cold climates. Ideal design for NV buildings should take full advantage of both types of ventilation. In hot humid climates, natural ventilation is the major measure to maintain human thermal comfort and IAQ.

7.2.1.1 Passive cooling process

In building science, passive cooling is the term designated as the cooling technologies without employing mechanical equipments (or non-renewable energy consumption). The building and occupant can be cooled down through some processes which can be categorized as:

- *Convective cooling*: the heat transfer process caused by the movement of the air on the surface of occupant's body or building elements. This process is governed by the surface characteristics, the contact area, temperature difference between the air and the element to be cooled and wind velocity.
- *Evaporative cooling*: evaporation of water takes the sensible heat of surrounding environment and converts it into latent heat, thus cooling down building surfaces and occupant's skin.
- *Radiant cooling*: the heat of building elements is gradually dissipated into the atmosphere by long-wave radiation, especially during nighttime when temperature of the sky vault drops.
- *Cooling by conduction*: building elements are cooled down by a direct contact with cooling fluid (e.g. cool sea water loop) or heat sink (e.g. the earth).

Natural ventilation is a typical convective cooling process through which excessive heat of the human body and building structure is removed by the airflow. Cooling by natural ventilation is the most common cooling strategy in hot humid climates. Air movement provides two cooling effects, namely bodily cooling and structural cooling. Hence, it offers a great possibility to maximize thermal comfort at minimum energy cost.

7.2.1.2 Bodily cooling by airflows

Bodily cooling by airflows is based on the cooling effect of sweat evaporation and convection. Air velocity must exceed a limit of stagnant air, approximately 0.2 m/s, and then the cooling effect can be perceived. For optimum cooling efficiency, airflow should be directed to the occupant's area. In hot and humid climates, an appropriate shelter sometimes includes only the floor and well-insulated roof to protect the occupant from sun and rain. Walls can be porous or even removed for the purpose of achieving maximum ventilation. Under hot and humid conditions, temperature difference between day and night becomes

insignificant and structural cooling by night ventilation is possibly inefficient. Hence, bodily cooling becomes very important. Bodily cooling can be enhanced at any time by the use of electric fans, e.g. ceiling fan, if natural ventilation is not available. Figure 7-7 shows how the air in a room of 4 m x 4 m x 3.2 m is stirred up by a normal ceiling fan (diameter of 1.2 m, outlet velocity of 2.5 m/s). This figure shows that a ceiling fan can considerably improve occupants' thermal sensation by generating higher air velocities in the occupied area.

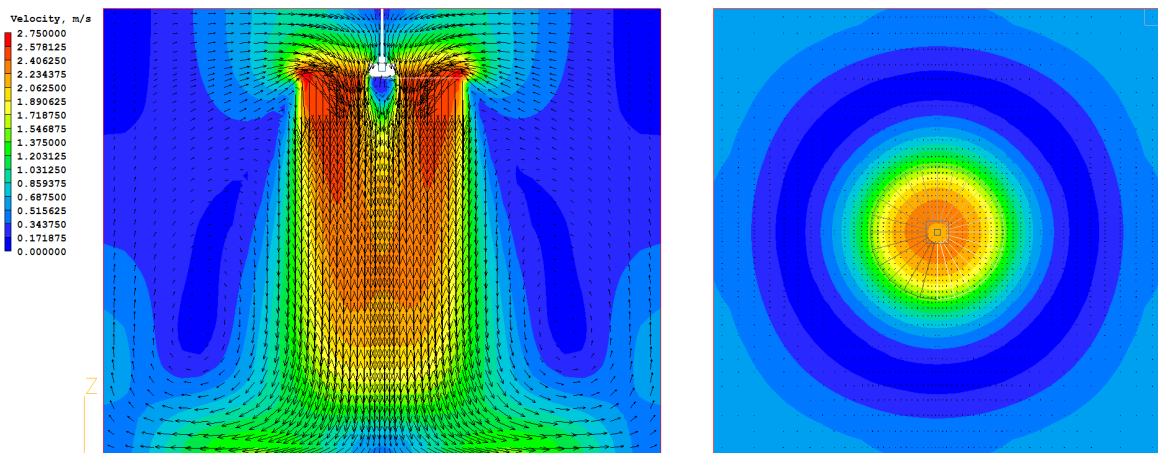


Figure 7-7: Airflow created by a ceiling fan on the central vertical plan (left) and horizontal plan at 1.1 m above the floor (right) - result given by a CFD simulation

7.2.1.3 Building structure cooling by the combination of thermal mass and nocturnal ventilation

Buildings with heavy structural mass usually have high thermal inertial which can smooth out the daily variation of indoor temperature. During nighttime when outdoor temperature is within or below the comfort zone, the thermal mass should be cooled down by long-wave radiation into the sky or by “flushing” the stored heat in the mass with nocturnal ventilation. The cooled thermal mass will serve as a heat sink for the next day which effectively reduces peak indoor temperature. Structure cooling is very effective under large daily temperature variation, e.g. in hot arid climates. In hot humid climates, the cooling effect of nocturnal ventilation should be intensified by the support of mechanical ventilation (Nguyen & Reiter, 2012c). Natural nocturnal ventilation may lower daytime peak indoor temperature by an amount equal to 15% of the outdoor temperature range, compared with that of an unventilated building with similar thermal mass (Legacy Resources Management Program, 1990).

When daytime temperature is above the upper limit of comfort temperature, bodily cooling requires air movement in occupied areas while the building must be closed to maximize and prolong the effect of pre-cooled structural mass. These requirements are therefore mutually exclusive. In such a case, bodily cooling can be achieved by stirring indoor air with ceiling fans or other mechanical equipments.

7.2.1.4 Design strategies to promote natural ventilation

Under the climate of Vietnam, ventilation caused by stack effect seems inefficient for passive cooling because of relative small difference of indoor - outdoor temperature. Instead, it can provide sufficient air change to meet IAQ requirement in winter when openings are normally closed. This section therefore focuses mainly on wind-driven ventilation by which thermal comfort can be improved. There are three major factors that affect the movement of the air mass within and around the buildings, including:

- Building site and surrounding landscape,
- Building orientation, shape, and envelope design,
- Internal arrangement of building elements such as rooms, internal doors, partitions, furniture.

There are a large number of available design solutions for natural ventilation. Some of these may however conflict with other requirements (e.g. solar orientation, solar shading, fire safety, security...) and designers have to take them into consideration as a whole. Table 7-6 shows some recommendations and rules of thumb for building design to enhance natural ventilation in hot humid climates. The guidelines were extracted, refined and summarized from some references (Legacy Resources Management Program, 1990; Allard, 1998; Aynsley, 2007; Patricia & José, 2008; Khan, et al., 2008; ASHRAE, 2009; Nguyen & Reiter, 2011a).

Table 7-6: Recommendations and rules of thumb for better natural ventilation

Building site and surrounding landscape	<p>Building site should avoid enclosed valleys and sheltered locations where air is often stagnant. Designer should maintain adequate building spacing and organize proper site layout (e.g. scattered layout) to increase wind movement around buildings. Buildings should not be located within the wake of any obstruction by a clear spacing of at least 5 times the height of the upwind building.</p> <p>Buildings should be placed upwind of or far away from pollution sources. Big tree must be carefully planted in prevailing wind directions so that the wake region of the canopy does not</p>
---	---

	<p>cover the inlet openings. Rows of trees and hedges can direct air towards or away from a building; thus can help control wind velocity. They can also be used to generate suction zones for outlet openings.</p> <p>Grassy open area may cool down the wind before it reaches the building. Sunlit manmade open areas may heat the air above them and should be minimized.</p> <p>Large bodies of water (e.g. lake) may absorb heat and moderate temperature of coming wind.</p>
<p>Building orientation, shape, and envelope design</p>	<p>Building orientation should maximize exposure to summer wind directions. Shape of building determines the length of ventilation path, hence a narrow plan form facilitates cross ventilation. The building long axis and the majority of external doors and windows should be oriented perpendicular (or $\pm 20^\circ$) to prevailing summer breezes.</p> <p>Some architectural elements such as wingwalls, parapet walls, balconies, window overhangs, and roof overhangs strongly affect the wind pressure distribution on building façades and thus the flow rates through openings. Wingwalls are used to promote ventilation in rooms with windows on one external wall only; up to 100% increase of the air flow rate may be yielded. Long roof overhangs can increase ventilation by blocking the airstream in the corner of front wall; increasing the positive pressure outside the window and thereby the airflow through it. Solar chimneys, rotary vents or wind traps are also some strategies to enhance ventilation in hot conditions.</p> <p>Square or vertical windows are generally less effective than horizontal counterparts. Sliding windows should be avoided. Greatest flow rate of a cross ventilated room is observed if areas of inlet and outlet openings are nearly equal. An outlet smaller than the inlet provides more uniform but lower airspeed throughout the space while higher inlet velocities can be achieved in the reversed case. Openings should be placed properly so as to direct the airflow to occupied areas, that is, within 1.8 m of floor level, to increase direct cooling effects. Horizontal and vertical shading devices may promote wind movement if they are properly designed.</p> <p>As wind velocity profile near ground is logarithmic, rooms elevated from the ground may experience stronger wind and ventilation potential may increase up to 30% over that of rooms on grade.</p>
<p>Internal arrangement of building elements such as internal spaces, doors, partitions, furniture.</p>	<p>Internal partitions should not abruptly obstruct the airstream from inlet openings, but they can be placed to redistribute airflow within the space. They should be placed far from inlet openings to minimize the dissipation of wind kinetic energy. Flow between the building's inlets and outlets should be respected to preserve wind energy. Oversized furniture can significantly affect or obstruct room airflow patterns. Thus laying out furniture plan should be made with care.</p> <p>Vertical air-shaft or opened staircase can be used as air outlet in cross ventilation. Courtyard, lightwell can act as outlets in compact buildings and high density urban areas to improve cross ventilation and natural lighting. Wind catchers and external wind scoops may act as inlets, driving cool wind into the center of a building. A wind catcher can be combined with a solar chimney to improve effectiveness. Ceiling configuration has small effect and can be omitted in preliminary design. The use of ceiling fans or portable oscillating fans provides inexpensive air stirring when natural ventilation is not satisfied.</p>

As presented above, passive cooling techniques by natural ventilation are abundant and the choice for each specific problem is the responsibility of designers. Moreover, the use patterns of building occupants (e.g. opening control) also have considerable effects on the effectiveness of natural ventilation (as can be seen in section 7.1). As a demonstration, the subsequent sections will discuss specific ventilation solutions for each case-study house in detail.

7.2.2 Case study on natural ventilation using the CFD technique

In this section, natural ventilation is investigated in the three case-study houses. It was hypothesized that ventilation of these houses can be improved by a number of passive solutions. The houses in the present conditions were assumed to be retransformed and thereby having new configurations. The airflow patterns and ventilation flow rates in the house before and after transformation were examined by the CFD simulation. The advantages and drawbacks of the solutions will be analyzed, followed by discussions and recommendations.

7.2.2.1 Improving ventilation by a courtyard implemented in the detached house

Original design of the detached house creates a long central corridor. This corridor often suffers from darkness and stuffiness, particularly when internal doors are closed. Furthermore, all rooms are single-side ventilation zones thereby decreasing the potential of cross ventilation and consequently thermal comfort in hot weather. This study therefore proposes a simple solution to deal with this shortcoming. A new courtyard of 1.6 m x 4 m was implemented into the core of the house (see Figure 7-8). Two courtyard-facing windows were added in the bedroom 1 and 2. A small change was made to rearrange the bedrooms and the toilet, but the overall structure and function of the house have not changed. The courtyard was expected to provide sufficient natural light and to generate a central suction zone thereby promoting cross ventilation through the surrounding rooms.

In the CFD model, thickness of all internal walls was assumed 200 mm (instead of 100 mm) to reduce CFD mesh density and consequently simulation time. The chamfered corners of the house were ignored to prevent possible CFD errors. In all cases, the toilets were closed and the CFD code treats these toilets as blockages.

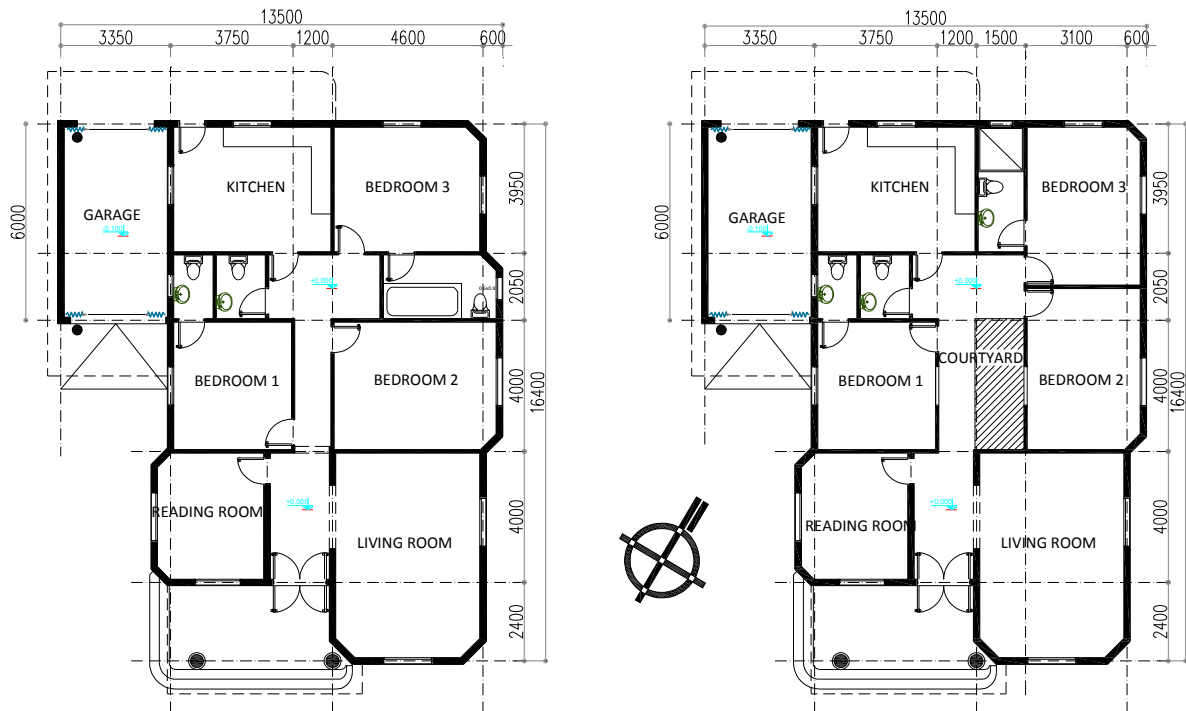


Figure 7-8: Floor plan of the detached house before (left) and after implementing the courtyard (right) in the central corridor

The CFD domain was 160 m x 160 m x 40 m. After some tests, the domain was finally discretized by a structured Cartesian grid system of 120 x 132 x 45 cells (712800 cells). Lower numbers of cells caused CFD errors because the smallest cell couldn't catch smallest architectural details. A higher number of cells possibly causes numerical divergences and significantly extends simulation time. The inlet wind speed at height of 10 m is assumed 1.85 m/s (annual average wind speed in Danang). As in urban areas, the wind profile follows the power law with exponent α of 0.17 - between category 2 and 3 in ASHRAE handbook (ASHRAE, 2009). The RNG k- ϵ turbulence model was applied for solving variables. The *equilibrium Logarithmic wall-function method* was applied for the flow field near the ground and solid surfaces. The SIMPLEST algorithm (Spalding, 2009) was selected to decouple pressure variable from partial differential equations. The Hybrid scheme was used to interpolate variable values at faces between cells. The simulations were considered isothermal.

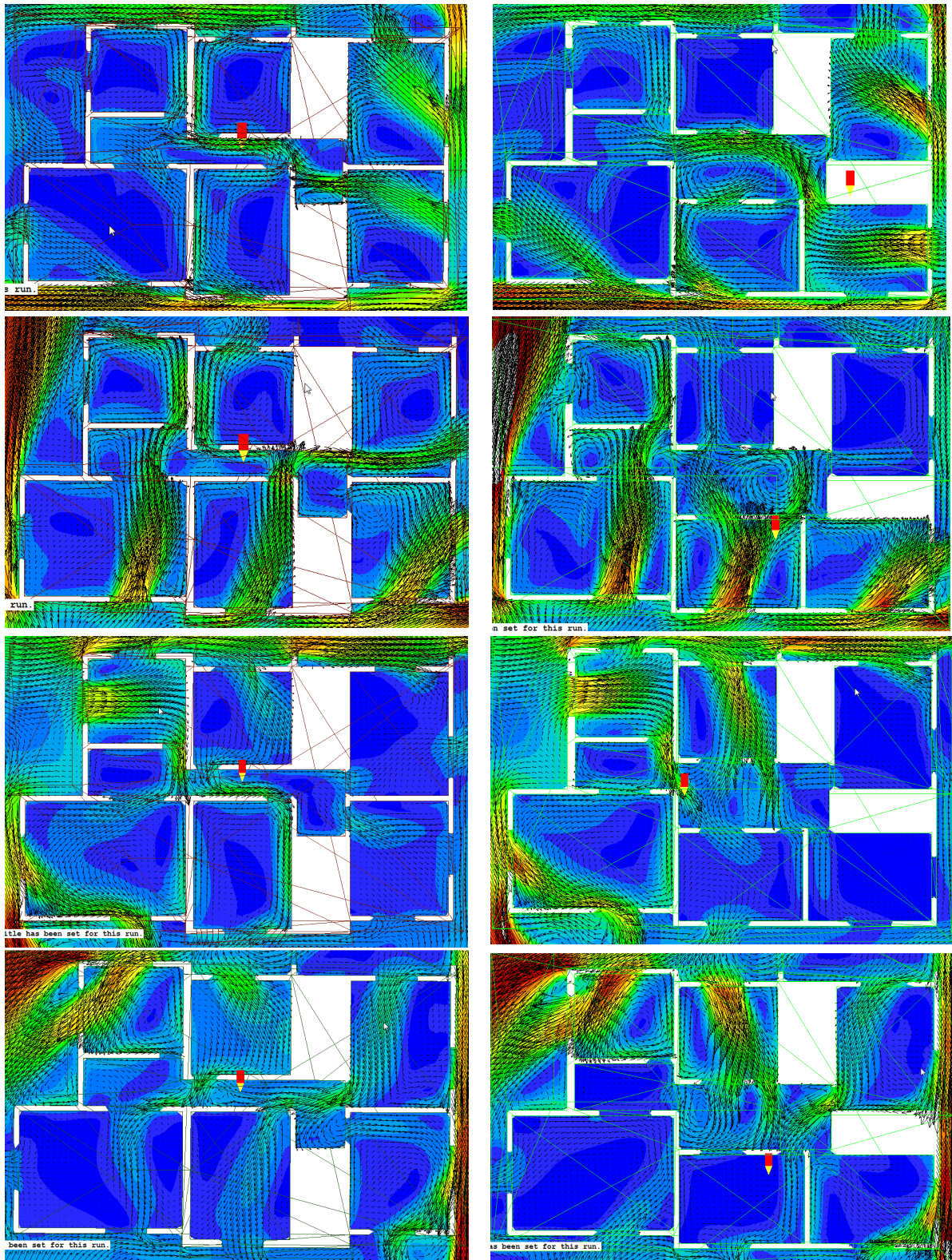


Figure 7-9: Time average wind velocity in the original detached house (left) and courtyard house (right). Velocity range from 0 to 1.5 m/s (from dark blue to red). Wind comes from the North, East, South and West, respectively

Though prevailing summer wind in Vietnam reaches the mainland from the sea, for an overall assessment, approaching wind in this series of simulations was assumed from four directions: North, East, West and South. Eight successful runs were completed among many trial runs which were mainly to correct numerical errors caused by the models and the grid system. All simulations were performed on a PC with CPU Intel Core i5 M460 (4 x 2.53 MHz). As the model was rather sophisticated and the grid system was dense, most simulations were rather unstable and required strict and continuous relaxation control. Time required for complete convergence varied from 8 h up to 12 h, depending on the cases and CFD convergence control during simulation.

Figure 7-9 compares the flow fields in the detached house and the courtyard house on the floor plan at height of 1.25 m. As can be seen, the wind condition in the corridor was significantly improved. Wind movement creates some vortexes in the corridor thereby stirring the air and removing humidity and odor concentration. In the courtyard house, the maximum wind speed in the region near inlet windows was much higher. Also, wind conditions in the rooms facing the wind (hereafter called “front rooms”) were much better, but those in the rooms behind the front rooms (hereafter called “rear rooms”) were slightly lower.

Table 7-7: Mean wind velocity in the main occupied spaces

Wind from		Max wind velocity (m/s)				Mean wind velocity (m/s)			
		Bed.1	Bed. 2	Bed. 3	Living	Bed.1	Bed. 2	Bed. 3	Living
North	No courtyard	0.58	0.53	0.80	0.47	Still air	Still air	0.33	Still air
	With courtyard	0.40	0.87	1.01	0.68	Still air	0.21	0.59	0.21
East	No courtyard	0.64	0.78	1.02	1.09	0.16	0.36	0.50	0.48
	With courtyard	0.36	1.23	1.22	1.21	0.19	0.48	0.52	0.58
South	No courtyard	0.47	0.56	0.41	0.93	0.21	Still air	0.20	0.21
	With courtyard	0.91	0.28	0.25	1.20	0.48	Still air	Still air	0.26
West	No courtyard	0.69	0.44	0.80	0.36	0.33	0.25	Still air	Still air
	With courtyard	1.15	0.36	0.88	0.32	0.57	Still air	Still air	Still air

Note: “Still air” indicates that mean air velocity is lower than or equal to 0.15 m/s

Table 7-7 compares the max and mean wind velocities at height of 1.1 m in three bedrooms and living room of these two houses. The mean velocity was calculated by the average values of four symmetrical points in a room. It can be observed that mean wind velocities in all rooms of the courtyard house were slightly better than those of no-courtyard

counterpart (observed mean velocity improvement was 0.11 m/s). Meanwhile, the maximum wind velocities in the courtyard house show significant improvements (see bold numbers in the Table) with an average difference of 0.28 m/s.

In order to understand the mechanism through which the courtyard enhanced the air flow in the house, the 3-D airflow patterns in the courtyard house were examined as shown in Figure 7-10. The courtyard is located in the center of the house (see the white arrows in the figure). Due to space constraint, only the cases of North and East wind are shown. In all cases, the wind strongly moved up in the courtyard and dissipated into the atmosphere. This “buoyancy” flow caused a certain static pressure drop in the courtyard thereby promoting cross ventilation in the front rooms, slightly reducing the ventilation rate of the rear rooms. Quite similar flow patterns were also observed with South and West wind.

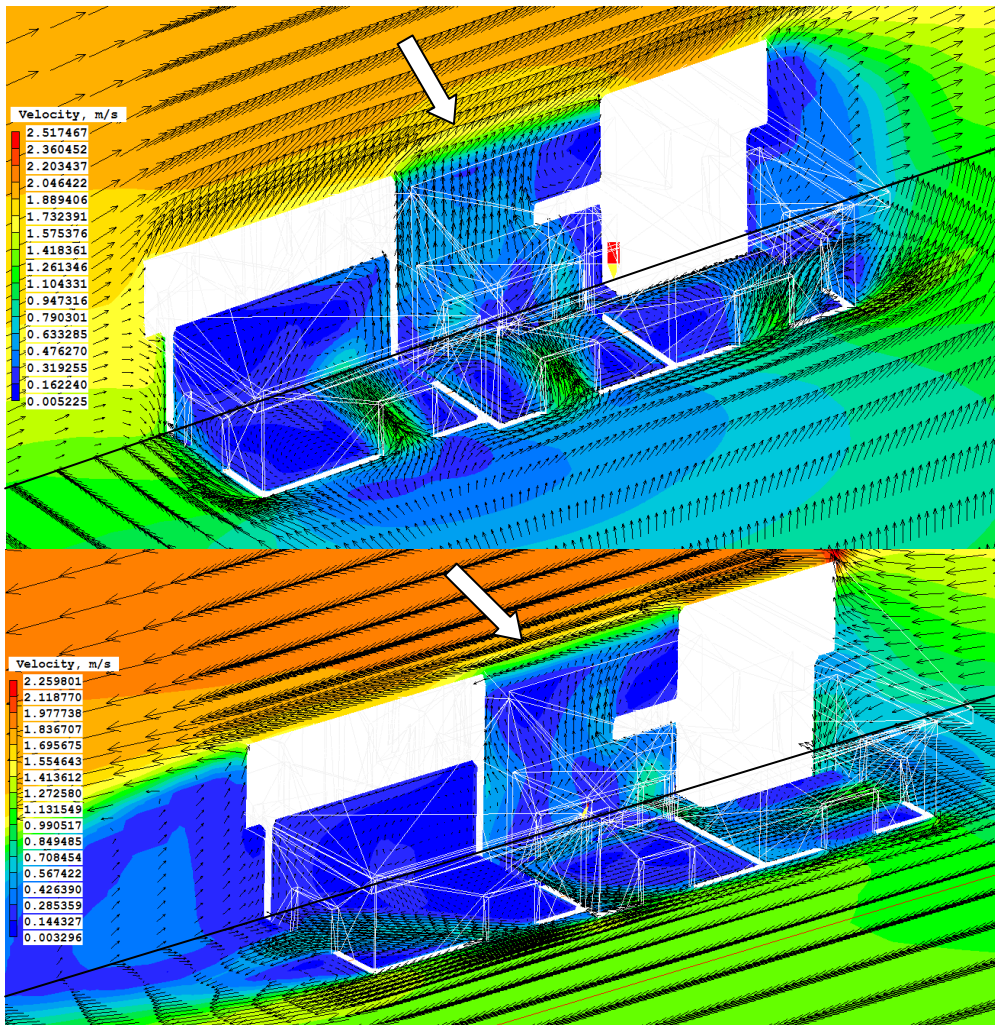


Figure 7-10: Airflow in the courtyard when the wind reaches the house from East (above) and North (below). The velocity field are displayed on both horizontal and vertical plans.

These observations indicate that the courtyard acts as an outlet, generating a suction zone thus promoting cross ventilation. The increase of the airflow in the front rooms is expected to be much higher if the rear rooms are partly or fully closed. When the front rooms are closed, the courtyard may promote ventilation through the rear rooms. The presence of the courtyard therefore provides occupants more choices to control ventilation and airflow in the house.

7.2.2.2 Improving ventilation by a lightwell implemented in the row house

The central rooms of the original row house have seriously suffered from darkness and stuffiness because they do not have any connection with the outdoor environment. A new lightwell of 2.35 m x 3.60 m is inserted into the core of the house. Unlike the case of the detached house where the courtyard is primarily to promote cross ventilation, the row house practically needs a lightwell for better ventilation as well as daylight and sunshine in rooms facing the lightwell. As can be seen from Figure 7-11, the bedroom 2, the toilet, the corridor and ground floor will obtain some benefits from the presence of the lightwell. It was hypothesized that the lightwell enhances cross ventilation, thereby increasing indoor wind velocity and improving thermal comfort. Anyway, it is necessary to note that a bedroom of the house must be sacrificed for the presence of the lightwell.

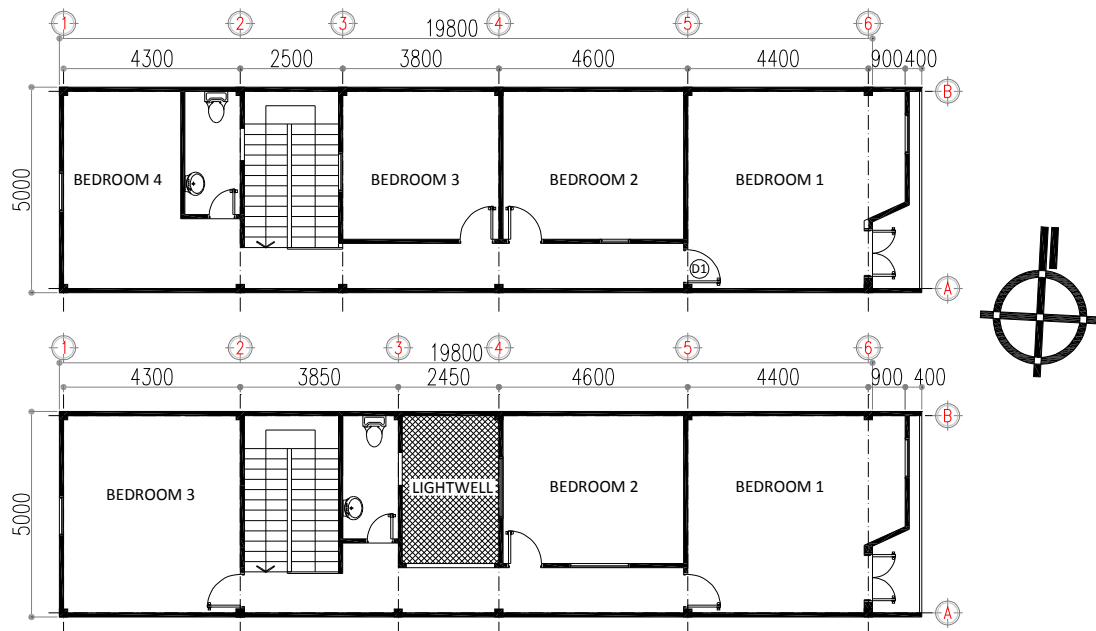


Figure 7-11: Second floor plan before (above) and after implementing the lightwell (below) in the row house. CFD results will show the cross sections and first floor plans.

The CFD domain was remained unchanged (160 m x 160 m x 40 m). The CFD boundary conditions and numerical schemes of the detached house were reused, except that the grid was slightly adjusted (140 x 76 x 50 grid cells) to suit the new building model. Figure 7-12 shows the CFD domain, the building model and part of the grid setting. In the CFD model, the adjacent, rear and frontal houses of the row house was included to partially imitate the actual background. Thickness of all internal walls was assumed 200 mm (instead of 100 mm) to reduce CFD mesh density and consequently simulation time. In all cases, the toilets were closed and the CFD code considers them as blockages. Doors and windows were assumed open.

As the house is nearly symmetrical through East-West axis, five wind directions were investigated, including East, South-East, South, South-West, and West wind. These wind directions were chosen as they cover almost cool summer breezes in Vietnam. In reality, ten successful runs were finished after many trail runs. Minimum time required for convergence is approximately 6 h.

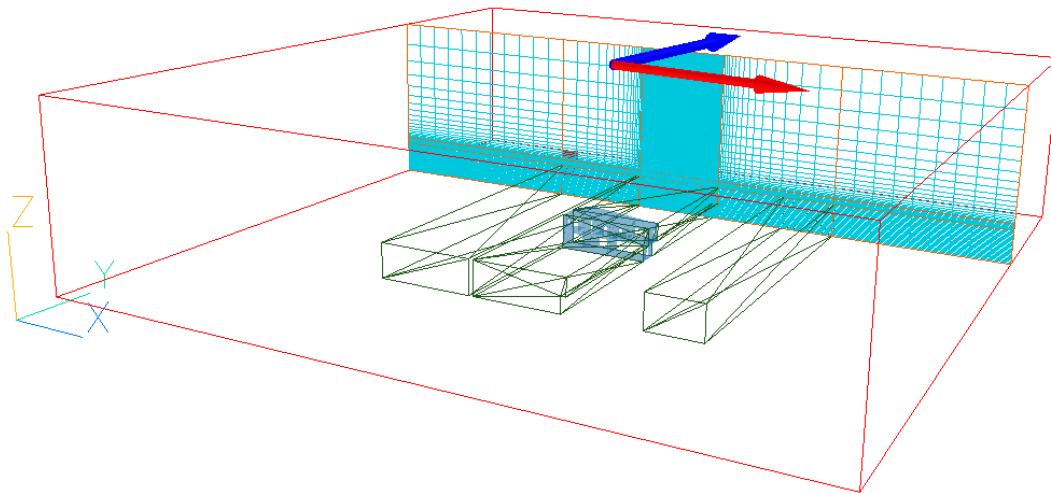


Figure 7-12: The CFD domain and X-Z plane grid solution of the row house and adjacent blocks. The row house is in the center. Red and blue arrows indicate the wind direction and true North, respectively.

To examine the airflow in the house before and after implementing the lightwell, the wind velocity along the longitudinal section of the house was analyzed. Figure 7-13 shows time average wind velocity along the central longitudinal sections of the house without and with the lightwell. All five wind directions were presented. The color contour indicates the magnitude of velocity – from 0 m/s to 0.5 m/s.

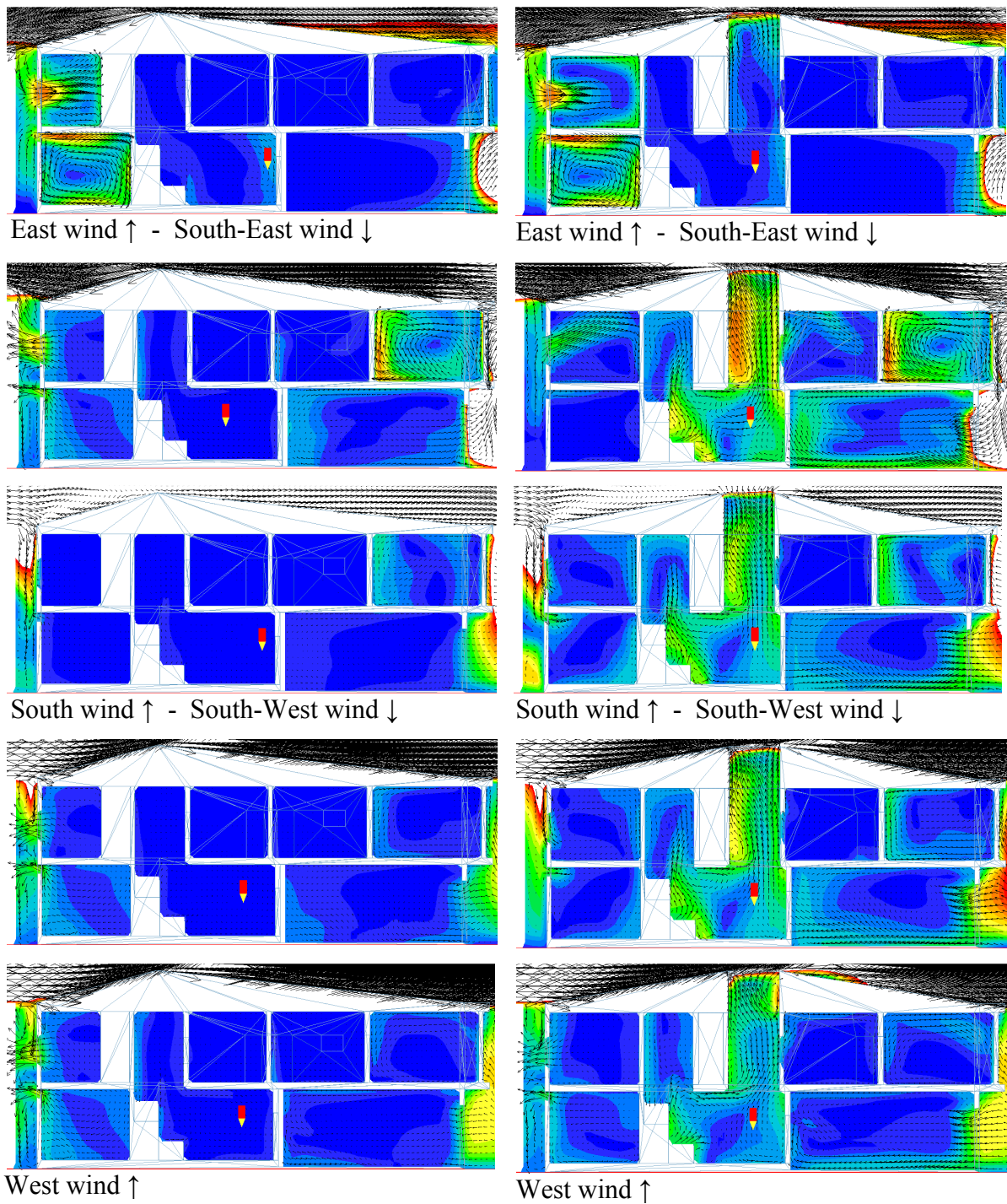


Figure 7-13: Central cross section of the house with the lightwell (right) and without the lightwell (left). Velocity range from 0 to 0.5 m/s (from dark blue to red)

The wind conditions in the house were improved by the presence of the lightwell. However, the improvements varied depending on the wind directions. Greatest improvement was observed when the wind reached the house from South-East while the

East wind only generated a slight improvement. Maximum velocity mostly occurred in the lightwell while wind in the room facing courtyard was almost still.

A clear observation is that indoor wind velocity is much smaller than outdoor counterpart, even if the lightwell was added. Average indoor wind could only reach 0.25 m/s while outdoor reference wind speed was 1.85 m/s. Absolute maximum indoor wind velocity was 0.72 m/s, observed at the door connecting the bedroom 1 and the corridor. It is obvious that wind velocity of around 0.25 m/s does not offer considerable bodily cooling. However, slight improvement of velocity strongly affects the air flow rate and thus IAQ.

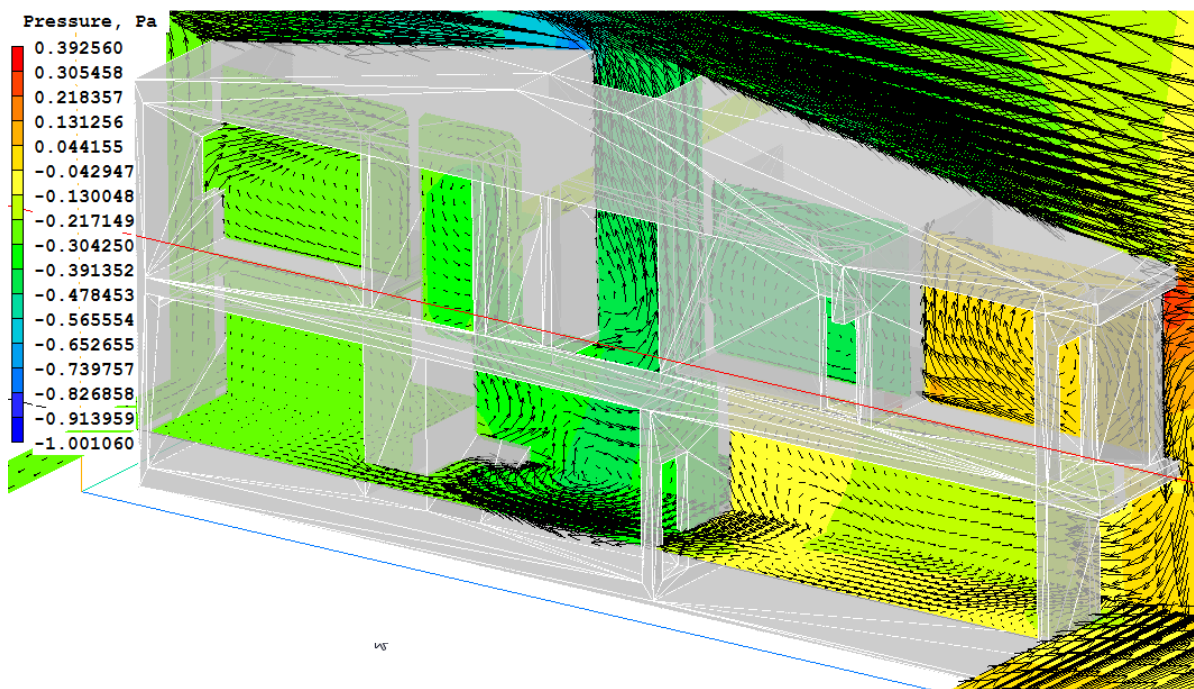


Figure 7-14: Detailed airflow and static pressure distribution in the house and lightwell (Side walls of the house are removed for internal view) - South-East wind

To explain the role of the lightwell, the airflow in the house and distribution of static pressure was examined in detail as shown in Figure 7-14. It can be seen that a low pressure zone was established on the top of the lightwell, creating a strong upward airflow. Consequently, the lightwell functioned as an outlet opening, expelling the air from the house. It is stated that with low pitched roof and flat roof, the negative pressure on the entire roof area always exists (Legacy Resources Management Program, 1990). This negative pressure maintains a suction force on the top of the lightwell, expelling the air from it. Similar airflow patterns in the lightwell were also observed with other wind directions. This

outflow will become more useful if indoor air is heated and blown up into the lightwell by the buoyancy force.

There are two possible reasons that caused small indoor velocity. Firstly, the pressure difference in the best case (South-East wind) between front openings and the lightwell was small, around 0.5 Pa. It is because the row house is surrounded by adjacent houses, it is therefore dipped into a shadow region of the wind generated by surrounding houses, significantly reducing wind dynamic pressure. Secondly, the zigzag indoor airflow caused by the arrangement of openings generates much wind turbulence. The turbulence rapidly dissipates wind kinetic energy and converts it into internal energy (e.g. heat) thereby reducing wind velocity (Kobayashi, et al., 2007; Nguyen & Reiter, 2011a). This lost of kinetic energy is not reversible.

In brief, the CFD analysis clearly indicated that the row house in the present form suffered from very poor ventilation, compared with the detached house. The implementation of a lightwell considerably improves the IAQ and ventilation flow rate, but bodily cooling was nearly impossible as indoor wind speed was not sufficient. In any case, the presence of lightwell in such housing type is, however, essential for not only better ventilation but also good natural lighting and sunshine.

7.2.2.3 Improving ventilation for the apartment by changing window configurations

As discussed in section 5.2.3, the monitoring data indicated that the apartment was fairly well ventilated. As a proof, Figure 7-15 shows the average ACH in two bedrooms of the apartment during a typical year in Danang. Means ACH of both bedrooms were mostly above 1 and frequently exceed 2. Means ACH through a year of the bedroom 1 and 2 are 1.86 and 1.36, respectively. These flow rates were based on an assumption that all windows and doors (including internal doors) were kept open. These conditions allowed the wind to flow through many rooms, creating cross ventilation. Nevertheless, in reality these conditions (all doors are opened) are not always true. Internal doors, especially bedroom doors, are usually closed due to privacy reasons and single-sided ventilation therefore becomes the dominant ventilation phenomenon.

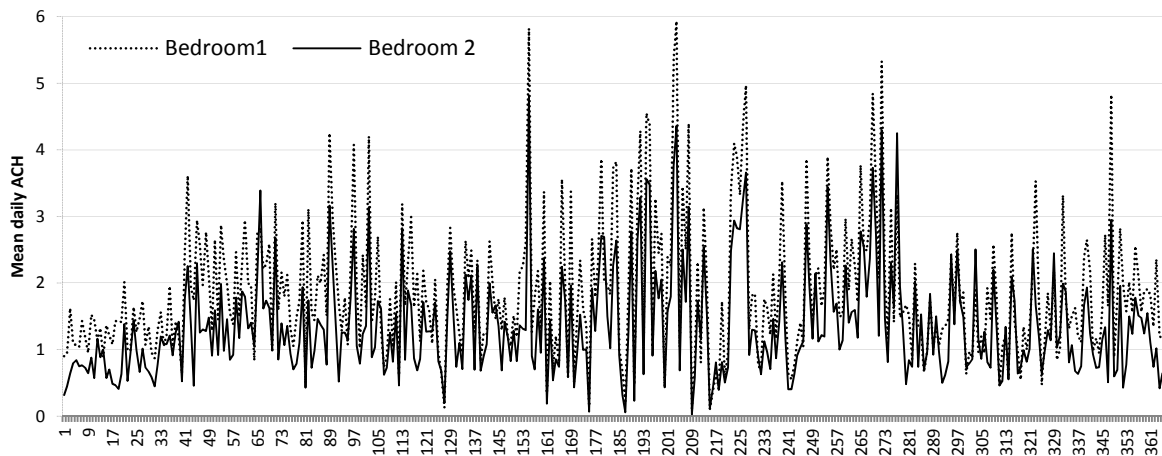


Figure 7-15: Average daily ACH in two bedrooms of the apartment during a year – result given by EnergyPlus airflow network simulation with the calibrated model

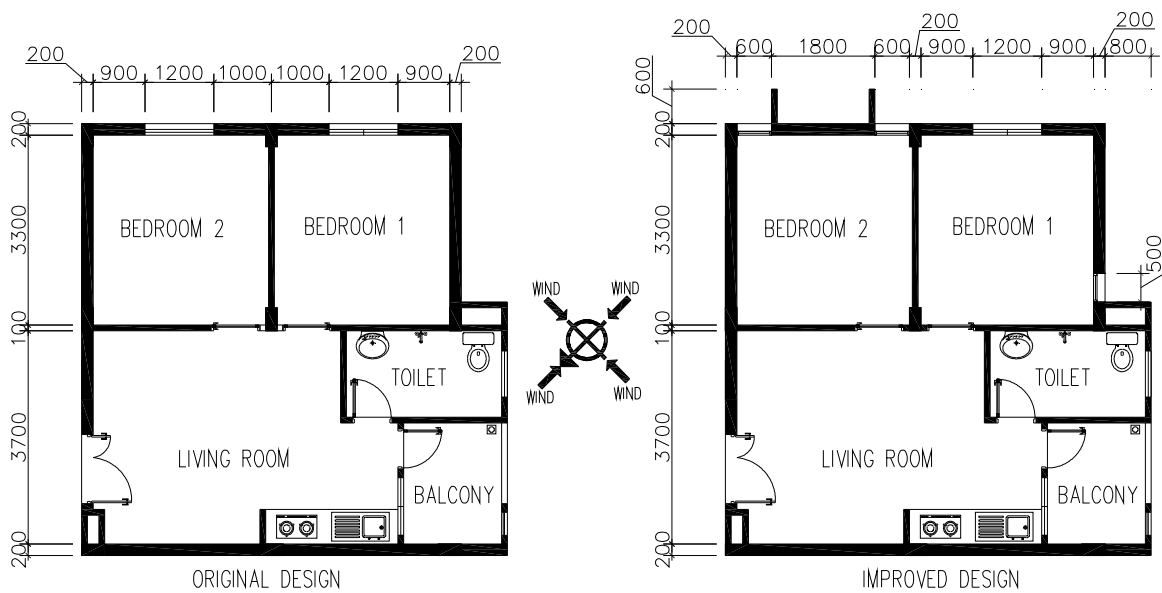


Figure 7-16: Plan of the original apartment (left) and the improved apartment (right). The true North and wind directions in CFD analysis are highlighted in the center

Single-side ventilation often results in poor ventilation rates. But the effect of single-side ventilation can be improved by some modifications on the external windows. The use of wingwalls is such a solution for single-sided ventilation. During 1960s, Givoni (1969; 1994) conducted some wind tunnel experiments on room models with and without wingwalls. His aim was to examine the effect of wingwalls on a single-sided ventilated space. His results indicated that the ventilation flow rate and the mean indoor wind speed

were significantly increased in a single-sided ventilated room incorporated with wingwalls, compared with that without wingwalls.

The present study examines the potential of ventilation improvement of using wingwalls and rearranging external windows of the apartment by the CFD technique. The window configuration of the original apartment was slightly modified as shown in Figure 7-16. In the bedroom 1, a small window of 0.5 m x 1.4 m was added. In bedroom 2, the original window was replaced by 2 separated windows with vertical wingwalls. Each wingwall has the total area of 0.96 m² (0.6 m x 1.6 m). Total opening area of bedroom 2 was kept unchanged. It is worthy of note that new windows are protected from the Sun better than the originals. Doors of the bedrooms are assumed close; thus only the airflow in two bedrooms will be considered (the living room does not have any change).

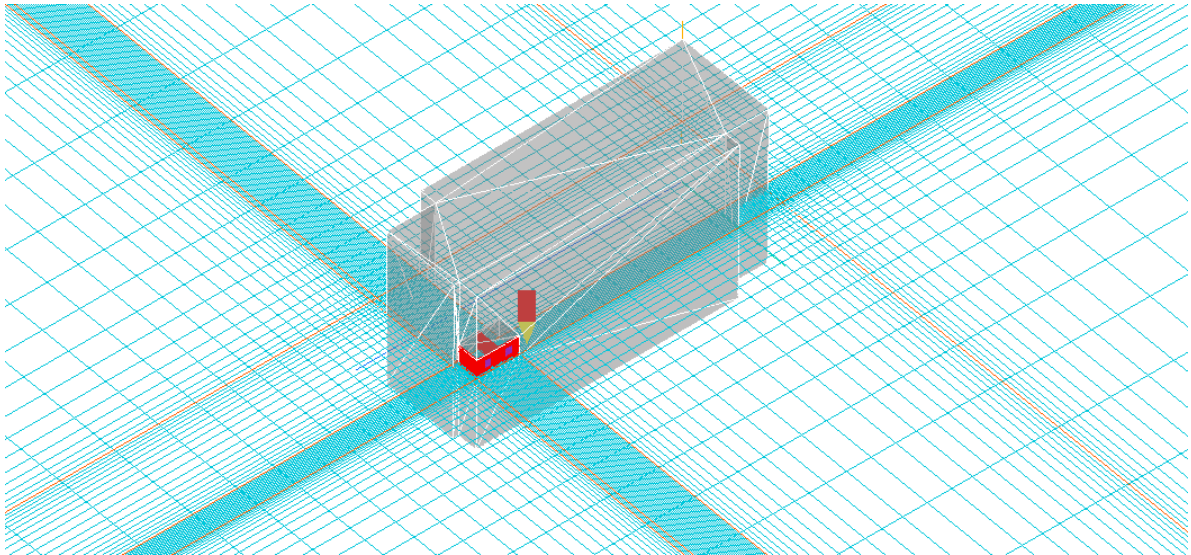


Figure 7-17: The 7-storey building, the apartment on the 4th floor and the grid system in the center of the CFD domain

In the CFD analysis, both the bedrooms and the whole apartment building were modeled. The building model was placed in a CFD domain of 300 m x 300 m x 60 m. Other boundary conditions and numerical schemes of the detached house and row house were reused. To fit the apartment building model into the CFD domain, size of the CFD domain was increased. The domain was discretized into a 3-D structured Cartesian grid system which consists of 103 x 78 x 62 grid cells (498108 cells). Figure 7-17 shows the building model and part of the grid setting. Very dense grid was imposed on the apartment and near

the hard surfaces of the building. As the grid was sophisticated, continuous relaxation control and convergence monitor were required during all simulations.

Four wind directions, including North, East, South and West wind, were tested on the two models of the apartment. The East wind is the dominant wind direction during warm periods in Danang. These wind directions put the apartment onto both windward and leeward sides of the building, thus the effectiveness of wingwalls and cross ventilation in various situations can be evaluated. Convergence of each simulation was reached after about more than 10 hours. Totally, 8 successful simulations were confirmed.

To compare the ventilation performance of different models and cases, both the ventilation flow rate and indoor wind speed were considered. The volumetric flow rate Q can be obtained by several methods. In simple design calculations, the flow rate through a cross-ventilated model was computed by an empirical method based on Bernoulli equation. In this study, Q was calculated by using the definition of Q . In cross-ventilated cases with incompressible fluid ($\rho = constant$), given an opening area A at the inlet, and a fluid flowing through it with uniform velocity U and an angle θ away from the perpendicular direction to A , the flow rate is defined as:

$$Q = UA \cos \theta \quad (7.1)$$

For a non-uniform flow, considering the mean velocity (\bar{U}) in the direction perpendicular to the area A , equation (7.1) becomes:

$$Q = \int_A u dA = \sum_{i=1}^n u_{i,A} A_i = \bar{U} A \quad (7.2)$$

where

A is the area of the windward window;

$u_{i,A}$ indicates the wind velocity through A_i ;

A_i refers to the i^{th} differential of A .

\bar{U} on the window area was computed by composing some short commands in Phoenics. Higher CFD grid resolution on the window area will give a more accurate value. Therefore, Q can easily be calculated with high accuracy.

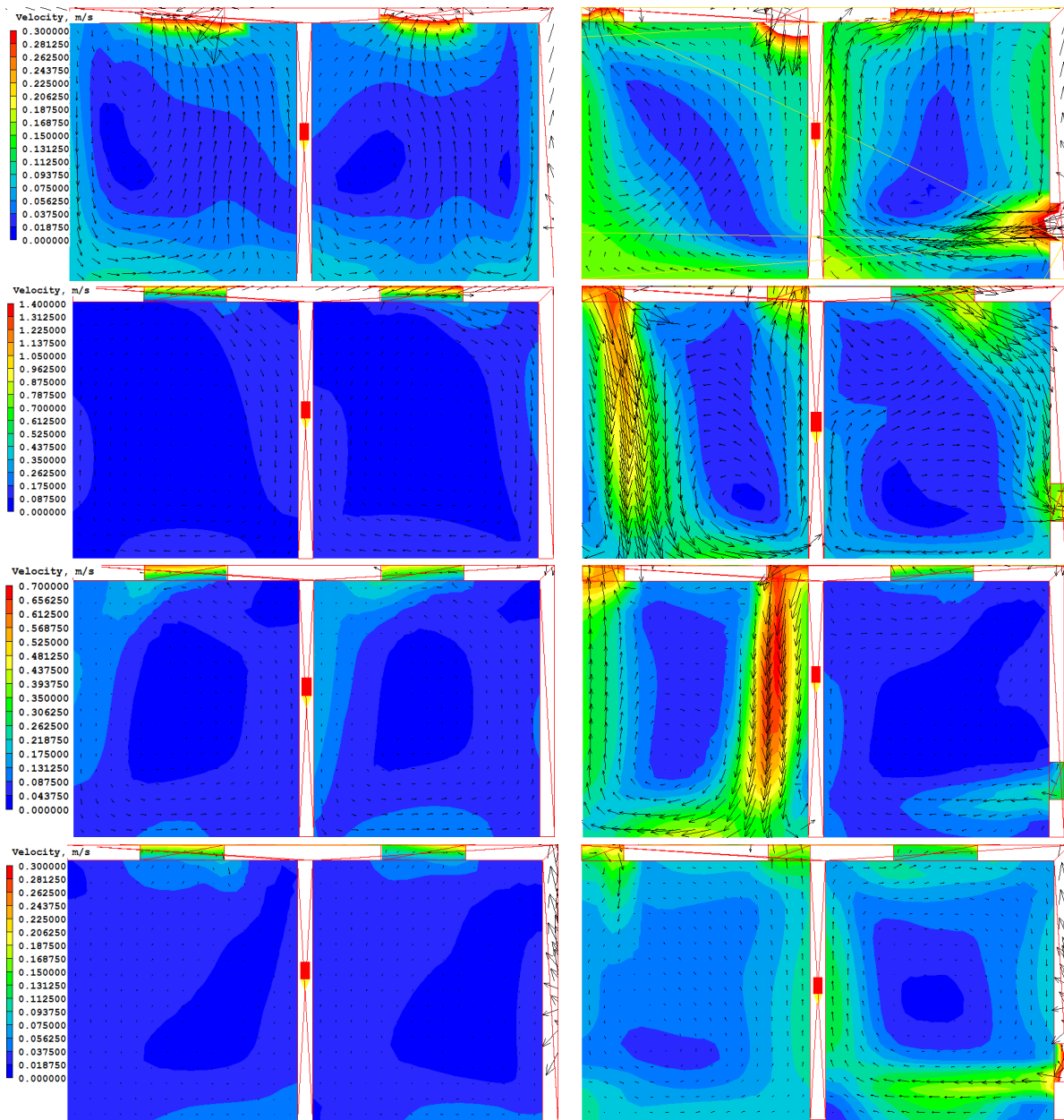


Figure 7-18: Velocity contour on the horizontal plan 1.1 m above the floor in the original apartment (left) and the improved apartment (right). The contour keys are shown on the left. (From top to bottom: North wind, East wind, South wind and West wind, respectively)

The airflows in the bedrooms of the original and improved apartments were compared in Figure 7-18. In most cases, the bedrooms with improved window configuration experienced much higher air velocity. In the improved apartment, the wind condition in the bedroom 2 was better than that of the bedroom 1. The differences were more explicit if the bedrooms were in the windward side (the case of East and South wind). These indicate that the modifications on the windows have a significant effect on natural ventilation. Figure

7-19 explains how the wingwalls and new window configurations promote ventilation. Significant pressure drops between the inlet and the outlet were observed in both two bedrooms. Locating in a special position of the building, the bedroom 1 has two external walls and the openings on these two walls are of course adequate for cross ventilation. The pressure drop on these openings was about 0.85 Pa. Like many other rooms in the building, the location of the bedroom 2 is more disadvantage because only one external wall is available for ventilation. The implementation of the wingwalls increased the pressure drop between openings to around 1.7 Pa; thereby strongly driving the wind in and out the room. The wingwall is, therefore, very effective in single-sided ventilation.

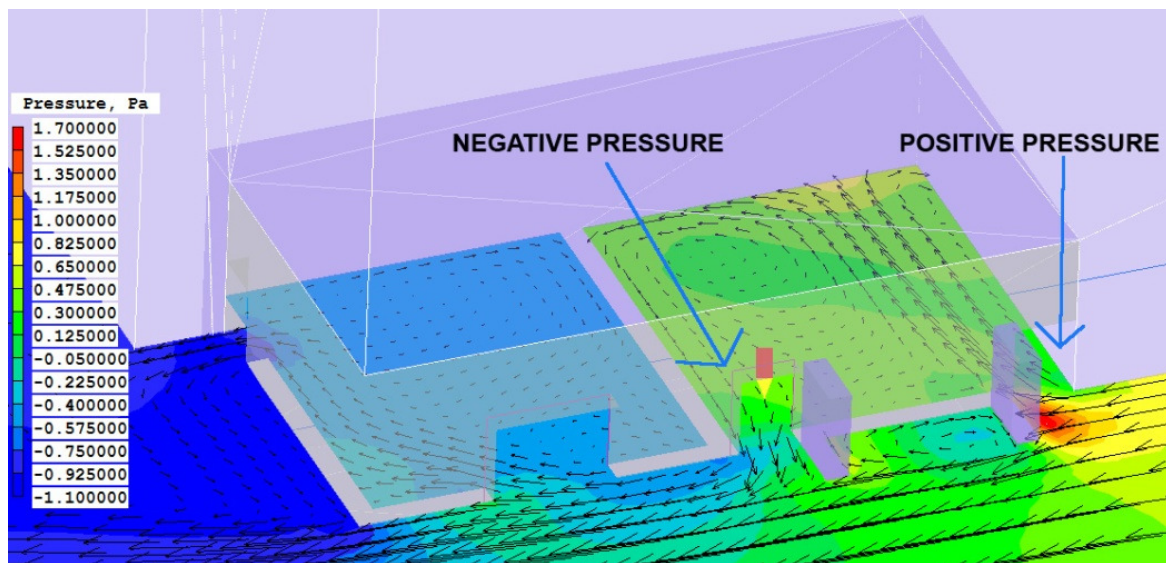


Figure 7-19: Static pressure distribution around the openings of the improved apartment in the case of East wind

The ventilation performance of the improved design is quantitatively compared with that of the original design. The mean indoor air velocity and the ventilation rate are considered. The performances are listed in Table 7-8 and then are compared in Figure 7-20.

Table 7-8: Mean air velocity and ventilation flow rate in the bedrooms

		North wind		East wind		South wind		West wind	
		V_a^*	Q^{**}	V_a	Q	V_a	Q	V_a	Q
Original apartment	Bedroom 1	0.05	0.015	0.09	0.023	0.07	0.026	0.02	0.017
	Bedroom 2	0.05	0.017	0.07	0.020	0.06	0.014	0.02	0.019
Improved apartment	Bedroom 1	0.08	0.32	0.26	1.15	0.05	0.13	0.07	0.11
	Bedroom 2	0.08	0.11	0.40	0.81	0.24	0.50	0.06	0.11

* V_a is mean air velocity on the horizontal plan 1.1 m above the floor, m/s

** Q is ventilation flow rate through the openings, m^3/s

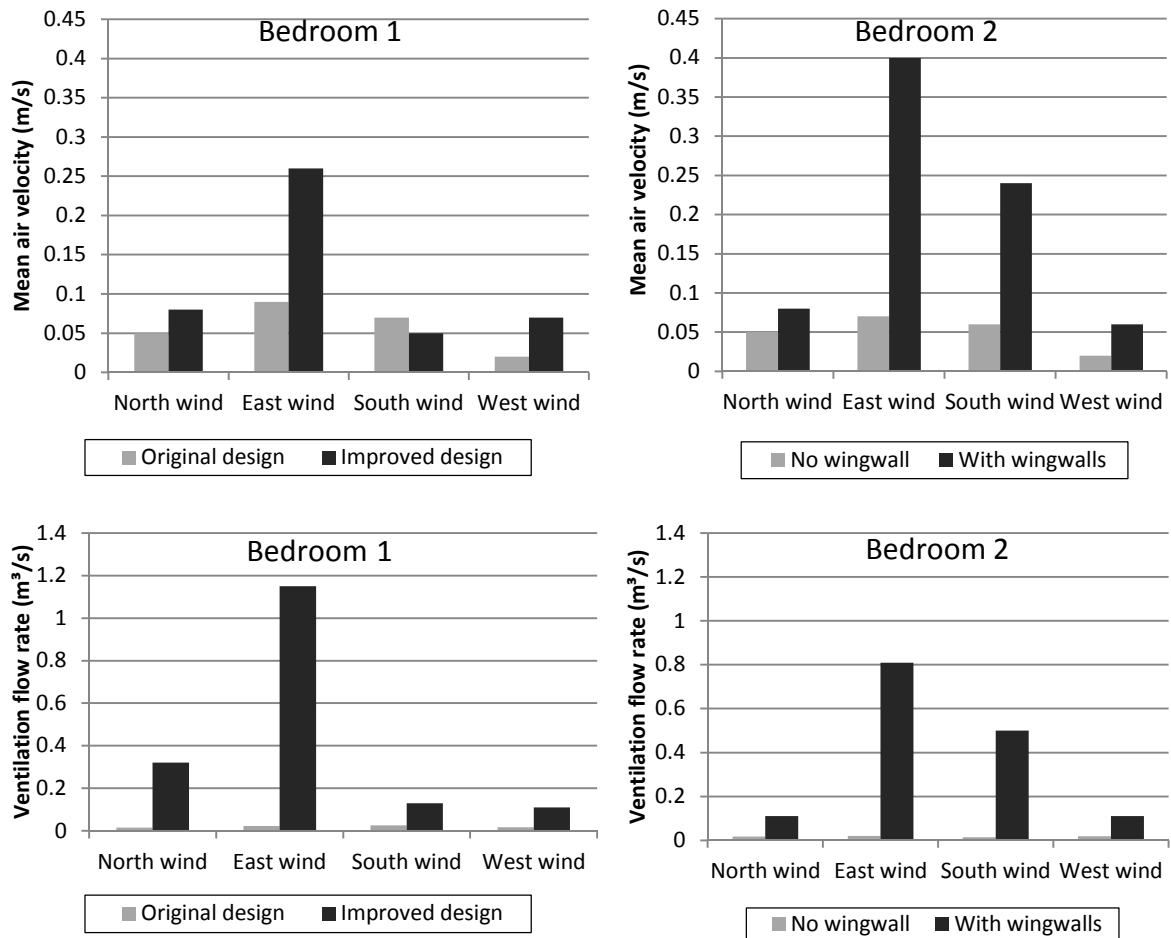


Figure 7-20: Comparison of mean air velocity (of 56 points on the working plan - 1.1 m above the floor) and ventilation flow rates in the original bedrooms and the improved bedrooms

As can be seen, the improved apartment performed much better than the original in both ventilation rates and air velocity. The air velocity and ventilation rates in the original apartment were very low and rather stable, regardless of the wind direction. In contrast in the improved apartment, the mean air velocity was increased up to 5.7 times (bedroom 2, East wind) while the ventilation rate can be 50 times higher (bedroom 1, East wind). However, the significance of improvement strongly depends on the direction of wind. When the wind reaches the apartment from the rear sides (North or West wind), the increases of wind speed in all bedrooms are not significant enough to give any bodily cooling effect; but the increases of ventilation rates are still very considerable. Hence, it is relevant to conclude that the effect of window arrangement and wingwalls always exists, regardless of the direction of wind.

The increase of ventilation rates refers to much better IAQ. The increase of air velocity may contribute to direct bodily cooling and in some cases can be perceived by the occupants if air velocity is above 0.15 m/s. Maximum indoor wind speed (about 1.1 m/s) was observed in the case of East wind, near the inlet window of the bedroom 2. According to ISO 7730 (ISO, 2005), the maximum cooling effect of this increased wind speed is equal to 3°C increase of operative temperature. Also in the case of East wind, the average wind speed in the bedroom 2 may provide an average cooling effect of 1°C, compared with a still air condition. In summary, the improved window configurations are capable to enhance ventilation and thereby occupants' thermal comfort and satisfaction.

7.3 Auxiliary strategies to improve building thermal performance

In practice, there are some less common climate responsive strategies for passive heating and cooling purposes through which thermal comfort can be improved. These strategies usually require complex systems and installation which have considerably limited their popularity. This thesis therefore describes these strategies in brief.

7.3.1 Climate responsive heating techniques

The most common passive heating technique is to take advantage of the low solar angle in winter and the greenhouse effect to warm equator-facing spaces up. During summer periods when the Sun angle is usually high, the equator-facing façades are shaded by proper shading devices (see Figure 7-21). This method is rather common in temperate climates in Northern hemisphere. However, at low latitudes, this technique is rarely applied due to some constraints: the solar angle is still high in winter; strong diffused solar radiation may penetrate into the building through glazing façades, even if they are well protected from direct solar radiation. In Hanoi, a space of 100 m² with a 10 m² South-facing window is able to maintain indoor temperature at 22.3°C constantly when outdoor temperature is 17.4°C (Nguyen & Reiter, 2012a).

A Trombe wall system is another effective passive heating technique. It is a massive sun-facing wall, separated from the outdoor air by a single or double layer of glass and an air gap (see Figure 7-21). The wall is usually painted with dark colors to maximize its solar absorptance. This system absorbs and accumulates solar energy and gradually delivers it towards the interior. Thanks to the glass layer, the heat absorbed in the wall does not lose to

the outdoors. The air gap can be ventilated in different ways in summer and winter so as to drive the hot air mass to the interior/exterior. Trombe walls must be shaded in summer periods to prevent overheating. A well-designed Trombe wall may provide 20% of the total annual heating demand of a building in temperate climates (Torcellini & Pless, 2004).

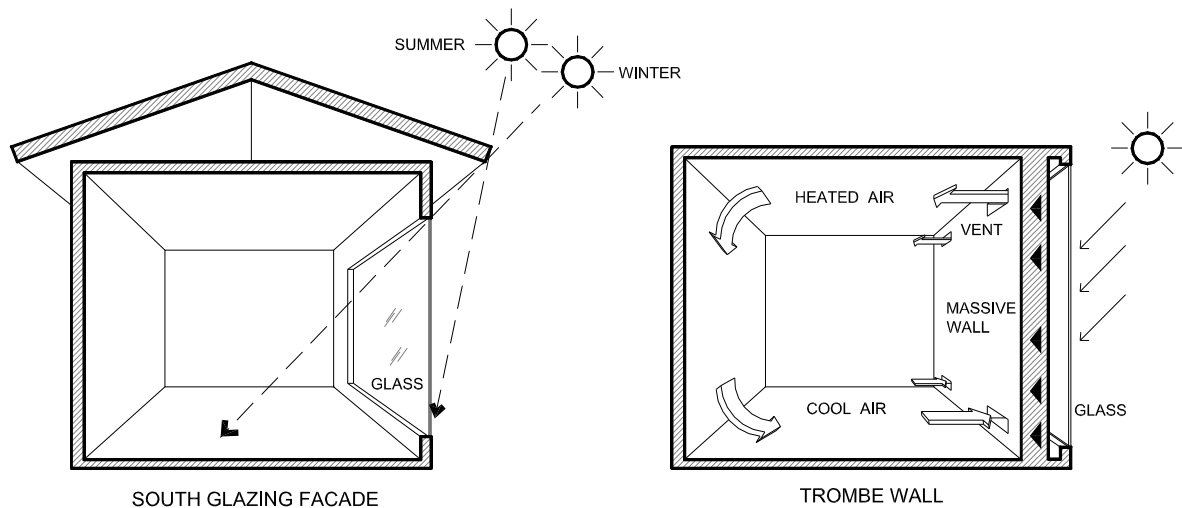


Figure 7-21: Examples of an equator-facing façade and Trombe wall

Some other strategies such as sun space, using wall color, double-skin façades... can be used to increase the solar heat received by the building.

7.3.2 Climate responsive cooling techniques

In hot climates, the major heat flux often penetrates through the roof. Keeping the roof cool and stable is crucial. Instead of using thermal insulation, green roof or roof pond or roof spray systems can be used for this purpose.

Green roof can be seen as a roof which covers by vegetation, planting on a number of soil layers. To bear the load and water pressure from the soil as well as the vegetation, the roof is often supported by a waterproofing hard structure such as a concrete slab. A green roof can play many roles simultaneously, such as providing thermal resistance and thermal mass effects, absorbing rainwater, lowering ambient temperature by evaporation and photosynthesis, creating natural shelter for insects. In hot humid climates, roof gardens have significant cooling effects with a reduction of about 10° to 30°C of roof surface temperature, depending on the roof types, vegetation types and settings, and the weather (Wong, et al., 2007). A simple form of the green roof was successfully applied in vernacular architecture in Vietnam in which the roof of vernacular houses was generally made from

thick and damped fired roof tiles which facilitate the growth of the wild grass (see Figure 6-3, houses C, D, F). Such damp roofs with wild grass can significantly reduce the roof surface temperature. A vegetation screen on building façades and openings can play the role of shading devices, keeping the building envelope cool.

A roof pond system consists of a pond of water on a roof structure, using to remove the sensible heat of the roof by evaporative cooling. A movable layer of insulation floating on the water surface is often used to shield the water mass from solar radiation during day time. Common problems of a roof pond are the heavy load on the roof and risk of water leakage to the layers beneath. The operation of the top cover is also troublesome. This solution is therefore not really attractive. A roof spray system combines a low-energy water pump and spray heads to cool the roof based on the passive cooling effect of water evaporation. Roof spray systems can operate in both day time and nighttime. These systems are presented in Figure 7-22.

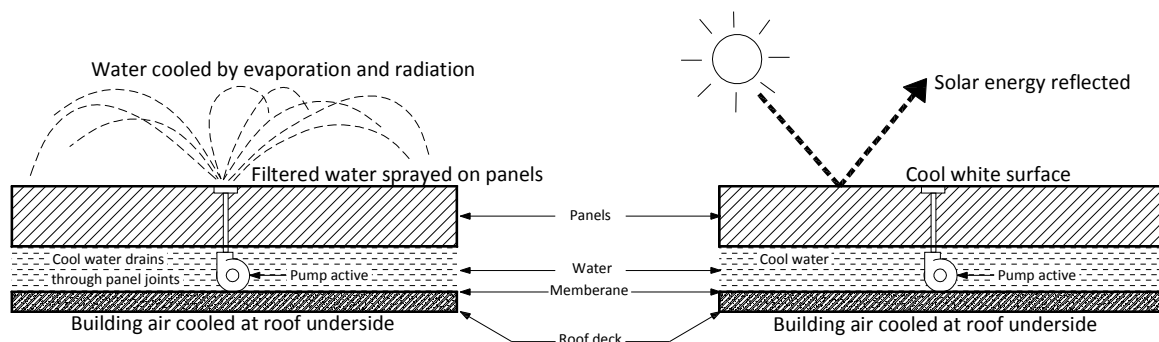


Figure 7-22: Roof spray and roof pond in nighttime and daytime, respectively – adapted from (Givoni, 1994)

As stated in (Tiwari, et al., 1982), experimental results has shown that by using a roof spray system, a drop of 27°C of peak roof temperature was observed, compared to a reduction of 23°C in the case of the roof pond. Surface temperature of the beneath ceiling was observed to follow a drop of 15°C and 13°C in the cases of roof spray and roof pond, respectively. Indoor air temperature has benefited a drop of 3.5°C and of 3°C in these cases.

Some other cooling techniques can be found in the literature such as radiant cooling (e.g. by high-mass roofs with openable insulation), ventilation cooling by earth tubes, cooling by the earth heat sink...However, they are sometimes not completely passive and their applications are rather limited.

7.4 Chapter conclusion

This chapter looks for the climate responsive design strategies to improve thermal performance and natural ventilation of the case-study houses. Potential solutions were discussed and derived from the analysis by both qualitative and quantitative assessment. The parametric simulation method has been used as the major measure to evaluate the effect of each solution on thermal performance of the houses. EnergyPlus and Phoenics programs were used for the thermal dynamics simulations and CFD simulations.

The results of the thermal simulation have shown that the parametric simulation method could reduce uncomfortable periods in NV houses by nearly a half (about 44.9%). Thermal performance of 5/9 improved houses was classified as “good”. Through the results of the thermal simulation, this study derived the best climate responsive design solutions for each climatic region. The design parameters of these solutions were presented in Table 7-4. The effects of each parameter on the thermal performance of the houses were outlined. As the relationship between these design parameters and the performance is non-linear, it is not easy to combine them to produce an optimal performance of the houses.

This chapter has briefly reviewed the passive cooling methods by natural ventilation. The case-study houses were used to demonstrate the effects of three improved design solutions, namely the courtyard, the lightwell and the wingwalls, on natural ventilation. Under a stable wind boundary condition, the results of the CFD simulation have quantitatively shown the considerable improvement in the indoor wind velocity and the ventilation flow rate and thereby comfort improvement. However, it is still very difficult to evaluate the long-term effect of these improved designs on ventilation and the thermal performance of the houses by coupling the present CFD technique with the building thermal simulation due to very time-consuming CFD simulations.

Some less common climate responsive strategies and their efficiency were also discussed qualitatively. These strategies and the previously discussed solutions have provided a broad and complete overview on climate responsive design in hot and humid climates.

CHAPTER 8

COMBINATION OF DESIGN STRATEGIES TO OPTIMIZE THERMAL COMFORT

This chapter describes a procedure through which the design objectives (thermal comfort, building energy consumption) are optimized using a two-step simulation-based optimization method. The name of the method itself indicates that the procedure will be conducted through two phases, namely (i) sensitivity analysis and (ii) optimization. Subsequent sections will discuss these two issues in detail.

8.1 Monte Carlo-based sensitivity analysis

8.1.1 A brief introduction of sensitivity analysis

Sensitivity is a generic concept. The term ‘sensitivity analysis’ (SA) has been variously defined by different communities due to the differences in methods used, problem settings, aims and demands. Until recently, SA has been conceived and defined as a local measure of the effect of a given input on the output (Saltelli, et al., 2004). If a change of an input parameter X produces a change in the output parameter Y and these changes can be measured, then we can determine the sensitivity of Y with respect to X (Lam & Hui, 1996). This measure of sensitivity can be obtained by the calculation via a direct or an indirect approach, system derivatives such as $S_{X_j} = \partial Y / \partial X_j$, where Y is the output of interest and X_j is the input factor (Saltelli, et al., 2004).

In building research using the simulation-based approach, the SA is often quantified by the difference in simulated results caused by the changes of input parameters. A SA provides designers a robust tool to quantify the effect of various design parameters and to identify sources of uncertainties. Lam and Hui (1996) performed an intensive study on the effects of various design parameters on building energy consumption. They used a simple

'local' sensitivity test and the simulation tool DOE-2 to examine an office model in Hong Kong. As the variation of each design parameter was considered separately, their study could not quantify the complex interactions between design factors. The results were therefore somewhat unconvincing. Heiselberg et al. (2009, p. 2036) used the Morris's method (Morris, 1991) - a local sensitivity method - to perform a SA for an office building in Denmark to measure the influence of design parameters on total building energy demand. They concluded that *"a SA in the early stages of the design process can give important information about which design parameters to focus on in the next phases of the design"* and *"improve the efficiency of the design process and be very useful in an optimization of building performance"*. Hopfe and Hensen (2011) performed an uncertainty analysis and SA of building annual cooling and heating demands on three groups of input parameters, including: physical parameters, design parameters and scenario parameters. The perturbation of input parameters was generated by the Latin hypercube sampling method and the Standardized Rank Regression Coefficient (SRRC) was used as a quantitative measure of sensitivity. This study revealed that the infiltration rate and the room geometry were among the most sensitive parameters of the model. Through SA, Eisenhower et al. (2011, p. 2785) found that *"the most sensitive parameters of the model relate to building operation (i.e. scheduling), and also find that a low energy building design is more robust to parameter variations than the conventional design"*.

The above mentioned studies show a preliminary insight of the importance and applications of SA among building research communities. In this thesis, the technique of SA was employed to assess the significance of various design parameters in the outputs of EnergyPlus program. The result of SA will be then applied in the subsequent steps – the optimization - of this research.

The philosophy of SA is that if we understand the relationships and the relative importance of design parameters on the building performance, we can easily improve the building performance by selecting appropriate design parameters. In BPS, the SA is used for a range of purposes and may provide some benefits as follows (Pannell, 1997):

- To quantify the sensitivity of the results of a simulation tool in the presence of uncertainty of input factors. In other word, the significance of each input is qualitatively and quantitatively measured. By varying an input and examining its

effect on the outcome of a model, a SA provides a “what-if analysis” (decision support).

- To explore the relationships between the inputs and outputs of a building model through a simulation tool.
- To reduce the uncertainty in the simulation outputs by setting the significant inputs with care. Consequently, this helps to simplify settings of the model by ignoring inputs that have no or small effects on the outputs.
- To detect errors in the model by detecting unexpected outputs in the relationships with inputs (quality assurance).
- To support an optimization by looking for regions in the space of input factors where the simulation output is maximum (or minimum).

8.1.2 Methodologies of sensitivity analysis

There are a number of approaches used in SA which can be distinguished by their methods, purposes, sensitivity indices... However, a typical procedure of SA follows a few standard steps as outlined below (Saltelli, et al., 2004):

- Step 1: Defining the goal of the analysis and then the form of the output function that is of major concern for the analysis.
- Step 2: Deciding which input factors have to be included in the analysis.
- Step 3: Estimating the uncertainty of each input by assigning a range and its probability density function (e.g. uniform, normal, log-normal...).
- Step 4: Choosing a SA method on the basis of: the natures of the problem at hand, the number of model evaluations and model execution time, the presence of a correlation structure between inputs factors.
- Step 5: Generating an input sample which includes N input vectors. The sampling method must follow the method chosen for the SA.
- Step 6: Running the model on N input vectors of the input sample to produce N corresponding outputs.
- Step 7: Analyzing the model inputs and outputs to draw conclusions using the method chosen in step 4.

Sometimes, this procedure may be repeated many times (e.g. in high-dimensional problems where unimportant input factors must be screened out before performing a full

SA). In most cases, the selection of a SA method in step 4 is crucial to the success of the analysis. The methods for SA are therefore the core problem in SA research. There are a large number of SA methods and they may be classified in some different ways. Hamby (1994) provided a comprehensive review on SA methods according to which SA methods could be addressed in three groups:

- Those that evaluate the output on one variable at a time (contains 6 methods);
- Those that are based on the generation of sample of input vectors and an associated outputs (contains 10 methods);
- Those that perform a partitioning of a particular input vector based on the resulting output vector (contains 4 methods).

Similarly in another study (Heiselberg, et al., 2009), the SA was grouped into three classes: *'local' sensitivity methods*, *global sensitivity methods*, and *screening methods*. 'Local' sensitivity methods are also often based on an one-parameter-at-a-time (OAT) approach in which the variation of the model outputs is considered under the variation of one design parameter, while all other design parameters are held constant (Heiselberg, et al., 2009). The global sensitivity approach is referred to a number of SA methods where the sensitivity of an input factor is evaluated by varying all other input factors as well. This approach is usually done by generating a large number of input vectors and model evaluations. The screening method is a particular variance of the sampling-based method with an aim of reducing computational cost in high-dimensionality models. In this method, the impact of changing the value of each input factor is evaluated in turn and the sensitivity index is evaluated by the averages of the partial derivatives at different points in the input space. The method of Morris (1991) is one of the most commonly used screening methods.

According to Frey et al. (2003), the SA methods may be broadly categorized into 3 groups. This work briefly represents these 3 groups in very short descriptions as follows:

- "Mathematical approach" typically involves calculating the output for a few values of an input within the possible range. It basically consists of the Nominal Range Sensitivity Analysis Method, the Differential Sensitivity Analysis, the method of Morris, most of the methods using the OAT approach...
- "Statistical (or probabilistic) approach" involves running of a large number of model evaluations on an input sample which is usually generated randomly.

Depending upon the method, one or more inputs are varied at a time. Statistical methods allow one to quantify the effect of simultaneous interactions among multiple inputs (Frey, et al., 2003). The statistical approach includes: the linear Regression Analysis (RA), the analysis of variance (ANOVA), the Response Surface Method (RSM), the Fourier Amplitude Sensitivity Test (FAST), the Mutual Information Index (MII), Sobol's method, methods using statistical indices: PEAR, SPEAR, SRC, Standardized rank regression coefficient...

- "Graphical assessment" gives a qualitative measure of sensitivity using graphs, charts, or surfaces of pairs of inputs – corresponding outputs. It can be used to strengthen the results of other quantitative methods for better interpretation. The most common forms of "graphical assessment" are the Scatter Plot and the Regression Analysis.

8.1.3 The selected approach of SA for the present study

As mentioned earlier, the choice of SA methods basically depends on the natures of the problem at hand. In this work we explore three EnergyPlus thermal models of three housing types; hence the present problem is related to simulation outputs of these thermal models.

In BPS, the natures of simulated outputs are typically multi-modal, non-linear (Wetter & Polak, 2004), computational expensive; and they are the result of simultaneous coupled interactions among multiple inputs. The sensitivity of such a problem should not be measured by linear coefficients of correlation (useful for strong linear problems). Furthermore, a 'local' SA may omit the simultaneous interactions among input factors, thus it may distort the sensitivity measure of input factors. Based upon these points, this work decided to perform global SAs which are based on the Monte Carlo method. This global SA approach is also referred to as the "Monte Carlo-based method". A Monte Carlo-based SA provides statistical answers to problems by running multiple model evaluations with probabilistically generated model inputs, and then the results of these evaluations are used to determine the sensitivity indices (Joint Research Centre - European Commission, 2008). The Monte Carlo-based SA used in this chapter consists of 4 major steps as follows:

- Identifying which simulation inputs should be included in the SA and what are the probability distribution functions of these variables.

- Generating a sample of N input vectors for the simulation model (EnergyPlus thermal models) by a probability *sampling method*.
- Run the simulation model N times on the input sample to produce N associated outputs.
- Calculating the *sensitivity indices* for each input, ranking them and drawing necessary conclusions.

At present, there are a number of *sampling methods*. The Latin Hypercube Sampling (LHS) method was selected for all sample generations. The LHS is a form of stratified sampling that can be used for multiple input factors. This sampling method is used so as to reduce the number of model evaluations necessary for a Monte Carlo analysis. The LHS method has been widely used in different engineering researches with both simple and very complicated computational models (Novák, et al., 1998). A short description of the LHS method in building SA can be found in (Kotek, et al., 2007). It is generally agreed that the LHS performs better than the random sampling method and is able to achieve a better coverage of the sample space of the input factors (Joint Research Centre - European Commission, 2008).

In SimLab, there are some highly reliable indices for measuring sensitivity of a non-linear and non-monotonic system, including those obtained by Sobol's method and the FAST method (see SimLab manual for details of their algorithms). However these methods require a very large number of model evaluations that tends to be inappropriate due to time-consuming EnergyPlus simulations. For example, for a system with 29 input variables, at least 960 simulations are needed for calculating Sobol's sensitivity index. The Morris method, on the other hand, needs quite few numbers of simulations, but it can only give a qualitative estimation of variable sensitivity, and it cannot distinguish the non-linearity of an input variable from the interaction with other variables (Yang, 2011). According to these obstacles, the author decided to use regression-based sensitivity indices which require a reasonable number of simulations.

The first sensitivity index used in this study was the *Partial Correlation Coefficient* (PCC). The PCC reveals the strength of the correlation between an output Y and an associated input vector X_j which was cleaned off any effect due to the correlation between the vector X_j and other input vectors. In other words, the PCCs provide a measure of a

variable importance that tends to exclude the effects of other variables (Joint Research Centre - European Commission, 2008). The PCC performs fairly well even if there are strong correlations among input variables.

The second index of variable sensitivity was the *Standardized Rank Regression Coefficients* (SRRC). The SRRC is based on regression analysis, but is improved by applying the *rank transformation* of the input and output values (i.e. replacing these values with their ranks). The SRRC can provide satisfactory prediction even if: (i) the input variables are uncorrelated, and (ii) the relationships between input variables and corresponding outputs are non-linear and monotonic. Nevertheless in the presence of strong non-monotonicity (usually occurs with low influential variables), the rank given by the SRRC may become dubious or sometimes misleading. The PCC and SRRC can be obtained by using some simple calculations. The reader may refer to SimLab manual for further details.

In Monte Carlo-based SA, most sensitivity indices are subject to uncertainty because they are calculated based on a limited sample of input vectors. The higher the number of random inputs is, the more reliable sensitivity indices are achieved. The PCC and SRRC tend to supplement each other in measuring sensitivity. Hence, they are expected to provide more explicit, multidimensional evaluations than that given by only one index (e.g. PCC or SRRC alone). More details about the LHS method, the equations for the PCC and SRRC can be found in some references (Hamby, 1994; Frey, et al., 2003; Saltelli, et al., 2004; Joint Research Centre - European Commission, 2008).

In this work, steps 2 (generating an input sample) and 4 (calculating sensitivity indices) of the Monte Carlo-based method were carried out with the support of SimLab – a software package for uncertainty and sensitivity analysis (Joint Research Centre - European Commission, 2011). Step 3 was done using the parametric simulation function in EnergyPlus and the results were extracted and then embedded into SimLab (for step 4) by a special technique. This technique was developed in Microsoft Excel[®] by the author, allowing one to extract automatically the results from hundreds of EnergyPlus output files and to convert them into a predefined format readable by SimLab. This SA process is summarized and illustrated in Figure 8-1.

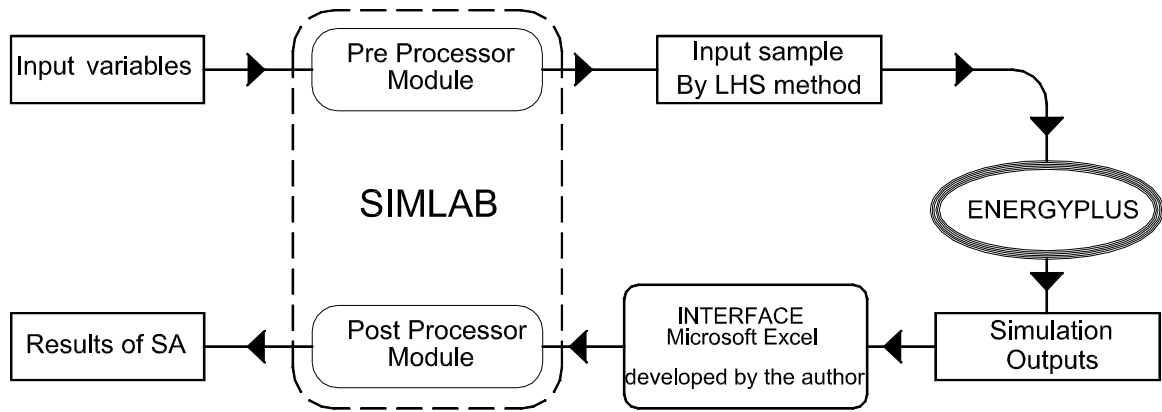


Figure 8-1: The full process of a SA using SimLab and EnergyPlus

8.1.4 Sensitivity analysis of the EnergyPlus thermal models

The aims of the thesis are not only to study and optimize the thermal environment in NV buildings but also to examine energy saving strategies in AC buildings. Hence, in the following series of SAs, two operating modes of the case-study houses were examined: NV and AC houses.

In the NV houses, the external openings were controlled by 10 common ventilation schemes in hot humid climates as shown in Table 8-1. The name of each ventilation scheme was codified by an integer number – from 400 to 409 – so that these ventilation schemes are readable by numerical simulation and optimization tools. This trick was also applied for many other categorical design options used in next stages of the research, e.g. wall types, roof types, window types...

Table 8-1: Common ventilation schemes applied in NV buildings

Ventilation schemes and their corresponding var. names in EnergyPlus	Ventilation period	Ventilation during day time	Ventilation during nighttime
All year day time ventilation - 400	All year	Yes	No
All year night ventilation - 401	All year	No	Yes
All year ventilation - 402	All year	Yes	Yes
All year closed - 403	All year	No	No
Day time ventilation summer - 404	1 st May - 30 th September	Yes	No
Day ventilation summer + mild seasons - 405	1 st March - 31 th October	Yes	No
Night ventilation summer - 406	1 st May - 30 th September	No	Yes
Night ventilation summer + mild seasons - 407	1 st March - 31 th October	No	Yes
Full ventilation summer - 408	1 st May - 30 th September	Yes	Yes
Full ventilation summer + mild seasons - 409	1 st March - 31 th October	Yes	Yes

In the AC houses, each thermal zone was equipped with a Packed Terminal Air Conditioner (PTAC). Each PTAC consists of an electric heating coil, a single-speed cooling coil, a ‘draw through’ fan, an outdoor air mixer, a thermostat control and a temperature sensor. It was assumed that the heating coil efficiency is 1; the coefficient of performance (COP) of the cooling coil is 3; the efficiency of the fan blades and the fan motor are 0.7 and 0.8 respectively; heating and cooling supplied air temperatures of the PTAC are 50°C and 13°C. Other capacities (e.g. flow rates, power of the coils) of these components are automatically estimated by EnergyPlus to meet heating and cooling loads of the zone. In every house, each PTAC operates independently from the others. Energy consumption of a PTAC is the sum of heating electricity, total cooling electricity and fan electricity. Total energy consumption of the houses is the sum of electricity consumed by the lighting system, equipments and the PTACs.

Due to space and time constraints, the SAs will only be done with three housing types under the climate of Danang. This climatic region shows a balance between the Northern and the Southern climatic regions of Vietnam. This study therefore assumed that the SA results can be generalized for the whole Vietnam with a few exceptions noticed by the empirical knowledge.

8.1.4.1 SA of the row house model

For the NV row house, 29 variables were taken into consideration, including uncertainties in physical properties of materials, uncertainties in design and operation. The natures of these variables, probability distribution functions, and the assigned ranges were reported in Table 8-2. Similarly, for the AC row house, 34 variables were taken into consideration and their details were reported in Table 8-3.

Table 8-2: Variables considered in the SA of the NV row house

Description of input variables in the SA	Var. name	Variable type	Probability distribution function	Range*	Mean	Standard deviation
Ventilation strategy (open or close the openings)	x1	Discrete	With weight factors	400 – 409, step = 1		
Max equipment power – level1	x2	Continuous	Normal		160 W	20
Max equipment power – level2	x3	Continuous	Normal		80 W	15
Max equipment power – bedroom	x4	Continuous	Normal		160 W	20
Insulation thickness- ground floor	x5	Continuous	Uniform	0 – 0.03 m		

Description of input variables in the SA	Var. name	Variable type	Probability distribution function	Range*	Mean	Standard deviation
External wall type	x6	Discrete	With weight factors	100 – 106, step = 1		
Insulation thickness- roof	x7	Continuous	Uniform	0 – 0.04 m		
Insulation thickness- ceiling	x8	Continuous	Uniform	0 – 0.04 m		
Brick density (external wall)	x9	Continuous	Normal		1600 kg/m ³	200
Thickness - brick	x10	Continuous	Normal		0.07 m	0.008
External wall color	x11	Continuous	Uniform	0.25-0.85		
Concrete slab thickness	x12	Continuous	Normal		0.09 m	0.01
Concrete slab density	x13	Continuous	Normal		2600 kg/m ³	200
Roof color	x14	Continuous	Uniform	0.25-0.85		
EPS Insulation conductivity	x15	Continuous	Normal		0.035 W/m.K	0.003
Window type	x16	Discrete	Uniform	200; 201; 202; 203		
Thickness of internal mass	x17	Discrete	With weight factors	0.1; 0.15; 0.2; 0.25; 0.3 m		
Façade shading length	x18	Continuous	Uniform	0.2 -0.4 m		
Max number of occupant	x19	Discrete	Uniform	2; 3; 4; 5; 6		
Power of gas stove	x20	Continuous	Normal		400 W	200
Width of front window level 2	x21	Continuous	Uniform	1 - 2.0 m		
Width of backward window level 2	x22	Continuous	Uniform	1 – 2.5 m		
Crack front window level 2	x23	Continuous	Uniform	0.002-0.008 kg/m.s		
Discharge coefficient front window level 2	x24	Continuous	Normal		0.45	0.1
Crack backward window level 2	x25	Continuous	Uniform	0.004-0.012 kg/m.s		
Discharge coefficient backward window level 2	x26	Continuous	Normal		0.5	0.1
Discharge coefficient of the crack of attic	x27	Continuous	Uniform	0.18-0.35		
Height of backward window level 1	x28	Continuous	Uniform	0.4 – 0.8 m		
Width of entrance door	x29	Continuous	Uniform	2 – 3.7 m		

*For discrete variables, each number represents a codified name of a building composition or schedule in EnergyPlus (e.g. 402 means “all year ventilation”)

Table 8-3: Variables considered in the SA of the AC row house

Description of input variables in the SA	Var. name	Variable type	Probability distribution function	Range*	Mean	Standard deviation
Azimuth	x1	Continuous	Normal		-7.5°	8
Max equipment power – level1	x2	Continuous	Normal		160 W	20
Max equipment power – level2	x3	Continuous	Normal		80 W	15
Max equipment power – bedroom	x4	Continuous	Normal		160 W	20
Insulation thickness- ground floor	x5	Continuous	Uniform	0 – 0.03 m		
External wall type	x6	Discrete	With weight factors	100 – 105, step = 1		
Insulation thickness- roof	x7	Continuous	Uniform	0 – 0.04 m		
Insulation thickness- ceiling	x8	Continuous	Uniform	0 – 0.04 m		
Brick density	x9	Continuous	Normal		1600 kg/m ³	200
Thickness – brick	x10	Continuous	Normal		0.07 m	0.008
External wall color	x11	Continuous	Uniform	0.25-0.85		
Concrete slab thickness	x12	Continuous	Normal		0.09 m	0.01
Concrete slab density	x13	Continuous	Normal		2600 kg/m ³	200
Roof color	x14	Continuous	Uniform	0.25-0.85		
EPS Insulation conductivity	x15	Continuous	Normal		0.035 W/m.K	0.003
Window type	x16	Discrete	Uniform	200; 201; 202; 203*		
Thickness of internal mass	x17	Discrete	With weight factors	10; 15; 20; 25; 30 mm		
Façade shading length	x18	Continuous	Uniform	200 – 500 mm		
Max number of occupant in each zone	x19	Discrete	Uniform	2; 3; 4; 5; 6		
Power of gas stove	x20	Continuous	Normal		400 W	100
Width of front window level 2	x21	Continuous	Uniform	1 - 2.0 m		
Height of backward window level 1	x22	Continuous	Uniform	0.4 - 0.8 m		
Width of backward window level 2	x23	Continuous	Uniform	1 – 2.5 m		
Width of entrance door	x24	Continuous	Uniform	2 – 3.7 m		
Infiltration of level 1	x25	Continuous	Normal		0.015 m ³ /s	0.003
Infiltration of level 2	x26	Continuous	Normal		0.008 m ³ /s	0.003
Infiltration of Bedroom	x27	Continuous	Normal		0.01 m ³ /s	0.003
Infiltration of the attic	x28	Continuous	Uniform		0.003 m ³ /s	0.001

Description of input variables in the SA	Var. name	Variable type	Probability distribution function	Range*	Mean	Standard deviation
HVAC Fan blades efficiency	x29	Continuous	Uniform	0.6 – 0.7		
HVAC Fan motor efficiency	x30	Continuous	Uniform	0.8 – 0.9		
HVAC Cooling coil COP**	x31	Continuous	Normal		3	0.13
HVAC Heating coil efficiency**	x32	Continuous	Uniform	0.95 - 1		
HVAC Heating setpoint***	x33	Continuous	Uniform	20° – 23°		
HVAC Cooling setpoint***	x34	Continuous	Uniform	26° - 27.5°		

*For discrete variables, each number often represents a codified name of a building composition or schedule in EnergyPlus (e.g. 101 means “220mm brick wall - no insulation or air gap”)

** Heating and cooling coil efficiency may be reduced due to the hygiene condition of the coils

***To ensure PPD does not exceed 20%, the HVAC setpoints are 20° - 26° in winter (0.8 clo, 1.2 M, 0.1 m/s, 50% RH) and 23° - 27.5° in summer (0.5 clo, 1.2 M, 0.15 m/s, 50% RH), PPDs are about 15%, plus 5% of dissatisfied occupant due to local thermal discomfort (cold floor, draught, dry air...)

The number of model evaluations (simulations) needed for a reliable Monte Carlo analysis is still subject to debate. This number must be large enough to assure convergence of the sensitivity indices, but should not be too large to delay the SA process. Yang (2011) carried out a study on the convergence issue in SA using the HYMOD model (a model using in hydrology). He reported that the sample size of 500 was needed for the regression-based method. However, this value seems to be too high in building simulation. Although no explanation was mentioned, SimLab recommends the sample size of 1.5 up to 10 times the number of input factors. In (Kotek, et al., 2007; Hopfe & Hensen, 2011) the authors used the sample size of 200 for complex building systems.

In the NV case, the input variables were randomly sampled 180 times by the LHS method, generating 180 input vectors for EnergyPlus. This number of input vectors is 6 times higher than the number of variables and it well exceeds 44 - the minimum value recommended by SimLab (1.5 times x 29 variables \approx 44). Figure 8-2 presents the Cobwebs plot of 180 random input vectors for the NV house in EnergyPlus. As can be seen, the values of each input variable follow its assigned probability distribution function in Table 8-2 and they are spread randomly over their ranges. Similarly, in the AC case, the 34 input variables were also randomly sampled by the LHS method, resulting in 200 input vectors for EnergyPlus simulation.

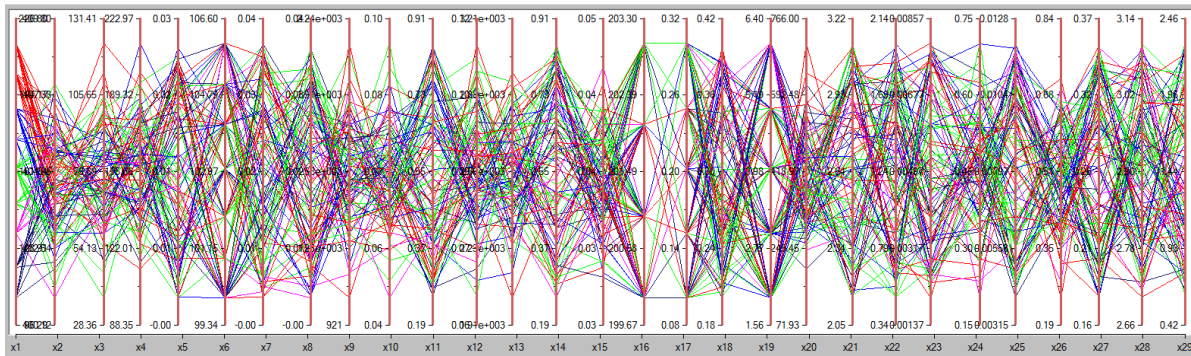


Figure 8-2: Cobwebs plot of 180 input vectors generated by the LHS method

The 180 (or 200) input vectors were implemented into EnergyPlus for 180 (or 200) corresponding simulation runs. The simulated results of these 180 (or 200) runs were extracted and embedded into SimLab where sensitivity indices of the input variables were calculated. The EnergyPlus outputs in consideration for SAs were the Total Discomfort Hours (TDH) and Total Energy Consumption (TEC) in the NV and AC houses, respectively.

The calculated PCCs and SRRCs of the input parameters of the NV and AC houses were sorted from the largest to the smallest as shown in Figure 8-3. The higher the absolute PCC and SRRC are, the more influential the parameter is. The positive / negative sign of the PCC or SRRC indicates the proportional / inverse relationship between a variable and the TDH. Based on the sensitivity rankings and the PCCs – SRRCs, the variables were categorized into three groups: the highly influential group (on top), the moderately influential group and the less influential group (bottom).

In the first group, it is clear that the predictions of the most sensitive variables by the PCC and SRRC were quite consistent in both NV and AC houses. In the NV house, it can be stated that *the roof color, the roof thermal insulation and ventilation schemes* are the most influential factors of the TDH. Their PCCs and SRRCs were much higher than those of the remaining, indicating that their influences on simulated results were significant. They should therefore be chosen with care during the design process. In the AC house, the *roof color* and the *number of occupant* is as important as the roof parameters. The *HVAC cooling setpoint, the roof insulation, and the cooling coil COP* were among this first group. The *HVAC heating setpoint*, in contrast, was completely not influential possibly due to the warm climate of Danang; but it may become much influential in Hanoi due to the cold winter in

the North of Vietnam. The most important things obtained from this result were that the heat flow through the metal roof of the row house must be strictly controlled for better indoor environment and energy saving.



Figure 8-3: Sensitivity rankings via the PCC and SRRC – the row house

To quantify how much influence the most sensitive parameter generates on the TDHs and the TECs, scatter plots of ‘roof color versus TDHs and TECs’ were examined as

shown in Figure 8-4. Each point in these graphs represents the mean of 10 input-output observations. Regardless of the variation of other variables, strong linear correlations can be observed as the coefficients of determination were 0.85 and 0.73 in the NV and AC cases, respectively. It can be said that bright or reflective roofs should be the best choice for such a climate.

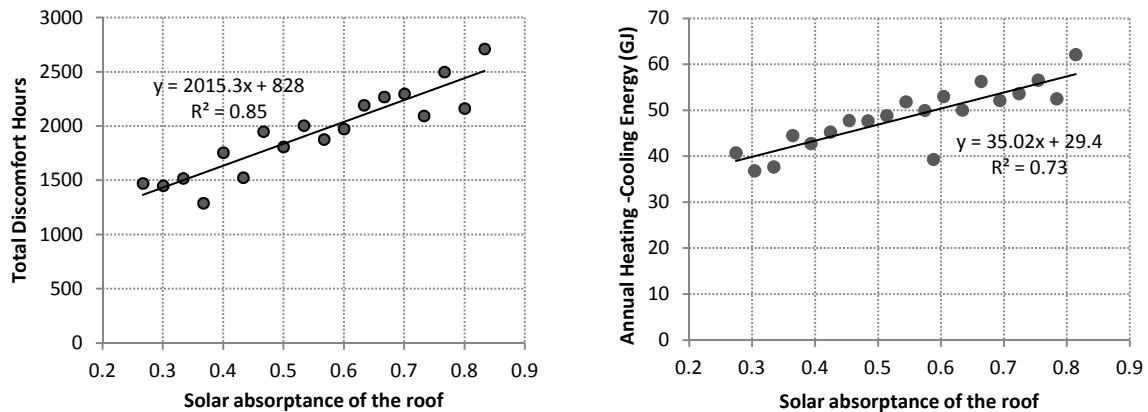


Figure 8-4: Correlations between the roof color and the TDHs and TECs

In the second group, the input parameters were much less influential than those of the first group. On the other hand, they have rather uniform PCCs and SRRCs, their ranking are thus not strictly accurate. They can be considered moderately influential factors. The less sensitive parameters were rather similar in both PCC and SRRC rankings. Notably, the *building orientation* and the remaining variables of the HVAC setting were among this group. Surprisingly, the *infiltration rates* of all AC thermal zones were dropped into the less influential group. There are two possible explanations: (i) the infiltration rates were assumed too small that their variations did not have any considerable influence, or (ii) the infiltration rate of each zone (not the whole building) may have a marginal effect on the total energy of the house. The author was in favor of the second hypothesis.

8.1.4.2 SA of the detached house model

The SA of the detached house was also conducted with the AC and NV cases. Similar to the row house, the detached house model was subject to the variations of 29 (the NV case) and 34 (the AC case) input parameters. Details of these input parameters and their variation ranges are reported in the Appendix A. These parameters were randomly sampled by the LHS method, generating a large number of input vectors for EnergyPlus. Totally 180 simulation runs of the NV case and 200 runs of the AC case were launched by the parametric function of EnergyPlus. The simulated results were passed to SimLab for SA.

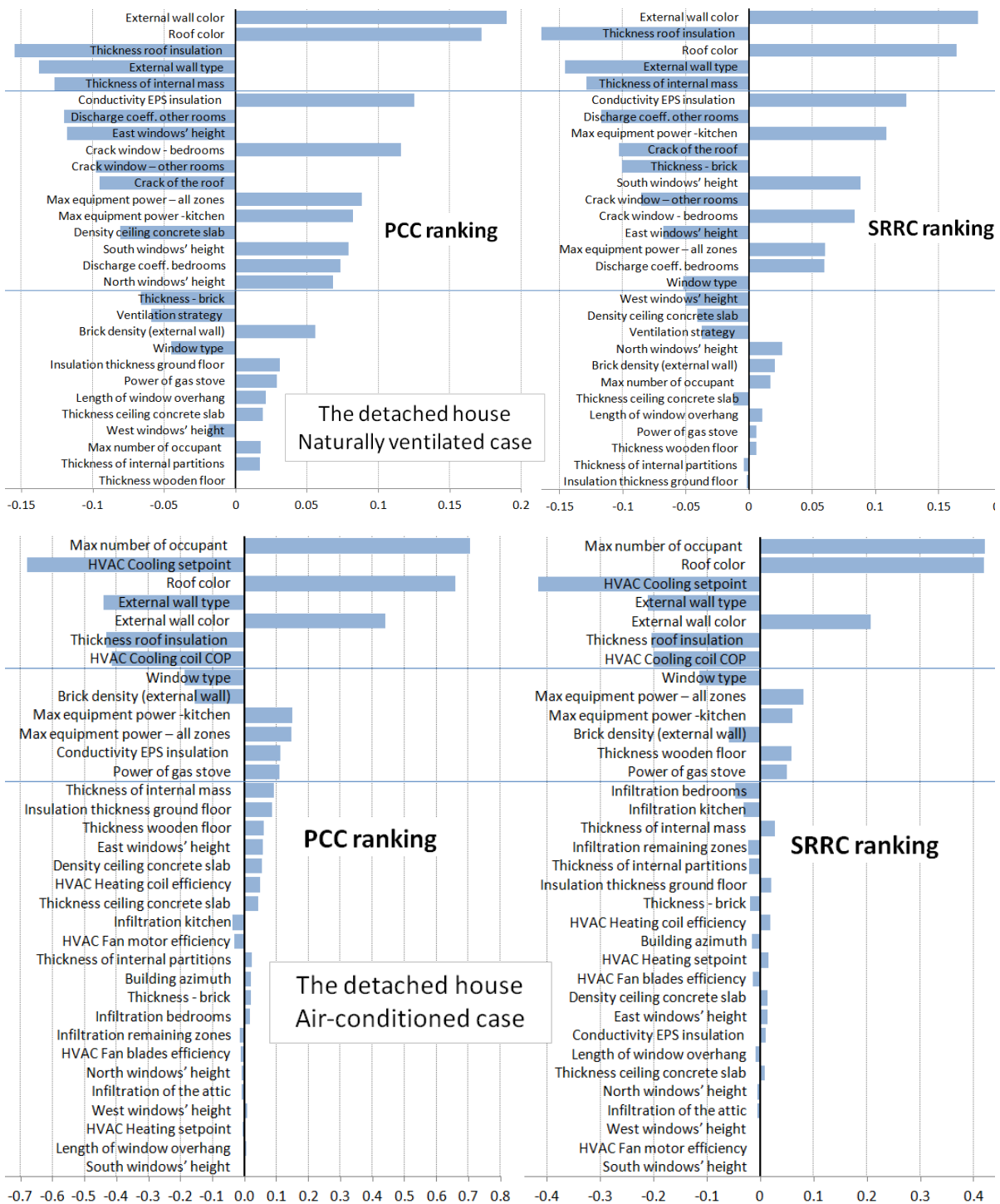


Figure 8-5: Sensitivity rankings via the PCC and SRRC - the detached house

Figure 8-5 shows the sensitivity ranking of input parameters of the detached house. The parameters related to building envelopes, the number of occupants and the HVAC cooling setpoint continued to play important roles. It was notable that many input

parameters of the NV house did not have the same influential measures as their counterparts of the AC house. For example: the *thickness of internal mass* was ranked 5th in the NV case, but ranked 15th in the AC case. Similarly, the *number of occupant* was also ranked differently in these two cases. This reveals that the design of NV and AC buildings must take these parameters into account in different priorities as being ranked in Figure 8-5.

In the NV case, it was abnormal that *ventilation strategy* parameter was not highly ranked by both PCC and SRRC. In fact, this may not be correct. This low ranking was possibly caused by the disorder of this discrete variable (the *ventilation strategy*), resulting in the non-linear relationship between ventilation strategies and the TDHs. The coefficient of determination R^2 of 0.09 was fairly low and the variation of TDHs was non-monotonic (see Figure 8-6a). In this case, the PCC and SRRC may not produce accurate rankings of such a variable.

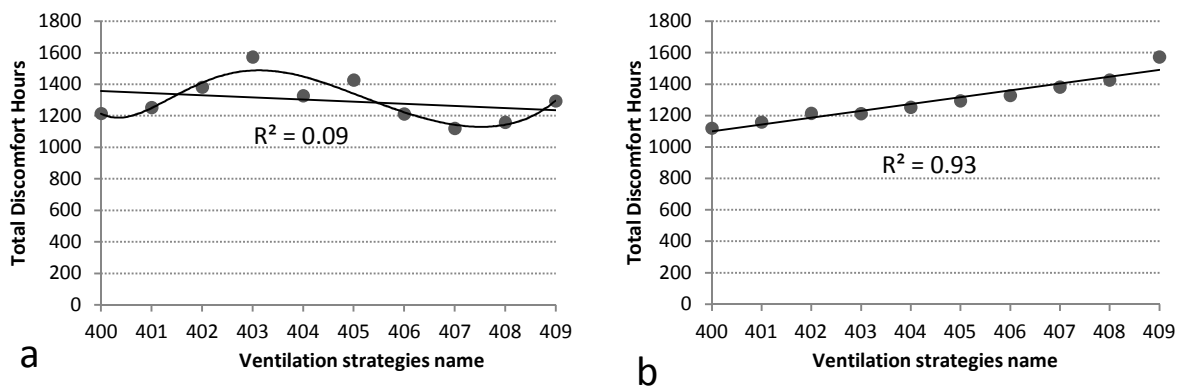


Figure 8-6: Non-linear non-monotonic relationship between ventilation strategies and TDHs (a) and strong correlation if the codified names were reordered (b)

We tried to reorder (by empirical experience) the codified names of the ventilation strategies in EnergyPlus input files so that the change of TDHs was monotonic (see Figure 8-6b). For instance, strategy ‘407’ is now reassigned ‘400’; ‘403’ now becomes ‘409’... Then we performed another SA on these new input files. The ventilation strategies were still unchanged (only the codified names were changed). The new SA result indicated that the sensitivity index of *ventilation strategy* changed considerably and it was ranked 2nd among 29 variables. This result proved that the TDH was highly sensitive to the ventilation strategies although this is not always reflected in the SA results. Thus they should be treated with much respect in the simulation of NV houses. The regression-based SA of discrete variables also needs special assessment to avoid incorrect ranking.

8.1.4.3 SA of the apartment model

Since 24 to 25 input parameters of the apartment were varied, there were 180 simulations for each NV or AC case. The sensitivity indices PCC and SRRC of input parameters are shown in Figure 8-7. The most influential group was almost related to the building envelope, ventilation strategy and the internal heat source. The HVAC cooling setpoint is obviously highly influential in any hot climates.

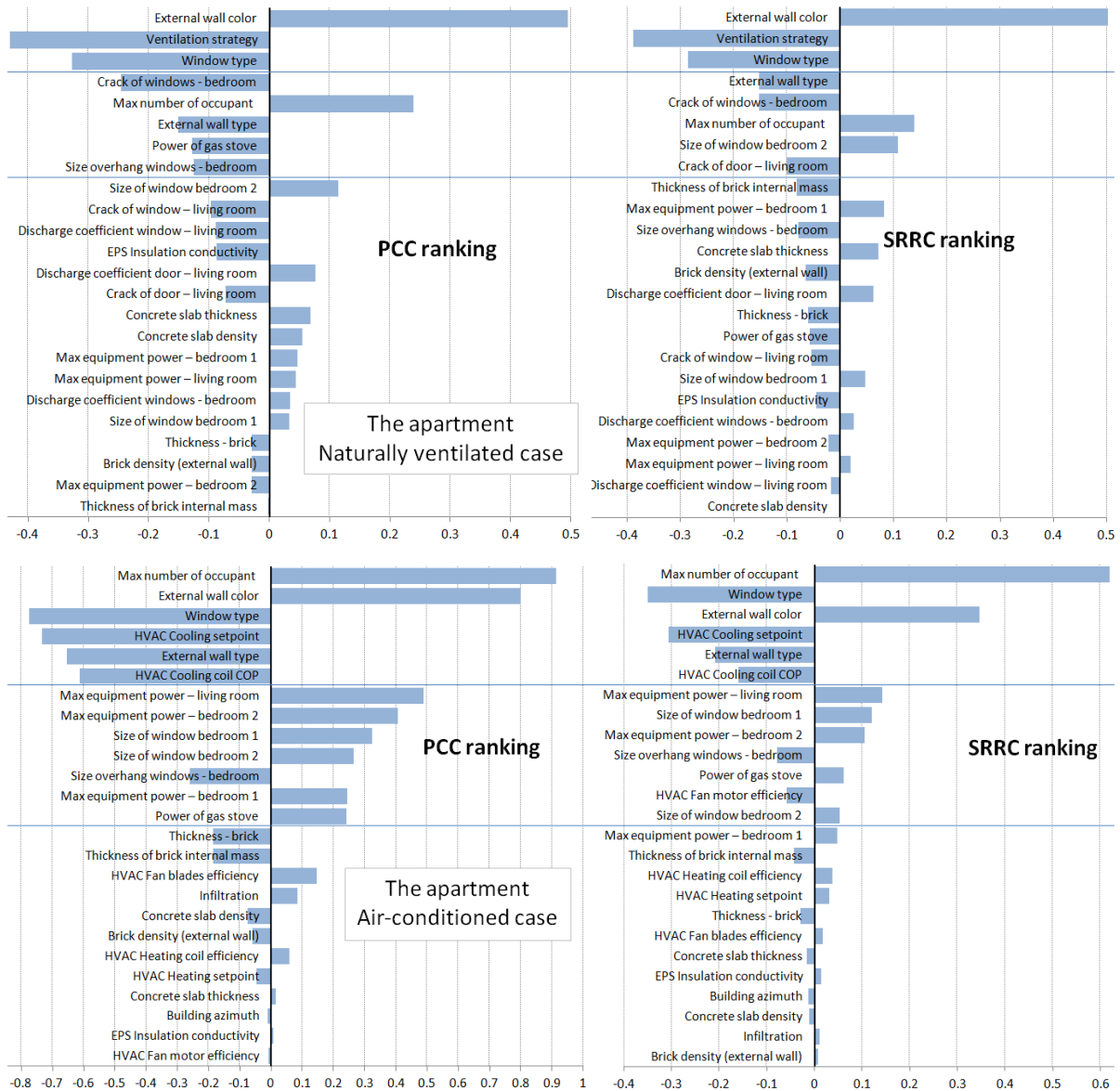


Figure 8-7: Sensitivity rankings via the PCC and SRRC – the apartment

From the SA of three case-study houses, it was found that in hot climates the COP (coefficient of performance) of the HVAC cooling coil is always highly influential to energy

consumption. A small increase of the COP may result in much energy saving. A high COP can be maintained by selecting appropriate cooling technologies (e.g. air-conditioner with inverter technology) or good periodic maintenances.

It was not difficult to recognize that the rankings of the PCC and the SRRC were quite consistent among the most influential parameters because the correlations between inputs and outputs are usually high, but not really in agreement in the remaining parts. It was simply because significant/weak correlations between these parameters and simulation outputs. The accuracy of the PCC and SRRC reduces if this correlation is not significant. Consequently, the orders of low influential parameters were not strictly accurate. It was stated that regression methods are highly reliable if the model response is approximately linear (e.g. R^2 greater than 0.7); if the model response is strongly non-linear (say R^2 smaller than 0.3), this method may result in unreliable predictions (Saltelli, et al., 2004).

This series of SA provides a very clear insight of the influence of building parameters on the design objectives. In NV buildings, the building envelope and ventilation strategy are the most influential factors. Meanwhile, the building envelope, the thermostat of HVAC systems and internal heat sources are significant in AC buildings. The results of SA may help designers to quickly choose appropriate solutions for their design problem. It might also be useful for making choices in building renovation and retrofit.

8.1.4.4 Uncertainty of simulation outputs due to variations of inputs

This section examines the uncertainty of simulation outputs caused by the variations of inputs. Table 8-4 shows statistical features of these output samples. In the light of uncertainty, among the NV houses, the apartment shows the best thermal performance, followed by the detached house. The row house shows the worst thermal performance. It can also be seen that the detached house was a little more robust to variables' variations than the others. In term of energy consumption, the AC detached house consumed much more energy than the row house and the apartment. Higher energy consumption in the detached house was possibly caused by the strong exposure of building surfaces to the outdoor environment, resulting in much heat gain and loss. Meanwhile, large side walls of the row house (and the apartment) adjacent to other houses (apartments) were modeled as adiabatic surfaces (no heat transfer). Surprisingly, in terms of energy density, the row house seems the most efficient model in which the energy density was nearly a half of the detached house while that of the apartment was much higher than the other houses.

Table 8-4: Statistical features of the samples of simulation outputs

	Total Discomfort Hours		Total Energy Consumption		
	Mean (h)	Standard deviation	Mean (GJ)	Standard deviation	Energy density (GJ/m ² .year)
Row house	1936	679	29.20	5.31	0.143
Detached house	1288	531	42.67	8.02	0.275
Apartment	1098	657	15.76	2.38	0.325

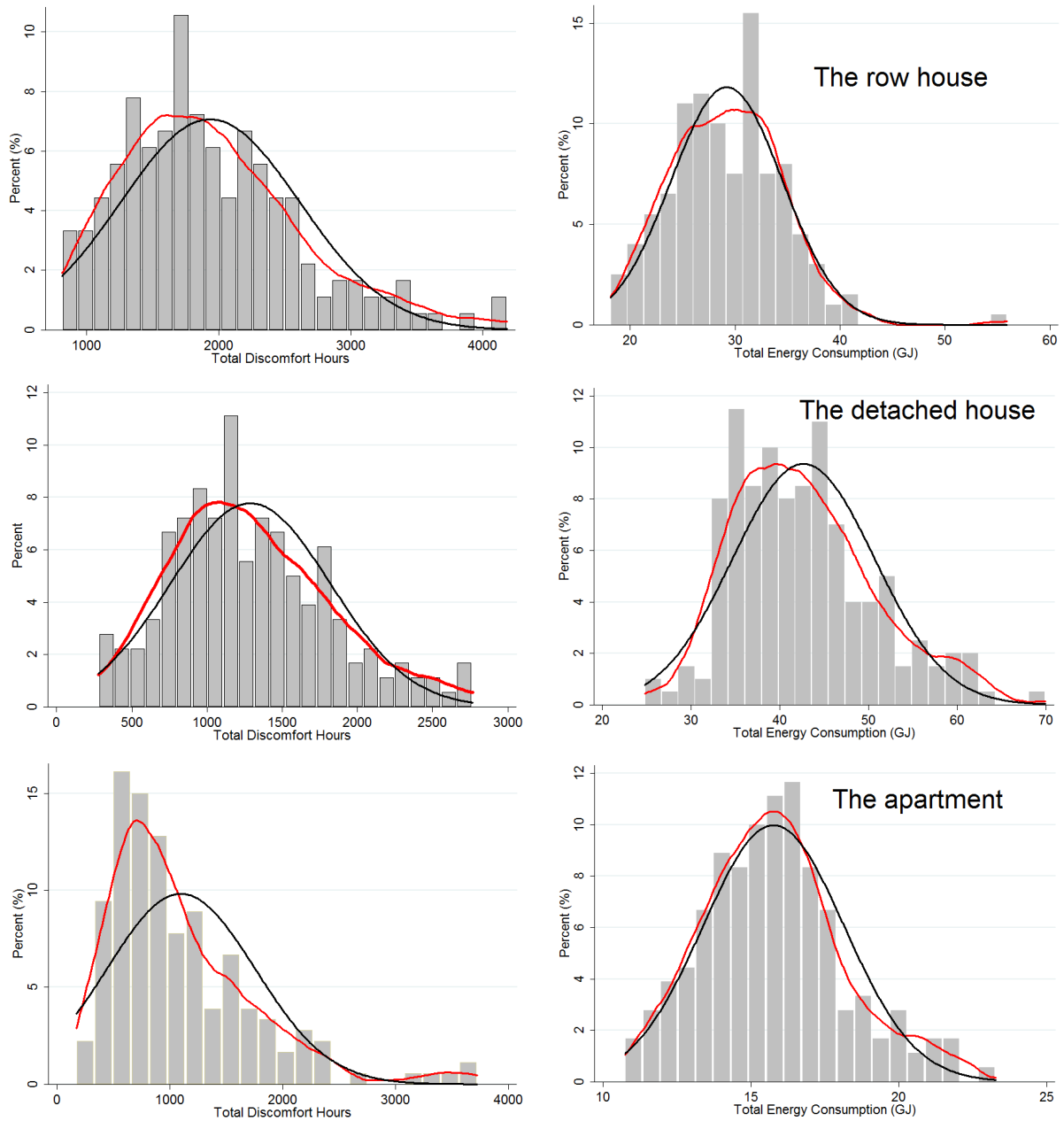


Figure 8-8: Probability distribution of simulation outputs

Figure 8-8 shows the probability distributions of TDHs and TECs in response to the variations of input parameters. The normal density curves (black) present the standard distributions, corresponding to the arithmetical means of the samples. Meanwhile, the Epanechnikov density curves (red) reproduce actual distributions of the output samples. Most Epanechnikov density curves were slightly asymmetrical with small positive skewnesses.

As can be seen, the TDH varied in a wide range from 250 h to 4200 h and the TEC from 11 GJ to 70 GJ. The strong variations of the THD and TEC indicate that these simulation outputs were subject to severe uncertainties, revealing great potentials of comfort and energy improvement. Hence, an important task of designers is to make the building more robust to the changes and to minimize the TDH and TEC.

8.2 Optimizing building thermal performance by numerical optimization

8.2.1 An introduction of numerical optimization

The application of computer simulations for handling complex engineering systems has emerged in some recent decades. In building science, designers often use a dynamic thermal simulation program to analyze thermal and energy behaviors of a building and to achieve specific targets, e.g. low energy consumption or acceptable thermal environment. CHAPTER 7 of this thesis illustrated an approach known as ‘parametric study’ to improve thermal performance and natural ventilation of the three case-study houses. According to this method, each input variable is varied to see the effect on a design objective while all other variables are kept unchanged. This procedure may be repeated iteratively with other variables. This approach is usually time-consuming while it might yield only partial improvement because of the complex non-linear interactions of input variables on simulated results.

To achieve an optimal solution (or a solution near the optimum) to a problem with less time and labor, the objective target (or the objective function¹⁸) of a numerical building model is usually “solved” by iterative methods, which construct infinite sequences, of progressively better approximations to a “solution”, i.e., a point in the search-space that

¹⁸ The objective function is (a) simulation outputs that need to be optimized, e.g. building energy consumption, length of time during which comfort criteria are not satisfied.

satisfies an optimality condition (Wetter, 2009). Due to the iterative nature of the procedures, these methods are usually based on computer programs. Such methods are often known as ‘numerical optimization’ or ‘simulation-based optimization’.

The applications of numerical optimization have been considered since the year 80s and 90s based on the rapid growth of computational sciences and mathematical optimization methods. However, most studies in building engineering which combined a building energy simulation tool with an optimization ‘engine’ have been published in the late 2000s although the first efforts were found much earlier. A pioneer study in optimization of building engineering systems was presented by Wright in 1986 when he applied the Direct Search method in optimizing HVAC systems (Wright, 1986). The Genetic algorithm was then introduced and applied in the optimization of building envelopes, HVAC systems and control (Wright, 1994; Wright, et al., 2002). In 2001, Wetter (2001) first introduced the optimization program GenOpt with different optimization algorithms that significantly contributed to optimization solutions in building engineering. GenOpt was originally developed for the BPS community hence it offers architects and engineers many advantages in their simulation works. Another optimization toolkit which has similar optimization capabilities to GenOpt is Dakota (Adams, et al., 2009). Dakota provides a framework for single, multi-objective or surrogate-based optimization, parameter estimation, uncertainty quantification, and sensitivity analysis to the simulation-based community, but its usage requires advanced programming knowledge. Some other optimization programs, e.g. BEopt, TopLight, MATLAB, GoSUM, LIONSolver... have also been developed, providing many more appropriate methodological frameworks to the simulation-based optimization community. Consequently, numerous optimization researches have been carried out, aiming to optimize building design, passive strategies, energy consumption, performance of HVAC systems, construction cost, life cycle cost, environmental impacts...

Due to cost constraints, residential buildings in Vietnam usually exploit natural ventilation as the major cooling strategy and IAQ control. HVAC systems are rarely used, thus indoor comfort is mainly achieved by passive design strategies. Also, Vietnam almost lies in a hot humid region where the climate has significant influences on housing architecture. Hence, in Vietnam the construction cost and the thermal comfort are the matters of great concern, rather than the issue of building energy consumption.

8.2.2 Definition of an optimization problem and related nominations

Optimization refers to as the procedure (or procedures) of making something (as a design, system, or decision) as fully perfect, functional, or effective as possible. In mathematics, statistics and many other sciences, *mathematical optimization* is the process of finding the best solution to a problem from a set of available alternatives. By a common rule, an optimization problem is often stated in terms of minimization because a maximization problem can always be translated into a minimization one by changing the sign of the objective function. Thus in simple cases, (mathematical) optimization problems can be defined as:

Given a function $f : X \rightarrow \mathbb{R}$, sought an element $x_0 \in X$ subject to $h(x_0) = 0$ or $h(x_0) \geq 0$ such that

$$\begin{cases} f(x_0) \leq f(x), \quad \forall x \in X \\ g(x_0) \geq 0 \end{cases} \quad (8.1)$$

where $f(x)$ is a real function; X is the domain of $f(x)$; \mathbb{R} is the set of real number; the functions $h(x)$ is the *constraint(s) of independent variables*; $g(x)$ is the *constraint(s) of dependant variables*.

The function $f(x)$ to be minimized (or maximized) is called the *objective function* (or *cost function*); the domain X of $f(x)$ is called the *search-space*. Each element x_i ($x_i \in X$) is called a *candidate solution* or a *feasible solution*. The element x_0 is called the *optimal solution*.

In many engineering problems, the domain X of $f(x)$ is usually a sub-set of \mathbb{R}^n , or $X \subseteq \mathbb{R}^n$. Thus each element $x \in X$ is a *design vector* with n dimensions, that is to say $\vec{x}_i = (x_{i1}, x_{i2}, \dots, x_{in})$. $x_{i1}, x_{i2}, \dots, x_{in}$ are called design variables. Generally, each design vector $\vec{x}_i \in X$ must satisfy $-\infty \leq l_i \leq x_i \leq u_i \leq \infty$, for $i \in \{1, \dots, n\}$. l_i and u_i are called the *lower bound* and *upper bound* of the design vector \vec{x}_i .

Given a function $f : X \rightarrow \mathbb{R}$, an element $x^* \in X$ is called a *local minimum* if there exists some $\delta > 0$ so that $\forall x \in X$ and $|x - x^*| < \delta$ the expression $f(x^*) \leq f(x)$ always holds. It also means that there is a region $X_0 \subset X$ around x^* where the function values in

this region are always greater than or equal to the value at x^* . If the function $f(x)$ is non-convex, it may have several local minima. Similarly, given a function $f : X \rightarrow \mathbb{R}$, a vector $x^* \in X$ is called a *global minimum* if $f(x^*) \leq f(x)$, $\forall x \in X$. A certain function $f(x)$ may have more than one global minimum. A *local maximum* or a *global maximum* is defined in a similar way.

In a numerical building system, each input parameter is a design variable; a set of input parameters that constitutes a complete design solution is a design vector; the algorithms implemented in the simulation program are the objective functions. As it is impossible to determinably write the simulation outputs as the function of the inputs, the objective function in building simulation programs is a “black box” function that one cannot derive any analytic information or derivatives of the function (Nielsen, 2002).

8.2.3 Optimization methodology

In this study, to optimize building costs and thermal comfort performance by the simulation-based optimization, an appropriate dynamic thermal simulation tool, namely EnergyPlus 6.0 (Crawley, et al., 2001) was used in this study. It should be noted that only version 6.0 or later is able to perform the life cycle cost analysis. EnergyPlus was directly coupled with GenOpt - an optimization program (Wetter, 2009) - to minimize different combined objective functions. GenOpt is a generic optimization program that can perform optimization of a user-prescribed cost function by choosing an optimization algorithm among an algorithm library.

In some cases, each simulation may require several minutes to hours to complete if the building model consists of many thermal zones and systems. Consequently, the direct coupling between a building simulation tool and an optimization ‘engine’ would be very time-consuming and other approaches should be used (e.g. surrogate-based optimization or artificial neural network). In the cases of this work, the building models are rather simple and do not require much simulation time; the direct coupling is therefore considered suitable and may yield most accurate information of optimal solutions. Figure 8-9, which was slightly modified from the origin in GenOpt manual (Wetter, 2009), shows how EnergyPlus is coupled with this optimization program. After each iteration, EnergyPlus is regularly restarted by a batch file (*.bat) embedded in GenOpt.

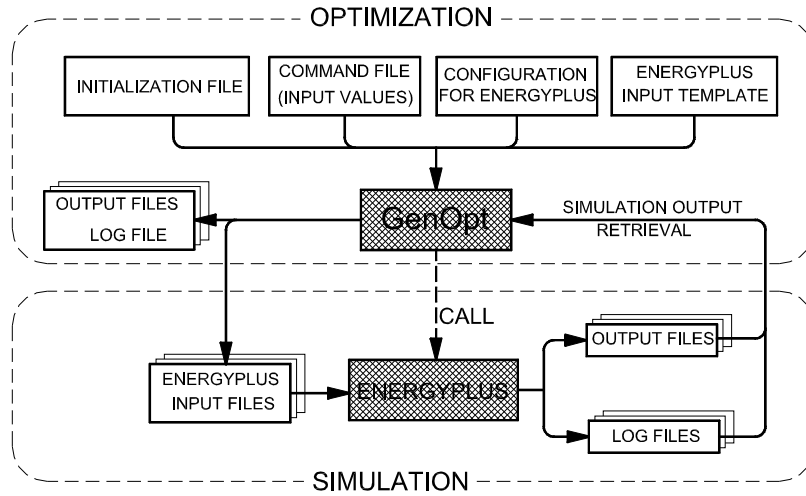


Figure 8-9: Coupling principle between GenOpt and EnergyPlus

The optimization will be performed on both NV models and AC models of three case-study houses. It is therefore essential to define appropriate methods for calculating the ventilation rate and infiltration rate in these houses. For the NV houses, the natural ventilation phenomenon was modeled by using the Airflow network model that was carefully reported in section 5.4 of this thesis. For the AC houses, the openings were assumed being closed all the time. The infiltration rate becomes an important input parameter. EnergyPlus provides a method which relates the air infiltration rate with outdoor conditions as follows:

$$Q = I_i * F_{schedule} (A + B * \Delta T + C * V_{outdoor} + D * V_{outdoor}^2) \quad (8.2)$$

where

Q is air infiltration rate (m^3/s);

I_i is reference infiltration flow rate (m^3/s);

$F_{schedule}$ is hourly schedule, prescribed by user (from 0 to 1);

ΔT ($T_{zone} - T_{out}$) is difference between indoor and outdoor temperature ($^{\circ}\text{C}$);

$V_{outdoor}$ is hourly outdoor wind speed (m/s);

A , B , C and D are coefficients, prescribed by user.

Typical values for A , B , C and D are still subject to debate (Ernest Orlando Lawrence Berkeley National Lab, 2010b). Based on some parametric runs, we assumed $(F_{schedule}, A, B, C, D) = (1.00, 0.20, 0.08, 0.18, 0.02)$ for most thermal zones of the models.

These coefficients produce an infiltration of 0.01 m³/s (at ΔT of 5°C and wind speed of 2 m/s), which corresponds to a typical summer condition in Hanoi at noontime.

In BPS, the reliability of simulated results varies from software to software and would be dominated by user’s experience. Each version of EnergyPlus was extensively tested using industry standard methods¹⁹. However possible uncertainties and errors may occur if an EnergyPlus model is not calibrated. The present study therefore assumed that the housing models can produce reliable results with no user calibration. Also, since one-year weather files of three sites were used, the 50-year life cycle cost analysis assumed that the impacts of climate change during 50 coming years are small and can be neglected.

8.2.4 Parameters of design and strategies considered in the optimization

Based on the results of the SA reported in section 8.1.4, the significant parameters were selected for the optimization. This sensitivity-based selection strategy is expected to improve the efficiency of the optimization because insignificant variables were expelled from the optimization. As the design of the three houses and the importance of design parameters in each house are different, the selections were therefore done on a case-by-case procedure. Table 8-5 and Table 8-6 show the selected variables and their properties of the NV and AC apartments, respectively. The variables of the detached houses and the row houses were reported in the Appendix B.

Table 8-5: Design parameters used in the optimization of the NV apartment

Numerical (continuous) variables and their variation ranges						
Design parameter	Opt. variable	Min value	Initial value	Max value	Step size	Number of case
External solar absorptance [dimensionless]	x ₁	0.25	0.35	0.75	0.1	6
Window bedroom 1 - crack infiltration [kg/s-m]	x ₂	0.004	0.01	0.012	0.002	5
Door balcony - crack infiltration [kg/s-m]	x ₃	0.004	0.004	0.012	0.002	5
Bedroom 1 window width (height = 1.42m) [m]	x ₄	1.2	1.2	2.2	0.2	6
Bedroom 2 window width (height = 1.42m) [m]	x ₅	1.2	1.2	2.2	0.2	6
Bedroom 1 window overhang [m]	x ₆	0	0.2	0.8	0.2	5
Bedroom 2 window overhang [m]	x ₇	0	0.2	0.8	0.2	5
External wall horizontal shading – East [m]	x ₈	0	0.2	0.6	0.2	4
External wall horizontal shading – West [m]	x ₉	0	0.2	0.6	0.2	4

¹⁹ See http://apps1.eere.energy.gov/buildings/energyplus/energyplus_testing.cfm

Categorical design options and strategies (discrete variables)					
Design parameter	Design choices	Opt. variable	Discrete value	Item cost (\$/m ²)	Number of case
External walls	110mm two-side plaster brick wall	x ₁₀	100	20	7
	220mm brick wall with no gap		101	28	
	220mm brick wall with air gap 2cm		102*	29	
	220mm brick wall with 1cm central EPS		103	30	
	220mm brick wall with 2cm central EPS		104	32.5	
	220mm brick wall with 3cm central EPS		105	35	
	220mm brick wall with 4cm central EPS		106	38	
Window glazing type	Clear glazed 6mm	x ₁₁	200	43	5
	Bronze film glazed 6mm -		201*	60	
	Double clear glazed with air gap 6mm		202	90	
	Double bronze film glazed with air gap 6mm		203	115	
	Double reflective glazed - 13mm Argon		204	135	
Ventilation strategy	From 400, 401, 402*, ..., 409 (see details of these ventilation strategies in Table 7-3)	x ₁₂	400 to 409	No cost	10
Internal thermal mass	Thermal mass 100mm thickness	x ₁₃	600	20	4
	Thermal mass 170mm thickness		601*	26	
	Thermal mass 240mm thickness		602	31	
	Thermal mass 310mm thickness		603	36.5	

*: Initial value

Table 8-6: Design parameters used in the optimization of the AC apartment

Numerical (continuous) variables and their variation ranges						
Design parameter	Opt. variable	Min value	Initial value	Max value	Step size	Number of case
External solar absorptance [dimensionless]	x ₁	0.25	0.35	0.75	0.1	6
Infiltration rate - all zones [m ³ /s]	x ₂	0.004	0.01	0.012	0.002	5
EPS insulation conductivity [W/m.K]	x ₃	0.029	0.032	0.041	0.003	5
Bedroom 1 window width (height = 1.42m) [m]	x ₄	1.2	1.2	2.2	0.2	6
Bedroom 2 window width (height = 1.42m) [m]	x ₅	1.2	1.2	2.2	0.2	6
Bedroom 1 window overhang [m]	x ₆	0	0.2	0.8	0.2	5
Bedroom 2 window overhang [m]	x ₇	0	0.2	0.8	0.2	5
External wall horizontal shading – East [m]	x ₈	0	0.2	0.6	0.2	4
External wall horizontal shading – West [m]	x ₉	0	0.2	0.6	0.2	4
Categorical design options and strategies (discrete variables)						
Design parameter	Design choices	Opt. variable	Discrete value	Item cost (\$/m ²)	Number of case	
External walls	110mm two-side plaster brick wall	x ₁₀	100	20	7	
	220mm brick wall with no gap		101	28		

	220mm brick wall with air gap 2cm		102*	29	
	220mm brick wall with 1cm central EPS		103	30	
	220mm brick wall with 2cm central EPS		104	32.5	
	220mm brick wall with 3cm central EPS		105	35	
	220mm brick wall with 4cm central EPS		106	38	
Window glazing type	Clear glazed 6mm	x ₁₁	200	43	5
	Bronze film glazed 6mm		201*	60	
	Double clear glazed with air gap 6mm		202	90	
	Double bronze film glazed, air gap 6mm		203	115	
	Double reflective glazed - 13mm Argon		204	135	
Internal thermal mass	Thermal mass 100mm thickness	x ₁₂	600	20	4
	Thermal mass 170mm thickness		601*	26	
	Thermal mass 240mm thickness		602	31	
	Thermal mass 310mm thickness		603	36.5	

*: Initial value

It is necessary to discuss the thermostat of the AC houses again. To ensure PPD does not exceed 20%, the HVAC setpoints are 20° - 26° in winter (0.8 clo, 1.2 M, 0.1 m/s, 50% RH) and 23° - 27.5° in summer (0.5 clo, 1.2 M, 0.15 m/s, 50% RH), PPDs are about 15%, plus 5% of dissatisfied occupant due to local thermal discomfort such as cold floor, draught, dry air...

The search-space in the optimization of the NV apartment has $4^3 \times 5^5 \times 6^3 \times 7 \times 10 \approx 3.02 \times 10^9$ candidate solutions. The search-space in the AC case includes $4^3 \times 5^5 \times 6^3 \times 7 \approx 3.02 \times 10^8$ candidate solutions. If the parametric simulation method is used and each simulation takes approximately 2 minutes to complete, it takes about 11492 years to examine all the search-space of the NV case. It is obvious that the parametric runs cannot be applied in such extremely large search-spaces and the optimization method seems to be the unique solution for exploring these search-spaces.

8.2.5 The choice of optimization algorithms for the present problem

The demand of a search-method that works efficiently on a specific optimization problem has led to various optimization algorithms. In most engineering optimization problems using the simulation-based approach, objective functions (simulation outputs) are generally non-linear, multi-modal, discontinuous and hence non-differentiable (Wetter & Polak, 2004). Some algorithms developed for solving such problems fail to draw a distinction between local optimal solutions and global optimal solutions, and consider the

former as final solutions to the problem. As an example, if the simulation program contains empirical assigned values (e.g. wind pressure coefficient), adaptive solvers with loose precision settings or iterative solvers using a convergence criterion, such as those in EnergyPlus, they may cause the cost function to be discontinuous. Hence gradient-based optimization algorithms, e.g. Discrete Armijo Gradient (Polak, 1997), that require smoothness of the cost function usually fail to reach the global minimum (Wetter & Wright, 2004). Consequently, the choice of optimization algorithm for a specific problem is crucial to yield the greatest reduction. In this work, the nature of the problem in consideration is summarized in the following:

- The “black box” objective functions are non-linear, discontinuous and hence non-differentiable,
- The input includes both continuous and discrete variables, so non-linear non-monotonic simulation outputs may occur (see Figure 8-6 for the effect of discrete variables on the simulation output),
- High number of variables in the optimization, i.e. usually greater than 10, resulting in very large search-spaces.

This type of optimization problem often requires heuristic optimization methods to search the search-space in a more or less intelligent way. Wetter and Wright (2004) compared the performance of 9 optimization algorithms and some variances by two numerical experiments on simple and complex EnergyPlus models. They reported that for 5/6 tests, the Hybrid algorithm achieved the biggest cost reduction but required a little more simulations than the standard Genetic algorithm. The Hybrid algorithm is a combination of the Particle Swarm Optimization (PSO) and the Hooke-Jeeves algorithm. A full description of these algorithms can be found in (Wetter, 2009).

The PSO algorithms belong to the population-based probabilistic optimization family. The first PSO algorithm was presented by Eberthart and Kennedy (1995). The search of the PSO mimics the social behavior of a flock of birds or a school of fish. In the PSO, each candidate solution is called a “particle”. The search is initially started with a number of particles called a “generation”. As the search processes, each particle changes its location (both the direction and velocity) towards a point of a lower objective function value known from previous generations, mimicking the cognitive behavior; at the same time it

moves towards the best location so far found by its neighbors, mimicking the social behavior of an individual in a swarm. This displacement is controlled by two parameters in the PSO: *cognitive acceleration* and *behavior acceleration*. Besides, to control how fast the population collapses into a point (the convergence speed), a *constriction coefficient* can be used in the PSO to reduce the velocity of particles. Another feature of the PSO used in this study is that the search is not taken over all points in the search-space. Instead, it is only performed on a mesh generated by the “*step size*” of independent variables. In each evaluation of the objective functions, continuous variables are replaced by the closest feasible mesh points while discrete variables still remain unchanged. This mesh is controlled by the *Neighborhood Typology* settings. Because the PSO search typically clusters around a point during the last iterations, the PSO on a mesh (of independent continuous variables) reduces considerably the number of simulation runs called by the PSO (Wetter, 2009).

The Hooke-Jeeves algorithm was initially proposed by Hooke and Jeeves (1961) and then modified by some authors. This algorithm performs the search on a mesh of independent variables through steps and loops presented in Figure 8-10. It does not require the gradient of the cost function; hence it can be used on functions that are not continuous or non-differentiable. Nevertheless, on multi-modal objective functions Hooke-Jeeves algorithm may be trapped in a local minimum, several sets of starting points are therefore recommended (Kampf, et al., 2010). Important parameters to control the Hooke-Jeeves algorithm are the *mesh size divider* and the *number of step reduction*.

The Hybrid PSO - Hooke-Jeeves algorithm is capable to work efficiently since it initially performs a global search by the PSO on a mesh, then the Hooke-Jeeves algorithm refines the search locally. This combination increases the possibility of the search to get close to the global minimum rather than only a local one (Wetter & Wright, 2004). On the other hand, as the PSO does not require the continuity of the objective functions, it accepts both continuous and discrete variables of the cases in question. In (Nguyen & Reiter, 2012b), the author compared the efficiency of the Hybrid algorithm and the PSO algorithm (version inertial weight) by using 3 different objective functions. All optimal results found by the Hybrid algorithm were better than the results of the PSO while the Hybrid cases offered reductions of about 50% of optimization time. For these reasons, the Hybrid algorithm was selected for this study.

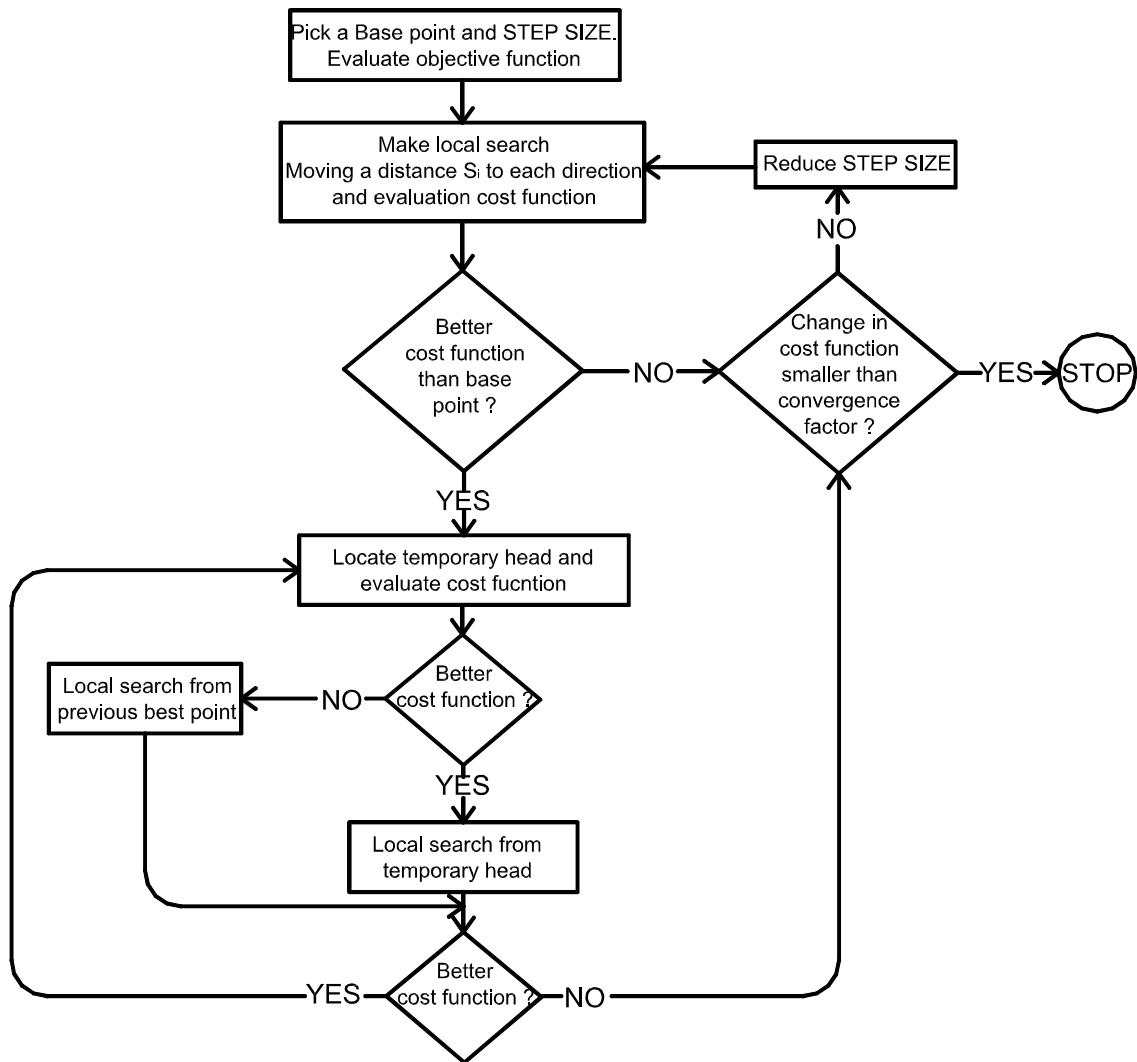


Figure 8-10: Diagram of the Hooke-Jeeves search logic²⁰

Performance of an optimization algorithm depends not only on its nature, but also on the setting parameters as pointed out in (Wetter & Wright, 2004). The important settings of the Hybrid algorithm were identified through some trials and were fixed as follows:

*** For the PSO algorithm**

```

NeighborhoodTopology = vonNeumann;
NeighborhoodSize = 5;
NumberOfParticle = 49;
NumberOfGeneration = 55;
Seed = 1;
CognitiveAcceleration = 2.05;
SocialAcceleration = 2.05;
MaxVelocityGainContinuous = 0.2;
MaxVelocityDiscrete = 4;
ConstrictionGain = 1;
  
```

*** For the Hooke-Jeeves algorithm**

```

MeshSizeDivider = 2;
InitialMeshSizeExponent = 0;
MeshSizeExponentIncrement = 1;
NumberOfStepReduction = 4;
  
```

²⁰ Rebuilt from <http://files.vlsi.uwindsor.ca/88-521/index.htm> [Accessed January 2013]

As can be seen, we chose the *number of particles* per generation of 49 to match with the large search-space. The population size of 49 is expected to be large enough to allow the search to process from the first generation while it results in acceptable optimization time. To prevent the PSO from being trapped early into a stationary point, the *constriction gain* was increased from 0.5 to 1. It was observed that with a higher *constriction gain*, the particles were more spread out in the early generations, offering more chance to catch the global minimum (Wetter & Wright, 2004). We also slightly adjust the *cognitive acceleration* and *social acceleration*. The settings also allow the Hooke-Jeeves algorithm to refine 4 times the mesh of the continuous variables after the last evaluation of the PSO. These settings provide good optimization results with both standard benchmark functions²¹ and real-world applications using EnergyPlus as being tested in (Kampf, et al., 2010). The number of generation was fixed at 55 for all optimizations. Our observations indicated that most optimization runs reached convergence after around 30th to 45th generations and some exceptions at 47th to 50th.

8.2.6 The establishment of objective functions

The choice of a building design solution is a non-linear multi-objective optimization process, hence it often requires a trade-off among conflicting design criteria, e.g. the initial construction cost, the operating cost, and occupant's thermal comfort (Wright, et al., 2002). The most common approach is to use the concept of Pareto optimality in which a set of trade-off solutions (Pareto set) is examined and appropriate solutions are then determined. This approach requires special features of optimization algorithms and expensive optimization time.

A more simplistic approach, namely "a priori", is to assign a weight factor to each criterion and the objective function will be simply the weighted sum of these criteria. As an example, we examine an optimization problem of a thermal zone which consists of a construction cost function $f_c(X)$ and a comfort performance function $f_p(X)$. These functions could be integrated into a single objective function by assigning two weight factors (a and b) or considering the second as a penalty function of the first:

²¹ Ackley function, Rastrigin function, Rosenbrock function, Sphere function and Constraint function

$$f(X) = a * f_c(X) + b * f_p(X) \quad (8.3)$$

or $f(X) = f_c(X) * f_p(X)$

In the present work, the “a priori” approach was used to combine two design criteria into one objective function which consists of the construction cost and comfort performance; or the construction cost and the operating cost. We established two objective functions for the NV cases and one for the AC cases.

In the NV cases, to find the best combination of various design parameters in response to the climates so as to achieve the best thermal comfort condition in the houses, the objective function [A] was established to minimize uncomfortable periods during a year:

$$f(x) \triangleq TDH(x) \quad (8.4)$$

In the above equation, the $TDH(x)$ is the simulated Total Discomfort Hours during a year. It is the thermal comfort indicator associated with the adaptive thermal comfort model for South-East Asia that was discussed earlier in section 5.6.1.

In NV buildings, the operating cost of different solutions is assumed to be similar. In most developing countries, the initial construction cost is an important decision making indicator. This study therefore minimizes the initial construction cost which is constrained by a TDH criterion so that $TDH\% \leq 10\%$. The objective function [B] was defined as:

$$f(x) \triangleq \frac{f_c(x)}{COST_{max}} + 10[\max(0, TDH\%(x) - 10)]^2 \quad (8.5)$$

where $f_c(x)$ is simulated initial construction cost of the house; $COST_{max}$ is the estimated maximum construction cost so that the equation $f_c(x) \leq COST_{max}$ always holds; $TDH\%(x)$ is the simulated percentage of Total Discomfort Hours during a year ($TDH\% = TDH * 100 / 8760$).

In the right side of the objective function [B], the first term is always smaller than or equal to 1; the rightmost term is a penalty function. This penalty function will add a large positive term to the objective function $f(x)$ if the thermal comfort criterion is violated (i.e. $TDH > 10\%$). In contrast, this penalty function is always zero if comfort criterion is satisfied (i.e. $TDH \leq 10\%$). The acceptable thermal comfort threshold is $TDH \leq 10\%$ (see discussions in Table 5-9 section 5.6.1).

In the AC case, since the indoor thermal environment is controlled by the PTAC systems (see section 8.1.4), this study therefore minimizes the life cycle cost of the house which consists of the initial construction cost and the 50-year operating cost. The demolition, transportation and waste management cost are assumed to be similar in all solutions. Thus the objective function [C] is the building Life Cycle Cost (LCC), defined as:

$$f(x) \triangleq f_c(x) + f_o^{50}(x) \quad (8.6)$$

where $f_c(x)$ is initial construction cost (present value); $f_o^{50}(x)$ is total 50-year operating cost (present value).

Using LCC provides a comprehensive approach to combine the initial construction cost and the projected future costs into a single measure, called the “present value” (Ernest Orlando Lawrence Berkeley National Lab, 2010a). To include this into the analysis in EnergyPlus, we assumed an inflation rate of 2.5% per year, a discount rate of 1%, an electricity price escalation rate of 0.6% (the price of electricity and various fuels does not change at the same rate as the inflation). Other annual maintenance cost, replacement cost and profit from salvage are also included in the analysis (see Table 8-7). The current electricity price in Vietnam is 0.0741 \$/kWh (EVN, 2013). The initial construction cost is calculated by EnergyPlus based on estimated component costs (MOC, 2011) as listed in Table 2. Other secondary costs related to building construction, e.g. miscellaneous cost, design and engineering fees, contractor fee, contingency, permission, bonding and insurance, commissioning fee, equipment cost, foundation cost... are also included in the analysis as shown in Table 8-7.

Table 8-7: Other costs and fees (exchange rate 1\$ = 20840VND)

Item name	Row house	Detach house	Apartment	Frequency
HVAC system cost	970 \$/unitary	480.67 \$/unitary	480.67 \$/unitary	Initial cost
Total interior equipment cost (estimated)	700 \$	2400 \$	480 \$	Initial cost
Foundation cost (estimated)	2,500 \$	3200 \$	800 \$	Initial cost
Miscellaneous cost	5%	5%	5%	Initial cost
Design and engineering fees	5%	5%	5%	Initial cost
Contractor fee	32.67 \$/m ²	42.00 \$/m ²	32.67 \$/m ²	Initial cost
Contingency fee	0%	0%	0%	Initial cost
Building permission, bonding and insurance	0.3%	0.3%	0.3%	Initial cost
Commissioning fee	0.5%	0.5%	0.5%	Initial cost
Maintenance cost	250 \$	300 \$	100 \$	Every 2 years
Replacement cost	1400 \$	2200 \$	1400 \$	Every 10 years
Profit from salvage	-50 \$	-50 \$	-25 \$	Every 10 years

8.2.7 Optimization results

In this work, the optimization was performed on 3 housing models under 3 climatic regions so as to minimize 3 objective functions. As a result, 27 optimization runs were completed successfully. Total time required for this task was nearly one month. However, there were two optimization runs that did not result in any solutions because the constraints of the objective function were not satisfied. Table 8-8 listed the lowest objective values of the 27 optimization runs. The Appendix C reports all the inputs of the optimal solutions of all cases. The subsequent sections present the analysis on these optimization results.

Table 8-8: Lowest values of the objective functions found in 27 optimization runs

House type	Location	Objective function [A]	Objective function [B]	Objective function [C]
		Minimum TDH (hour)	Minimum construction cost that satisfies TDH <10% (US\$)	Minimum LCC (US\$)
Row house	Hanoi	984.75	no solution	84631.04
	Danang	38.08	35492.95	84326.37
	Hochiminh	10.33	35492.95	91823.62
Detached house	Hanoi	1483.75	no solution	127734.11
	Danang	14.35	56815.57	124220.59
	Hochiminh	0.85	56341.51	133670.32
Apartment	Hanoi	514.08	10683.4	38657.73
	Danang	21.25	9688.39	40364.87
	Hochiminh	127.5	9598.25	46378.86

8.2.7.1 Optimization time and convergence issue

The optimization time is almost equal to the total time required for running all the simulations that the optimization algorithm launches. The number of simulations again depends on the natures of the objective function because the objective function will strongly affect the convergence of the optimization. The convergence of the Hybrid algorithm can be confirmed when the minimum point is found by the PSO algorithm and then the search clusters around this point. Once the optimization is convergent, the search of the Hybrid algorithm will be processed much quicker than that during the initial generations. Figure 8-11 shows an example of the improvement of the cost function and the convergence in the optimization of the AC detached house in Hochiminh city. This figure also shows two phases in the optimization which was done by the PSO and the Hooke-Jeeves algorithm.

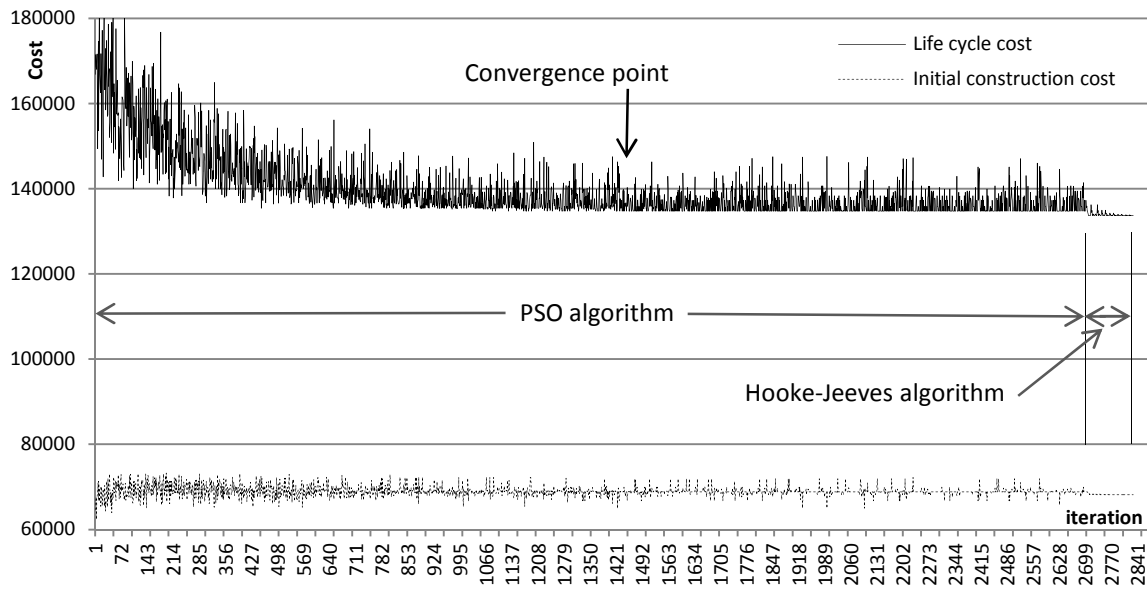


Figure 8-11: A typical optimization process (AC detached house, cost function [C])

During the optimization, it was found that the convergence of the three objective functions was rather different. Table 8-9 reports in detail the time and convergence issues of the detached house. The simulation time for the NV cases (function [A] and [B]) is much greater than that of the AC cases (function [C]) due to the coupling between the airflow network model and the thermal simulation module. Even if the lowest point was found much early, the function [B] required longest time because of the complex structure of the penalty function in [B]. It can also be observed that the total optimization time is still significant.

Table 8-9: Time and convergence issues in the optimization of the detached house

Location	Objective function	Operating mode	Smallest number of generation required for convergence	Total time of the optimization*
Hanoi	[A]	NV Detached house	36	14:38:50
	[B]	NV Detached house	No solution	-
	[C]	AC Detached house	21	09:03:23
Danang	[A]	NV Detached house	31	14:46:01
	[B]	NV Detached house	41	19:22:42
	[C]	AC Detached house	30	08:41:46
Hochiminh city	[A]	NV Detached house	47	17:12:20
	[B]	NV Detached house	17	18:40:16
	[C]	AC Detached house	29	10:20:30

* The optimization ran on 3 processors, thus 3 simulations could run in parallel. The optimization was performed on a PC with the processor Intel Core i5 M460 (4 x 2.53 GHz), 4 GB RAM.

All optimization runs achieved convergence, confirming that the number of generations was correctly set. The optimization results were therefore the best solutions found by the Hybrid algorithm.

8.2.7.2 Efficiency of the simulation-based optimization method

It is important to know the capability of the simulation-based optimization method in improving a design target such as indoor environment quality or building energy consumption. This allows designers to choose an appropriate method among a number of available approaches that can satisfy their time budget, resources and design objectives. To quantify the efficiency of the optimization method, this study compared the optimization results with the corresponding reference data.

Firstly, TDHs of the optimal NV houses found by the objective function [A] were compared with the references established in section 5.6.1. The TDHs of the improved houses by the parametric simulation method in section 7.1.6 was also included in the comparison. Figure 8-12 graphically presents the result.

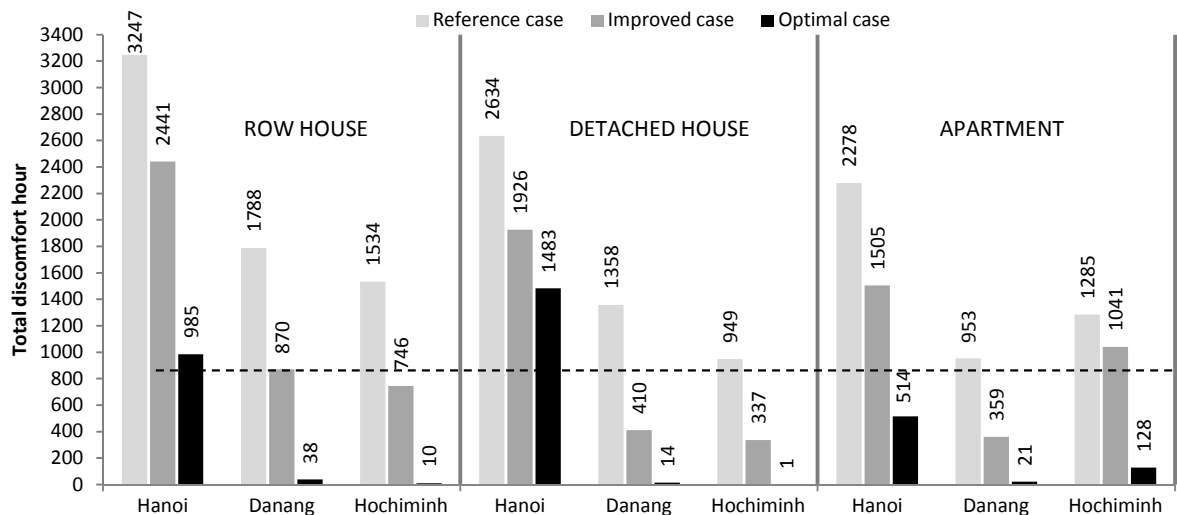


Figure 8-12: Comparison of the TDHs in the NV houses. The horizontal line indicates the acceptable threshold of the TDH.

It can be observed that the optimal cases offered great reductions of the TDH. The largest reduction of 99.9% occurred in the detached house in Hochiminh city. The smallest reduction of 43.7% can be observed in the detached house in Hanoi. The optimal cases always outperform the improved cases. Average TDH reduction of the optimal cases was 86.1% while that of the improved cases was only 44.9%. It is worthy of note that most of

the optimal houses were nearly perfect, in term of the TDH; thus energy for mechanical heating and cooling systems is not required. In Hanoi, the optimal row house and detached house did not satisfy the thermal comfort criterion, indicating that other heating – cooling methods are needed. The thermal classification of the optimal houses shown in Table 8-10 reveals that significant improvements were made on these houses.

Table 8-10: Thermal classification of the optimal houses

	% of time comfort limit is exceeded	Classification
Row house - Hanoi	11.24	Poor
Row house - Danang	0.43	Nearly excellent*
Row house – Hochiminh city	0.11	Nearly excellent
Detached house - Hanoi	16.92	Poor
Detached house - Danang	0.16	Nearly excellent
Detached house – Hochiminh city	0.01	Nearly excellent
Apartment - Hanoi	5.87	Good
Apartment - Danang	0.24	Nearly excellent
Apartment – Hochiminh city	1.46	Good

* ‘Nearly excellent’ means that the TDH is smaller than 1% of a year

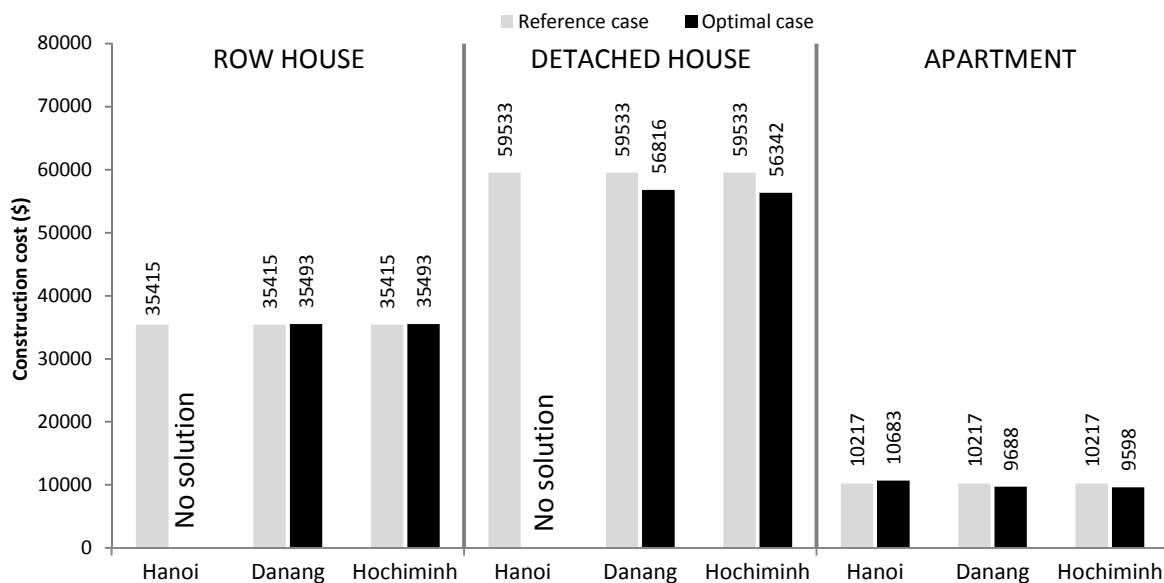


Figure 8-13: Minimum cost of the NV houses that satisfy thermal comfort criterion

Secondly, the minimum construction cost required for acceptable thermal comfort was compared with that of the reference houses as shown in Figure 8-13. It can be seen that the most of the minimum costs were not able to be reduced, compared with the reference costs. Nevertheless, the optimal houses found by the objective function [B] were thermally

comfortable all year round with the TDH below 10%. In Hanoi, the row house and the detached house had no answer to the problem.

Finally, the life cycle cost defined by equation (8.6) of the optimal cases and that of the reference cases were compared as shown in Figure 8-14. It can be observed that the LCC reductions were not as significant as the TDH reductions. The reduction amounts by the optimization were fairly uniform with an average reduction of 14.6% of the LCC.

In conclusion, the reduction of the cost functions or the efficiency of the optimization method may vary in a wide range, from 0% to 99.9%. The reductions depend on characteristics of the design objective. The optimization of the objective function [A] resulted in significant reductions of the TDH with an average of 86.1%. Nevertheless, cost reductions for the objective function [C] were not really significant as the average reduction only reached 14.6%. The study also shows the considerable potential of the optimization in comfort improvement and energy saving through the reductions of the LCC. The benefit given by the simulation-based optimization is actually remarkable while the computational cost is gradually decreased by advances in computational technologies. Since the work to couple EnergyPlus - GenOpt and then to define the optimization problems takes only a few hours, the optimization method shows a very promising applicability and can yield considerable economic gains.

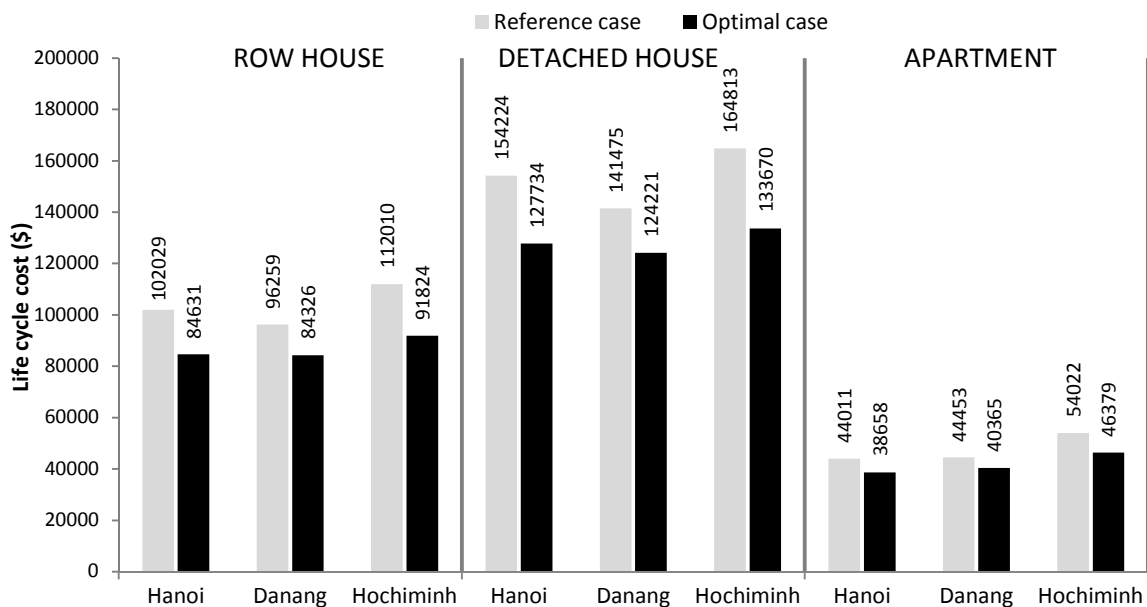


Figure 8-14: Optimal LCCs, compared with LCCs of the reference cases

8.2.7.3 Optimal solutions for the NV houses

Details of the optimization results were shown in the Appendix C. All these results are reported in the form of numerical data and they are certainly not easy to understand. In this section, the interpretation of these data was done and reported. From the optimization results of the objective function [A], for an ideal thermal comfort condition in NV residential buildings, the design strategies for each climatic region in Vietnam should follow the guides as shown in Table 8-11.

Table 8-11: Design guides for optimal thermal comfort in NV residential buildings

Design parameter	Hanoi	Danang	Hochiminh city
External wall color	Brightest color should be used; if the house has many thermal zones on the ground, darker color scheme can be used		Brightest color should be used
Roof color	In most cases, reflective roof or roof with brightest color must be used		
Opening crack infiltration	Crack infiltration should be minimized to prevent heat exchange when openings are closed. Very small increased infiltration may be required, but this is not common. Strong infiltration was not observed in any cases		
Infiltration of the attic	Small openings (if any) combined with less infiltration		Largest openings (if any) and well ventilated attic are preferred
Glazed window area	Minimize glazed areas on building façades even if high performance glass is used. If glazed windows are inevitable, they must be shaded or protected from solar radiation.		
Length of window overhang	Largest shading devices are highly recommended in most cases	Generally large shading devices are better, but there are some exceptions	Largest shading devices are highly recommended in most cases
External wall type	22cm brick wall with a high level of thermal insulation (4 cm) is recommended		
Glazed window type	High performance glazed windows are recommended		
Roof insulation	Highest level of thermal insulation for steel sheet roofs to protect the roof attic from overheating. Thermal insulation for ceiling is also recommended		
Ventilation scheme	Night ventilation during summer periods (combined with massive internal structures) is recommended. In other periods the openings should be kept closed		Night ventilation during hot weather is highly recommended
Floor on the ground	Minimized insulation so as to facilitate the heat exchange between the earth and thermal zones on the ground floor, no exception		
Internal thermal mass	Structures with high thermal inertia are recommended. However, thermal mass should be used in conjunction with a suitable ventilation scheme to maximize the efficiency of thermal inertia of the mass		

It is necessary to note that all optimal solutions of the objective function [A] consistently require combinations of massive internal structures and night ventilation during warm and hot periods. This requirement may increase indoor humidity and CO₂

concentration due to limited ventilation during day time. In such a case, occupants still feel thermally comfortable but they may find IAQ unacceptable.

This study therefore performed another series of optimization to test another scenario according to which **ventilation is always available during warm and hot periods**. The optimization results of this scenario showed that the optimal design variables were almost unchanged while new minimum TDHs slightly increased (in Danang, new TDH% were 3.2%, 0.9% and 2.7% in the optimal row house, detached house and apartment, respectively). Notably, a high insulation level in external walls and internal walls with high thermal inertia were still required in new optimal NV houses regardless of ventilation schemes during warm and hot periods.

It can be seen that the design guides in Table 8-11 will result in increases of construction cost because of the increases of thermal mass, thermal insulation, stronger air tightness and high performance glazed windows. By comparing the construction costs of the case-study houses with those of the optimal houses, this study found that average increases of construction cost of the optimal row houses, the detached houses and the apartments were 22.7%, 12.0% and 23.4%, respectively. In the context of Vietnam, these increases of construction cost are considered significant. It is therefore relevant that both thermal comfort criterion and construction cost should be considered in a mutual relationship. The optimization results of the objective function [B] provide solutions for comfortable housing models at moderate cost. Table 8-12 shows how to obtain this objective through some simple guides.

In Table 8-12, the optimal low-cost houses in Danang and Hochiminh city are simply the combinations of smallest and low-cost building components with some passive features of the building envelope and appropriate ventilation schemes. This simple requirement makes low-cost housing quite feasible in these regions thanks to their warm climates.

The climate of Hanoi is more unfavorable; thus a comfortable house usually requires higher total investment and more robust design than those in other regions in Vietnam. In many cases, it is very difficult to create comfortable dwellings without mechanical heating-cooling systems. This work therefore recommends that the design of low-cost residential buildings in Hanoi must be carefully considered under the light of both occupants' comfort and building cost.

Table 8-12: Design guides for low-cost house with acceptable indoor thermal comfort

Design parameter	Hanoi	Danang	Hochiminh city
External wall color	Brightest color (e.g. white) should be used	Very bright colors (e.g. light blue, light green, yellow, pink...) should be used	Brightest color (e.g. white) should be used
Roof color	No information	Reflective roof or roof with brightest color must be used	
Opening crack infiltration	Smallest infiltration	Air tightness is not very important as moderate infiltration in many cases is allowed. However, a few exceptions (good air tightness) can be observed.	
Infiltration of the attic	No information	Generally, attic spaces should be well ventilated, using large ventilation holes	
Glazed window area	Smallest glazed areas		
Length of window overhang	All regions require small overhangs / shading devices (this requirement seems to reduce construction cost rather than improving thermal comfort. Larger overhangs in optimal solutions can further improve thermal comfort)		
External wall type	22cm brick wall with 4cm insulation	11cm brick wall to reduce cost	
Glazed window type	High performance glazed windows	Simplest single glazed windows to reduce cost	
Roof insulation	No information	No insulation so as to reduce cost	
Ventilation scheme	Night ventilation during summer periods	Full ventilation or night ventilation in summer periods	There are some adequate ventilation schemes such as: full ventilation in summer and mild seasons, night ventilation summer, night ventilation all year round
Floor on the ground	No information	Minimized insulation so as to facilitate the heat exchange between the earth and thermal zones on the ground floor, no exception	
Internal thermal mass	Minimized thermal mass (it reduces construction cost, but it may increase discomfort periods)		

8.2.7.4 Optimal solutions for the AC houses

According to the optimization results, the design of optimal AC houses should follow the design guides as presented in Table 8-13. It can be seen that the optimal NV and AC houses were almost similar in all design features, except the choice of internal thermal mass. Generally, massive internal structures are only suitable for NV houses while it should be avoided in AC houses. It is likely that massive internal structures in the AC houses will require extra heating – cooling load for warming or cooling the high thermal inertia of the structures, resulting in profitless energy expenses. Conversely, in NV houses massive

internal structures can provide the high thermal inertia which is able to maintain a stable indoor condition. In hot climates, the effect of thermal mass can be maximized if it is used in conjunction with a nocturnal ventilation scheme.

Table 8-13: Design guides for AC residential buildings

Design parameter	Hanoi	Danang	Hochiminh city
External wall color	Brightest color (e.g. white) must be used		
Roof color	Reflective roof or roof with brightest color must be used		
Opening crack infiltration	Air infiltration must be minimized		
Infiltration of the attic	Airtight	Well ventilated attic	Airtight
Glazed window area	Smallest window area		
Length of window overhang	This design option may vary, depending on the housing types. The optimal row house and detached house require smallest window overhangs. The optimal apartment is quite different from the others, requiring largest overhangs for windows		
External wall type	22cm brick wall with a thick layer of thermal insulation (4cm)	22cm brick wall with or without a moderate layer of insulation (2cm)	22cm brick wall with a thick layer of thermal insulation (4cm)
Glazed window type	High performance glazed windows are recommended		
Roof insulation	Highest level of thermal insulation for steel sheet roofs to protect the roof attic from overheating. Thermal insulation for ceiling is also recommended		
Floor on the ground	Minimized insulation so as to facilitate the heat exchange between the earth and thermal zones on the ground floor		
Internal thermal mass	Minimized thermal mass		

8.3 Discussions and comparisons

8.3.1 Discussions

It is important to stress that an optimal solution is not simply the combination of the ‘best’ design variables. As an example, common design knowledge for hot humid climates indicates that large overhangs, light weight building envelopes, very large openings... should be used. These recommendations are not always true in the optimal cases found by the optimization method. Intrinsically, the design variables exhibit very complex interactions and nonlinear effects on the performance of a building. If all variables are varied simultaneously, the effect of each variable cannot be estimated by any linear principle. Hence, optimal buildings cannot be achieved by trial and error, even with experienced designers. Optimization is clearly a very effective method to achieve the best (or nearly best) solutions to a specific building design problem.

In another aspect, a design variable of an optimum solution is not necessarily the best choice for a specific design situation. More specifically, the best solution given by the parametric simulation method is not necessarily the solution given by the optimization method. For example, assuming that the thermal performance of the apartment in Hanoi needs to be improved by changing the composition of external walls alone, the best option is not the “220mm brick wall with 4mm EPS insulation” (as indicated by the optimal solution), but it should be the “220mm brick wall with 10mm EPS insulation” (as indicated by the parametric simulation method - see section 7.1.1). **So it is easy to recognize that the optimization method is more suitable for the design of new buildings during which many design variables can be controlled and adjusted simultaneously. Conversely, in a building renovation project improvements can be achieved through a few modifications which are easily defined by the parametric simulation method.**

It is necessary to discuss a limitation of the thermal dynamic simulation method. In reality, buildings with large openings may enhance natural ventilation and thereby possibly improving thermal comfort due to elevated air velocity. On the other hand, large openings are able to promote the efficiency of night ventilation in buildings with massive building structures. However, most thermal simulation tools cannot take the cooling effect of instantaneous airflows into calculations of thermal comfort indices. Thus in building thermal simulation, larger windows only increase the air flow rates and the heat gain/loss through the building envelope, but perhaps predicted thermal comfort will not be improved by natural ventilation. Consequently, small windows usually result in better building thermal performance. That is possibly the reason why in the optimization smallest windows have been required for optimal thermal comfort. Hence a question has been raised as to whether large or small openings should be used in Vietnam. A possible answer is to follow the experience of the vernacular architecture in Vietnam (see CHAPTER 6), according to which multiple openings can be used and must be well shaded and/or using 2-layer windows (see Table 6-4). In any case, glazed surfaces on building facades should be avoided or minimized.

In a recent study (Nguyen & Reiter, 2013) the climate responsive design strategies for a simple model of a rectangular detached house in Vietnam (see Figure 8-15) were investigated using the simulation-based optimization method. This is the generic simplified

model for many housing types and typologies; thus optimization results may reveal appropriate design principles that can be considered as the reference for more sophisticated buildings. The design variables and objective functions in this study were similar to those in the present work.

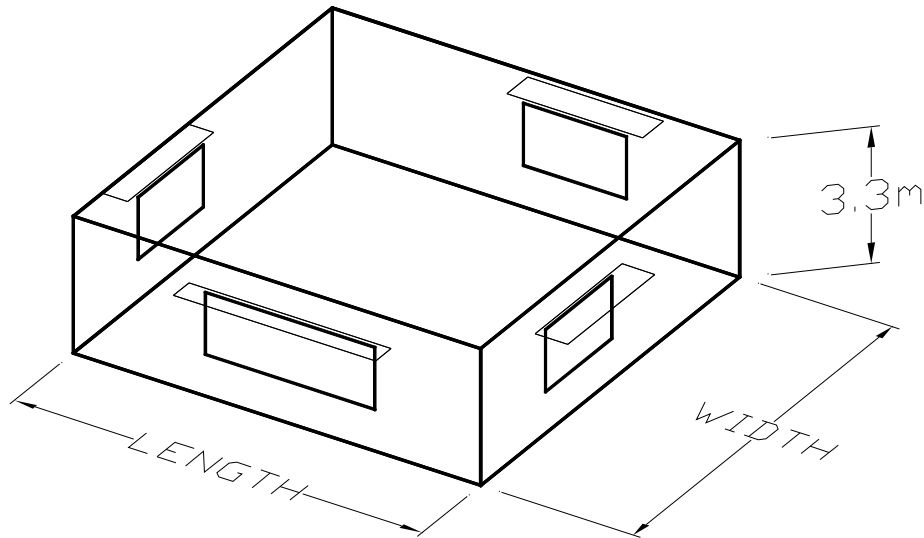


Figure 8-15: The simple rectangular housing model (Nguyen & Reiter, 2013)

The design guides for three climatic regions of Vietnam were derived as shown in Figure 8-16. In Figure 8-16, the design variables were normalized so that their values vary between 0 and 1. By comparing the optimization results of this chapter and this figure, it can be seen that there is a good agreement among them although the housing models are different. In addition, the figure also recommends optimal building orientations and shape according to which (i) the shape of NV buildings should be long and narrow and the building long axis should be shifted to an East-West orientation and (ii) the shape of AC buildings should be square or nearly square to minimize the total area of the envelope.

The design of NV and AC houses has some notable differences such as the building shape and thermal mass. The internal thermal mass is only required in NV buildings, maybe for night pre-cooling when night ventilation is applied. The shape of the AC houses should be square or nearly square while an East-West long rectangular geometry is suitable for the NV houses. These indicate that designers should take environmental control methods, e.g. NV or AC running modes, into consideration in initial stages of the design process so as to propose adequate solutions.

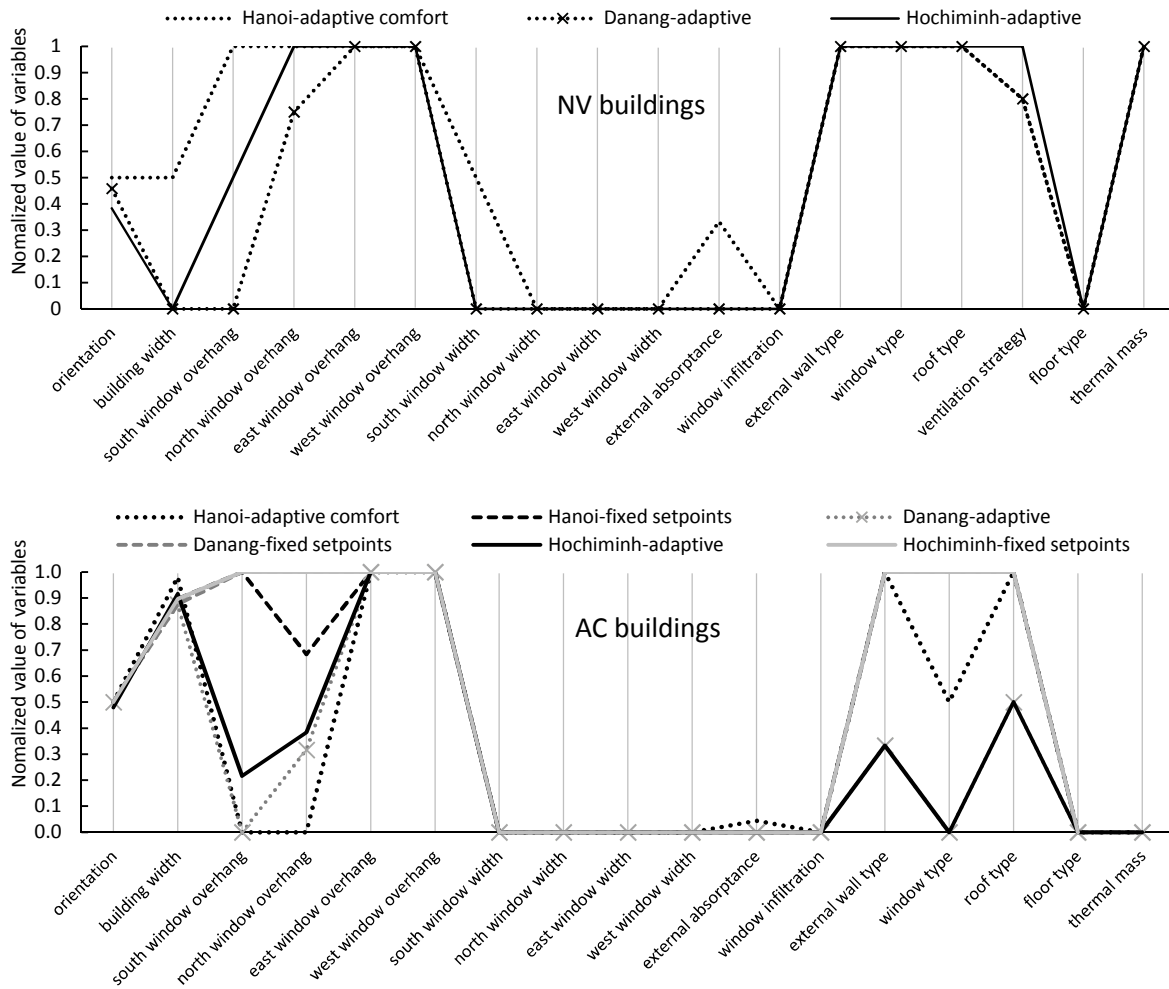


Figure 8-16: Design guides for an isolated rectangular housing model (AC houses use a fixed thermostat and an 'adaptive' thermostat)

8.3.2 Comparison of the findings of this work with results of earlier studies

In order to examine the agreement as well as the reliability of the results, the optimal design guides of the present work were compared with the recommendations of other authors, methods and the experience of the vernacular housing in Vietnam. Table 8-14 shows the result of the qualitative comparison. In this comparison, the 5-point Likert scale (Likert, 1932) was employed to estimate different degrees of agreement.

Due to a number of differences in study conditions, climate classification methods and semantic contents of the statements, these comparisons have to be considered with much care. It can be seen that 3 design choices found by this work were strongly rejected by the earlier recommendations, indicating that these design choices are, at any rate, not

reliable. They were “less ventilation - attic space”, “night ventilation scheme during hot weather conditions” and “massive building structure”. There are some reasons for these disagreements among which the assessment criteria, the different contexts and the semantic issues are possibly important. Most authors disagreed with the strategy “massive building structure” and “night ventilation” because of the concern of damp indoor air during day time when no ventilation occurs.

Table 8-14: Findings of the present work and those of other authors and tools

Main findings of the present work	The findings of other authors				Recommendations by other methods		
	(Givoni, 1969)	(Olgyay, 1963)	(Koenigsberger et al., 1973)	(Szokolay, 2004)	Vernacular housing	Climate Consultant	Mahoney tables
Long rectangular building shape – East-West building long axis	?	✓✓	✓✓	✓✓	?	?	✓✓
Light external wall color	✓✓	✓✓	✓✓	✓	✓✓	✓✓	?
Light or reflective roof color	✓	✓✓	✓✓	✓✓	?	✓✓	?
Minimized infiltration when openings are closed	?	?	?	?	?	?	?
Less ventilation - attic space (in Hanoi and Danang)	✗	✗	✗	✗	✗	?	?
Well ventilated attic space (in Hochiminh city)	✓✓	✓	✓✓	✓✓	✓	✓✓	?
Smallest glazed window area	?	?	?	?	?	✓	?
Large shading device	✓✓	✓✓	✓✓	?	✓✓	✓✓	?
Well insulated external walls (by optimization)	✓✓	✗	✓✓	✓	✗	?	?
Simple external walls, except Hanoi (by parametric simulation)	✗	✓	?	?	✓	✓	?
High performance glazed window	?	?	?	?	?	✓	?
Strong roof and ceiling insulation	✓✓	✓✓	✓✓	✓	✓	✓✓	✓✓
Night ventilation during hot weather conditions (by optimization)	✗	?	✗	✗	?	?	?
Full day ventilation during hot weather conditions (by parametric simulation)	✓✓	✓	✓	?	?	?	?
No insulation for floor on the ground	?	?	?	✓	✓✓	?	?
Massive building structure	✗✗	✗	✗✗	✓✗	✗	✓✓	✗✗

✓✓: strongly agree; ✓: agree; ?: Neither agree nor disagree; ✗✗: strongly disagree; ✗: disagree;

In Table 8-14, the symbol “✓✗” occurs once with the choice of thermal mass, indicating a hybrid construction type recommended by Szokolay (2004). He proposed that lightweight construction can be applied to bedrooms of a house while massive structures for other daytime rooms (living, dining, kitchen).

Based on the results of Nguyen and Reiter (2013) and the result of the optimization using “forced” ventilation scheme in section 8.2.7.3, the optimal choices should be revised as follows:

- Well ventilated attic space combined with an insulated ceiling,
- Full day ventilation during hot weather conditions (or night ventilation scheme combined with controlled ventilation in day time),
- Light weight and well insulated external building structures combined with massive internal structures.

These solutions may result in a slight increase of the TDH, but in compensation the IAQ (humidity, concentration, air movement, and natural light) will be improved considerably.

The choice “smallest glazed window area” has hardly been mentioned by the previous authors. Conversely, these authors recommended large to very large openings to facilitate natural ventilation. Nevertheless, in any case large openings must be shaded and protected well from both direct irradiation and diffused irradiation which are almost equally important in hot humid climates. Other recommendations of this work were in good agreement with those of other authors, confirming that they are highly reliable.

8.4 Chapter conclusion

This chapter was developed through two phases with the aim of optimizing the thermal comfort and cost in both NV and AC housing models. In the first phase, the sensitivity of these three models to the variation of design parameters was quantitatively measured by using a Monte Carlo-based sensitivity analysis. Parameters that have significant impacts on the outputs of these models were selected for use in the second phase – optimization. In this phase, the thermal comfort and the construction cost in NV houses and the life cycle cost in AC houses were optimized by the simulation-based optimization method.

Through the sensitivity analysis, the most important parameters of each housing model were derived. These parameters have significant impacts on the thermal performance as well as energy consumption of a house. The most important groups in NV houses were the roof configurations, the ventilation scheme, and the external building envelope. In the AC houses, the roof configurations, the heating cooling setpoints, the COP of the PTACs and the building envelope showed significant impacts on the energy consumption.

It is necessary to stress that by simply using a bright wall color (e.g. white or light yellow), it is possible to significantly improve indoor thermal comfort and reduce energy consumption by the houses. This study also emphasizes that thermal insulation in metal roof should be a compulsory design requirement (e.g. in building codes) because the roof thermal insulation is the most significant parameter in many cases.

The optimal cases obtained by the optimization method showed significant thermal comfort improvements with the average reduction of the TDH of 86.1%. Improvements of the building LCC were much more modest with the average reduction of only 14.6%. The specific design guides for each climatic region of Vietnam to obtain optimal building performance were derived from the optimal models. After the discussion and the rigorous comparison, general design recommendations for Vietnam were also outlined.

Some discrepancies among the solutions given by the parametric simulation method and optimization method indicated that these methods should be used in accordance with the problem at hand. In new building design, the optimization method should be used as all design variables can be controlled. In building renovation and retrofit with limited design options, the parametric simulation method seems to be more suitable.

CHAPTER 9

CONCLUSIONS AND FURTHER WORKS

The last chapter summarizes the main original contributions developed in this thesis and provides general design recommendations for the three climate regions in Vietnam. It also outlines possible future extensions of this thesis through new researches.

9.1 Original contributions of the thesis

9.1.1 A simple climate-comfort analysis tool for hot humid climates

A considerable number of climate analysis tools have been developed during recent years for some applications in building design. However, these climate analysis tools are not easy to use in building design by professionals due to their complexity. Some others require stringent environmental conditions of thermal comfort so as to apply in developed countries and/or in temperate climates. At different levels, these tools are inappropriate or inaccurate for applications in developing countries for two reasons: (i) developing countries mostly lie in hot and humid regions; and (ii) people usually have much lower expectation due to the adaptation mechanism.

In this thesis, an improved climate-comfort analysis method was developed and presented through its fundamental algorithms. Its prediction relies on the basis of data derived from TMY weather files which provide the most typical weather pattern and detailed weather information of a region. The method has some positive features. Firstly, it is simple and easy for use by building designers. Secondly, its settings are easy to be modified by users to meet different criteria of thermal comfort and climate types, including the hot humid climate. Finally, the analysis outputs are flexible and can be establish at different levels of details. The analysis results of three climatic regions of Vietnam have demonstrated the basic capabilities of the method. This can be refined and applied by

software programmers to develop computer weather analysis tools and comfort assessment tools in building simulation.

9.1.2 An adaptive thermal comfort model for South-East Asia

The present work successfully developed a thermal comfort model based on the adaptive theory. The reliability of the model was confirmed by the huge database that the model relied on and stringent criteria in statistics. The model can be used to predict comfort temperature of occupants in NV buildings in Vietnam as well as in South-East Asia, provided that adaptive behaviors of occupants are allowed. This thesis also introduced a method used to calculate the length of the comfort period in a year given by a climate, providing an estimate of minimum comfort performance that must be satisfied by every NV building.

Applications of this adaptive comfort model have indicated that the comfort temperature in South-East Asia is slightly higher than that of the world as predicted by the ASHRAE adaptive comfort model (ASHRAE, 2004). This is the consequence of long-term adaptation to hot and humid weather conditions in the region, resulting in looser acceptable thermal environment (or greater percentage of satisfied occupants) and potential cooling energy saving. This adaptive comfort model is therefore valuable in terms of both thermal comfort studies and strategies towards a greener built environment.

9.1.3 Thermal performance of vernacular housing and current housing typologies in Vietnam

A comprehensive investigation on climate responsive strategies applied in vernacular housing in Vietnam was carried out by using both qualitative and quantitative assessment methods. It was found that natural ventilation, building orientation, building shape and solar shading were the most commonly-used strategies in vernacular housing. The modeling results of a case-study vernacular house in Hanoi show relatively stable indoor temperature, regardless of the fluctuations of the outdoor temperature; the indoor condition is generally thermally acceptable but the house failed to protect occupants from cold weather, showing the interest of applying more sophisticated design solutions, e.g. using thermal insulation, Trombe walls. This study provides valuable lessons for modern applications and gives evidence that humans can live in harmony with nature without

consuming much energy. Vernacular housing has provided valuable social, cultural and scientific values, confirming the need to preserve vernacular architecture in Vietnam.

This thesis includes also indoor comfort assessments of the current housing stock in Vietnam. Three most common housing prototypes in Vietnam were selected: an urban row house, a detached house and an apartment. Various techniques (in situ monitoring, building thermal simulation, CFD and airflow network modeling, numerical model calibration, parametric simulation method) were used to assess and improve the thermal performances and natural ventilation of these houses. The detached house and the apartment perform better than the row house under the hot humid climate of Vietnam. The discomfort period is generally longer, for the three house types, in the North of Vietnam than in the central and South of Vietnam. Generally, indoor comfort is not guaranteed by the current design in Vietnam. Today, comfort improvement strategies for building design are really needed, in order to prevent the cold in the North of Vietnam and the overheating in all regions. Thermal performances of these houses are considered as references for the current design assessment in Vietnam and will be useful for numerous other building researches.

9.1.4 A new bioclimatic approach towards sustainable architecture

The conventional method to bioclimatic architecture was mostly based on the works of Olgyay and Givoni. This thesis demonstrates an innovative, comprehensive methodology to establish design strategies for comfortable, low-energy and low-cost buildings in a climate by using the simulation-based approach. Using this approach, the relationship between the climate and the climate responsive design is established through the optimization process on computer building models.

Although this is not a new idea in building research, the comprehensive procedure (both parametric simulation and optimization methods) used in this thesis seems to be more efficient in improving building performance and could provide more explicit results. This procedure was also a pioneering effort in quantifying the efficiency of two most common simulation-based design methods (parametric simulation and optimization method) in improving two building performance indicators: thermal comfort and energy consumption. Such information helps to answer the question whether a specific threshold of building performance can be achieved or satisfied even before starting a design process. Thus the efficiency is a basis for the selection of a design method.

9.2 Conclusions and recommendations

9.2.1 Comfort model for Vietnamese

In NV buildings, the mean neutral operative temperatures found in Vietnam and in South-East Asia were almost identical, around 27.9°C. This was about 2.2°C higher than the comfort temperature in climate-controlled environment, showing a deviatory effect of human adaptation on thermal comfort. However, the neutral standard effective temperatures in both AC and NV buildings were almost the same, about 25.5° - 25.7° SET*, indicating that the deviation of neutral operative temperature in NV buildings was mainly caused by behavioral adaptation (changing clothing, wind speed, activities...).

Through a meta-analysis, the thesis found a correlation between neutral operative temperature and monthly mean outdoor temperature in NV buildings. This correlation can be expressed by a linear function as follows:

$$T_{comf} = 0.341T_{out} + 18.83 \quad (9.1)$$

where T_{comf} is comfort temperature; T_{out} is monthly mean outdoor temperature.

This linear function shows a periodical variation of the neutral temperature in accordance with prevailing outdoor conditions. Individual adaptation is mainly the reason of this variation. Finally, the changeable comfort temperature has questioned the rationality of the fixed HVAC thermostat in climate-controlled buildings, revealing a huge potential of building energy saving in hot climates.

9.2.2 The significance of design parameters

During the building design process, designers should be aware of the significance of design parameters so as to optimize the performance of the building. Through the Monte Carlo-based SA, the present work provides an insight of variables' significance in both NV and AC houses. The results of SA may help designers in selecting suitable solutions for their design problem. It is also useful for making choices in building renovation and retrofit.

Based on the SA of the case-study houses under the climate of Danang, the sensitivities of the TDH and TEC to the variation of design variables were defined. In NV buildings, the configuration of building envelopes (e.g. roof, external walls...) and ventilation strategies are the most influential factors. Meanwhile, the building envelope, the

thermostat, COP of HVAC systems and internal heat sources are significant in AC buildings. The SA has indicated that roof insulation and roof color play very important roles in controlling the outdoor – indoor heat flow. However, the practice in Vietnam has shown that the metal roof was not obtained enough attention of designers that usually results in poor building performance. This incorrect design thinking must be changed.

This analysis assumed that the SA with the climate of Danang could provide generic results for the whole Vietnam. However, this hypothesis needs to be verified by further investigations with other climate patterns.

9.2.3 Climate responsive design for optimal thermal comfort

This thesis studied the climate responsive design strategies by both the parametric simulation method and the optimization method. These two methods were based on different assumptions (e.g. climate change during 50 coming years is neglected) and their results were not the same in some categories. Their applications are therefore different as reported in the following guides and recommendations.

** For building renovation:*

Building renovation usually limits the design choices according to the context, building status, construction budget, urban design laws... Designers may have only a few design options. In such cases, the solutions derived from the parametric method can be used. Each solution can be applied separately as they almost result in positive effects on indoor thermal comfort. Table 9-1 summarized the results for the three climatic regions of Vietnam.

Table 9-1: Design guides and recommendations for building renovation

Hanoi	Danang	Hochiminh city
High level of thermal insulation for external walls	220mm brick wall with an air gap between two brick layers is effective	220mm brick wall without thermal insulation
Air leakage through external openings should be limited	Air leakage through external openings is NOT significant	
Full day ventilation OR night ventilation during summer and mild seasons	Full day ventilation OR night ventilation during summer and mild seasons	3 ventilation schemes can be used, depending on a specific situation. However, full year ventilation is always a good choice for most cases with possible slight decrease of thermal comfort.
Use brightest color for external walls; highest level of thermal insulation for the roof; largest overhangs for glazed windows; windows with low U-value; massive structures (NV buildings only).		

** For design of new buildings:*

In the design of new buildings, designers are able to control all design variables and they can vary these variables simultaneously with fewer constraints. This design situation can be seen as an optimization problem in which the designers are the “optimization engine” and the design variables are optimization parameters. It is therefore relevant that the design principles derived from the optimization and comparison in CHAPTER 8 can be applied. The optimal design principles for the three climatic regions of Vietnam are presented in Table 9-2.

Table 9-2: Optimal combinations of design variables for new buildings

Hanoi	Danang	Hochiminh city
Rectangular building plan with moderate building width, building long axis shifts to the East-West direction	Longest and narrowest building plan and building long axis shifts to the East-West direction	
Bright color for the roof and external walls can be used, but exception does exist, especially in Hanoi		Brightest color for the roof and external walls is compulsory
Maximize window overhangs	Maximize window overhangs, but there are some exceptions	Maximize window overhangs
Minimize ventilation roof attic		Well ventilated roof attic
Night ventilation – only in summer		All year night ventilations due to hot weather all year round
Minimize air leakage through external openings (small increased leakage may be required, but not common); minimize glazed areas on building façades; 220mm brick walls with a high level of thermal insulation; Highest level of thermal insulation for both the roof and ceiling; high performance windows; massive structures (NV buildings only); ground floor slabs without insulation.		

Due to very complex, non-linear interactions among design variables, these combinations must be respected as strictly as possible, unless non-optimal or unexpected results may occur.

In warm and humid climates, ventilation is always preferred to prevent damp air in occupied spaces. However in some cases, night ventilation during hot weather is required for pre-cooling thermal mass and day time ventilation is consequently limited. This thesis therefore recommends that indoor humidity must be controlled by using dehumidification devices or simply using periodical ventilation powered by electric fans. Another choice is to allow natural ventilation all the time with slight sacrifice of thermal comfort.

In hot and humid climates, glazed windows should be minimized to avoid overheating due to strong solar radiation. On the other hand, natural ventilation needs large openings to promote ventilation rates. These requirements are likely contradictory. This study proposes that large glazed windows can be used, provided that they are protected from both direct and diffused radiation (e.g. using vertical roller blinds, French windows).

**For low-cost housing:*

The design of an optimal low-cost dwelling with acceptable indoor thermal comfort is nearly the same; but the demand of reducing the construction cost leads to the cut-off of thermal insulation and massive building structures. These simple requirements make low-cost housing quite feasible in the warm central and south regions of Vietnam. The climate of Hanoi is more unfavorable; thus comfortable houses usually need higher investment such as thermal insulation or mechanical heating and cooling systems.

**For AC buildings:*

The design of AC buildings to minimize energy consumption and operating cost is nearly similar to that of NV counterparts, except that internal thermal mass and external building areas should be minimized. The ideal shape of such a building type should be square or nearly square to minimize the building envelope area. Heat from gas stoves, electric appliances... is very important thermal loads in AC buildings and should be expelled from the house by forced ventilation.

9.2.4 The efficiency of different design methods

By comparing the performances of the reference cases, the improve cases and the optimal cases, the efficiency of the parametric simulation method and optimization method could be derived. This thesis found that the optimization method significantly outperforms the parametric simulation method. In NV houses, the average reductions of the reference TDHs by these two methods were 44.9% and 86.1%, respectively. On the other hand, as the optimal (or nearly optimal) solution can be obtained after an unique simulation setting, the optimization method requires less time and possibly fewer users' errors, compared with the parametric simulation method.

The level of cost reduction by the optimization method was found unstable. It depends on the nature of cost functions and may vary in a very wide range. This study has observed a reduction of the TDH up to 99.9% while the maximum reduction of the LCC

was only 18.0%. Average reductions of the TDHs and LCCs were 86.1% and 14.6%, respectively. Discomfort was nearly eliminated in most of the optimal NV houses. The optimization method offers a great support to architects and engineers in reaching passive buildings and even approaching zero energy buildings.

9.3 Further works

9.3.1 Sustainable housing under the perspective of building materials

This thesis has discussed the role of building materials with respect to the thermal comfort issue in a limited vision, i.e. only the EPS and some other common materials were examined. In practice, building materials can play a greater role in governing indoor air humidity, temperature and its fluctuation and thereby thermal comfort. Furthermore, the choice of building materials is among the most important measures to control building cost and the environmental impacts of a building during its life cycle. Vernacular housing in Vietnam has used many renewable, environmentally friendly materials while still maintained acceptable indoor thermal conditions. Local materials and self-fabricated materials are other attractive subjects related to housing sustainability. It is therefore interesting to further explore these issues of building materials under the context of Vietnam.

9.3.2 Feasibility of adaptive thermal comfort in climate-controlled buildings

Conventional AC buildings often apply fixed heating and cooling setpoints in controlling the HVAC system. These setpoints are usually based on the preferred temperature found by the experiments in climate chambers. However, in reality neutral temperature may vary in accordance with the climate through adaptive actions of occupants. Consequently, HVAC setpoints in accordance with the adaptive comfort temperature is possibly an alternative solution which may offer significant energy saving. McCartney and Nicol (2002) stated that occupants' satisfaction did not decrease if adaptive setpoints were imposed in AC office buildings. Some questions have arisen as to whether adaptive setpoints will interfere with occupant's satisfaction and performance in residential buildings and how much energy can be saved by the HVAC system using adaptive control algorithms. Such questions are obviously promising directions for the next research.

9.3.3 Climate responsive solutions for non-residential buildings

Non-residential buildings can be defined as buildings other than dwellings or buildings in which less than half of its gross floor area is used for dwelling purposes. In reality, non-residential buildings also occupy a considerable portion in the building stock of the country. Such buildings often have various functions and correspondingly different occupancy patterns; thus these buildings require special design and strategies which considerably differ from the design of residential facilities. Non-residential buildings are usually public buildings where users' work performance and energy consumption are the major concerns of designers. Climate responsive design strategies for non-residential buildings have become an interesting subject to study. The aim of such research will be to minimize discomfort (improve work performance) and to minimize energy demand for heating, cooling and lighting systems.

9.3.4 Passive design towards zero energy buildings in Vietnam

In a general sense, a 'zero energy building' is a building which has a total annual sum of zero energy/exergy transfer across the building-district boundary in a district energy system (Marszal, et al., 2011) and/or zero carbon emissions annually. Locating in the tropics, the climate of Vietnam offers many advantages to attain this target. This thesis has pointed out that in Vietnam comfortable NV buildings can be achieved, without using mechanical heating and cooling systems, by applying the optimization method. Consequently, further studies are needed to evaluate the validity and applicability of the 'zero energy building' concept in Vietnam through passive design and advanced renewable energy technologies (to compensate the energy consumption due to lighting, cooking, electric appliances, etc).

9.4 Towards sustainable housing in Vietnam

By focusing on climate responsive design strategies for housing in Vietnam, this thesis has developed new assessment tools and architectural recommendations that will be very useful for various actors involved in the development of the built environment. The new simple climate analysis tool for humid climates will help architects and offers the possibility of future developments to software programmers. The current thermal comfort

standard in Vietnam should evolve to take into account the adaptive thermal comfort model for South-East Asia developed in this thesis. This adaptive comfort model will also be very useful for building engineers as well as for future researches on comfortable buildings in Vietnam. The studies on current housing types and vernacular houses in Vietnam will enrich the teaching of architecture. They can also help to develop a political awareness of the importance of preserving vernacular dwellings and increasing Vietnamese current quality of life through a better housing design. The climate responsive design strategies developed in this thesis successfully provide general guidelines and recommendations for improved Vietnamese housing design towards comfortable and sustainable architecture; they will be useful for architecture teachers and building designers. The efficiency study on the parametric simulation method and the optimization method opens a new research field and will help building engineers to reach passive or zero-energy buildings.

Finally, although it is impossible to thoroughly cover all the aspects sustainable housing by this thesis alone, this work has provided analyzes, recommendations and lines of thought in relation to the three dimensions of sustainable housing. As the main goal of this thesis was to improve the quality of living environments and occupants' comfort, the social dimension represents the core of this thesis. Housing issue in Vietnam is still a big concern as in 2008, 72.2% of the existing housing was semi-permanent or temporary and 89.2% of the poor did not have a permanent shelter. These houses are extremely vulnerable to natural disasters, which occur very often in Vietnam, and indoor comfort is entirely not ensured by the current design. As a response to sustainability, this thesis has developed design strategies toward comfortable, energy-efficient housing with acceptable building cost.

The main results of the thesis in the social dimension are the new simple climate analysis tool, the adaptive thermal comfort model for South-East Asia and the climate responsive design strategies for Vietnamese housing that should improve future comfort requirements as well as buildings design. This thesis shows that it is possible to nearly eliminate discomfort in NV houses in Vietnam: the optimization method leads to an average reduction of 86,1% of the total predicted discomfort hours. The socio-cultural dimension has also been addressed by the study on vernacular and traditional architecture in Vietnam, showing the importance of preserving this cultural heritage.

The environmental dimension has been enhanced by the focus on naturally ventilated buildings, ensuring energy savings and reducing environmental impacts. This thesis shows that the comfort optimization method is really effective in reaching passive buildings and even approaching zero energy buildings in Vietnam. Note also that the adaptive comfort model developed has questioned the rationality of the fixed HVAC thermostat in climate-controlled buildings, revealing a huge potential of building energy saving in hot climates.

The economic dimension has been addressed by the optimization process of the construction cost of NV buildings and by a life-cycle cost optimization of AC buildings, providing strategies for affordable climate responsive housing in Vietnam.

The author hopes that this thesis is a first step towards more extensive research on large-scale development of sustainable housing in Vietnam as well as complementary aspects of sustainability in built environments such as urban planning issues, water management, biodiversity, etc.

REFERENCES

- Adams, B. M. et al., 2009. *"DAKOTA, A Multilevel Parallel Object-Oriented Framework for Design Optimization, Parameter Estimation, Uncertainty Quantification, and Sensitivity Analysis: Version 5.0 User's Manual"*. Livermore, CA: Sandia National Laboratory.
- Allard, F., 1998. *Natural ventilation in buildings – A design Handbook*. London: James & James.
- Andamon, M. M., 2005. *PhD thesis: Building climatology and thermal comfort – Thermal environment and occupant responses in Philippine office buildings*. Adelaide: University of Adelaide.
- Aronin, J. E., 1953. *Climate and Architecture*. New York: Reinhold Publishing Corporation.
- ASHRAE, 1992. *ASHRAE standard 55-1992: Thermal Environmental Conditions for Human Occupancy*. Atlanta GA: ASHRAE, Inc..
- ASHRAE, 2002. *ASHRAE Guideline 14-2002: Measurement of energy and demand savings*. Atlanta GA: ASHRAE, Inc..
- ASHRAE, 2004. *ASHRAE standard 55-2004: Thermal Environmental Conditions for Human Occupancy*. Atlanta GA: ASHRAE, Inc..
- ASHRAE, 2004b. *ASHRAE standard 62.1-2004. Ventilation for acceptable Indoor Air Quality*. Atlanta GA: ASHRAE, Inc..
- ASHRAE, 2009. *ASHRAE handbook of Fundamentals*. Atlanta GA: ASHRAE, Inc..
- Auliciems, A., 1981. Towards a psycho-physiological model of thermal perceptions. *Int. J. of Biometeorology*, 25(109-122).
- Auliciems, A. & Szokolay, S. V., 2007. *Thermal comfort (in PLEA notes no.3)*. Brisbane: PLEA and University of Queensland.
- Autodesk, 2011. Autodesk Ecotect Analysis 2011. Available at www.students.autodesk.com [Accessed 01 Jun 2010].
- Axley, J. W., Emmerich, S. J. & Walton, G. N., 2002. Modeling the performance of a naturally ventilated commercial building with a multizone coupled thermal/airflow simulation tool. *ASHRAE Transactions*, 108(2), p. 1260–1275.
- Aynsley, R., 2007. *Natural Ventilation in Passive Design*, Adelaide: The Royal Australian Institute of Architects.
- Bakker, A., 2012. Computational Fluid Dynamics Lectures. Available at <http://www.bakker.org> [Last accessed 07 October 2012].
- Barbason, M. & Reiter, S., 2010. *About the choice of turbulence model in building physics simulation*. New York, Syracuse University.
- Barbason, M. & Reiter, S., 2011. *A validation process for CFD use in building physics – study of contaminant dispersion*. Leuven, Université Catholique de Louvain / Université de Liège / Universiteit Gent, pp. 1-10.
- Bay, J. H. & Ong, B. L., 2006. *Tropical sustainable architecture - Social and environmental dimensions*. 1st ed. Oxford: Architectural Press.

- Berge, B., 2001. *The ecology building materials*. Oxford: Architectural Press.
- Bouden, B. & Ghrab, N., 2005. An adaptive thermal comfort model for the Tunisian context: a field study results. *Energy and Buildings*, Volume 37, p. 952–963.
- Bou-Saada, T. E. & Haberl, J. S., 1995. *An improved procedure for developing a calibrated hourly simulation models*. Madison, Wisconsin, IBPSA.
- Brager, G. S. & de Dear, R. J., 1998. Thermal adaptation in the built environment: a literature review. *Energy and Buildings*, Issue 27, pp. 83-96.
- Brager, G. S. & de Dear, R. J., 2000. A standard for natural ventilation. *ASHRAE Journal*, Volume 42(10), pp. 21-28.
- Bronson, J. D., 1992. *Calibrating DOE-2 to weather and non-weather dependent loads for a commercial building*. M.S. thesis: Texas A&M University.
- Bui, Q. B. & Morel, J. C., 2009. Assessing the anisotropy of rammed earth. *Construction and Building Materials*, 23(9), p. 3005–3011.
- Cañas, I. & Martín, S., 2004. Recovery of Spanish vernacular construction as a model of bioclimatic architecture.. *Building and Environment*, Volume 39, pp. 1477-95.
- Cândido, C., de Dear, R. J., Lamberts, R. & Bittencourt, L., 2010. Air movement acceptability limits and thermal comfort in Brazil's hot humid climate zone. *Building and Environment*, Volume 45, p. 222–229.
- CEN, 2007. *CEN Standard EN15251: Indoor environmental input parameters for design and assessment of energy performance of buildings - addressing indoor air quality, thermal environment, lighting and acoustics*.. Brussels: Comité Européen de Normalisation.
- CHAM Co., 2010. PHOENICS 2010. Available from <http://www.cham.co.uk> [Accessed 25th June 2010].
- Chen, Q., 1995. Comparison of different k-ε models for indoor airflow computations. Part B, Fundamentals. *Numerical Heat Transfer*, Volume 28(3), p. 353–69.
- Chen, Q., 2009. Ventilation performance prediction for buildings: A method overview and recent applications. *Building and Environment*, Volume 44, p. 848–58.
- Chung, T. M. & Tong, W. C., 1990. Thermal comfort study of young Chinese people in Hong Kong. *Building and Environment*, 25(4), pp. 317-328.
- CIBSE, 1997. *Natural Ventilation in Non-domestic Buildings, Applications Manual AM10*.. London: The Chartered Institution of Building Services Engineers.
- CIBSE, 1999. *Environmental design - CIBSE guide A*. London: The Chartered Institution of Building Service Engineers.
- Claridge, D. E. et al., 2003. *Manual of procedures for calibrating simulations of building systems*, Berkeley, CA: Lawrence Berkeley National Laboratory.
- Coch, H., 1998. Bioclimatism in vernacular architecture. *Renewable and Sustainable Energy Reviews*, 2(1-2), pp. 67-87.
- CPHSC, 2010. *The 2009 Vietnam population and housing census: completed results*, Hanoi: Statistics Publishing House.
- Crawley, D. et al., 2001. EnergyPlus: creating a new-generation building energy simulation program. *Energy and Buildings*, Volume 33, pp. 319-331.
- de Dear, R. J., 2010. Thermal comfort prediction calculator. Available at <http://web.arch.usyd.edu.au> [Accessed 12 Nov 2010].
- de Dear, R. J. & Brager, G. S., 1998. Developing an adaptive model of thermal comfort and preference. *ASHRAE Transactions*, Volume 104(1a), pp. 145-167.

- de Dear, R. J. & Brager, G. S., 2002. Thermal comfort in naturally ventilated buildings: revisions to ASHRAE Standard 55. *Energy and Buildings*, Volume 34, p. 549–561.
- de Dear, R. J., Brager, G. S. & Cooper, D., 1997. *Final report – ASHRAE Project RP-884: Developing an Adaptive Model of Thermal Comfort and Preference*, Atlanta, GA: ASHRAE Inc..
- de Dear, R. J., Leow, K. G. & Ameen, A., 1991. Thermal Comfort in the Humid Tropics - Part II: Climate Chamber Experiments on Thermal Acceptability in Singapore. *ASHRAE Transactions*, 97(1), pp. 874-879.
- Dili, A. S., Naseer, M. A. & Varghese, T. Z., 2010. Passive control methods of Kerala traditional architecture for a comfortable indoor environment: Comparative investigation during various periods of rainy season.. *Building and Environment*, Volume 45, pp. 2218-2230.
- Eberhart, R. C. & Kennedy, J., 1995. *A new optimizer using particle swarm theory*. Nagoya, IEEE, pp. 39-43.
- Eisenhower, B. et al., 2011. *A comparative study on uncertainty propagation in high performance building design*. Sydney, IBPSA Australasia and AIRAH, pp. 2785-2792.
- Emmerich, S. J., 1997. *Use of computational fluid dynamics to analyze indoor air quality issues - Report NISTIR 5997*. USA: National Institute of Standards and Technology.
- Ernest Orlando Lawrence Berkeley National Lab, 2010a. *EnergyPlus Engineering Reference*. Berkely: LBNL.
- Ernest Orlando Lawrence Berkeley National Lab, 2010b. *The Encyclopedic Reference to EnergyPlus Input and Output - Version October 2010*. Berkeley: LBNL.
- EVN, 2013. Vietnam electricity price. Available at www.evn.com.vn [Accessed January 2013].
- Fanger, P. O., 1970. *Thermal comfort*. Copenhagen: Danish Technical Press.
- Fanger, P. O., 1982. *Thermal comfort*. Malabar, FL: R.E. Krieger Publishing Co..
- Fanger, P. O., Højbjerg, J. & Thomsen, J. O. B., 1974. Thermal comfort conditions in the morning and in the evening. *Int. J. Biometeor*, Volume 8(1), pp. 16-22.
- Fanger, P. O. & Tøftum, J., 2002. Extension of the PMV model to non-air-conditioned buildings in warm climates.. *Energy and buildings*, Volume 34, pp. 533-6.
- Feriadi, H. & Wong, N. H., 2004. Thermal comfort for naturally ventilated houses in Indonesia. *Energy and Buildings*, Volume 36, p. 614–626.
- Frey, H. C., Mokhtari, A. & Danish, T., 2003. *Evaluation of Selected Sensitivity Analysis Methods Based Upon Applications to Two Food Safety Process Risk Models*, Raleigh - North Carolina: North Carolina State University.
- Gagge, A. P., Fobelets, A. P. & Berglund, L. G., 1986. A standard predictive index of human response to the thermal environment. *ASHRAE Transactions*, 92(2B), pp. 709-731.
- Gagge, A. P., Stolwijk, J. & Nishi, Y., 1971. An effective temperature scale based on a simple model of human physiological regulatory response. *ASHRAE Transactions*, 71(1), pp. 247-262.
- Gao, Y. & Chow, W. K., 2005. Numerical studies on air flow around a cube. *Journal of Wind Engineering and Industrial Aerodynamics*, Volume 93, p. 115–135.

- Gebremedhin, K. G. & Wu, B. X., 2003. Characterization of flow field in a ventilated space and simulation of heat exchange between cows and their environment. *Journal of Thermal Biology*, Volume 28(4), pp. 301-19.
- Givoni, B., 1969. *Man climate and architecture*. Oxford: Elsevier publishing Co.Ltd.
- Givoni, B., 1994. *Passive and low energy cooling of buildings*. New York: Van Nostrand Reinhold.
- Givoni, B., 1998. *Climate Considerations in Building and Urban Design*. New York: John Wiley & Sons.
- Glass, G. V., 1976. Primary, secondary, and meta-analysis of research. *Educational Researcher*, Volume 5, pp. 3-8.
- Glicksman, L. & Lin, J., 2006. *Sustainable urban housing in China*. 1st ed. Dordrecht: Springer.
- Glória Gomes, M., Rodrigues, A. M. & Mendes, P., 2005. Experimental and numerical study of wind pressures on irregular-plan shapes. *Journal of Wind Engineering and Industrial Aerodynamics*, Volume 93, pp. 741-56.
- Griffiths, I., 1990. *Thermal comfort studies in buildings with passive solar features, field studies*. UK: Report of the Commission of the European Community.
- Hamby, D. M., 1994. A review of techniques for parameter sensitivity analysis of environmental models. *Environmental Monitoring and Assessment*, 32(2), pp. 135-154.
- Hammond, G. & Jones, C., 2008. *Inventory of carbon and energy, version 1.6a*. Bath: The University of Bath.
- Ha, N. M., 2002. *Prospects on Housing Construction Industry in Urban Areas of Vietnam*. Tokyo, IIBH.
- Heiselberg, P. et al., 2009. Application of sensitivity analysis in design of sustainable buildings. *Renewable Energy*, Volume 34, p. 2030–2036.
- Heisenberg, P., Murakami, S. & Roulet, C. A., 1998. *Ventilation of large spaces in buildings - Analysis and prediction techniques*. Aalborg: Kolding Trykcenter A/S.
- Henninger, J. H., 1984. *Solar absorptance of some common spacecraft thermal-control coatings*. Maryland: NASA.
- Hensel, H., 1981. *Temperature reception and thermal comfort*. London: Academic press.
- Hoang, H. T., 2002. *Architecture in tropical climate*. 2nd ed. Hanoi: Construction Publishing House.
- Hooke, R. & Jeeves, J., 1961. 'Direct Search' Solution of Numerical and Statistical Problems. *Journal of the Association for Computing Machinery*, Volume 8(2), pp. 212-229.
- Hopfe, C. J. & Hensen, J. L. M., 2011. Uncertainty analysis in building performance simulation for design support. *Energy and Buildings*, Volume 43, p. 2798–2805.
- Hopfe, C. J., Hensen, J. L. M. & Plokker, W., 2007. *Uncertainty and sensitivity analysis for detailed design support*. Beijing, IBPSA, pp. 1799-1804.
- Huang, H., Ooka, R., Chen, H. & Kato, S., 2009. Optimum design for smoke-control system in buildings considering robustness using CFD and Genetic Algorithms. *Building and Environment*, Volume 44(11), pp. 2218-2227.
- Humphreys, M., 1978. Outdoor temperature and comfort indoor. *Building research and practice*, Volume 6(2), pp. 92-105.

- Humphreys, M. & Nicol, J. F., 1998. Understanding the adaptive approach to thermal comfort. *ASHRAE Technical Data Bulletin*, 14(1), pp. 1-14.
- Humphreys, M. & Nicol, J. F., 2000. Outdoor temperature and indoor thermal comfort: raising the precision of the relationship for the 1998 ASHRAE database of field studies. *ASHRAE Transactions*, 206(2), pp. 485-492.
- Humphreys, M., Nicol, J. F. & Raja, I. A., 2007. Field studies of indoor thermal comfort and the progress of the adaptive approach. *Journal of Advances on Building Energy Research*, Volume 1, p. 55–88.
- Hunter, J. E. & Schmidt, F. L., 1990. *Methods of Meta-Analysis: Correcting Error and Bias in Research Findings*. California; London; New Delhi: SAGE Publications.
- Hussein, I. & Rahman, M. H. A., 2009. Field Study on Thermal Comfort in Malaysia. *European Journal of Scientific Research*, Volume 37(1), pp. 134-152.
- Hyde, R., 2008. *Bioclimatic housing - Innovative designs for warm climates*. 1 ed. London: Earthscan.
- Hyland, R. W. & Wexler, A., 1983. Formulations for the thermodynamic properties of the saturated phases of H₂O from 173.15 K to 473.15 K. *ASHRAE Transactions*, 89(2A), pp. 500-519.
- Ibrahim, E., Shao, L. & Riffat, F. B., 2003. Performance of porous ceramic evaporators for building cooling application. *Energy and Buildings*, Volume 35, p. 941–949.
- IES, 2010. Virtual Environment Pro 6.0. Available at <http://www.iesve.com/software/ve-pro> [Last accessed 10 Aug 2010].
- Institute of Construction Science and Technology, 2009. *Vietnam Building Code 2009 - QCVN 02: 2009/BXD - Natural Physical & Climatic Data for Construction*. Hanoi: Ministry of Construction of Vietnam.
- International Association for the Properties of Water and Steam, 2007. *Revised release on the IAPWS industrial formulation 1997 for the thermodynamic properties of water and steam*, Oakville, ON: IAPWS.
- ISO, 1995. *ISO 9920: Ergonomics of the thermal environment - estimation of the thermal insulation and evaporative resistance of a clothing ensemble*. Geneva: ISO.
- ISO, 1998. *ISO 7726-1998: Ergonomics of the thermal environment – Instruments for measuring of physical quantities*. Geneva: ISO.
- ISO, 2005. *ISO 7730-2005: Ergonomics of the thermal environment - Analytical determination and interpretation of thermal comfort using calculation of the PMV and PPD indices and local thermal comfort criteria..* Geneva: ISO.
- IUCN, 1980. *World Conservation Strategy - Living resource conservation for sustainable development*, Gland, Switzerland: IUCN-UNEP-WWF.
- Izuba energies, 2010. Pleiades-Comfie software. Available at <http://www.izuba.fr> [Accessed 7 Apr 2010].
- Jiang, Y. et al., 2003. Natural ventilation in buildings: measurement in a wind tunnel and numerical simulation with large-eddy simulation. *Journal of Wind Engineering and Industrial Aerodynamics*, Volume 91, p. 331–353.
- Joint Research Centre - European Commission, 2008. *Simlab 2.2 Reference Manual*. Brussels: JRC.
- Joint Research Centre - European Commission, 2011. Simlab - Software package for uncertainty and sensitivity analysis. Downloadable for free at: <http://simlab.jrc.ec.europa.eu> [Last accessed 10 Dec 2012].

- Kampf, J. H., Wetter, M. & Robinson, D., 2010. A comparison of global optimisation algorithms with standard benchmark functions and real-world applications using EnergyPlus. *Journal of Building Performance Simulation*, Volume 3, pp. 103-120.
- Kenedy, J. F., 2004. *Building without borders*. Gabriola Island: New society publisher.
- Khan, N., Su, Y. & Riffat, F. B., 2008. A review on wind driven ventilation techniques. *Energy and Buildings*, Volume 40, p. 1586–1604.
- Kobayashi, T. et al., 2007. *Stream Tube Analysis of Cross-Ventilated Simple-shaped Model and Detached House*. Sendai, Tohoku University.
- Koenigsberger, O. H., Ingersoll, T. G., Mayhew, A. & Szokolay, S. V., 1973. *Manual of tropical housing and building*. 1st ed. New York: Longman publisher.
- Koppen, W. & Geiger, R., 1936. *Handbuch der Klimatologie*. Berlin: Gebruder Borntraeger.
- Kotek, P., Jordán, F., Kabele, K. & Hensen, J., 2007. *Technique for uncertainty and sensitivity analysis for sustainable building energy systems performance calculation*. Beijing, Online version, pp. 629-636.
- Kubota, T., Toe Hooi Chyee, D. & Ahmad, S., 2009. The effects of night ventilation technique on indoor thermal environment for residential buildings in hot-humid climate of Malaysia. *Energy and Buildings*, Volume 41, pp. 829-839.
- La Roche, P., 2012. *Carbon-Neutral Architectural Design*. 1st ed. Boca Raton, FL: CRC Press.
- Ladeine, F. & Nearon, M., 1997. CFD applications in the HVAC&R industry. *ASHRAE Journal*, Volume 39 (1), p. 44.
- Lam, J. C. & Hui, S. C. M., 1996. Sensitivity analysis of energy performance of office buildings. *Building and Environment*, 31(1), pp. 27-39.
- Lauder, B. E. & Spalding, D. B., 1974. The numerical computation of turbulent flows. *Computational Methods Appl, Mechanical Engineering*, Volume 3, pp. 269-289.
- Legacy Resources Management Program, 1990. *Cooling buildings by natural ventilation*. Washington: U.S. Department of Defense.
- Liébard, A. & de Herde, A., 2005. *Traité d'architecture et d'urbanisme bioclimatiques. Concevoir, édifier et aménager avec le développement durable*. Baume-les-Dames: Observ'ER.
- Likert, R., 1932. A Technique for the Measurement of Attitudes. *Archives of Psychology*, Volume 140, p. 1–55.
- Li, Q. et al., 2009. CFD study of the thermal environment in an air-conditioned train station building. *Building and Environment*, Volume 44, p. 1452–1465.
- Loomans, M., 1998. *The Measurement and Simulation of Indoor Air Flow*. PhD Thesis: Eindhoven university of Technology.
- Ly, P., Birkeland, J. & Demirbilek, N., 2010. *Towards sustainable housing for Vietnam*. Auckland, NZ, New Zealand Society for Sustainability Engineering and Science, pp. 348-361.
- Manioğlu, G. & Yılmaz, Z., 2008. Energy efficient design strategies in the hot dry area of Turkey. *Building and Environment*, Volume 43, p. 1301–1309.
- Manoj, K. S., Sadhan, M. & Atreya, S. K., 2011. Adaptive thermal comfort model for different climatic zones of North-East India. *Applied energy*, Volume 88, p. 2420–2428.
- Marszal, A. J. et al., 2011. Zero Energy Building – A review of definitions and calculation methodologies. *Energy and Buildings*, Volume 43, pp. 971-979.

- McCartney, K. J. & Nicol, J. F., 2002. Developing an adaptive control algorithm for Europe. *Energy and Buildings*, Volume 34, p. 623–635.
- McCullough, E. A., Jones, B. W. & Huck, J., 1985. A comprehensive data base for estimating clothing insulation. *ASHRAE Transactions*, Volume 91(2), pp. 29-47.
- McCullough, E. A. & Wyon, D. P., 1983. Insulation characteristics of winter and summer indoor clothing. *ASHRAE Transactions*, Volume 89(Part 2B), pp. 614-633.
- McMinn, J. & Polo, M., 2005. *Sustainable architecture as a cultural project*. Tokyo, SB05Tokyo National Conference Board, pp. 4537-4544.
- Ministry of Science and Technology, 2005. *TCVN 7438:2004: Ergonomics. Moderate thermal environments. Determination of the PMV and PPD indices and specification of the conditions for thermal comfort*. Hanoi: Ministry of Science and Technology.
- Ministry of Science and Technology, 2010. *Ventilation-air conditioning - Design standards*. Hanoi: Construction Publishing House.
- MOC, 1991. *TCXD 29:1991: Natural illumination in civil building-Design standard*. Hanoi: Ministry of Construction of Vietnam.
- MOC, 2004. *TCXDVN 306: 2004: Dwelling and public buildings - Parameters for micro climates in the room*. Hanoi: Ministry of Construction.
- MOC, 2010. *Proceedings of the seminar "Effective and economic usage of energy and resources in building sector"*. Hanoi, MOC.
- MOC, 2011. Construction price 09 August 2011. Available at www.moc.gov.vn [Accessed August 2011].
- Morris, M. D., 1991. Factorial sampling plans for preliminary computational experiments. *Technometrics*, 33(2), pp. 161-174.
- Murakami, S., 1998. Overview of turbulence models applied in CWE-1997. *Journal of Wind Engineering and Industrial Aerodynamics*, Volume 74-76, pp. 1-24.
- Murakami, S., Kato, S., Ooka, R. & Shiraishi, Y., 2004. Design of a porous-type residential building model with low environmental load in hot and humid Asia. *Energy and Buildings*, Volume 36, p. 1181–1189.
- Nguyen, A. T. & Reiter, S., 2011a. The effect of ceiling configurations on indoor air motion and ventilation flow rates. *Building and Environment*, Volume 46, pp. 1211-1222.
- Nguyen, A. T. & Reiter, S., 2011b. *Passive cooling and heating potential in Vietnam using graphical method and Typical Meteorological Year weather file*. Lausanne, EPFL, pp. 323-328.
- Nguyen, A. T. & Reiter, S., 2012a. A climate analysis tool for passive heating and cooling strategies in hot humid climate based on Typical Meteorological Year data sets. *Energy and Buildings*, Volume <http://dx.doi.org/10.1016/j.enbuild.2012.08.050>.
- Nguyen, A. T. & Reiter, S., 2012b. *Optimum design of low-cost housing in developing countries using nonsmooth simulation-based optimization*. Lima, Peru, Pontificia Universidad Catolica del Peru.
- Nguyen, A. T. & Reiter, S., 2012c. An investigation on thermal performance of a low cost apartment in hot humid climate of Danang. *Energy and Buildings*, Volume 47, pp. 237-246.
- Nguyen, A. T. & Reiter, S., 2013. Passive designs and strategies for low-cost housing using simulation-based optimization and different thermal comfort criteria. *Journal of Building Performance Simulation* (doi:10.1080/19401493.2013.770067).

- Nguyen, A. T., Singh, M. K. & Reiter, S., 2012. An adaptive thermal comfort model for hot humid South-East Asia. *Building and Environment*, Volume 56, pp. 291-300.
- Nguyen, A. T., Tran, Q. B., Tran, D. Q. & Reiter, S., 2011. An investigation on climate responsive design strategies of vernacular housing in Vietnam. *Building and Environment*, Volume 46, pp. 2088-2106.
- Nicol, J. F., 2004. Adaptive thermal comfort standards in the hot-humid tropics. *Energy and Buildings*, Volume 36, pp. 628-637.
- Nicol, J. F. & Humphreys, M., 2002. Adaptive thermal comfort and sustainable thermal standards for buildings. *Energy and buildings*, Volume 34, pp. 563 - 572.
- Nicol, J. F. & Humphreys, M., 2010. Derivation of the adaptive equations for thermal comfort in free-running buildings in European standard EN15251. *Building and Environment*, Volume 45, p. 11-17.
- Nicol, J. F. & Humphreys, M. A., 1973. Thermal comfort as part of a selfregulating system. *Building Research and Practice*, Volume 1(3), pp. 174-179.
- Nicol, J. F. & McCartney, K. J., 2001. *SCATS: Final Report—Public*. Oxford: Oxford Brookes University.
- Nielsen, M., 1974 (result reported by Fanger P.O.). *Studies on the relation between sensations of comfort, degree of heating and physiological reactions*. København: Boligopvarmningsudvalgets meddelelse nr. 3.
- Nielsen, T. R., 2002. *Optimization of buildings with respect to energy and indoor environment*. PhD thesis: Danmarks Techniske Universitet.
- Nishi, Y., 1981. *Measurement of thermal balance of man*. New York, Elsevier.
- Novák, D., Teplý, B. & Keršner, Z., 1998. *The role of Latin Hypercube sampling method in reliability engineering*. Rotterdam, Brookfield, Vt. : A.A. Balkema, pp. 403-409.
- O'Cofaigh, E., Olley, J. A. & Owen, L., 1996. *The Climatic Dwelling: An Introduction to Climate-Responsive Residential Architecture*. 1st ed. London: James & James.
- Office of Energy Efficiency and Renewable Energy, 2012. EnergyPlus Energy Simulation Software - Testing and validation. Available at http://apps1.eere.energy.gov/buildings/energyplus/energyplus_testing.cfm [Accessed 5 August 2012].
- Olesen, B. W., 1985. A new and simpler method for estimating the thermal insulation of a clothing ensemble. *ASHRAE Transactions*, Volume 91(2b), pp. 478-492.
- Olesen, B. W. & Dukes-DuBos, F. N., 1988. *International standards for assessing the effect of clothing on heat tolerance and comfort*. Philadelphia, PA, ASIM, pp. 17-30.
- Olgyay, V., 1963. *Design with climate - Bioclimatic approach to architectural regionalism*. New Jersey: Princeton University Press.
- Pannell, D. J., 1997. Sensitivity analysis of normative economic models: Theoretical framework and practical strategies. *Agricultural Economics*, Volume 16, pp. 139-152.
- Patel, V. C., Rodi, W. & Scheuere, G., 1985. Turbulence Models for Near-Wall and Low Reynolds Number Flows- A Review. *AIAA Journal*, Volume 23(9), pp. 1308-1319.
- Patricia, R. C. D. & José, K. F., 2008. *An air circulation comparative study between the application of short and long wind-catchers in a confined space: case of House VI of "Vila" 37*. Dublin, University College Dublin, p. 393.

- Peel, M. C., Finlayson, B. L. & McMahon, T. A., 2007. Updated world map of the Koppen-Geiger climate classification. *Hydrol. Earth Syst. Sci.*, Volume 11, p. 1633–1644.
- Pérez-Lombarda, L., Ortiz, J. & Pout, C., 2008. A review on buildings energy consumption information. *Energy and Buildings*, 40(3), p. 394–398.
- Peuportier, B., 2005. *Bancs d'essais de logiciels de simulation thermique*. La Rochelle, IBPSA.
- Pham, D. N., 2002. *Bioclimatic architecture (in Vietnamese)*. Hanoi: Construction Publishing House.
- Pham, D. N., Nguyen, T. H. & Tran, Q. B., 1998. *Climate responsive design strategies in Vietnam (in Vietnamese)*. 1st ed. Hanoi: Science and Technology Publishing House.
- Pham, N. D., Pham, D. N. & Luong, M., 1980. *Building Physics (in Vietnamese)*. 1st ed. Hanoi: Construction Publishing House.
- Polak, E., 1997. Optimization, Algorithms and Consistent Approximations. *Applied Mathematical Sciences*, Volume 124, p. 779.
- Reiter, S., 2010. Assessing wind comfort in urban planning. *Environment and Planning B: Planning and Design*, 37(5), p. 857–873.
- Roaf, S., Fuentes, M. & Thomas, S., 2001. *Ecohouse: A design guide*. Oxford: Architectural Press.
- Rohles, F. H., 1973. The revised modal comfort envelope. *ASHRAE Transactions*, 79(2), p. 52.
- Rohles, F. H. & Nevins, R. G., 1971. The nature of thermal comfort for sedentary man. *ASHRAE Transactions*, 77(1), p. 239.
- Rosenthal, R., 1979. The "File Drawer Problem" and the Tolerance for Null Results. *Psychological Bulletin*, Volume 86(3), p. 638–641.
- Saltelli, A., Tarantola, S., Campolongo, F. & Ratto, M., 2004. *Sensitivity analysis in practice*. Chichester: John Wiley & Sons.
- Santamouris, M., 2006. *Environmental Design of Urban Buildings: An Integrated Approach*. 1st ed. London: Earthscan.
- Sevilgen, G. & Kilic, M., 2011. Numerical analysis of air flow, heat transfer, moisture transport and thermal comfort in a room heated by two-panel radiators. *Energy and Buildings*, Volume 43, p. 137–146.
- Singh, M. K., 2010. *Bioclimatic design of built environment for North-East India*. PhD thesis: Indian Institute of Technology.
- Smith, P. F., 2005. *Architecture in a climate of change*. 2nd ed. Oxford: Architectural Press.
- Spalding, D. B., 2009. The phoenics encyclopedia. Available from: http://www.cham.co.uk/phoenics/d_polis/d_enc/encindex.htm [Accessed 20 Nov 2010].
- Spence, R. J. S. & Cook, D. J., 1983. *Building materials in developing countries*. Oxford: John Wiley & Sons.
- Stamou, A. & Katsiris, I., 2006. Verification of a CFD model for indoor airflow and heat transfer. *Building and Environment*, Volume 41, p. 1171–1181.
- Stolwijk, J. A. J. & Hardy, J. D., 1966. Partitional calorimetric studies of response of man to thermal transients. *Journal of Applied Physiology*, Volume 21, p. 967.
- Szokolay, S. V., 2004. *Introduction to architectural science*. Oxford: Elsevier Science.

- Takahashi, K. et al., 2004. Measurement of thermal environment in Kyoto city and its prediction by CFD simulation. *Energy and Buildings*, Volume 36, p. 771–779.
- Tanabe, S., Kimura, K. & Hara, T., 1987. Thermal comfort requirements during the summer season in Japan. *ASHRAE Transactions*, 93(1).
- The Philippine builder, 2012. Evaporative cooler. Available at www.philippine-builder.com [Accessed 2 Feb 2012].
- Thomas, T. G. & Williams, J. J. R., 1999. Simulation of skewed turbulent flow past a surface mounted cube. *Journal of Wind Engineering and Industrial Aerodynamics*, Volume 81, pp. 347-360.
- Tiwari, G. N., Kumar, A. & Sodha, M. S., 1982. A review—cooling by water evaporation over roof. *Energy conversion and Management*, Volume 22, pp. 143-53..
- Torcellini, P. & Pless, S., 2004. *Trombe Walls in Low-energy Buildings: Practical Experiences*. Colorado: National Renewable Energy Laboratory.
- Tran, T. Q. H., 2005. *A study on the history of Viet's traditional timber houses in Vietnam*. Ph.D thesis: Tokyo Metropolitan University.
- Tsuchiya, M. et al., 1997. Development of a new k- ϵ model for flow and pressure fields around bluff body. *J. Wind Eng. Ind. Aerodynamics*, Volume 67-68, p. 169–182.
- U.S. Department of Energy, 2012. Weather data. Available at <http://apps1.eere.energy.gov> [Accessed 07 Jan 2012].
- UCLA, 2011. Climate consultant 5. Available at www.energy-design-tools.aud.ucla.edu [Accessed 08 Feb 2011].
- UIA, 1993. *Final report of UIA World Congress*. Chicago: UIA.
- van der Linden, A. C., Boerstra, A. C. & Kurvers, S. R., 2002. *Thermal indoor climate as a building performance - Proposal for new criteria, design aids and assessment methods in The Netherlands*. Hongkong, Elsevier Science Ltd., pp. 1375-1382.
- Versteeg, H. K. & Malalasekera, W., 1995. *An Introduction to Computational Fluid Dynamics: The Finite Volume Method*. Harlow, England: Addison Wesley Longman, Ltd..
- Vickery, B. J., Aynsley, R. M. & Melbourne, W., 1977. *Architectural aerodynamics*. 2nd ed. Amsterdam: Elsevier Science Ltd.
- Vissilia, A. M., 2009. Evaluation of a sustainable Greek vernacular settlement and its landscape: Architectural typology and building physics. *Building and Environment*, Volume 44, pp. 1095-1106.
- Walker, R., 2010. Density of materials. Available on <http://www.simetric.co.uk> [Accessed 7 Oct 2010].
- Walton, G. N., 1989. Airflow network models for element-based building airflow modeling. *ASHRAE Transaction*, Volume 95(2), p. 611–620.
- Wang, L. & Wong, N. H., 2007. The impacts of ventilation strategies and facade on indoor thermal environment for naturally ventilated residential buildings in Singapore. *Building and Environment*, Volume 42, p. 4006–4015.
- Watson, D. & Labs, K., 1983. *Climatic design: energy-efficient building principles and practices*. London: McGraw-Hill.
- Wendt, J. F., 2009. *Computational fluid dynamics: An introduction*. 3rd ed. Berlin: Springer Verlag.
- Wetter, M., 2001. *GenOpt, A generic optimization program*. Rio de Janeiro, IBPSA, pp. 601-608.

- Wetter, M., 2009. *GenOpt, Generic optimization program - User manual, version 3.0.0. Technical report LBNL-5419*. s.l.:Lawrence Berkeley National Laboratory.
- Wetter, M. & Polak, E., 2004. A convergent optimization method using pattern search algorithms with adaptive precision simulation. *Building Services Engineering Research and Technology*, Volume 25(4), p. 327–338.
- Wetter, M. & Wright, J. A., 2004. A comparison of deterministic and probabilistic optimization algorithms for nonsmooth simulation-based optimization. *Building and Environment*, Volume 39, p. 989 – 999.
- Wilcox, D. C., 1998. *Turbulence modeling for CFD*. 2nd ed. La Canada: DCW Industries.
- Wong, N. H. et al., 2002. Thermal comfort evaluation of naturally ventilated public housing in Singapore. *Building and Environment*, Volume 37, pp. 1267-1277.
- Wong, N. H., Lam, K. P. & Feriadi, H., 1999. The Use of Performance-based Simulation Tools for Building Design and Evaluation: A Singapore Perspective. *Building and Environment*, Volume 35, pp. 709-736.
- Wong, N. H., Tan, P. Y. & Chen, Y., 2007. Study of thermal performance of extensive rooftop greenery systems in the tropical climate. *Building and Environment*, Volume 42, pp. 25-54.
- World Commission on Environment and Development, 1987. *Our common futur*. Oxford: Oxford University Press.
- Wright, J. A., 1986. *The optimised design of HVAC systems*. PhD thesis: Loughborough University of Technology.
- Wright, J. A., 1994. *Optimum Sizing of HVAC Systems by Genetic Algorithm*. Liege, University of Liege, pp. 503-523.
- Wright, J. A., Loosemore, H. A. & Farmani, R., 2002. Optimization of Building Thermal Design and Control by Multi-Criterion Genetic Algorithm. *Energy and Buildings*, Volume 34(9), pp. 959-972.
- Xing, T. B. S. & Stern, F., 2010. (Presentation) Introduction to Computational Fluid Dynamics (CFD). *The University of Iowa*.
- Yagloglou, C. P. & Miller, W. E., 1925. Effective temperature with clothing. *ASHVE Transactions*, Volume 31, p. 89.
- Yakhot, V. & Orszag, S. A., 1986. Renormalization group analysis of turbulence. I. Basic theory. *Journal of Scientific Computing*, Volume 1(1), pp. 3-51.
- Yakhot, V. et al., 1992. Development of turbulence models for shear flows by a double expansion technique. *Phys. Fluids*, Volume A4, p. 1510–1520.
- Yang, J., 2011. Convergence and uncertainty analyses in Monte-Carlo based sensitivity analysis. *Environmental Modelling & Software*, Volume 26, pp. 444-457.
- Yoshino, H., Hasegawa, K. & Matsumoto, S., 2007. Passive cooling effect of traditional Japanese building's features. *International Journal of Management of Environmental Quality*, Volume 18-5, pp. 578-590.
- Zhang, W. & Chen, Q., 2000. Large eddy simulation of indoor airflow with a filtered dynamic subgrid scale model. *International Journal of Heat and Mass Transfer* 2000;, Volume 43, pp. 3219-3231.
- Zhang, Y. et al., 2010. Thermal comfort in naturally ventilated buildings in hot-humid area of China. *Building and Environment*, Volume 45, pp. 2562-2570.

Number of references: 220

LIST OF FIGURES

Figure 1-1: The three pillars of sustainable development (Liébard & de Herde, 2005).....	2
Figure 1-2: The hierarchy of sustainability in architecture.....	4
Figure 1-3: The workflow of the thesis	13
Figure 2-1: The building bioclimatic chart of Olgay (left) and Givoni (right).....	18
Figure 2-2: Heat exchange between man and his environment	23
Figure 2-3: Heat balance mechanism and body temperature.....	24
Figure 2-4: The comfort chart recommended by ASHRAE (2004)	28
Figure 2-5: PPD as the function of PMV	30
Figure 2-6: The concentric model of a man and his environment (Gagge, et al., 1971)	31
Figure 2-7: The change in comfort temperature with monthly mean outdoor temperature (Humphreys, 1978)	33
Figure 3-1: Distribution of indoor operative temperature and relative humidity in NV (left) and AC buildings (right) of all surveys	44
Figure 3-2: Weighted regression of mean $T_{i,o}$ versus mean TSV. Smallest and largest sample sizes in NV buildings (left) are 1 and 430, and in AC buildings (right) are 1 and 225.	46
Figure 3-3: Weighted regression of mean ET^* versus mean TSV. Smallest and largest sample sizes in NV buildings (left) are 2 and 298, and in AC buildings (right) are 2 and 229.	46
Figure 3-4: Weighted regression of mean SET^* versus mean TSV. Smallest and largest sample sizes in NV buildings (left) are 1 and 118, and in AC buildings (right) are 1 and 93.	48
Figure 3-5: Sensitivity of resulted adaptive comfort model with different ‘Griffiths constants’(left) and the relationship between Griffiths constant and regression slope of adaptive comfort equation (right)	49
Figure 3-6: Relationship between Griffiths constant and correlation coefficient of adaptive comfort equation	50
Figure 3-7: Slope of the regression in relation to the standard deviation of indoor operative temperature. Each point represents the slope of linear regression of a survey in a country, in NV or AC buildings. The survey in Guangzhou was divided into two	

surveys: hot season and mild seasons (Smallest and largest sample sizes are 97 and 762, respectively).....	51
Figure 3-8: Predicted comfort temperature. Each bubble represents mean vote corresponding to a mean monthly temperature. For NV buildings (left): largest bubble size: 569, smallest bubble size: 14. For AC buildings (right): largest bubble size: 458, smallest bubble size: 21. 95% confidence intervals of the regression line were also shown.....	52
Figure 3-9: Change of mean thermal sensation vote corresponding to deviation from comfort temperature. Each point represents mean of 50 votes.....	53
Figure 3-10: Corrected PMV versus thermal sensation vote in warm climate.....	54
Figure 3-11: Measuring equipments used and class room arrangement in the survey (The downward arrow indicates the position of the data logger in the middle of the classroom).....	57
Figure 3-12: Screen shot of the questionnaire (in Vietnamese) used in the survey.....	58
Figure 3-13: Weighted regression between Operative temperature and Thermal Sensation Vote in NV buildings in Vietnam. Each point represents mean thermal sensation vote of a class (Smallest and largest sample sizes are 10 and 95, respectively)....	60
Figure 3-14: Observed neutral operative temperature corresponding to each month by linear regression. Each point represents mean vote of a class.....	61
Figure 4-1: The map of Vietnam and three selected sites for this study.....	67
Figure 4-2: Köppen - Geiger climate classification map for Vietnam (see (Peel, et al., 2007) for the legend of other climatic regions).....	68
Figure 4-3: Statistical temperature, humidity, solar radiation and rainfall of selected sites..	69
Figure 4-4: Sun chart diagram and wind regimes in the selected sites.....	70
Figure 4-5: Sample output of Mahoney tables – general recommendations for Hanoi.....	75
Figure 4-6: Sample output of Mahoney tables – detail recommendations for Hanoi.....	75
Figure 4-7: Incorrect prediction of the comfort zone for Hanoi by Ecotect (Autodesk, 2011).....	78
Figure 4-8: Comfort zone proposed for Vietnamese and its control potential zones.....	79
Figure 4-9: Hourly plot weather data on Building psychrometric chart at standard atmospheric pressure (101.325 kPa).....	86
Figure 4-10: All year cumulative comfort using passive heating and cooling strategies (NV: natural ventilation; DEC: direct evaporative cooling; PSH: passive solar heating).....	89
Figure 4-11: Cumulative comfort during 4 seasons in Hanoi by passive strategies (NV: natural ventilation; DEC: direct evaporative cooling; PSH: passive solar heating).....	90
Figure 4-12: Natural comfort and cumulative comfort by natural ventilation during 12 months in Hanoi.....	91

Figure 4-13: The climate of Hanoi on the adaptive comfort model of South-East Asia	92
Figure 5-1: Locations of the 3 case-study houses (black round dots) and the Meteorological station (square dot) in Danang city.....	97
Figure 5-2: Three case-study houses and the locations of measuring equipments.....	99
Figure 5-3: Indoor - outdoor temperature and humidity during 31 days of May	101
Figure 5-4: EnergyPlus program schematic, its modules and capabilities (Ernest Orlando Lawrence Berkeley National Lab, 2010a)	104
Figure 5-5: Typical steps of a CFD study (Xing & Stern, 2010).....	107
Figure 5-6: Locations of wind velocity measurement on the symmetrical section of the model (thick dark block) and model configurations (all dimensions in mm).....	111
Figure 5-7: Typical velocity distribution in near-wall region (after (Wilcox, 1998))	113
Figure 5-8: Incorrect prediction of recirculation above a cube by the k-ε model (a); the correction by the method of Gao and Chow (b) and wind tunnel experiment (c)	116
Figure 5-9: Mean velocity U/U_{ref} on 9 vertical lines at center section of the model (Black dots: experiment; solid line: numerical results)	117
Figure 5-10: Mean velocity V/U_{ref} on 9 vertical lines at center section of the model (Black dots: experiment; solid line: numerical results)	118
Figure 5-11: Wind velocity distribution around the model by RNG k-ε simulation in this study (left) and in the practical experiment (right)	119
Figure 5-12: 3D housing models in EnergyPlus. Rectangular planes around the houses represent adjacent buildings and trees. Adjacent buildings of the apartment are not shown.	120
Figure 5-13: Simulated WPC surface contours of the wind from the South (180°) – the apartment is on the 4 th floor of the building on the left.	123
Figure 5-14: The creation of a weather file for EnergyPlus and calibration procedure	127
Figure 5-15: Comparison between simulated and measured temperature in the bedroom – row house.....	131
Figure 5-16: Tuning progress with input modifications (left) and linear regression analysis of run #1 vs. run #9 (right) - row house.	131
Figure 5-17: Measured versus predicted relative humidity in the bedroom – row house ...	132
Figure 5-18: Comparison between simulated and measured temperature in the bedroom 1- detached house.....	134
Figure 5-19: Tuning progress with input modifications (left) and linear regression analysis of run #1 vs. run #6 (right) – detached house	135
Figure 5-20: Measured versus predicted relative humidity - bedroom 1, detached house ..	135

Figure 5-21: Tuning progress with input modifications (left) and linear regression analysis of run #1 vs. run #8 (right) – apartment.....	137
Figure 5-22: Comparison between simulated and measured temperature / humidity in the bedroom 1- apartment.....	138
Figure 5-23: The contradictory of predicted results given by the two comfort criteria.....	142
Figure 5-24: Monthly mean indoor relative humidity of major thermal zones through the reference year.....	144
Figure 5-25: From top to bottom: hourly temperature of the row house under the climate of Hanoi, Danang and Hochiminh city respectively (all thermal zones are presented).....	146
Figure 5-26: From top to bottom: hourly temperature of the detached house under the climate of Hanoi, Danang and Hochiminh city respectively (for clarity, temperature of the bedroom 1 + 2 and living room are shown).....	147
Figure 5-27: From top to bottom: hourly temperature of the apartment under the climate of Hanoi, Danang and Hochiminh city respectively (all thermal zones are presented).....	148
Figure 6-1: The innovative approach proposed and applied to this research	152
Figure 6-2: Traditional life on boats affected the housing style of Viet people: (a) ancient boat and (b) ancient house found on Dong Son bronze drum 6 th century BC; (c) current Viet communal house	153
Figure 6-3: Architectural details of the selected houses A, B, C, D, E, and F	154
Figure 6-4: Frequency of use of different climatic responsive strategies.....	165
Figure 6-5: Distribution of measuring points (1, 2,..., 10 are illumination measuring points; A, B,..., E correspond with measuring points of other variables).....	166
Figure 6-6: Average air temperature, relative humidity and scalar wind velocity at surveyed points in a typical summer and winter day (measurement at point E in summer was unavailable due to construction work being done there).....	167
Figure 6-7: Change of temperature, humidity and wind velocity at some survey points during a typical summer and winter day.....	168
Figure 6-8: Indoor thermal comfort evaluation by the building psychrometric chart developed for hot humid climate (Nguyen & Reiter, 2011b).....	169
Figure 6-9: Indoor illuminance compared with Building code (15h, 16 th December)	169
Figure 6-10: Distribution of static pressure and time-averaged velocity in case D with side corridor opened (above) and case E with side corridor closed (below)	172
Figure 6-11: Three cases in the study of solar shading effectiveness (14h; 11 th July).....	173
Figure 6-12: Shading effectiveness on the hottest day - 11 th July (above) and monthly average shading percentage of the vertical façades (below).....	174
Figure 6-13: Building model for the simulation on thermal performance.....	175

Figure 6-14: Temperature variation in the living room over one year	175
Figure 6-15: Hourly plot of living room air temperature on the adaptive comfort model during a year	176
Figure 6-16: Cumulative percentage of living room temperature over base temperature 13.9°C (left) and below base temperature 32°C (right) during TMY	176
Figure 7-1: Thermal performance of the houses with various types of the external walls..	180
Figure 7-2: Thermal performance of the houses before and after installing thermal insulation into the roof.....	182
Figure 7-3: Thermal performances of the case-study houses with various external wall colors.....	185
Figure 7-4: Thermal performances of the case-study houses with different ventilation schemes	186
Figure 7-5: Effects of other strategies on thermal condition of the case-study houses	187
Figure 7-6: Thermal performances of the houses if combined strategies are used. The horizontal line indicates the acceptable threshold of TDH.....	189
Figure 7-7: Airflow created by a ceiling fan on the central vertical plan (left) and horizontal plan at 1.1 m above the floor (right) - result given by a CFD simulation	192
Figure 7-8: Floor plan of the detached house before (left) and after implementing the courtyard (right) in the central corridor	196
Figure 7-9: Time average wind velocity in the original detached house (left) and courtyard house (right). Velocity range from 0 to 1.5 m/s (from dark blue to red). Wind comes from the North, East, South and West, respectively.....	197
Figure 7-10: Airflow in the courtyard when the wind reaches the house from East (above) and North (below). The velocity field are displayed on both horizontal and vertical plans.	199
Figure 7-11: Second floor plan before (above) and after implementing the lightwell (below) in the row house. CFD results will show the cross sections and first floor plans. .	200
Figure 7-12: The CFD domain and X-Z plane grid solution of the row house and adjacent blocks. The row house is in the center. Red and blue arrows indicate the wind direction and true North, respectively.....	201
Figure 7-13: Central cross section of the house with the lightwell (right) and without the lightwell (left). Velocity range from 0 to 0.5 m/s (from dark blue to red)	202
Figure 7-14: Detailed airflow and static pressure distribution in the house and lightwell (Side walls of the house are removed for internal view) - South-East wind	203
Figure 7-15: Average daily ACH in two bedrooms of the apartment during a year – result given by EnergyPlus airflow network simulation with the calibrated model.....	205

Figure 7-16: Plan of the original apartment (left) and the improved apartment (right). The true North and wind directions in CFD analysis are highlighted in the center	205
Figure 7-17: The 7-storey building, the apartment on the 4 th floor and the grid system in the center of the CFD domain.....	206
Figure 7-18: Velocity contour on the horizontal plan 1.1 m above the floor in the original apartment (left) and the improved apartment (right). The contour keys are shown on the left. (From top to bottom: North wind, East wind, South wind and West wind, respectively).....	208
Figure 7-19: Static pressure distribution around the openings of the improved apartment in the case of East wind	209
Figure 7-20: Comparison of mean air velocity (of 56 points on the working plan - 1.1 m above the floor) and ventilation flow rates in the original bedrooms and the improved bedrooms.....	210
Figure 7-21: Examples of an equator –facing façade and Trombe wall.....	212
Figure 7-22: Roof spray and roof pond in nighttime and day time, respectively – adapted from (Givoni, 1994).....	213
Figure 8-1: The full process of a SA using SimLab and EnergyPlus	222
Figure 8-2: Cobwebs plot of 180 input vectors generated by the LHS method	227
Figure 8-3: Sensitivity rankings via the PCC and SRRC – the row house.....	228
Figure 8-4: Correlations between the roof color and the TDHs and TECs	229
Figure 8-5: Sensitivity rankings via the PCC and SRRC - the detached house.....	230
Figure 8-6: Non-linear non-monotonic relationship between ventilation strategies and TDHs (a) and strong correlation if the codified names were reordered (b).....	231
Figure 8-7: Sensitivity rankings via the PCC and SRRC – the apartment	232
Figure 8-8: Probability distribution of simulation outputs	234
Figure 8-9: Coupling principle between GenOpt and EnergyPlus	239
Figure 8-10: Diagram of the Hooke-Jeeves search logic.....	245
Figure 8-11: A typical optimization process (AC detached house, cost function [C]).....	250
Figure 8-12: Comparison of the TDHs in the NV houses. The horizontal line indicates the acceptable threshold of the TDH.	251
Figure 8-13: Minimum cost of the NV houses that satisfy thermal comfort criterion	252
Figure 8-14: Optimal LCCs, compared with LCCs of the reference cases	253
Figure 8-15: The simple rectangular housing model (Nguyen & Reiter, 2013).....	259
Figure 8-16: Design guides for an isolated rectangular housing model (AC houses use a fixed thermostat and an ‘adaptive’ thermostat)	260

LIST OF TABLES

Table 1-1: Percentage of the final energy consumption used in commercial and residential buildings in 2004 (Pérez-Lombarda, et al., 2008).....	3
Table 1-2: Monthly income per capita by urban and rural region - unit: 1000 VND (At exchange rate of 1USD \approx 17.000 VND) (CPHSC, 2010).....	7
Table 1-3: Living area per capita by type of house, urban-rural region (Unit: m ²).....	7
Table 1-4: Percentage of house by housing condition, urban - rural area (CPHSC, 2010).....	8
Table 2-1: Three major bioclimatic approaches in the evolutionary order.....	20
Table 2-2: ASHRAE and Bedford thermal sensation scales	26
Table 2-3: Thermal sensation prediction by temperature and humidity (adapted from (La Roche, 2012)).....	27
Table 2-4: Sensation prediction and neutral temperature of different groups of subjects.....	27
Table 2-5: Thermal sensation and comfort scale of the two-node model.....	32
Table 3-1: Summary of the field survey database for the present adaptive model.....	39
Table 3-2: Mean observed neutral temperature in South-East Asia	47
Table 3-3: The role of Griffiths constant in the establishment of adaptive comfort equation and its correlation R ²	50
Table 3-4: Results of some statistical significance tests of some parameters and variables' attributes in NV buildings	55
Table 3-5: Technical specifications of measuring instruments.....	58
Table 3-6: Statistical results of the survey.....	59
Table 3-7: Comparison between predicted and observed comfort temperature	62
Table 4-1: Comfort of the climates of Vietnam and corresponding design guidelines proposed by Climate Consultant 5.3	72
Table 4-2: Design strategies recommended by Mahoney tables	76
Table 4-3: Potential comfort improvement by each strategy.....	89
Table 4-4: Results of climate analysis by the adaptive comfort model	93
Table 5-1: Basic features of the case-study houses	98
Table 5-2: Details of the boundary conditions and computational parameters	115
Table 5-3: Wind pressure coefficient of the row house.....	124
Table 5-4: Wind pressure coefficient of the detached house.....	124
Table 5-5: Wind pressure coefficient of the apartment	125
Table 5-6: Row house calibration runs	129
Table 5-7: Detached house calibration runs.....	133

Table 5-8: The apartment - calibration runs	136
Table 5-9: Classification system of thermal performance for NV buildings.....	141
Table 5-10: Thermal performance in a year of the row houses	141
Table 5-11: Thermal performance in a year of the detached house (only 5 major thermal zones of the house were considered)	141
Table 5-12: Thermal performance in a year of the apartment	142
Table 6-1: General information about the houses in question	155
Table 6-2: Types of materials used in the houses investigated.....	155
Table 6-3: Most used materials and their properties.....	156
Table 6-4: Qualitative investigation of bioclimatic design strategies used in traditional architecture in Vietnam.....	158
Table 6-5: Measurement instruments and their properties	166
Table 6-6: Vietnam building code of natural illumination for residential facilities	166
Table 6-7: Characteristics of air flow field through the model.....	171
Table 7-1: Retrofit choices for the external walls and their corresponding U-values	180
Table 7-2: Retrofit choices for the roof and their corresponding U-values	182
Table 7-3: Description of the ventilation strategies.....	184
Table 7-4: Recommended changes for the houses to obtain improved performances	188
Table 7-5: Thermal classification of the improved houses	190
Table 7-6: Recommendations and rules of thumb for better natural ventilation	193
Table 7-7: Mean wind velocity in the main occupied spaces	198
Table 7-8: Mean air velocity and ventilation flow rate in the bedrooms.....	209
Table 8-1: Common ventilation schemes applied in NV buildings.....	222
Table 8-2: Variables considered in the SA of the NV row house.....	223
Table 8-3: Variables considered in the SA of the AC row house.....	225
Table 8-4: Statistical features of the samples of simulation outputs	234
Table 8-5: Design parameters used in the optimization of the NV apartment.....	240
Table 8-6: Design parameters used in the optimization of the AC apartment.....	241
Table 8-7: Other costs and fees (exchange rate 1\$ = 20840VND).....	248
Table 8-8: Lowest values of the objective functions found in 27 optimization runs.....	249
Table 8-9: Time and convergence issues in the optimization of the detached house	250
Table 8-10: Thermal classification of the optimal houses	252
Table 8-11: Design guides for optimal thermal comfort in NV residential buildings	254
Table 8-12: Design guides for low-cost house with acceptable indoor thermal comfort	256
Table 8-13: Design guides for AC residential buildings	257
Table 8-14: Findings of the present work and those of other authors and tools.....	261
Table 9-1: Design guides and recommendations for building renovation.....	268
Table 9-2: Optimal combinations of design variables for new buildings.....	269

APPENDIX A

VARIABLES NATURES AND RANGES IN THE SENSITIVITY ANALYSIS

Table A-1: The NV **detached house**

Description of input variables tested in the SA	Var. name	Variable type	Probability distribution function	Range*	Mean	Standard deviation
Ventilation strategy (open or close the openings)	x1	Discrete	With weight factors	400 – 409, step = 1		
Max equipment power – all zones	x2	Continuous	Normal		120 W	20
Max equipment power -kitchen	x3	Continuous	Normal		400 W	40
Thickness wooden floor	x4	Continuous	Uniform	0.01 – 0.025 m		
Insulation thickness ground floor	x5	Continuous	Uniform	0 – 0.03 m		
External wall type	x6	Discrete	With weight factors	100 – 106, step = 1		
Thickness roof insulation	x7	Continuous	Uniform	0 – 0.04 m		
Thickness of internal partitions	x8	Continuous	Uniform	0.08 - 0.25 m		
Brick density (external wall)	x9	Continuous	Normal		1600 kg/m ³	200
Thickness - brick	x10	Continuous	Normal		0.07 m	0.008
External wall color	x11	Continuous	Uniform	0.25 - 0.85		
Thickness ceiling concrete slab	x12	Continuous	Normal		0.12 m	0.01
Density ceiling concrete slab	x13	Continuous	Normal		2700 kg/m ³	200
Roof color	x14	Continuous	Uniform	0.25 - 0.85		
Conductivity EPS insulation	x15	Continuous	Normal		0.035 W/m.K	0.003
Window type	x16	Discrete	Uniform	200; 201; 202; 203		
Thickness of internal mass	x17	Discrete	With weight factors	0.1; 0.15; 0.2; 0.25; 0.3 m		
Length of window overhang	x18	Continuous	Uniform	0 – 0.8 m		
Max number of occupant	x19	Discrete	Uniform	3; 4; 5; 6; 7		

Description of input variables tested in the SA	Var. name	Variable type	Probability distribution function	Range*	Mean	Standard deviation
Power of gas stove	x20	Continuous	Normal		500 W	200
Crack of the roof	x21	Continuous	Normal		0.065 kg/m.s	0.01
Crack window - bedrooms	x22	Continuous	Uniform	0.001 – 0.005 kg/m.s		
Crack window – other rooms	x23	Continuous	Uniform	0.001 – 0.006 kg/m.s		
Discharge coeff. bedrooms	x24	Continuous	Uniform	0.18 – 0.35		
Discharge coeff. other rooms	x25	Continuous	Uniform	0.2 – 0.4		
North windows' height	x26	Continuous	Uniform	2.6 – 3.2 m		
South windows' height	x27	Continuous	Uniform	2.6 – 3.2 m		
East windows' height	x28	Continuous	Uniform	2.6 – 3.2 m		
West windows' height	x29	Continuous	Uniform			

Table A-2: The AC detached house

Description of input variables tested in the SA	Var. name	Variable type	Probability distribution function	Range*	Mean	Standard deviation
Building azimuth	x1	Continuous	Normal		-27°	10
Max equipment power – all zones	x2	Continuous	Normal		120 W	20
Max equipment power -kitchen	x3	Continuous	Normal		400 W	40
Thickness wooden floor	x4	Continuous	Uniform	0.01 – 0.025 m		
Insulation thickness ground floor	x5	Continuous	Uniform	0 – 0.03 m		
External wall type	x6	Discrete	With weight factors	100 – 106, step = 1		
Thickness roof insulation	x7	Continuous	Uniform	0 – 0.04 m		
Thickness of internal partitions	x8	Continuous	Uniform	0.08 - 0.25 m		
Brick density (external wall)	x9	Continuous	Normal		1600 kg/m ³	200
Thickness - brick	x10	Continuous	Normal		0.07 m	0.008
External wall color	x11	Continuous	Uniform	0.25 - 0.85		
Thickness ceiling concrete slab	x12	Continuous	Normal		0.12 m	0.01
Density ceiling concrete slab	x13	Continuous	Normal		2700 kg/m ³	200
Roof color	x14	Continuous	Uniform	0.25 - 0.85		
Conductivity EPS insulation	x15	Continuous	Normal		0.035 W/m.K	0.003

Description of input variables tested in the SA	Var. name	Variable type	Probability distribution function	Range*	Mean	Standard deviation
Window type	x16	Discrete	Uniform	200; 201; 202; 203		
Thickness of internal mass	x17	Discrete	With weight factors	0.1; 0.15; 0.2; 0.25; 0.3 m		
Length of window overhang	x18	Continuous	Uniform	0 – 0.8 m		
Max number of occupant	x19	Discrete	Uniform	3; 4; 5; 6; 7		
Power of gas stove	x20	Continuous	Normal		500 W	200
Infiltration of the attic	x21	Continuous	Normal		0.01 m ³ /s	0.002
Infiltration bedrooms	x22	Continuous	Normal		0.01 m ³ /s	0.002
Infiltration kitchen	x23	Continuous	Normal		0.01 m ³ /s	0.002
Infiltration remaining zones	x24	Continuous	Normal		0.01 m ³ /s	0.002
HVAC Cooling setpoint	x25	Continuous	Uniform	26° - 27.5°		
North windows' height	x26	Continuous	Uniform	2.6 – 3.2 m		
South windows' height	x27	Continuous	Uniform	2.6 – 3.2 m		
East windows' height	x28	Continuous	Uniform	2.6 – 3.2 m		
West windows' height	x29	Continuous	Uniform	2.6 – 3.2 m		
HVAC Fan blades efficiency	x30	Continuous	Uniform	0.6 – 0.7		
HVAC Fan motor efficiency	x31	Continuous	Uniform	0.8 – 0.9		
HVAC Cooling coil COP	x32	Continuous	Normal		3	0.13
HVAC Heating coil efficiency	x33	Continuous	Uniform	0.95 - 1		
HVAC Heating setpoint	x34	Continuous	Uniform	20° – 23°		

Table A-3: The NV **apartment**

Item	Var. name	Variable type	Probability distribution function	Range*	Mean	Standard deviation
Ventilation strategy	x1	Discrete	With weight factors	400 – 409, step = 1		
Max equipment power – living room	x2	Continuous	Normal		200 W	22
Max equipment power – bedroom 1	x3	Continuous	Normal		60 W	10
Max equipment power – bedroom 2	x4	Continuous	Normal		80 W	12
External wall type	x5	Discrete	With weight factors	100 – 105, step = 1		
Size overhang windows - bedroom	x6	Continuous	Uniform	0.1- 0.8 m		
Size of window bedroom 1	x7	Continuous	Uniform	1 – 2.2 m	5.2-6.4	
Size of window bedroom 2	x8	Continuous	Uniform	1 – 2.2 m	2-3.2	

Item	Var. name	Variable type	Probability distribution function	Range*	Mean	Standard deviation
Brick density (external wall)	x9	Continuous	Normal		1600 kg/m ³	200
Thickness - brick	x10	Continuous	Uniform	0.06 – 0.1 m		
External wall color	x11	Continuous	Uniform	0.25-0.85		
Concrete slab thickness	x12	Continuous	Normal		0.09 m	0.01
Concrete slab density	x13	Continuous	Normal		2600 kg/m ³	200
EPS Insulation conductivity	x14	Continuous	Normal		0.035 W/m.K	0.003
Window type	x15	Discrete	Uniform	200; 201; 202; 203		
Thickness of brick internal mass	x16	Discrete	With weight factors	10; 15; 20; 25 mm		
Max number of occupant	x17	Discrete	Uniform	2; 3; 4		
Power of gas stove	x18	Continuous	Normal		400 W	100
Discharge coefficient windows - bedroom	x19	Continuous	Normal		0.4	0.1
Crack of windows - bedroom	x20	Continuous	Uniform	0.004-0.014 kg/m.s		
Discharge coefficient window – living room	x21	Continuous	Normal		0.3	0.08
Crack of window – living room	x22	Continuous	Uniform	0.003 – 0.008 kg/m.s		
Discharge coefficient door – living room	x23	Continuous	Normal		0.35	0.08
Crack of door – living room	x24	Continuous	Uniform	0.003 – 0.008 kg/m.s		

Table A-4: The AC apartment

Item	Var. name	Variable type	Probability distribution function	Range*	Mean	Standard deviation
Building azimuth	x1	Continuous	Normal		135°	10
Max equipment power – living room	x2	Continuous	Normal		200 W	22
Max equipment power – bedroom 1	x3	Continuous	Normal		60 W	10
Max equipment power – bedroom 2	x4	Continuous	Normal		80 W	12
External wall type	x5	Discrete	With weight	100 – 105,		

Item	Var. name	Variable type	Probability distribution function	Range*	Mean	Standard deviation
			factors	step = 1		
Size overhang windows - bedroom	x6	Continuous	Uniform	0.2- 0.8 m		
Size of window bedroom 1	x7	Continuous	Uniform	1 – 2.2 m	5.2-6.4	
Size of window bedroom 2	x8	Continuous	Uniform	1 – 2.2 m	2-3.2	
Brick density (external wall)	x9	Continuous	Normal		1600 kg/m ³	200
Thickness - brick	x10	Continuous	Uniform	0.06 – 0.1 m		
External wall color	x11	Continuous	Uniform	0.25-0.85		
Concrete slab thickness	x12	Continuous	Normal		0.09 m	0.01
Concrete slab density	x13	Continuous	Normal		2600 kg/m ³	200
EPS Insulation conductivity	x14	Continuous	Normal		0.035 W/m.K	0.003
Window type	x15	Discrete	Uniform	200; 201; 202; 203		
Thickness of brick internal mass	x16	Discrete	With weight factors	10; 15; 20; 25 mm		
Max number of occupant	x17	Discrete	Uniform	2; 3; 4		
Power of gas stove	x18	Continuous	Normal		400 W	100
Infiltration	x19	Continuous	Uniform	0.25 – 0.5 ACH		
HVAC Heating setpoint	x20	Continuous	Uniform	20° - 23°		
HVAC Cooling setpoint	x21	Continuous	Uniform	26° - 27.5°		
HVAC Fan blades efficiency	x22	Continuous	Uniform	0.6 – 0.7		
HVAC Fan motor efficiency	x23	Continuous	Uniform	0.8 – 0.9		
HVAC Cooling coil COP	x24	Continuous	Normal		3	0.13
HVAC Heating coil efficiency	x25	Continuous	Uniform	0.95 - 1		

APPENDIX B

OPTIMIZATION PARAMETERS

Table B-1: Design parameters used in the optimization of the NV row house

Numerical (continuous) variables and their variation ranges						
Design parameter	Opt. variable	Min value	Initial value	Max value	Step size	Number of case
Solar absorptance – external wall [dimensionless]	x_1	0.25	0.35	0.75	0.1	6
Solar absorptance – roof [dimensionless]	x_2	0.25	0.35	0.75	0.1	6
Crack infiltration - Opening level 1 [kg/s-m]	x_3	0.004	0.008	0.012	0.002	5
Crack infiltration - Opening level 2 [kg/s-m]	x_4	0.004	0.006	0.012	0.002	5
Opening sizing factor – roof attic [kg/s-m]	x_5	0.2	0.4	1.0	0.2	5
Width - Front window (height = 1.9m) [m]	x_6	1.0	2.0	2.2	0.2	7
Width - Entrance door (height = 2.9m) [m]	x_7	1.6	3.2	3.6	0.4	5
Width - Backward window level 2 (height = 1.2m) [m]	x_8	1	1.5	3	0.5	5
Length - Front facade shading device [m]	x_9	0.05	0.05	0.65	0.2	3
Categorical design options and strategies (discrete variables)						
Design parameter	Design choices	Opt. variable	Discrete value	Item cost (\$/m ²)	Number of case	
External walls	110mm two-side plaster brick wall	x_{10}	100*	20	7	
	220mm brick wall with no gap		101	28		
	220mm brick wall with air gap 2cm		102	29		
	220mm brick wall with 1cm central EPS		103	30		
	220mm brick wall with 2cm central EPS		104	32.5		
	220mm brick wall with 3cm central EPS		105	35		
	220mm brick wall with 4cm central EPS		106	38		
Window glazing type	Clear glazed 6mm	x_{11}	200*	43	5	
	Bronze film glazed 6mm -		201	60		
	Double clear glazed with air gap 6mm		202	90		
	Double bronze film glazed with air gap 6mm		203	115		
	Double reflective glazed - 13mm Argon		204	135		
Roof types	Corrugated metal roof	x_{12}	300*	11	5	
	Corrugated metal roof + 1cm insulation		301	13.5		
	Corrugated metal roof + 2 cm insulation		302	15		

	Corrugated metal roof + 3 cm insulation		303	16.5	
	Corrugated metal roof + 4 cm insulation		304	18.5	
Ventilation strategy	From 400, 401, 402*, ..., 409 (see details of these ventilation strategies in Table 7-3)	x_{13}		No cost	10
Ground floor types	Concrete slab + ceramic tile finish	x_{14}	500*	34	4
	Concrete slab+ 1cm insulation + wooden tile finish		501	43.5	
	Concrete slab+ 2cm insulation + wooden tile finish		502	45	
	Concrete slab+ 3cm insulation + wooden tile finish		503	47	
Internal thermal mass	Thermal mass 100mm thickness	x_{15}	600*	20	4
	Thermal mass 170mm thickness		601	26	
	Thermal mass 240mm thickness		602	31	
	Thermal mass 310mm thickness		603	36.5	

*: Initial value

The search-space includes $3 \times 4^2 \times 5^7 \times 6^2 \times 7^2 \times 10 \approx 6.62 \times 10^{10}$ candidate solutions.

Table B-2: Design parameters used in the optimization of the AC row house

Numerical (continuous) variables and their variation ranges						
Design parameter	Opt. variable	Min value	Initial value	Max value	Step size	Number of case
Solar absorptance – external wall [dimensionless]	x_1	0.25	0.35	0.75	0.1	6
Solar absorptance – roof [dimensionless]	x_2	0.25	0.35	0.75	0.1	6
Total infiltration - level 1 [kg/s-m]	x_3	0.008	0.01	0.018	0.002	6
Total infiltration - level 2 [kg/s-m]	x_4	0.004	0.008	0.012	0.002	5
Total infiltration - bedroom [kg/s-m]	x_5	0.004	0.006	0.012	0.002	5
Width - Front window (height = 1.9m) [m]	x_6	1.0	2.0	2.2	0.2	7
Width - Entrance door (height = 2.9m) [m]	x_7	1.6	3.2	3.6	0.4	5
Width - Backward window level 2 (height = 1.2m) [m]	x_8	1	1.5	3	0.5	5
Length - Front facade shading device [m]	x_9	0.05	0.05	0.65	0.2	3
Categorical design options and strategies (discrete variables)						
Design parameter	Design choices	Opt. variable	Discrete value	Item cost (\$/m ²)	Number of case	
External walls	110mm two-side plaster brick wall	x_{10}	100*	20	7	
	220mm brick wall with no gap		101	28		
	220mm brick wall with air gap 2cm		102	29		
	220mm brick wall with 1cm central EPS		103	30		
	220mm brick wall with 2cm central EPS		104	32.5		
	220mm brick wall with 3cm central EPS		105	35		

	220mm brick wall with 4cm central EPS		106	38	
Window glazing type	Clear glazed 6mm	x ₁₁	200*	43	5
	Bronze film glazed 6mm -		201	60	
	Double clear glazed with air gap 6mm		202	90	
	Double bronze film glazed with air gap 6mm		203	115	
	Double reflective glazed - 13mm Argon		204	135	
Roof types	Corrugated metal roof	x ₁₂	300*	11	5
	Corrugated metal roof + 1cm insulation		301	13.5	
	Corrugated metal roof + 2 cm insulation		302	15	
	Corrugated metal roof + 3 cm insulation		303	16.5	
	Corrugated metal roof + 4 cm insulation		304	18.5	
Ground floor types	Concrete slab + ceramic tile finish	x ₁₃	500*	34	4
	Concrete slab+ 1cm insulation + wooden tile finish		501	43.5	
	Concrete slab+ 2cm insulation + wooden tile finish		502	45	
	Concrete slab+ 3cm insulation + wooden tile finish		503	47	
Internal thermal mass	Thermal mass 100mm thickness	x ₁₄	600*	20	4
	Thermal mass 170mm thickness		601	26	
	Thermal mass 240mm thickness		602	31	
	Thermal mass 310mm thickness		603	36.5	

*: Initial value

The search-space includes $3 \times 4^2 \times 5^6 \times 6^3 \times 7^2 \approx 7.94 \times 10^9$ candidate solutions.

Table B-3: Design parameters used in the optimization of the NV detached house

Numerical (continuous) variables and their variation ranges						
Design parameter	Opt. variable	Min value	Initial value	Max value	Step size	Number of case
Solar absorptance – external wall [dimensionless]	x ₁	0.25	0.35	0.75	0.1	6
Solar absorptance – roof [dimensionless]	x ₂	0.25	0.35	0.75	0.1	6
Crack infiltration – window bedrooms [kg/s-m]	x ₃	0.002	0.002	0.008	0.002	4
Crack infiltration – window other rooms [kg/s-m]	x ₄	0.002	0.002	0.008	0.002	4
Crack infiltration – the roof attic [kg/s-m]	x ₅	0.02	0.06	0.1	0.02	5
Height – East windows [m]	x ₆	1.2	1.6	1.8	0.2	4
Height – West windows [m]	x ₇	1.2	1.6	1.8	0.2	4
Height – North and South windows [m]	x ₈	1.2	1.6	1.8	0.2	4
Length – East window overhang [m]	x ₉	0.2	0.6	0.8	0.2	4
Length – West window overhang [m]	x ₁₀	0.2	0.6	0.8	0.2	4
Categorical design options and strategies (discrete variables)						
Design parameter	Design choices	Opt. variable	Discrete value	Item cost (\$/m ²)	Number of case	

External walls	110mm two-side plaster brick wall	x ₁₁	100	20	7
	220mm brick wall with no gap		101*	28	
	220mm brick wall with air gap 2cm		102	29	
	220mm brick wall with 1cm central EPS		103	30	
	220mm brick wall with 2cm central EPS		104	32.5	
	220mm brick wall with 3cm central EPS		105	35	
	220mm brick wall with 4cm central EPS		106	38	
Window glazing type	Clear glazed 6mm	x ₁₂	200*	43	5
	Bronze film glazed 6mm -		201	60	
	Double clear glazed with air gap 6mm		202	90	
	Double bronze film glazed with air gap 6mm		203	115	
	Double reflective glazed - 13mm Argon		204	135	
Roof types	Corrugated metal roof	x ₁₃	300*	11	5
	Corrugated metal roof + 1cm insulation		301	13.5	
	Corrugated metal roof + 2 cm insulation		302	15	
	Corrugated metal roof + 3 cm insulation		303	16.5	
	Corrugated metal roof + 4 cm insulation		304	18.5	
Ventilation strategy	From 400, 401, 402*, ..., 409 (see details of these ventilation strategies in Table 7-3)	x ₁₄	400 to 409	No cost	10
Ground floor types	Concrete slab + ceramic tile finish	x ₁₅	500	34	4
	Concrete slab+ 1cm insulation + wooden tile finish		501*	43.5	
	Concrete slab+ 2cm insulation + wooden tile finish		502	45	
	Concrete slab+ 3cm insulation + wooden tile finish		503	47	
Internal thermal mass	Thermal mass 100mm thickness	x ₁₆	600*	20	4
	Thermal mass 170mm thickness		601	26	
	Thermal mass 240mm thickness		602	31	
	Thermal mass 310mm thickness		603	36.5	

*: Initial value

The search-space includes $3 \times 4^2 \times 5^7 \times 6^2 \times 7^2 \times 10 \approx 6.62 \times 10^{10}$ candidate solutions.

Table B-4: Design parameters used in the optimization of the AC detached house

Numerical (continuous) variables and their variation ranges						
Design parameter	Opt. variable	Min value	Initial value	Max value	Step size	Number of case
Solar absorptance – external wall [dimensionless]	x ₁	0.25	0.35	0.75	0.1	6
Solar absorptance – roof [dimensionless]	x ₂	0.25	0.35	0.75	0.1	6
Infiltration bedroom [m ³ /s]	x ₃	0.002	0.006	0.01	0.002	5

Infiltration other zone [m ³ /s]	x ₄	0.002	0.006	0.01	0.002	5
Infiltration – roof attic [m ³ /s]	x ₅	0.004	0.004	0.01	0.002	4
Height – East windows [m]	x ₆	1.2	1.6	1.8	0.2	4
Height – West windows [m]	x ₇	1.2	1.6	1.8	0.2	4
Height – North and South windows [m]	x ₈	1.2	1.6	1.8	0.2	4
Length – East window overhang [m]	x ₉	0.2	0.6	0.8	0.2	4
Length – West window overhang [m]	x ₁₀	0.2	0.6	0.8	0.2	4
Categorical design options and strategies (discrete variables)						
Design parameter	Design choices	Opt. variable	Discrete value	Item cost (\$/m ²)	Number of case	
External walls	110mm two-side plaster brick wall	x ₁₁	100	20	7	
	220mm brick wall with no gap		101*	28		
	220mm brick wall with air gap 2cm		102	29		
	220mm brick wall with 1cm central EPS		103	30		
	220mm brick wall with 2cm central EPS		104	32.5		
	220mm brick wall with 3cm central EPS		105	35		
	220mm brick wall with 4cm central EPS		106	38		
Window glazing type	Clear glazed 6mm	x ₁₂	200*	43	5	
	Bronze film glazed 6mm -		201	60		
	Double clear glazed with air gap 6mm		202	90		
	Double bronze film glazed with air gap 6mm		203	115		
	Double reflective glazed - 13mm Argon		204	135		
Roof types	Corrugated metal roof	x ₁₃	300*	11	5	
	Corrugated metal roof + 1cm insulation		301	13.5		
	Corrugated metal roof + 2 cm insulation		302	15		
	Corrugated metal roof + 3 cm insulation		303	16.5		
	Corrugated metal roof + 4 cm insulation		304	18.5		
Ground floor types	Concrete slab + ceramic tile finish	x ₁₄	500	34	4	
	Concrete slab+ 1cm insulation + wooden tile finish		501*	43.5		
	Concrete slab+ 2cm insulation + wooden tile finish		502	45		
	Concrete slab+ 3cm insulation + wooden tile finish		503	47		
Internal thermal mass	Thermal mass 100mm thickness	x ₁₅	600*	20	4	
	Thermal mass 170mm thickness		601	26		
	Thermal mass 240mm thickness		602	31		
	Thermal mass 310mm thickness		603	36.5		

*: Initial value

The search-space includes $3 \times 4^2 \times 5^6 \times 6^3 \times 7^2 \approx 7.94 \times 10^9$ candidate solutions.

APPENDIX C

DETAILS OF THE OPTIMIZATION RESULTS

Table C-1: Optimization results of the NV houses – objective function [A]

	Hanoi			Danang			Hochiminh		
	Row house	Detached house	Apart.	Row house	Detached house	Apart.	Row house	Detached house	Apart.
x1	0.2625	0.75	0.25	0.25	0.75	0.25	0.25	0.25	0.25
x2	0.25	0.4125	0.004	0.25	0.25	0.004	0.25	0.25	0.004
x3	0.004	0.002	0.008	0.004	0.002	0.006	0.004	0.002	0.008
x4	0.004	0.002	1.2	0.004	0.002	1.2	0.004	0.004	1.2
x5	0.2	0.02	1.2	0.225	0.02	1.2	1	0.06	1.2
x6	1	1.2	0.8	1	1.2	0.4	1	1.2	0.8
x7	1.6	1.2	0.8	1.6	1.2	0.8	1.6	1.2	0.8
x8	1	1.2	0.6	3	1.2	0.4	1.03125	1.2	0.6
x9	0.65	0.8	0.55	0.65	0.8	0.2	0.65	0.8	0.4
x10	106	0.2	106	106	0.25	106	106	0.8	106
x11	204	106	204	204	106	204	204	106	204
x12	304	204	406	304	204	406	304	204	401
x13	406	304	603	406	304	603	407	304	603
x14	500	406		500	406		500	403	
x15	603	500		603	500		603	500	
x16		603			603			603	

Table C-2: Optimization results of the NV houses – objective function [B]

	Hanoi			Danang			Hochiminh		
	Row house	Detached house	Apart.	Row house	Detached house	Apart.	Row house	Detached house	Apart.
x1	No solution		0.25	0.35	0.35	0.25	0.25	0.25	0.25
x2			0.004	0.25	0.25	0.008	0.25	0.25	0.008
x3			0.004	0.012	0.004	0.006	0.004	0.004	0.004
x4			1.2	0.004	0.008	1.4	0.012	0.008	1.2
x5			1.2	0.6	0.08	1.2	1	0.04	1.2
x6			0.1	1	1.2	0	1	1.2	0
x7			0	1.6	1.2	0	1.6	1.2	0

	Hanoi			Danang			Hochiminh		
	Row house	Detached house	Apart.	Row house	Detached house	Apart.	Row house	Detached house	Apart.
x8	No solution		0.2	1	1.2	0.2	1	1.2	0
x9			0	0.05	0.2	0.2	0.05	0.2	0
x10			104	100	0.2	100	100	0.2	100
x11			204	200	100	200	200	100	200
x12			406	300	200	406	300	200	401
x13			600	408	301	600	409	300	600
x14				500	406		500	406	
x15				600	500		600	500	
x16					600			600	

Table C-3: Optimization results of the AC houses – objective function [C]

	Hanoi			Danang			Hochiminh		
	Row house	Detached house	Apart.	Row house	Detached house	Apart.	Row house	Detached house	Apart.
x1	0.25	0.25	0.25	0.25	0.25	0.25	0.25	0.25	0.25
x2	0.25	0.25	0.004	0.25	0.25	0.004	0.25	0.25	0.004
x3	0.008	0.002	0.029	0.008	0.002	0.029	0.008	0.002	0.029
x4	0.004	0.002	1.2	0.004	0.002	1.2	0.004	0.002	1.2
x5	0.004	0.004	1.2	0.004	0.01	1.2	0.004	0.004	1.2
x6	1	1.2	0.8	1	1.2	0.8	1	1.2	0.8
x7	1.6	1.2	0.8	1.6	1.2	0.8	1.6	1.2	0.8
x8	1	1.2	0	1	1.2	0	1	1.2	0
x9	0.05	0.2	0	0.05	0.2	0	0.05	0.2	0
x10	106	0.2	105	104	0.2	102	106	0.2	106
x11	204	106	204	204	104	204	204	106	204
x12	304	204	600	304	204	600	304	204	600
x13	500	304		500	304		500	304	
x14	600	500		600	500		600	500	
x15		600			600			600	